UNIVERSITATEA DE MEDICINĂ ȘI FARMACIE
GRIGORE T. POPA IAȘI

HABILITATION THESIS

Iași

2023

UNIVERSITATEA DE MEDICINĂ ȘI FARMACIE
GRIGORE T. POPA IAȘI

THROMBOSIS AND CARDIOVASCULAR DISEASE ÎN VARIOUS CLINICAL SCENARIOS

Associate Professor:
Radu-Florin POPA, MD, PhD

2023

Table of Contents:

ABBREVIATIONS

ADS - Adipose-derived relaxing factor
AHA - American Heart Association
ASA - Acetylsalicylic acid
ATS - Atherosclerosis, atherosclerotic carotid artery disease
B-mode - Brightness mode
BMP-4 - Bone morphogenic protein-4
BMP-7 - Bone morphogenic protein-7
CAD - Coronary artery disease
CCL - Chemokine (C-C motif) ligand
CCL5 - Chemokine ligand 5
CEA - Carotid endarterectomy
$\chi 2$ test - Chi-square test
COX-2 - Cyclooxygenase-2
CRP - C-reactive protein
CT - Computed tomography
DAB- 3,3'Diaminobenzidine
D-E - Doppler echocardiography
Doppler - Doppler ultrasound
ECM - Extracellular matrix
ECST - European Carotid Surgery trial
ED - Emergency department
eNOS - Endothelial nitric oxide synthase
ERK1/2 - Extracellular signal-regulated kinase 1/2
ET-1 - Endothelin-1
FDA - Food and Drug Administration
GHS-R - Growth-hormone secretagogue receptor
GHS-R1a - Growth hormone secretagogue receptor type 1a
GM-CSF - Granulocyte-macrophage colony-stimulating factor
GOT - Glutamic oxaloacetic transaminase
GOAT - Ghrelin O-acyl transferase
GSM - Gray scale median
HIF-1a - Hypoxia-inducible factor 1 alpha
HP - Histopathological
HRP - Horseradish peroxidase
IHC - Immunohistochemical
ICAM-1 - Intercellular adhesion molecule 1
IFN-γ - Interferon-gamma
IL - Interleukin
IL-6 - Interleukin 6
ICA - Internal carotid artery
MCP-1 - Monocyte chemoattractant protein-1
MRI - Magnetic resonance imaging
MMP - Matrix metalloproteinase
MS - Metabolic syndrome
NADPH - Nicotinamide adenine dinucleotide phosphate
NO - Nitric oxide
NOAC - Non-vitamin K antagonist oral anticoagulants
NPY - Neuropeptide Y

NYHA - New York Heart Association
OPG - Osteoprotegerin
OPN - Osteopontin
p-value - Probability value
PI3K/Akt - Phosphoinositide 3-kinase/Akt
PFO - Patent foramen ovale
PPARγ - Peroxisome proliferator-activated receptor gamma
PVAT - Perivascular adipose tissue
RANTES - Regulated upon activation, normal T cell expressed and secreted
ROS - Reactive oxygen species
RV - Right
sCD40L - Soluble CD40 ligand
SPSS - Statistical Package for the Social Sciences
TGF-β - Transforming growth factor beta
TIA - Transient ischemic attack
TLR4 - Toll-like receptor 4
TNF-α - Tumor necrosis factor-alpha
TNFR - Tumor necrosis factor receptor
TRAIL - TNF-related apoptosis-inducing ligand
TSP-1 - Thrombospondin-1
TEE - Transesophageal echocardiography
US - Ultrasound
VCAM-1 - Vascular cell adhesion molecule 1
VEGF - Vascular endothelial growth factor

REZUMATUL TEZEI

Această teză de abilitare intitulată **„TROMBOZA ȘI BOALA CARDIOVASCULARĂ ÎN DIVERSE SCENARII CLINICE”** oferă o perspectivă organică asupra activității mele clinice, didactice și științifice din perioada postdoctorală. Atât boala cardiovasculară, cât și patologia trombotică reprezintă niște domenii de cercetare complexe, în continuă dinamică și interconectate, iar această lucrare își propune să reflecte aplicabilitatea clinică a modelelor experimentale studiate. Totodată, doresc să subliniez principalele direcții de dezvoltare ale carierei mele universitare din punct de vedere clinic, didactic și al activităților de cercetare științifică.

Prima parte a tezei de abilitare cuprinde un sinopsis al carierei mele academice, profesionale și științifice, precum și a principalelor realizări profesionale obținute de-a lungul timpului, concretizate prin obținerea unui brevet de invenție și recunoscute prin principalii indicatori ai evaluării științifice (indice Hirsch de 6 și 75 de citări).

SECȚIUNEA I a tezei de abilitare cuprinde 4 capitole care reflectă activitatea mea științifică. Primul capitol reunește 4 studii care au evaluat rolul grelinei în progresia plăcilor de aterom, osteopontina și osteoprotegerina ca markeri ai instabilității plăcilor de aterom, corelația dintre markerii ecografici și histopatologici pentru plăcile de aterom carotidiene, precum și caracterizarea ecografică a acestora.

Cel de-al doilea capitol a descris multiple abordări imagistice pentru evaluarea foramen ovale patent, precum și rolul secțiunilor de 3 vase-trahee în screening-ul anomaliilor congenitale cardiace. Al treilea capitol a relevat o influența vasculopatiilor trombotice asupra outcome-urilor obstetricale și reproductive, precum și managementul trombozei venoase profunde la gravide. Ultimul capitol a evaluat asocierea SARS-CoV-2 cu complicații trombotice și vasculare la populația adultă, negravidă.

SECȚIUNEA II enunță și explică direcțiile de dezvoltare profesională și cercetare științifică pe care mi le-am propus în să le dezvolt în următorii ani. Va fi evidențiată colaborarea mai strânsă cu studenții, cu promovarea activităților de învățare a abilităților practice chirurgicale și a activităților de cercetare științifică experimentală.

De asemenea, va fi promovată colaborarea cu colegii rezidenți și tineri specialiști pe multiple paliere precum dezvoltarea abilităților practice chirurgicale, a cercetării clinice, precum și diseminarea rezultatelor cercetării științifice. Nu în ultimul rând, vor fi punctate principalele posibilități și teme de cercetare clinică în domeniul ales, chirurgia cardiovasculară.

SECȚIUNEA III include o listă cu articole, cărți leși capitolele de carte care m-au ajutat la elaborarea acestei teze.

THESIS SUMMARY

This habilitation thesis entitled **"THROMBOSIS AND CARDIOVASCULAR DISEASE IN VARIOUS CLINICAL SCENARIOS"** provides an organic perspective on my postdoctoral clinical, teaching and scientific work. Both cardiovascular disease and thrombotic pathology represent complex, constantly dynamic and interconnected fields of research, and this paper aims to reflect the clinical applicability of the studied experimental models. At the same time, I want to emphasize the main development directions of my university career from the clinical, didactic and scientific research points of view.

The first part of the habilitation thesis includes a synopsis of my academic, professional and scientific career, as well as the main professional achievements obtained over time, concretized by obtaining an invention patent and recognized by the main indicators of scientific evaluation (Hirsch index of 6 and 75 citations).

SECTION I of the habilitation thesis includes 4 chapters that reflect my scientific activity. The first chapter brings together 4 studies that evaluated the role of ghrelin in the progression of atheroma plaques, osteopontin and osteoprotegerin as markers of atheroma plaque instability, the correlation between sonographic and histopathological markers for carotid atheroma plaques, as well as their sonographic characterization.

The second chapter described multiple imaging approaches for evaluating patent foramen ovale, as well as the role of 3-vessel-tracheal sections in screening for congenital cardiac anomalies. The third chapter revealed an influence of thrombotic vasculopathies on obstetric and reproductive outcomes, as well as the management of deep vein thrombosis in pregnant women. The last chapter assessed the association of SARS-CoV-2 with thrombotic and vascular complications in the adult, non-pregnant population.

SECTION II states and explains the directions of professional development and scientific research that I have proposed to develop in the coming years. Closer collaboration with students will be highlighted, with the promotion of learning practical surgical skills and experimental scientific research activities.

Collaboration with fellow residents and young specialists will also be promoted on multiple levels, such as the development of practical surgical skills, clinical research, as well as the dissemination of scientific research results. Last but not least, the main possibilities and themes of clinical research in the chosen field, cardiovascular surgery, will be pointed out.

SECTION III includes a list of articles, books, and book chapters that helped me develop this thesis.

SECTION I

Synopsis of clinical, academic, and scientific achievements

A. Clinical achievements

I graduated the Faculty of Medicine of „Grigore T. Popa" University of Medicine and Pharmacy of Iasi in 1984, and I completed a 3 years internship at the County Hospital from Botoșani, Romania. During this timeframe, I was able to consolidate my knowledge in various fields such as Obstetrics and Gynecology, General Surgery, and Pediatrics. At my personal request I fulfilled the last stages of this internship in Hlipiceni village from Botosani county, where I was able to use my professional skills for improving the health status of patients from all age categories and social backgrounds. I considered this clinical experience an immense opportunity for my personal and clinical development due to the great variety of medical situations that imposed complex thinking and innovative problem solving.

In the spring of 1988, following several residency exams, I was able to achieve a resident position as a General Surgeon. I completed the residency program at the third General Surgery clinic from "Saint Spiridon" Clinical Emergency Hospital, Iași, Romania, under the supervision of Professor Constantin Dolinescu. At the end of the second year of residency I obtained an assistant lecturer position, and I was transferred at the first General Surgery clinic from the same hospital, where I fulfilled the rest of my residency program under the supervision of Professor Victor Strat. During my residency, I had the opportunity to learn various surgical techniques that would later help me in difficult intraoperative situations, as well as the discipline of mind, which is an essential attribute of good surgeons.

In 1992, I obtained the degree of Specialist in the specialty General Surgery, and in the month of May of the same year I followed a 3-months internship on vascular surgery at the "Saint Elisabeth" Clinic in Bruxelles, Belgium, under the supervision of Professor Robert Van Gestel. During this internship, I was able to learn and consolidate basic vascular surgical skills by working in various clinical settings that were based on general surgery and vascular surgery.

Between 1992 and 1993 I was accepted by Professor Ralph Suy for a 1-year internship at the Clinical University Hospital Gasthuisberg from Leuven, Belgium. During this timeframe, I participated and operated all types of surgical procedures that were specific to the vascular surgery field, and I succeeded to pass all the final examinations with good results.

I returned to Romania in 1993, and I have continued my clinical activity as a general surgeon at the "Saint Spiridon" Clinical Emergency Hospital, but, at the same time, I became more and more interested in the vascular surgery procedures, participating predominantly at those who necessitated high surgical skills. This shift in the optics of my medical profession determined myself to pursue a 6-months internship at the "Professor Doctor C.C. Iliescu" Heart Institute, Fundeni, Bucharest, Romania. In this medical setting I was able to expand my level of surgical expertise in the heart surgery field, as well as in peripheral vascular surgery domain.

Between 1996 and 1997, after a thorough selection from the Romanian Public Health Ministry, I pursued an internship at Hadassah University Medical Center, from Jerusalem, Israel. I worked under the supervision of Professor Gideon Merrin in the Heart Surgery Department, and I accumulated extensive knowledge regarding top surgical techniques in the following fields: coronary artery surgery, heart valve surgery, and congenital heart defects surgery. These procedures required a high level of surgical expertise, and I was fortunate

enough to receive all technical support from this team, that also encouraged me to extensively study the myocardial energy preservation mechanisms as a separate research project.

Once again returned in Romania, I engaged in a 2-years internship at the "Professor Doctor C.C. Iliescu" Heart Institute, Fundeni, Bucharest, Romania, where I collaborated with Professor Dan Făgărășanu and Professor Vasile Cândea in Heart Surgery Specialty. I benefited from an extensive surgical expertise, and I was able to put into practice my surgical knowledge obtained from previous medical experiences.

I obtained a primary physician degree in general surgery in 1997, and I was willing to later fulfill my surgical background by completing my second surgical specialty- the cardiovascular surgery. Therefore, in 1998, I obtained the degree of Specialist in the specialty Cardiovascular Surgery. I worked as a primary general surgeon and a specialist cardiovascular surgeon in the Vascular Surgery Compartment that was then assimilated to the third General Surgery clinic from "Saint Spiridon" Clinical Emergency Hospital, Iași, Romania.

In 1999, I obtained a study fellowship in Belgium that allowed me to work under the supervision of Professor Schoevaerts in Mont-Goddine Hospital, for three months. I actively participated in the clinic's medical and surgical activity, performing numerous vascular and cardiac surgical interventions.

After completing this fellowship, I returned to work to the Vascular Surgery Compartment, where I performed over two thousand vascular surgery procedures that interested both arterial (arteriopathies, aneurisms, large vessels disease) and venous pathology. I developed the Vascular Surgery Compartment into a standalone clinic in the "Saint Spiridon" Clinical Emergency Hospital, that was able to attend all important traumatic and non-traumatic emergencies from Iasi County and from all over Moldavian region.

In 2003, I obtained a primary physician degree in vascular surgery, and since then I have constantly learned new surgical and management. I obtained professional competencies in general ultrasound, and followed multiple postgraduate specialization studies that allowed me to be constantly up to date with medical novelties.

From 2007 I put my greatest effort in the formation of an integrated service of vascular surgery. After many years of methodological, logistics, and medical work, "Saint Spiridon" Clinical Emergency Hospital has now a modern Clinical Department of Vascular Surgery that is able to manage some of the most complex vascular pathologies.

B. Academic achievements

A limited number of vascular surgeons throughout the country prioritize the act of instructing and communicating with students. I commenced my teaching endeavors in 1991, when I obtained an assistant lecturer position at the Cardiovascular Surgery discipline from the University of Medicine and Pharmacy "Grigore T. Popa", Iasi. In 2003, I became a Lecturer and head of the Cardiovascular Surgery discipline, while in 2014 I obtained an Assistant Professor position in the same institution, which I presently occupy with honor.

During my academic carrier, I have contributed to the development of curricula, practical workshops, case studies, and seminars for students of vascular surgery. I was the *Vascular Surgery* course coordinator for the third-year students, and I also coordinated optional courses such as *Step decisions in the diagnosis and treatment of peripheral vascular disease* or *Diagnostic and treatment algorithm of vascular disorders* for students in their fourth or fifth year of medical school.

I have devoted significant effort towards the facilitation of medical education at the University of Medicine and Pharmacy "Grigore T. Popa" for all three tiers of learners, including undergraduate students, residents, and postgraduate physicians. I contributed to the

development of educational resources and assessments of knowledge. I provided mentorship to a cohort of nine undergraduate students in their academic writing endeavors. Additionally, I facilitated the participation of residents in the production of scientific papers and syntheses pertaining to diverse subject matters.

It is important to note that I have consistently demonstrated a willingness to receive and incorporate feedback and recommendations from my learners. Additionally, I have actively participated in various events organized by student associations at our university, including workshops and conferences hosted by SSCR (Societatea Studențească de Chirurgie din România) and SSMI (Societatea Studenților Mediciniști Iași). My involvement in aforementioned occasions has consistently elicited authentic eagerness, thereby serving as a source of inspiration and encouragement. The extracurricular topics that have been covered include the diagnosis and treatment of aortic sub-renal aneurysms, carotid arteries stenosis, aortoiliac disease, femoropopliteal disease, aorto-iliac disease or vascular anastomosis.

The formation of a united and professional team in the Clinical Department of Vascular Surgery from “Saint Spiridon” Clinical Emergency Hospital needed intensive guidance and teaching. A team of primary physicians, specialty doctors, as well as vascular surgery residents is working in this department. I was certified as a trainer for preparing teaching staff, and I was a member of various commissions that evaluated candidates for a position in the university.

C. Scientific achievements

Research is an important part of every academic career, and numerous efforts should be made in order to clarify complex medical problems or to innovate the diagnostic and therapeutic approaches. My research career developed under the supervision of Professor Victor Strat who helped me in the process of fulfilling my doctoral research, that evaluated the actual therapeutical options for aortoiliac disease. Our results were gathered under a doctoral thesis that was publicly presented and evaluated in 2005.

I have contributed more than 30 research publications of various categories to international journals, some of which are regarded as high impact.

Following the completion of my PhD studies, I have constantly participated in several national and university research programs and grants, including:

1. Internal Grant Competition - UMF "Gr.T.Popa" Iasi: "Complex study of the atheroma plaque: predictive value for carotid restenosis" (Director of Grants, 2011);
2. Noninterventional, multicenter prospective National Clinical Study: "ATTEST: Assessment of Thromboprophylaxis for patients with major Surgery in current clinical practice" number DIREG_L_03699. Sponsored by Sanofi (Principal investigator, 2009)
3. Prospective study "Assessment of the effectiveness and safety of Vessel Due in the therapy of venous and arterial diseases for the inpatients at vascular surgery department".Contractor Alfa Wasermann (Project manager)
4. Multicentric International Epidemiological Study "Vein Consult Program" Protocol no. ICE-5682-50-ROM (Investigator)
5. Project ID POSDRU/87.1.3/S/62208-Diploma of excellence (participant; project manager Professor Norina Forna).
6. National Coordinator/Lecturer at the "Education Program in Venous Pathology" Credited by the Romanian College of Physicians (5100/08.11.2007) and supported by Servier Pharma Company.

7. National Coordinator/Lecturer at the "Education Program in Venous Pathology" Credited by the Romanian College of Physicians (153/13.01.2009) and supported by Servier Pharma Company.

One of the most important results of my research is represented by an invention patent (nr 133683) for an endovascular simulator dedicated to the blood flow and intravascular pressure analysis in the aortas of patients with complex aortic disorders. Also, the results of my work were disseminated throughout years in numerous national and international scientific manifestations.

I have always been interested in actively joining professional organizations from Romania and abroad in the disciplines of Vascular and Cardiac Surgery, as they are complementary to and helpful to my scientific, clinical, and academic pursuits. I belong to numerous scientific organizations such as:

- Society of Physicians and Naturalists and Medical-Surgical Journal of Iasi;
- Romanian Society of Surgery;
- Romanian Society of Angiology and Vascular Surgery;
- Romanian Society of Cardiovascular Surgery;
- Romanian Society of Vascular Surgery;
- European Society of Vascular Surgery (ESVS).

In addition, I am a founder member of the Vascular Surgery Society since 2013 and of the International Society of Endovascular Specialists (**ISEVS**) since 2018, as well as a Romanian Counselor in the European Society of Vascular Surgery Committee.

Chapter 1: Atherosclerotic plaques characterization

I.1.1. State of art

Hyperlipidemia and persistent inflammation are two characteristics of atherosclerotic plaques that are intricately connected by innate and adaptive immunological systems (1, 2). The pathology that underlies cardiovascular disease is atherosclerosis. Myocardial infarction and cerebral stroke are most often caused by unstable atherosclerotic plaque and subsequent atherothrombosis (3). Despite extremely effective choices being available to manage traditional cardiovascular risk factors, 17.8 million deaths worldwide were linked to cardiovascular disease in 2017, making it a persistently major global health issue (4, 5). The immune system and inflammation most likely play a significant role in this residual risk (5, 6).

Increased blood levels of low-density lipoprotein (LDL) and other cardiovascular risk factors, particularly metabolic syndrome or nicotine consumption, favor loss of endothelial integrity and endothelial activation, preferably at areas of low endothelial shear stress (7). This enables the buildup of lipids in the artery intima, where they are oxidized, collect, and are absorbed by macrophages and smooth muscle cells, leading to the development of foam cells (8, 9).

The innate and adaptive immune systems are chronically stimulated by modified lipids, which orchestrate a simmering low-grade inflammation of the vessel wall (10). A lipid-rich necrotic center is formed as a result of subsequent cell apoptosis and necroptosis, which are worsened by ineffective efferocytosis (the evacuation of dead cells by phagocytes). This results in the synthesis of thrombogenic tissue factor (9). The extracellular fibrous matrix, which helps to stabilize plaques, is broken down by necrotic center’s components and inflammatory cells, which thins the fibrous cap (8). The necrotic center's cells release hypoxia-inducible factors that encourage pathologic neoangiogenesis, which favors intraplaque hemorrhage and continued growth of the necrotic center.

Plaque calcification is triggered by untreated inflammation, which further lessens the plaque's mechanical stability (10). Numerous scientific researches have been performed in order to provide the best characterization of plaque instability, but very few imagistic and histopathological markers have proven to be effective in predicting adverse cerebrovascular outcomes. The present chapter aims to evaluate the role of ghrelin in the progression of atheroma plaques, osteopontin and osteoprotegerin as markers of atheroma plaque instability, the correlation between sonographic and histopathological markers for carotid atheroma plaques, as well as their sonographic characterization.

Personal contributions:

1. Peiu SN, **Popa RF**, Akad F, Cretu-Silivestru IS, Mihai BM, Visnevschi A, Vudu L, Tamba B, Oboroceanu T, Timofte D, Mocanu V. Perivascular Adipose Tissue Inflammation: The Anti-Inflammatory Role of Ghrelin in Atherosclerosis Progression. Applied Sciences. 2022; 12(7):3307.
2. Strobescu-Ciobanu C, Giuşcă SE, Căruntu ID, Amălinei C, Rusu A, Cojocaru E, **Popa RF**, Lupaşcu CD.Osteopontin and osteoprotegerin in atherosclerotic plaque - are they significant markers of plaque vulnerability? Rom J Morphol Embryol. 2020 Jul-Sep;61(3):793-801. doi: 10.47162/RJME.61.3.17. PMID: 33817720; PMCID: PMC8112796.

3. Cristina Strobescu-Ciobanu, **R. F. Popa**, Simona-Eliza Giușcă, Andreea Rusu, C. D.Lupașcu. CORRELATIONS BETWEEN GRAYSCALE AND HISTOPATHOLOGICAL PROPRIETIES OF CAROTID ATHEROSCLEROTIC PLAQUE. Med.Surg. J. –Rev. Med. Chir. Soc. Med. Nat., Iaşi –2020–vol. 124, no. 1
4. **Popa, Radu** & Cristina, Strobescu & Baroi, Genoveva & Raza, A & Fotea, Vasile. (2013). Complex utrasound study of the atherosclerotic plaque. Revista medico-chirurgicală a Societăţii de Medici şi Naturalişti din Iaşi. 117. 424-30.

I.1.2. Perivascular adipose tissue inflammation: the anti-inflammatory role of ghrelin in atherosclerosis progression

I.1.2.1 Introduction

The absence of atherosclerosis in myocardial bridges, which have no surrounding fat, led to the misleading hypothesis of a causal role of perivascular adipose tissue (PVAT) in atherosclerosis. PVAT is attached straight to the vascular wall and its adipokines can act directly upon the vascular wall, which for its part modifies PVAT secretome in bidirectional crosstalk. PVAT is neither a mere sustainer of the vascular system nor a risk factor for atherosclerosis. It exerts various protective vasodilatory, anti-inflammatory, and antioxidative effects.

PVAT-derived adipokines release anti-atherogenic factors, such as adiponectin, hydrogen sulfide, omentin, IL-10, IL-19, adipose-derived relaxing factor (ADRF), nitric oxide, hydrogen sulfide, and methyl palmitate. PVAT-derived adipocytokines with a vascular impact include adiponectin, leptin, nicotinamide phosphoribosyltransferase (NAMPT), omentin, chemerin, and resistin, with the first having the most detrimental impact. Adiponectin was shown to inhibit NADPH oxidase-mediated release of reactive oxygen species and to increase endothelial nitric oxide (NO) bioavailability. The anticontractile relaxing action is achieved by PVAT-released angiotensin (1–7), by potassium (K^+) channel opening in the plasma membrane of smooth muscle cells, by norepinephrine uptake through the organic cation transporter 3 (OCT-3), and the release of adiponectin mediated by the β 3-adrenoceptor (11, 12).

Human ghrelin ($C_{149}H_{249}N_{47}O_{42}$) is the endogenous ligand for growth-hormone secretagogue receptor (GHS-R), GHS-R1a being its functional form. Ghrelin is a 28 amino acid peptide secreted by the P/D1 cells, lining the stomach fundus. Human ghrelin differs from rat only in amino acids in position 11 and 12. In order to be recognized by the GHS-R1a receptor and to stimulate growth hormone release from the pituitary gland, the ghrelin's serine at position 3 is acylated by a fatty acid, the n-octanoic acid, near its N-terminal region, before secretion. Ghrelin acylation is triggered by an enzyme known as ghrelin O-acyl transferase (GOAT) (13). The non-modified ghrelin is called desacyl ghrelin and circulates as a free peptide, whereas acyl ghrelin is bound to lipoproteins. Plasma levels of desacyl ghrelin are about four or five times higher than those of acyl ghrelin in non-pathological states (14).

Ghrelin is a hormone that stimulates appetite and increases the volume of white adipose tissue. Ghrelin reduces insulin secretion and suppresses the production of adiponectin. Ghrelin plasma concentrations decrease after glucose and carbohydrate intake, but a high-fat diet does not reduce ghrelin concentrations (13). It is most abundantly expressed in specialized cells of the oxyntic glands of the gastric epithelium, but it is also present in both vascular and cardiac tissues (14, 15). Ghrelin inhibits cytokine release (IL-1 β, IL-6, and TNF-α) in endothelial cells by inhibiting the activation of NF-κB (16). Vasodilatory effects of ghrelin on arteries are induced by the antagonistic action of ghrelin on the

vasoconstrictor effect of endothelin-1 (ET-1). This vasodilatory response is associated with an increase in endothelial nitric oxide synthase production. The imbalance between the vasodilating NO and vasoconstricting ET-1 is solved by synthetic ghrelin administration in humans. The arterial infusion of ghrelin (200 ng/min) in humans mitigated the vasoconstrictive effects of ET-1 and stimulated NO-dependent vasodilation by increasing NO bioavailability (16).

In obese individuals, PVAT also increases in volume and this adipocyte hypertrophy provides less vasoprotective factors and more pro-inflammatory adipokines, such as leptin and resistin, pro-inflammatory cytokines (TNF-α, IL-6, GM-CSF), angiogenic factors (vascular endothelial growth factor—VEGF) and chemokines (RANTES or CCL5, MCP-1 or CCL2). PVAT-derived TNF-α and IL-6 stimulate ROS production and liver synthesis of C-reactive protein (CRP), which reduces NO production by decreasing the expression of eNOS (17).

The increased local inflammation and hypoxia suppress the cardioprotective properties of PVAT. Obese patients with metabolic syndrome (MS) have low levels of circulating ghrelin (18) and a compromised NO bioavailability associated with increased ET-1-mediated vasoconstriction (19). This makes obese and MS patients a suitable model for investigating the impact of ghrelin on vascular dysfunction.

I.1.2.2. Characteristics of PVAT

Obesity causes the dispersal of a visceral adipose tissue affected by systemic insulin resistance, dyslipidemia, with increased levels of proinflammatory cytokines and modified secretome. PVAT seems to share its origin with vascular smooth muscle cells and not with visceral or subcutaneous adipose tissue. PVAT consists of adipocytes, stromal cells with pre-adipocytes, fibroblasts, stem cells, inflammatory cells (macrophages, lymphocytes, and eosinophils), nerves, and vascular cells (12).

In rodents, PVAT shows many similarities with brown adipose tissue due to its well-vascularized structure and adipose morphology, whereas in humans PVAT resembles visceral adipose tissue (20). Extrapolation of rodent studies to humans is frequently deceptive in the research of either adipose tissues or inflammatory responses (21). Insufficient data on the appearance of PVAT is caused by these disparities between human and animal models. The shortage of human studies on PVAT has been caused by the lack of proper tools, but the advance of imaging techniques has already begun to change that (20).

The inflammation caused by obesity changes the appearance of PVAT. As the macrophages of the adipose tissue turn from anti-inflammatory (M2) into pro-inflammatory (M1), the PVAT of obese individuals shows higher levels of M1 polarized macrophages than in lean individuals. Therefore, PVAT has smaller adipocytes and lower levels of intracellular lipid accumulation.

Obesity induces a whitening of brown adipose tissue in some vascular segments, such as thoracic periaortic adipose tissue (12, 20). Aortic coarctation models in rats show a decreased number of adipocyte progenitor cells, with lower adipocyte formation and lipid accumulation. Differences in arterial pressure modify the adipogenic potential and stress relaxation in aortic PVATs (22).

PVAT surrounding different blood vessels has a heterogeneous density and appearance, resembling endothelial cells and smooth muscle cells from different vascular beds. In human coronary arteries, PVAT has diverse-shaped and smaller adipocytes with decreased adipogenic differentiation (23). In patients with abdominal aortic aneurysm, adipocytes are larger than in healthy individuals (24).

In atherosclerosis, the amount of PVAT correlates directly with the size of atherosclerotic plaque found in the corresponding vascular wall. In coronary artery disease, enlarged PVAT as measured on CT imaging or in post-mortem human coronary artery samples has higher volume near coronary artery segments with an atherosclerotic plaque as compared with no plaque areas. Plaque composition is also relevant for the structural changes of PVAT. Plaque with a lipid core and calcification was shown to be associated with an increased PVAT mass and macrophage infiltration in PVAT (25).

I.1.2.3. The anti-inflammatory role of ghrelin in adipose tissue macrophage infiltration in atherosclerosis

PVAT surrounding arteries may be involved in building up atherosclerotic plaque from outside the artery through infiltration of macrophages and proinflammatory factors. However, the reciprocal may be also true, and atherosclerosis may be the cause of inflammation in PVAT, as an expression of the bidirectional crosstalk between PVAT and the vascular wall. Adipocytokines secreted by PVAT may diffuse into the vascular wall and draw macrophages.

The PVAT on the atherosclerotic segments of the aorta has more macrophages as compared to atherosclerosis-free arteries in the same patient. In the epicardial adipose tissue of patients with coronary atherosclerosis, the number of proinflammatory M1 macrophages is more pronounced than in controls. The inflammation of PVATs is correlated with adventitial inflammation and atherosclerosis (25). In coronary artery disease (CAD), secretion of adipocytokines is higher in PVAT near non-stenotic than near stenotic coronary artery segments in patients undergoing coronary artery bypass graft surgery. PVAT macrophages are associated with atherosclerosis in the adjacent artery, but the anti-inflammatory M2 macrophages are more abundant, which suggests desensitization of the inflammatory response in PVAT in advanced CAD (26).

In perivascular adipocytes, the secretion of the MCP-1/CCL2 protein, with an important role in the pathogenesis of atherosclerosis, is up to 40-fold higher than in perirenal and subcutaneous adipocytes. Again, anti-inflammatory factors, such as adrenomedullin, are also synthesized by PVAT, suggesting a simultaneous protective role for the PVAT on the adjacent vessels (23). This balance between protective and detrimental effects exerted by PVAT on atherosclerosis could be disturbed by gut-derived antigens such as lipopolysaccharides, dietary lipids, hypoxia, or mechanical stress, which have a direct impact on inflammation and the accumulation of proinflammatory macrophages in adipose tissues.

In vivo animal models have shown that in obesity proinflammatory signaling in perivascular mesenchymal cells has a key role in chronic inflammation of white adipose tissues. TLR4 signaling in perivascular stromal cells mediates proinflammatory macrophage accumulation. Fibro-inflammatory progenitors, a specialized subpopulation of perivascular cells activated during metabolic inflammation, modulate macrophage homeostasis (27).

Ghrelin acts directly on adipocytes to stimulate adipogenesis through preadipocyte differentiation and antagonism of isoproterenol-induced lipolysis. The expression of ghrelin receptors in adipocytes is upregulated during preadipocyte differentiation (28). Ghrelin stimulates angiogenesis in the adipose tissue by inhibiting bone morphogenic protein-4 (BMP-4), which regulates adipogenic cell precursors differentiation, bone morphogenic protein-7 (BMP-7), involved in the formation of brown adipose tissue, and VEGF (29).

Ghrelin inhibits sympathetic efferents to brown adipose tissue and impairs the intracellular breakdown of triglycerides into free fatty acids (30), leading to weight gain. Although ghrelin acts as a neurotransmitter that modulates sympathetic activity to white and

brown adipose tissue, its role on lipid synthesis and mobilization and adipokine release in PVAT requires further investigation.

Lipid storage promotes vascular inflammation. However, high ghrelin levels improve outcomes in early atherosclerosis (31, 32). This anti-atherosclerotic effect is attributed to a balance between macrophage cholesterol uptake and efflux regulated by ghrelin and its GHS-R1a receptor. Ghrelin stimulates the expression of the adipogenic transcription factor peroxisome proliferator-activated receptor gamma (PPARγ) from adipocytes, which is associated with enhanced cholesterol efflux by macrophages and lower risk of atherosclerotic lesions (33).

Ghrelin protects against atherosclerosis by inhibiting the GRP78/CHOP/caspase-12 signaling pathway which involves endoplasmic reticulum stress-related proteins (34, 35). Gut microbiome products, such as trimethylamine-N-oxide are involved in atherogenesis. Ghrelin shows inverse correlations with trimethylamine N-oxide (36). The atherosclerotic process may be accelerated by endothelial cell apoptosis which causes deposition of lipids and fibrous elements on the arterial wall (37). The inhibition of hyperglycemia-induced apoptosis in endothelial cells and vascular smooth muscle cells (VSMC) is mediated by GHS-R1a receptors. Ghrelin directly inhibits VSMC apoptosis and proliferation by activation of the cAMP/PKA pathway (38). The stimulation of intracellular signaling pathways that inhibit apoptosis is achieved by phosphorylation and activation of ERK1/2 and PI3K/Akt (39-42). The inhibition of plaque angiogenesis caused by oxidized low-density lipoprotein is also mediated by GHS-R1a receptors. FGF-2, a modulator of angiogenesis that mediates atherosclerotic neovascularization, is inhibited by ghrelin in vitro and in vivo. Ghrelin inhibits hypoxia-induced changes in myocardial and pulmonary angiogenesis by decreasing protein HIF-1a and VEGF, a pro-angiogenic and antiapoptotic growth factor, in the cardiac and lung tissues (43, 44) [34,35]. Ghrelin helps improve endothelial function and inhibits endothelial injury by increasing NO bioactivity through the activation of endothelial nitric oxide synthase (eNOS) (18).

Obesity causes the dispersal of a visceral adipose tissue affected by systemic insulin resistance, dyslipidemia, with increased levels of proinflammatory cytokines and modified secretome. PVAT seems to share its origin with vascular smooth muscle cells and not with visceral or subcutaneous adipose tissue. PVAT consists of adipocytes whose appearance differs between healthy and diseased blood vessels, the latter being enlarged (18).

I.1.2.4. The role of ghrelin in inhibiting proinflammatory adipokine secretion

Ghrelin, the appetite-inducing hormone counteracts the effects of leptin, an adipokine regulating satiety. Ghrelin and leptin receptors are co-expressed in more than 90% of the neurons modulating their activity (45). Ghrelin levels decrease under prolonged exposure to leptin, as is the case in obese individuals, except for obesity in Prader–Willi syndrome, with high ghrelin levels.

Leptin induces ghrelin resistance. Ghrelin gene expression is reduced when leptin and IL-1 β are administered (46). Leptin suppresses ghrelin secretion by gastric cells and the expression of ghrelin receptors in the neuropeptide Y system (NPY) involved in the sympathetic nervous system-induced adipose tissue growth and vasoconstriction (47). However, ghrelin inhibits the leptin-induced release of pro-inflammatory cytokines by increasing prostacyclin production from endothelial cells (48).

Pro-inflammatory cytokines IL-1 β, IL-6, and TNF-α were shown to suppress appetite, especially in anxiety and stress (49), which may suggest an inhibiting effect on ghrelin. The anti-inflammatory effect of ghrelin on adipose tissue is achieved by inhibiting the TNF-α induced activation of caspases and apoptosis. Ghrelin limits the expression of autophagy-

related genes (50). An anti-inflammatory role of ghrelin in atherosclerosis is suggested by an increase in lipid infiltration, the expression of CD4 + T cells, MAC-3 macrophage antigens, and VCAM-1 and ICAM-1 adhesion molecules in aortic arches of ghrelin receptor knockout mice (41). The effects of ghrelin are summarized in Table I.1.

Table I.1. Actions of ghrelin related to adipose tissues, endothelium, and atherosclerosis

Determining Factors	Action	References
Adipose tissue	Increases the production of adiponectin, decreases the production of leptin and resistin.	Choi et al., 2003 (28) Yasuda et al., 2003 (30) Lelis et al., 2019 (29)
	Stimulates adipogenesis by reducing fat oxidation, increases food intake, and stimulates preadipocyte differentiation	
Adipose tissue inflammatory cells	Inhibits leptin-induced cytokine expression.	Dixit et al., 2004 (46) Perpetuo et al., 2021 (47)
Endothelium	Promotes endothelial cell proliferation, inhibits endothelial cell apoptosis and increases the expression of eNOS in arterial endothelial cells.	Tesauro et al., 2005 (18) Mengozzi et al., 2020 (17)
Atherosclerosis	Inhibits overproduction of inflammatory cytokines (IL-1, IL-6, IL-8, and TNF-α), suppresses MCP-1 and the NF-κB pathway and decreases the expression of Cox-2 in endothelial cells.	Bedendi et al., 2003 (48) Shu et al., 2013 (51) Ai et al., 2017 (34) Yang et al., 2020 (35) Virdis et al., 2016 (52)

Table legend: eNOS- Endothelial nitric oxide synthase; IL- Interleukin; TNF-α- Tumor necrosis factor-alpha; MCP-1- Monocyte chemoattractant protein-1; Cox-2- Cyclooxygenase-2.

I.1.2.5. Leukocyte–endothelial eell–platelet interaction

In the leukocyte-platelet aggregates which characterize atherosclerosis, platelets recruit and activate leukocytes. For their part, leukocytes act on the hemostatic system by activating platelets through immuno-thrombosis, contributing to either pro-inflammatory (cytokine and chemokine release, reactive oxygen production, and lymphocyte development) or anti-inflammatory effects (inhibited monocyte recruitment and cytokine or chemokine production via platelet receptor glycoprotein Ibα and sCD40L).

Platelets are involved in plaque rupture and atherothrombosis in an attempt to preserve blood vessel integrity. By recruiting immune cells, platelets accelerate the atherosclerotic process (53, 54). Moreover, the interactions with the vascular wall are also suspected to impair leukocyte recruitment by platelets, as platelets may interact directly with endothelial cells in atherosclerosis, under the influence of cytokines (55).

In healthy non-obese individuals, ghrelin was shown to exert no effects on either platelets or endothelial cells (56). Later studies have shown that ghrelin can inhibit platelet aggregation. Its antithrombotic effects were shown by the protective effects of ghrelin pre-treatment on liver coagulation disturbances in rats and by ghrelin involvement in the inhibition of MCP-1 expression, with indirect decreasing effects on platelet aggregation and adhesion (51, 57).

In excessive adipose tissue, chronic inflammation leads to increased platelet volume. Platelets become highly activated and aggregated. In obese adipose tissues of mice, the

interactions between leukocytes and endothelial cells are higher than in lean mice and the platelets are hyperactivated (58).

I.1.2.6. Inflammation and oxidative stress in PVAT. The role of ghrelin in vasoreactivity

PVAT influences vasodilation and vasocontraction and regulates vascular tone and diameter. PVAT-derived ROS can directly inhibit smooth muscle cell contractions by activating the receptor of NO, soluble guanylyl cyclase. Hydrogen peroxide release is another mechanism of PVAT-induced anticontractile vascular effects (59).

Healthy perivascular adipocytes inhibit vasoconstriction by activating the potassium channels in smooth muscle cells through the adipocyte-derived relaxing factor (ADRF). However, the vasodilatory effect of PVAT is mostly present in an association of intact endothelium with intact PVAT (23). In non-obese type 2 diabetes animal models, no relaxing properties of PVAT from rat aortas were found (60).

Ghrelin, a modulator of gastric motility, has kinetic properties which also impact the vascular tone. PVAT modifies the local production of angiotensinogen, which regulates blood pressure (61). Ghrelin inhibits angiotensin II-induced proliferation and contraction of human aortic smooth muscle cells (62). Ghrelin inhibits the vasoconstrictor angiotensin-II by increasing the intracellular concentration of cAMP and increasing the bioavailability of NO, which has vasodilatory properties. The decrease in blood pressure may be also mediated by the brain, where ghrelin suppresses sympathetic activity (47).

The vasodilatory effects of ghrelin (63) are confirmed by the finding that low ghrelin levels are associated with increased blood pressure (64). Ghrelin was found to suppress oxidative stress in hypertensive rats (65). High levels of ghrelin were associated with hypertension only in obese women (47). Ghrelin inhibits a major source of intravascular ROS formation, the isoform cyclooxygenase-2 (COX-2) found in hypertensive patients (52).

Ghrelin secretion declines with age (66), and aging is a major risk factor for atherosclerosis. The decreased levels of ghrelin are aggravated by MS, as obese and diabetic individuals are known to have low levels of ghrelin (67, 68).

The increase in adipose tissue mass has major implications on the characteristics of PVAT, with detrimental effects on vascular health. Due to its cardiovascular protective effects, ghrelin could compensate for these vascular dysfunctions.

However, various ghrelin polymorphisms, such as Leu72Met, indicate an increased risk of coronary artery disease (42). Moreover, despite its orexigenic effect, circulating ghrelin levels decline in obesity, diabetes, and MS, but this decrease applies to des-acyl ghrelin concentrations, the most abundant form of ghrelin, whereas acylated ghrelin remains unchanged or increases (50).

I.1.2.7. Conclusions

The present study collated the protective and detrimental effects of PVAT and ghrelin in inflammation and atherosclerosis and showed that ghrelin could also have an important role in vascular fat accumulation and pathophysiology.

Extensive research has been conducted on the role of ghrelin in vascular and adipose tissues.

The effect of ghrelin on PVAT remains poorly understood and should be further investigated.

The two isoforms of circulating ghrelin, acylated and des-acylated ghrelin should be analyzed independently, due to their distinct role in atherosclerosis protection and adipose tissue remodeling.

I.1.3. Osteopontin and osteoprotegerin in atherosclerotic plaque – are they significant markers of plaque vulnerability?

I.1.3.1. Introduction

More than 100 years after the first accepted definition (69), atherosclerosis (ATS) is still considered as a major, global health problem (70). The outlining usually used for this chronic condition includes the following characteristics: it is a prominent cause of vascular disease, the main clinical manifestations are ischemic heart disease, stroke and peripheral arterial disease, and the key pathological feature is the thickening of the arterial wall (69). The concept of atherosclerotic burden was introduced and agreed due to the impact of the disease on the general population, based on its predictive power for critical cardiovascular outcomes, followed by threatening complications and an increase rate of mortality (70, 71).

The deeper understanding of ATS pathology represents an important target in medical research. Remarkable results have been accumulated over time, leading to the identification and grouping of microscopic lesions in classifications whose relevance has been supported by clinicopathological correlations.

ATS has a progressive course affecting the large elastic and medium muscular arteries (72). The pathognomonic lesion is the atherosclerotic plaque, which develops either by thickening resulting in stenosis or fissure of vessels, generating a thrombotic material involved in the occurrence of ischemic events (72).

Thus, the assessment of the atherosclerotic lesion type allows not only a staging but also an insight into the dynamics of the pathogenic process. Therefore, the most reliable classification of atherosclerotic lesions, developed by the American Heart Association (AHA), sets the type of lesion by microscopic examination of certain elements, closely related to the developmental stages of this process (72, 73).

There is a paradigm shift in understanding the ATS pathology in the last years, by translation from tissue visible events to molecular mechanisms (5, 74-79). Classical data were supplemented by the involvement of the endothelial, muscular, and inflammatory cell, through specific signaling pathways and molecular crosstalk (5, 74-79).

Within this context, osteopontin (OPN) and osteoprotegerin (OPG) are two molecules that have been associated with the initiation and progression of ATS lesions, being linked to plaque vulnerability by modulating vascular calcification (80-82).

OPN is an extracellular matrix (ECM) protein that functions as a proinflammatory cytokine (83), beside binding potential of hydroxyapatite crystals to osteoblasts which has been originally described (84). It is also involved in most systemic inflammatory processes and tissue remodeling (83). The involvement of OPN in the pathogenic mechanism of ATS is supported by fibroblasts and macrophage's ability to synthesize OPN (83, 85). Clinical evidence has confirmed a correlation between plasma OPN levels and coronary and aortic ATS, with a noticeable increased value in large vessel lesions (86).

OPG, a protein in the tumor necrosis factor receptor (TNFR) family, acts on bone tissue as an inhibitor of bone resorption and inhibits the immune response (87). At cardiovascular level, OPG synthesized by macrophage and expressed by endothelial and smooth muscle cells has a protective role in the development of ATS (88). OPG is one of the

major components of endothelium-specific intracytoplasmic corpuscles, called Weibel–Palade bodies (89, 90).

In endothelial activation by tumor necrosis factor alpha (TNF-α) and interleukin-1β (IL-1β), the corpuscles are secreted into the extracellular environment, thus protecting the endothelium from the apoptotic process triggered by the TNF-related apoptosis-inducing ligand (TRAIL) pathway (89, 90). Moreover, OPG binds thrombospondin-1 (TSP-1), thus intervening in the regulation of vascular damage and thrombus formation (87). OPG expressed by smooth muscle cells of medial layer is preventing the calcification of the ECM, but not the resorption of the already deposited calcium (88, 91).

Concurrently with the pathogenic mechanism of ATS, the researchers' interest is also directed on its clinical and therapeutic management. A critical problem is the fact that the disease can remain asymptomatic for many years, complications often being the first clinical manifestation.

The progress made in the development of non-invasive cardiovascular techniques, folded up by the increase of patients' accessibility to these techniques has improved the prognosis for ATS, allowing a more accurate evaluation of early stages of the disease. Ultrasonography (US) represents the first line approach for diagnosis. US performances allow not only the identification of the lesion, but also determine the degree of stenosis (92, 93) and the associated risk. It is already known that the echolucent plaques are vulnerable and with a higher probability to determine transitional ischemic strokes.

Thus, imaging diagnosis can prevent dramatic ischemic lesions, by prioritizing those cases that require endarterectomy. Early diagnosis and therapy of atherosclerotic carotid artery disease have significantly reduced the risk of complications, mainly the stroke risk – the results being confirmed by two clinical trials targeting this issue (94, 95).

However, there are still limits related to the accuracy of imaging diagnosis. That is why researchers are testing additional markers that can enhance the quality of the diagnosis. Gray scale median (GSM) is an US marker for atherosclerotic plaque aspect (96, 97), but its value is still disputed in the literature.

Within this context of knowledge, the present research is based on the experience of the Department of Vascular Surgery, Sf. Spiridon Emergency County Hospital, Iaşi, Romania, in the diagnosis and surgical treatment of ATS lesions and completes our previous published reports on this subject (98, 99).

I.1.3.2. Aim

Specifically, our study aims to assess the OPN and OPG expression in advanced stages of carotid ATS, to analyze the correlation between these markers and the ultrasonographic plaque properties, pointing out the identification of possible patterns that can predict plaque vulnerability and risks of restenosis, after carotid endarterectomy (CEA).

I.1.3.3. Materials and methods

The study group comprised 49 consecutive patients (38 males and 11 females, average age 66±6.16 years old) diagnosed with carotid stenotic lesions and treated in the Department of Vascular Surgery, Sf. Spiridon Emergency County Hospital, Iaşi, from January 2015 to April 2018.

The selection of the patients was based on well-established inclusion criteria (namely 70–99% stenosis of internal carotid arteries without symptoms, 50–99% stenosis of internal carotid arteries associated with recent transitory ischemic attack or stroke). The exclusion

criteria included the presence of chronic autoimmune, endocrine, hepatic, renal or cardiac conditions, and neoplasms.

The study received the ethical approval of "Grigore T. Popa" University of Medicine and Pharmacy, Iaşi. Epidemiological, clinical characteristics, and preoperatory treatment for the patients in our group are summarized in Table I.2.

Table I.2. Epidemiology, clinical characteristics, and pre-operatory treatment

Characteristics	No. of cases	Percentage
Gender		
- Male	38	77.5%
- Female	11	22.5%
History of neurological symptoms		
- TIA	19	38.7%
- Stroke	18	36.7%
- Amaurosis fugax	3	6.1%
- Absent	9	18.4%
Risk factors		
- Hypertension	37	75.5%
- Dyslipidemia	20	40.8%
- Diabetes mellitus	15	30.6%
- Active smokers	10	20.4%
- Peripheral arterial disease	15	30.6%
Treatment		
- ASA/platelet aggregation inhibitors before admission	40	81.6%
- HMG-CoA reductase inhibitors before admission	48	97.9%

Table legend: ASA: Acetylsalicylic acid; HMG-CoA: β-Hydroxy-β-methylglutaryl coenzyme A; TIA: Transient ischemic attack.

The diagnosis was established using US, B-mode and Doppler [Siemens US equipment (X700)]. The examination of the common and internal carotid arteries was performed in supine position, the neck being rotated at 45º in the opposite direction. The degree of stenosis was measured and reported according to North American Symptomatic Carotid Endarterectomy Trial (NASCET) method (94).

The plaques were described and classified according to the Gray–Weale classes in two main categories: vulnerable and stable (100). Vulnerable plaques included anechogenic plaques with fibrous cap (type 1) or plaques with less than 25% of echogenic areas (type 2), whereas stable plaques category included the hyperechogenic ones, with reduced anechogenic zones (less than 25% – type 3) or with homogenous hyperechogenicity (type 4). After that, type 1 and type 2 plaques were grouped in echolucent plaques, whereas type 3 and 4 – in echogenic plaques.

All collected ultrasonographic images were analyzed by applying the GSM (97). The calculation of GSM (for each plaque) required an image-analysis technique performed by using Adobe Photoshop application and the following steps: image normalization, that ensures the decrease of the gain-induced variability characteristic for the image echogenicity; image segmentation, considering two values of reference: 0 for black (corresponding to the blood) and 255 for white (corresponding to the adventitia); selection of the plaque area with subsequent acquisition of the corresponding histogram.

The CEA specimens were standardly processed for histopathological (HP) and immunohistochemical (IHC) exams at the Laboratory of Histology. Serial sections were cut using a microtome, stained with Hematoxylin–Eosin and trichrome, and also prepared for IHC technique.

The microscopic exam in standard and special stainings allowed the classification of the atherosclerotic lesions using the criteria of AHA classification. For each plaque, several parameters for plaque vulnerability were noted, specifically: calcification, hemorrhage, ulceration, inflammation, and necrosis.

IHC technique was performed using two specific primary antibodies anti-OPN (rabbit polyclonal antibody, code: ab231484, 1:100 dilution) and anti-OPG (rabbit polyclonal antibody, code: ab183910, 1:1000 dilution). Tissue section were dewaxed in two baths of xylol and rehydration was done by immersion of slides in ethanol. To unmask the antigenic situs by heat-induced epitope retrieval, the slides were immersed in citrate buffer pH 6 and placed in a water bath at 97ºC, for 20 minutes. The reaction was developed with a specific Horseradish peroxidase (HRP)/3.3'Diaminobenzidine (DAB) detection kit using HRP-labeled Streptavidin, a biotinylated secondary antibody and DAB

The expression of the two biomarkers was quantified taking into consideration the intensity of the immunolabeling (low and high, respectively) and the extension of the immunopositive area inside the plaque. Therefore, negative lesions and those with low immunopositivity in less than 50% of the plaque area were classified as low OPN/OPG expression, and the lesions with high OPN/OPG expression were considered when the immunostaining was noted in more than 50% of the interest area defined in the plaques. The assessment was performed by three trained histopathologists. The final results were decided in consensus, in order to avoid the degree of subjectivity in the semi-quantitative assessment.

For statistical analysis, we used the Statistical Package for the Social Sciences (SPSS) program (version 19.0). Nominal variables were analyzed using the χ 2 (chi-squared) test and we considered a priori a p-value <0.05 as significant.

I.1.3.4. Results

The results of ultrasonographic examination revealed 33 patients who presented a degree of stenosis between 70–99%, 14 patients with stenosis between 60–69%, and two patients with stenosis between 50–59%.

All identified internal or common carotid lesions were classified as follows: 21 plaques as echolucent, and 28 plaques as echogenic. We noticed that most of the echolucent plaques were type 1 (16 cases), anechogenic with echogenic fibrous cap, whereas the echogenic plaques were predominantly type 3 (26 cases), characterized by hyperechogenicity mixed with less than 25% anechogenic zones.

By using the GSM score and a threshold of 37 based on the GSM value for quartile 25, 13 plaques were considered vulnerable (GSM <37), and 36 plaques were stable (GSM >37).

The microscopic exam showed 35 plaques with specific features for AHA type V (morphologically stable plaques) and 14 plaques with particular morphological changes for AHA type VI (morphologically unstable plaques).

The qualitative assessment of OPN and OPG in atherosclerotic plaques showed a fine granular expression pattern, with heterogeneous distribution and variable intensity (low, moderate, or high).

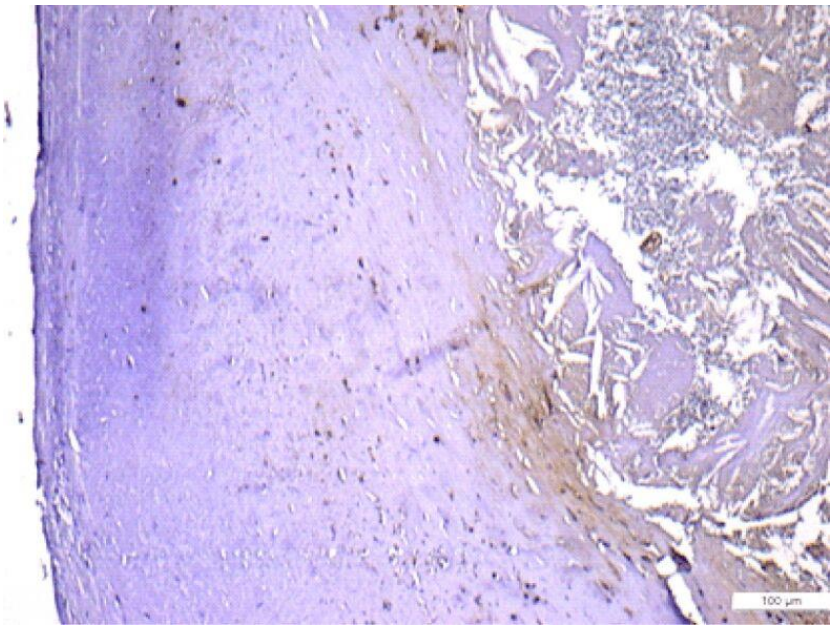

Figure I.1. Low OPN expression in the periphery of the lipid core (IHC staining with anti-OPN antibody, ×100). IHC: Immunohistochemical; OPN: Osteopontin

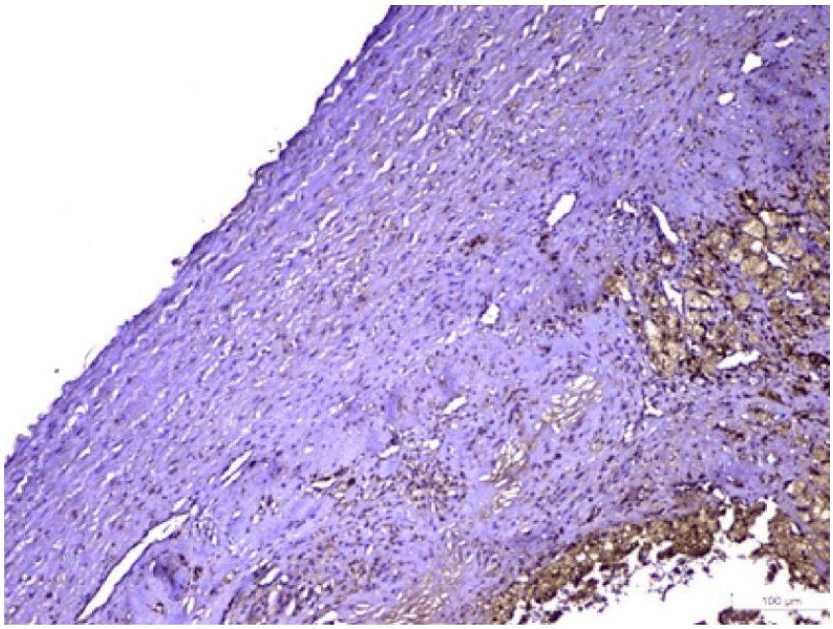

Figure I.2. Strong OPN expression in the periphery of the calcification area, in foamy macrophages, fibroblasts, and inflammatory cells of the plaque (IHC staining with anti-OPN antibody, ×100). IHC: Immunohistochemical; OPN: Osteopontin

OPN expression, with low or moderate intensity, was identified in the lipid core and in the areas adjacent to dystrophic calcifications in more than 50% of cases (Figure I.1).

High intensity expression of OPN was observed in the lipid core and very rarely in the ECM, only in plaques with moderate or well represented inflammatory infiltrate (Figure I.2).

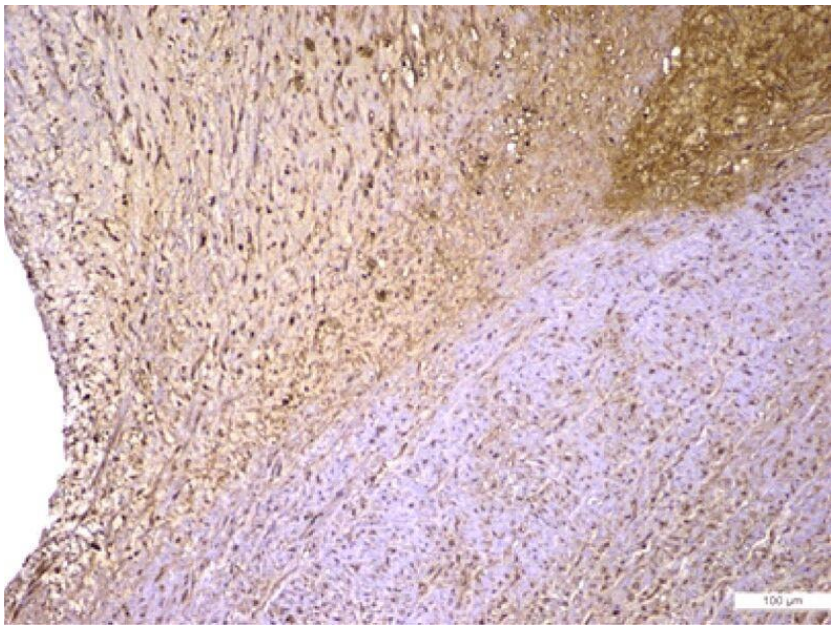

Figure I.3. Strong OPG expression in the fibro-lipid plaque (lipid core, smooth muscle cells, fibroblasts, extracellular matrix); smooth muscle cells OPG positive in the media (IHC staining with anti-OPG antibody, ×100). IHC: Immunohistochemical; OPG: Osteoprotegerin

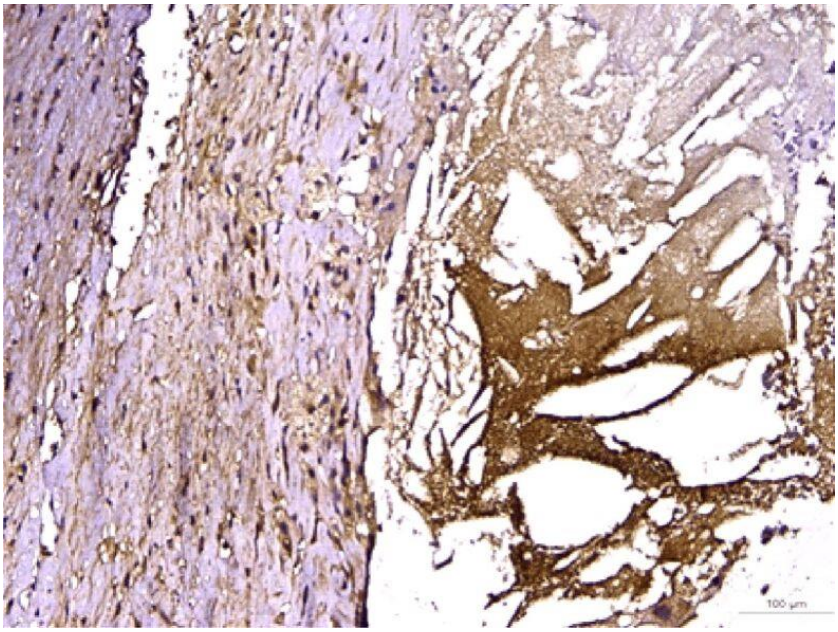

Figure I.4. Strong OPG expression in the lipid core, adjacent to cholesterol crystals, in the extracellular matrix and intracellular matrix resident cells (fibroblasts) or migrated cells (inflammatory elements) (IHC staining with anti-OPG antibody, ×100). IHC: Immunohistochemical; OPG: Osteoprotegerin

Cells expressing OPN were macrophages, myofibroblasts, and focal smooth muscle cells, but the intensity of expression was low. OPG high intensity expression was constantly identified in the intimal layers as fine granular areas within dystrophic calcification and around them, as well as in atheromatous core (Figures I.3 and I.4).

OPG was also identified in the ECM of plaques, occupying large areas (corresponding to increased synthesis), especially in plaques with associated inflammation or numerous smooth muscle cells. Areas containing foamy macrophages and smooth muscle cells in the

media were strongly positive for OPG. OPG was also focally observed in smooth muscle cells migrated to the fibrous cap. OPG decreased cellular expression was associated with increased expression of OPG in the ECM.

The semi-quantitative assessment based on the applied scoring system, revealed low OPN expression in 35 plaques and high expression in the other 14 plaques specimens. On the other hand, OPG was low in 16 plaques and high in 33 plaque specimens.

A significant statistical correlation was noticed between histological AHA type and ultrasonographic classification (echogenic versus echolucent) ($p<0.001$).

Ultrasonographic classification was correlated with hemorrhage ($p=0.013$), ulceration ($p=0.001$), inflammation ($p=0.004$), and necrosis ($p=0.025$), but no significant correlation was registered for the plaque calcification ($p=0.219$). There were no statistically significant differences between low versus high expression of intra-plaque OPN and OPG ($p=0.335$).

Statistical analysis showed significant correlation between OPN and plaque echogenicity ($p=0.011$), but not for OPG ($p=0.079$). Moreover, no statistical significance could be identified between OPG or OPN and GSM, neither as individual value nor as threshold.

Table I.3. OPN and OPG expression in correlation to morphological parameters

Morphological parameters	**OPN expression**	**p-value**	**χ2 test**	**OPG expression**	**p-value**	**χ2 test**
	Low	High		Low	High	
Calcification - Negative	6 (60%)	4 (40%)	0.370	2 (20%)	8 (80%)	0.339
Calcification - Positive	29 (74.4%)	10 (25.6%)		14 (35.9%)	25 (64.1%)	
Hemorrhage - Negative	31 (73.8%)	11 (26.2%)	0.366	15 (35.7%)	27 (64.3%)	0.263
Hemorrhage - Positive	4 (57.1%)	3 (42.9%)		1 (14.3%)	6 (85.7%)	
Ulceration - Negative	30 (81.1%)	7 (18.9%)	0.009	14 (37.8%)	23 (62.2%)	0.174
Ulceration - Positive	5 (41.7%)	7 (58.3%)		2 (16.7%)	10 (83.3%)	
Inflammation - Negative	29 (90.6%)	3 (9.4%)	<0.001	11 (34.4%)	21 (65.6%)	0.724
Inflammation - Positive	6 (35.3%)	11 (64.7%)		5 (29.4%)	12 (70.6%)	
Necrosis - Negative	27 (75%)	9 (25%)	0.357	13 (36.1%)	23 (63.9%)	0.390
Necrosis - Positive	8 (61.5%)	5 (38.5%)		3 (23.1%)	10 (76.9%)	
Morphologically stable plaques	28 (80%)	7 (20%)	0.036	13 (37.1%)	22 (62.9%)	0.289
Morphologically unstable plaques	7 (50%)	7 (50%)		3 (21.4%)	11 (78.6%)	

Table legend: OPG: Osteoprotegerin; OPN: Osteopontin.

Statistically significant differences were registered between OPN expression (low versus high) and plaque type (stable versus unstable) ($p=0.036$), and also for plaque ulceration ($p=0.009$) and inflammation ($p<0.001$). OPG expression (low versus high) did not reveal statistically significant differences with plaque type (stable versus unstable) and vulnerability plaque parameters, respectively (Table I.3).

I.1.3.5. Discussions

Currently, plaques removed by CEA which are not analyzed by standard histology are wasted. Several studies have emphasized that the histological analysis of the plaque specimens harvested during a CEA may provide insights in the atherosclerotic process of the entire vascular system (100-102). It is worth mentioning that the accurate diagnosis for ATS lesions is based on the histological exam, in accordance with AHA classification. Thus, the unstable plaques, susceptible to rupture have a central necrosis mass, rich inflammatory infiltrate, and a thin fibrous cap. On the other hand, the stable plaques show a small lipid core, few inflammatory cells, and a thick fibrous cap.

The histological characterization of the CEA specimens can be compared with imaging features of the plaques, leading to a more precise diagnosis for stable versus vulnerable plaques. These features have major implications in the prediction of the atherosclerotic process evolution, including the possible risk of a cerebral thromboembolism resulting in stroke, transient ischemic attacks or amaurosis fugax (103, 104).

We must highlight that in our study most carotid atherosclerotic plaques have been obtained from asymptomatic patients (either with no symptomatology at all or with cerebral ischemic events older than six months) and were echogenic, stabile plaques, with surgical indications for CEA due to stenosis severity.

The review of the literature reveals constant effort aiming to provide uniformity in reports on atherosclerotic plaque imaging, either US, computed tomography (CT) or magnetic resonance imaging (MRI) versus histology.

One of the first relevant paper on this topic, published in the 80's, reported that the echolucent plaques frequently present intraplaque hemorrhage in comparison with the echogenic ones (100). Another classification is based on the degree of plaque echogenicity, proposing three distinct types: hypoechogenic plaque, often associated with serious retinal phenomena, hyperechogenic plaque, correlated with an asymptomatic status, and intermediate echoic plaque, responsible for the occurrence of cerebrovascular symptoms (105). The presence of hemorrhage area represents a characteristic of hypoechogenic plaques, whereas necrosis and calcification do not have an echomorphologic predilection (105). This makes it difficult to distinguish by ultrasound techniques between calcified plaques and those with necrosis, thus limiting the diagnostic accuracy of this investigation and suggesting the need for additional histological analysis (105).

The comparative histological-imaging approach could provide a new perspective in establishing the type of atherosclerotic lesions by promoting a non-invasive investigation. Relevant data are provided by a review that analyzed 73 studies that compared carotid plaque imaging with carotid plaque histology (101). Unfortunately, this review revealed a large variety of histological and/or imaging techniques, including performance of the equipment and the examiner subjectivity, without a common methodology and measurement parameters. Therefore, the paper cannot offer an integrated, histological-imaging overview regarding the atheromatous process (101).

Histological assessment had been variable according to the processing method, type of section (cross-section in 66% and longitudinally in 4% of studies, respectively), thickness of the sample, staining, and not least the number of sections (101). From the total number of studies, the correlations between histology and imaging addressed the size of lipid core by reference to the fibrous layer in 77%, calcification in 66%, intra-plaque hemorrhage in 56%, surface-thrombus in 37%, rupture in 21%, inflammation in 12%, cap thickness in 10%, and plaque neovascularization in 4% (101).

The evaluation was predominantly qualitative and only 20 studies used computer-assisted image analysis in addition to classical histological exam to determine the percentage

of each element in the structure of plaque (101). On the other hand, even if the same imaging methods were used, with similar criteria ensuring the reproducibility of the study (i.e., Gray–Weale scale of ultrasonographic echogenicity), the results were extremely variable (101).

All these deficiencies led to the necessity to develop new reporting criteria that show atheromatous plaque characteristics from both histological and imaging point of view, in order to provide a diagnosis as accurate as possible (101). The correlation between the histological analysis and the imaging technique (US, CT or MRI) facilitates the atheromatous process staging and enables the development of appropriate therapeutic strategy in relation to the particularities of each reported investigation.

Relying on the classification of atherosclerotic plaques in echogenic or echolucent, our study identifies a strong correlation with histological examination and AHA plaque type, providing information about carotid plaque vulnerability by identifying hemorrhage ($p=0.013$), ulceration ($p=0.001$), inflammation ($p=0.004$) or necrosis ($p=0.025$) in echolucent plaques.

Although other studies showed significant correlation between high echogenicity and calcified plaques (106, 107)**,** our study did not confirm this association. Our results indicate that the echogenic plaques are predominantly calcified and also some of the echolucent, vulnerable plaques show a variable degree of calcification.

Thus, imaging diagnosis does not equal the specific ability of histopathology to refine lesions type and there is no perfect matching between US and the histological approach. US offer a two-dimensional image, with low potential to cover the entire plaque volume and it is dependent on the potential to overcome shadowing artefacts caused by calcified plaques (108). Unfortunately, US is characterized by low levels of reproducibility (109, 110) and GSM values have a very low level of correlation with HP examination results (111).

The optimization of the imaging techniques is an important step to promote non-invasive methods for diagnosis, but it cannot be done in the absence of histological contributions. Early diagnosis of atherosclerotic lesions and their predicable evolution are common goals of clinical and histological examinations. Any success in this approach provides new perspectives for a deeper understanding of ATS, a disease with significant incidence and impact in general population.

Classically, the etiopathogenesis of ATS involves metabolic, mechanical, infectious, or inflammatory lesions (72, 78). Nowadays, current trends in ATS research trigger the molecular pathogenesis that determines the onset and progression of disease. From the description of specific histological changes, the level of knowledge has deepened into specific mechanisms and pathways based on the synergistic action of products synthesized by vascular wall cells and circulating factors (112). Despite the progress made in deciphering the molecular interferences that lead to vascular damage and structural remodeling, there are still a multitude of unknown elements.

The extensive panel of molecular markers involved in the pathogenic mechanism of ATS includes OPN and OPG, considered as calcification markers. These bonematrix proteins seem to have an important role in mineral deposition and osteoclastogenesis inhibition and are expressed by most vascular cells (113, 114).

OPN is synthesized mainly by macrophages stimulated by numerous cytokines [i.e., angiotensin II, TNF-α, interferon-gamma (IFN-γ), and transforming growth factor beta (TGF-β), and various interleukins – IL-1, IL-2, IL-3], lipopolysaccharides and nitric oxide (115). Although OPN upregulation is still unknown, it seems that peroxisome proliferator-activated receptor gamma (PPARγ) has the main role, as an inhibitor of its gene expression. OPN acts by direct interaction with several types of membrane receptors belonging to integrin family and with cluster of differentiation 44R (CD44R) (116).

Once synthesized, OPN is responsible for several actions: it promotes adhesion, migration, and monocyte differentiation, stimulates matrix metalloproteinase (MMP)-2 and MMP-9 expression, stimulates phenotypic T1-lymphocytes differentiation, and inhibits T2-lymphocytes differentiation.

Given that MMPs are involved in degradation of the ECM, this effect is synergistic with the pro-migratory monocyte action (117). Thus, OPN has a crucial role in the recruitment of macrophages which, in turn, stimulate cytokine secretion and, consequently, cellular immunity is activated**.**

As a chemoattractant for inflammatory cells, OPN has an important role in healing and in vascular remodeling, and, supplementary, it has an inhibitory effect on calcification. Consequently, OPN could be responsible for the evolution of unstable plaques (118, 119).

A close relationship between plasma OPN levels and ATS has been demonstrated (86). In vulnerable plaques, increased OPN expression is associated with the association of inflammation and calcifications (120).

The major role of OPG is associated with bone turnover (87). The study of OPG expression in normal and pathological status is also demonstrating other functions, such as: promoter of cell survival, stimulator of tumor cells apoptosis and inhibitor of the immune response. The process of vascular calcification during ATS lesions progression has many similitudes with bone formation, without being identical phenomena (87, 91).

The role of OPG in the induction of osteogenesis analyzed by several experimental and clinical studies reveal contradictory data. Some reports indicate that the presence of OPG inhibits the mineralization process, thus having a potential role in preventing calcification in atheroma plaques (91). According to these data, the fibrous cap plaques are dominant in carotids (73%) and express more OPG, while calcified plaques are more common in femorals (93%) and show a lower OPG expression (121).

Increased OPG expression in carotid plaques is correlated with an increased number of macrophages (89). On the other hand, other reports show an increase in morbidity and mortality by cardiovascular disease associated with elevated serum OPG levels, as well as an increased OPG expression in unstable plaques (122-124). Thus, although OPG is unanimously accepted as a marker of ATS and of intraplaque stabilization, it is not clearly established whether it is a pathogenic factor or appears because of endothelial activation (122, 124, 125).

Our semi-quantitative analysis of OPN and OPG in atherosclerotic plaque, defining the expression as low and high, showed that in most cases (31 plaques) OPG and OPN had opposite expressions. However, OPG and OPN expression was similar in 18 cases (eight cases high and 10 cases low expression, respectively). These data support that OPG and OPN are co-expressed in carotid atherosclerotic plaques, as markers of inflammation and calcification processes.

From a clinical and histopathological point of view, the presence of calcification in the carotid plaque determines its stability and decreases the risk of rupture and the presence of symptomatology.

Our data support the dual role of the OPN. OPN was poorly expressed in 29 calcified plaques and in plaques without hemorrhage (31 plaques), ulceration (30 plaques), inflammation (29 plaques) or necrosis (27 plaques). The correlation of OPN expression with the presence of intraplaque ulceration and inflammation confirms its involvement in vulnerable morphological lesions ($p=0.036$).

Our data support the association of OPG with the mineralization process, OPG being strongly expressed in stable, calcified plaques. More specifically, OPG was highly positive in 33 plaques, 25 (75%) of them showing calcifications in histological examination. In addition

to these data, our study shows no statistical significance between GSM and AHA plaques type or the presence of OPN or OPG.

I.1.3.6. Conclusions

OPG and OPN co-exist in carotid atherosclerotic plaque demonstrating a modulatory role in inflammatory and calcification processes. OPG is strongly expressed in stable, calcified plaques, while OPN is poorly expressed in calcified plaques and in plaques without hemorrhage, ulceration, inflammation, or necrosis.

I.1.4. Correlations between grayscale and histopathological proprieties of carotid atherosclerotic plaque

I.1.4.1. Introduction

The high rate of strokes, 1.4 million/year and consequently the high mortality of 1.1 million/year among Europe citizens is alarming (93, 126, 127). The most common cause of TIA or stroke is carotid artery and vertebral artery atherosclerosis, or thrombosis and the neurological deficit can occur suddenly, in "full health" (128). The management of atherosclerotic carotid and vertebral artery disease is one of the most studied and discussed topic in the last years at each international vascular surgery meeting and was the topic of 2 major trials: The North American Symptomatic Carotid Endarterectomy Trial (NASCET) and The European Carotid Surgery trial (ECST) (94, 95). Identifying patients at risk for ischemic cerebral events is an important concern for vascular surgeons. Ultrasound is preferred for carotid artery imaging due to its accessibility, low cost and non-invasiveness (93). The association of B-mode and Doppler color flow imaging increases the possibility of quantifying the degree of stenosis (92, 93).

Previous studies have identified the ultrasonic echo lucent plaques as vulnerable and associated them with a higher probability of causing TIAs or ischemic strokes. GSM is an ultrasound-based risk marker that measures atherosclerotic plaque echogenicity (96, 97). Its value is still disputed in the literature. This prospective study aimed to determine if GSM is a predictor of carotid plaque vulnerability.

I.1.4.2. Materials and methods

Included in this study were 49 consecutive patients admitted to the Department of Vascular Surgery of the Iasi "Sf. Spiridon" County Clinical Emergency Hospital between January 2015 and April 2018 with indication for CEA. There were 38 male and 11 female patients, median age 66 years old (range 54-80), 34 patients being over age 65 years at the time of diagnosis.

The patients were selected from the cases with a high probability of advanced internal carotid artery (ICA) lesion referred from neurology departments, and from those with peripheral vascular disease already admitted to our department who screened positive for significant carotid artery stenosis.

The inclusion criteria were asymptomatic ICA stenosis greater than 70%, recent history of transient ischemic attack (TIA) and ICA stenosis of 50-99% with a history of stroke maintaining self-sufficiency. The exclusion criteria were autoimmune diseases, hypothyroidism, osteoporosis, hepatic insufficiency (GOT higher than 2.5 UI/L), chronic renal disease (creatinine above 2.0 mg/dL), ischemic heart disease classes III, IV NYHA, atrial fibrillation, malignancies (98).

All patients underwent a new Doppler ultrasound examination using a Siemens X 700 ultrasound system. B-mode settings for carotid exploration were saved and used each time trying to ensure uniformity throughout the study (figure I.5).

Figure I.5. Intrastenotic blood flow velocity at ICA bifurcation

Patients were examined supine with the neck rotated 45 degrees to the opposite side. A peripheral vascular transducer was used. Carotid arteries were examined bilaterally, both in transverse and longitudinal planes (using an angle < 60°). Stenosis was measured according to the NASCET method and was calculated as the ratio between minimal residual lumen diameter at the stenosis as the numerator and the diameter of the disease-free ICA segment above the stenosis (where the vessel walls were approximately parallel) as denominator, in correlation with Intrastenotic flow (92). The images were stored and transferred to a computer in order to calculate GSM for all study patients.

All images were normalized according to the method proposed by El-Atrozy et al. in order to eliminate gain-induced variability of echogenicity (97). The enhanced ultrasound images were processed using the computer software Adobe Photoshop and selecting two reference points: blood (black) and adventitia (white) (figure I.6). The GSM of blood was set to 0, while the GSM of adventitia was set to 255.

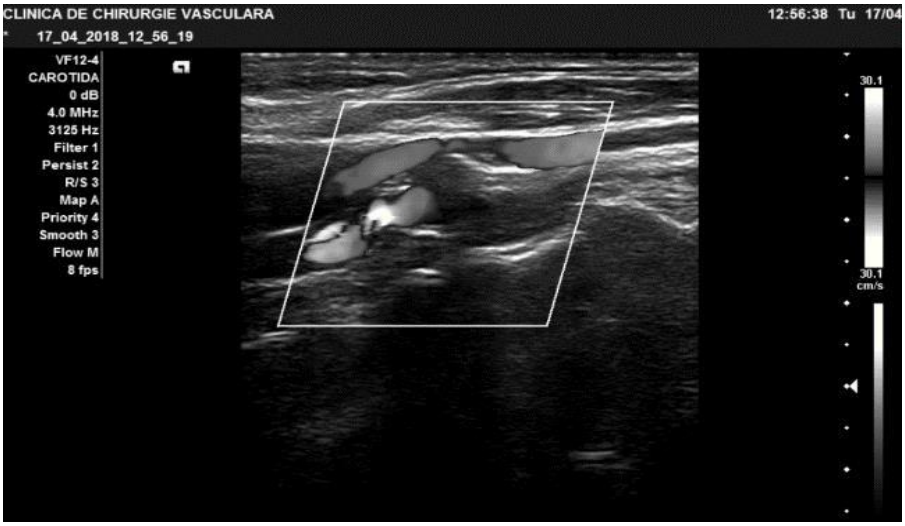

Figure I.6. Post-normalization US image

To determine the GSM for each carotid plaque the best segment for visualization was selected followed by the use of the histogram function of the software (97) (figure I.7).

Figure I.7. Histogram acquisition returning GSM value

All patients underwent carotid endarterectomy and patch angioplasty. Carotid endarterectomy specimens were processed by the standard paraffin embedded histology technique at the Histology Laboratory of the Iasi University of Medicine and Pharmacy. For each fragment, representative sections were selected and stained with hematoxylin and eosin. The lesions were analyzed by two pathologists who classified the atherosclerotic plaques according to the AHA criteria (73).

The microscopic examination of carotid ATS plaques was focused on three main components, namely the cells (smooth muscle cells, macrophages and other leukocytes), extracellular matrix and intraand extracellular lipids. Also determined was the presence or absence of the vulnerability factors (inflammation, LRNC, intraplaque hemorrhage or ulceration).

According to the histological criteria, the carotid ATS plaques belonged to two categories: stable, that includes type IV (atheroma) and type V (fibroatheroma) AHA lesions, and vulnerable, that comprises type VI AHA lesions (with erosions of the endothelium or fibrous cap, ulceration or intraplaque hemorrhage).

Statistical analysis was performed using SPSS software, Chi square descriptive test compared the ultrasound vulnerable plaques with GSM <=37 with the histopathologicaly-proven vulnerable plaques, AHA class VI.

I.1.4.3. Results

Ultrasound scanning diagnosed 33 patients with 70-99% carotid stenosis, 14 patients with 60-69% and only 2 patients with 50-59% carotid stenosis, the last 2 patients having an indication for carotid endarterectomy due to recent symptomatology.

GSM measured after ultrasound image normalization revealed a high grade of heterogeneity of plaques. GSM ranged from 8 to 130, median 48 (Table I.4). Values in the first quartile ranged from 8 to 37. Unstable plaques were more heterogenic, with higher transparency and lower GSM than stable plaques. Quartile 25 included 13 plaques with increased ultrasound-based vulnerability and higher echo transparency. Quartile 50 and Quartile 75 included 36 echogenic, stable plaques according to ultrasound criteria.

Table I.4. GSM value quartile distribution

Min	Q25	Median	Q75	Max
8	37	48	59	130

Of the total of 49 carotid ATS plaques, 14 were classified as unstable AHA type VI lesions (figures I.8 and I.9), with the following complications: intraplaque hemorrhage caused by the rupture of vessels in the granulation tissue of the atheroma in 2 cases, bleeding and ulceration in 5 cases and areas of erosion or irregular endothelial ulceration caused by plaque necrosis in 7 cases. The other 35 plaques were considered stable AHA type V lesions.

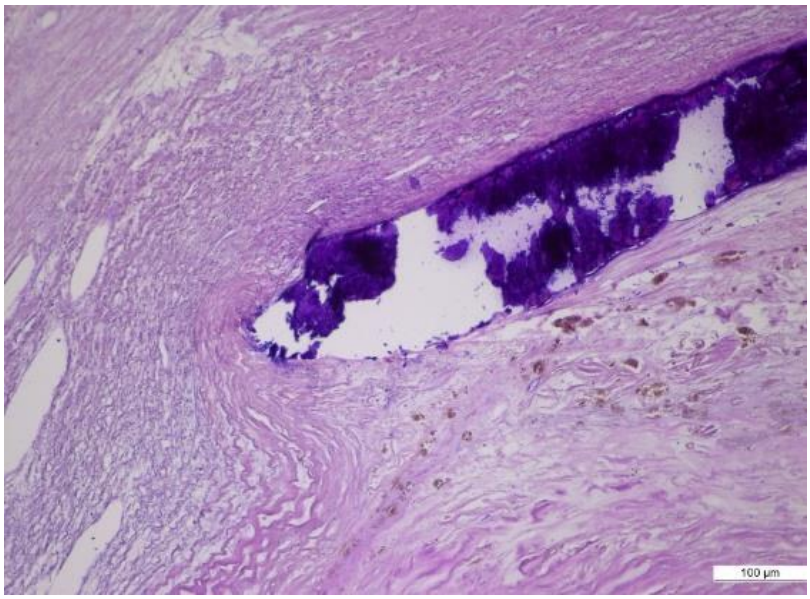

Figure I.8. Fibro lipidic plaque-compact calcification, destruction of internal elastic lamina (IEL) and marked compression of the media; adjacent to macrophage calcification loaded with hemosiderin pigment and neovascularization components, HEx100

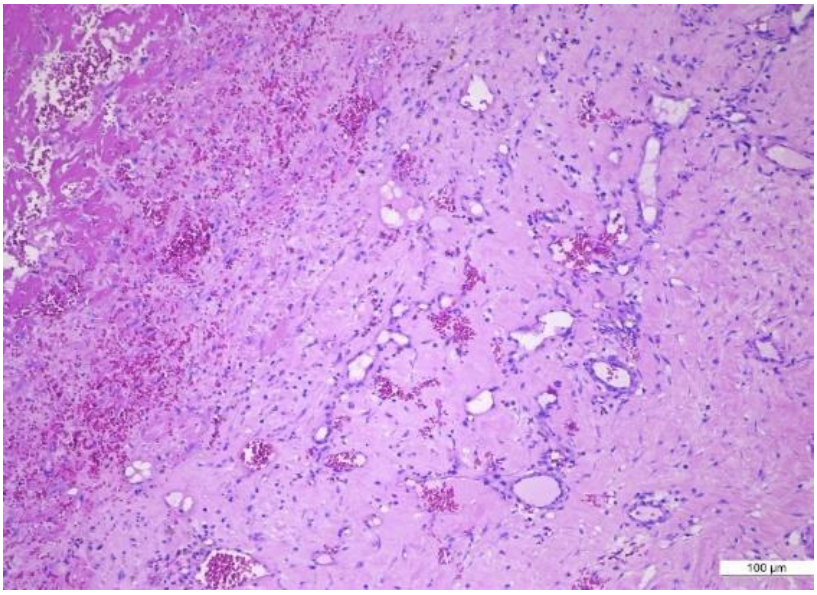

Figure I.9. Fibro-lipidic plaque-intraplaque hemorrhage, numerous capillaries of neoangiogenesis, associated inflammatory infiltrate, HEx100

Inflammation and necrosis of the atheromatous core, considered risk factors for plaque vulnerability, were found in 17 and 13 lesions, respectively. Dystrophic calcification was

present in 39 of the 49 ATS lesions. The plaques classified as vulnerable/stable by GSM and according to histopathological criteria were compared assuming that a lower GSM will be associated with histopathological plaque instability (table I.5).

Table I.5. GSM vs AHA plaque type - Cross tabulation

	Histopathological type		TOTAL
	Stabile	**Vulnerable**	
GSM>=37	26	10	36
GSM<37	9	4	13
TOTAL	35	14	49

Legend: GSM- gray scale median; AHA- American Heart Association

We found no direct correlation either between GSM (<=37 vs. >37) and type V or type VI plaque (p = 0.838), or the presence of each histopathological instability marker, namely ulceration (p = 0.73) and intraplaque hemorrhage (p = 0.29). Also, no statistically significant differences were found between GSM values and inflammation (p = 0.739).

GSM<37 strongly correlates independently with lipid-rich necrotic core, a morphological risk factor for plaque vulnerability. Of the 49 carotid plaques 13 showed signs of necrosis and 8 of these had GSM < 37 (p = 0.01).

I.1.4.4. Discussions

Although the histopathologic examination is the “gold standard” for identifying and staging ATS lesions, this examination can be performed only postoperatively as confirmation based on the morphological substrate. In this context, a constant concern of specialists in vascular surgery is the implementation of alternative non-invasive diagnostic methods, which to allow the identification of vulnerable carotid ATS lesions. The rapid development of imaging techniques (Doppler ultrasound, carotid angiography, angio-CT, angio-MRI) has led to real progress, facilitating the primary diagnosis and guiding the surgeon in making a therapeutic decision. Duplex ultrasound is “the firs line” imaging method for carotid artery (93). The Society of Radiologists recommended during the 2003 Ultrasound Consensus Conference that the final carotid artery ultrasound report should include velocity measurements, grayscale and color Doppler findings (129).

The relationship between echolucent plaque, plaque instability and presence of symptoms is proven (130). Echolucent plaques are more prone to rupture than dense fibrous echogenic plaques and are more common in patients with symptomatic cerebrovascular disease (131, 132).

Plaques with a higher GSM score are predominantly calcified plaques and are more stable and associated with a lower rate of cerebrovascular events (96). The GSM median of 48 and also the maximum at 130 show that most of our study patients had echogenic plaques. Also, in comparison with the results from other studies, our study showed higher median GSM values (96, 98). This is a consequence of the incidental discovery of carotid stenosis and that patients tend to present with more advanced disease or long after the symptomatic period

(the first 6 months after an ischemic event). This fact is also confirmed by the predominant presence of AHA type V plaques in our study group.

Accumulation of lipid-rich necrotic debris and smooth muscle cells are present in advanced carotid plaques. Unstable plaques usually have a thin fibrous cap with a necrotic core situated juxta luminal. Our study supports a prior finding that lower GSM values are associated with lipid-rich necrotic core (133, 134). In presence of ulceration the necrotic core is exposed, the ATS plaque is vulnerable, predisposing to thromboembolic events.

However, full overlap of diagnostic imaging classes with histopathologic diagnosis classes has not been obtained, yet. Our study highlights the discrepancies between the classification of the plaques into the unstable, vulnerable versus stable categories by using ultrasound and histology, respectively. Our results demonstrate the limitation of ultrasound imaging for the assessment of plaque vulnerability. Despite the great benefits of ultrasound examination, as a non-invasive method, the vascular surgeon must be aware that GSM results cannot offer a perfect, point to point mirror of the morphological background that characterizes the plaques in their biological environment.

No carotid restenosis was detected during the first 12 months of ultrasound follow-up. The patients are still under surveillance, the follow-up aiming to detect the possible occurrence of restenosis at 24-year follow-up and to correlate the recurrence with GSM and histological characteristics.

I.1.4.5. Conclusions

High-grade carotid stenosis, GSM higher than 37, and AHA type V carotid ATS plaques predominantly identified in our study group show that patients tend to present with more advanced disease. GSM < 37 strongly correlates with intraplaque necrosis, but in the absence of other correlations with the histopathological vulnerable plaque characteristics it leads to the conclusion that although ultrasound remains the best noninvasive method for assessing the carotid ATS plaques, GSM measurement can be time-consuming with little additional value in evaluating plaque vulnerability.

I.1.5. Complex ultrasound study of the atherosclerotic plaque

I.1.5.1. Introduction

Carotid surgery concept is wining ground both among neurologists who recommend and vascular and cardiovascular surgeons who perform an increased number of interventions. Regardless of the technique used (open surgery, stenting) we were interested in the tendency of the plaque to grow and determine stenosis.

The prevalence of significant internal carotid artery (ICA) stenosis (more than 50%) is 0.5% among the age range 50 - 59 years, 10% in elderly over 80 years and 20% in patients presenting lower limb peripheral arterial disease (103). Worldwide stroke is the third common cause of death. The prevalence of stroke after a transient ischemic attack (TIA) is 7% per year and the prevalence of stroke in an asymptomatic patient with a carotid stenosis larger than 80% is 3% per year (103).

The main cause of stroke is atheroembolism followed by the low blood flow through the stenosis. The benefit from surgery in terms of stroke prevention in patients with symptomatic 70 - 99% stenosis (NASCET criteria) is higher than the one obtained from medical treatment (103).

The available level I evidence suggests that in symptomatic patients' surgery is currently the best option. The recommendation was based on a meta-analysis by The

Cochrane Collaboration of eight randomized trials comparing carotid artery stenting with carotid endarterectomy (104). Patients with recent symptomatic stenosis (70-99%) are at highest risk of subsequent stroke. The efficacy of CEA falls with time (104).

Duplex ultrasound is the gold standard technique for carotid arteries evaluation. Ultrasound (US) uses B-mode US imaging and Doppler US to detect focal increases in blood flow velocity indicative of high-grade carotid stenosis. The peak systolic velocity is the most frequently used to measure the severity of stenosis.

Color Doppler technique increases the efficiency of the test, but it has not been shown to improve accuracy. US is 91-94% sensitive and 85-99% specific in detecting a significant stenosis of the ICA (135-137).

Doppler US is also useful in obtaining information about plaque composition. Intraplaque hemorrhage, which may increase the risk of embolism and impact on prognosis, can be visualized on high resolution B-mode (130, 135-139). The ratio of ICA peak systolic velocity to the common carotid artery (CCA) velocity predicting a high-grade stenosis sets the indication for surgery (140).

I.1.5.2. Materials and methods

The patients included in this study were selected based on the following criteria: patients referred by neurology departments with a high probability of advanced ICA lesion, patients with peripheral vascular disease already hospitalized in the vascular surgery department screened positive for significant carotid or femoral stenotic lesions, patients with arteriopathy hospitalized in cardiology and internal medicine departments diagnosed with significant femoral artery stenosis. 98% of the patients were diagnosed and selected in the Vascular Surgery Department. Before surgery all patients benefited from a new Doppler US (performed on Siemens EchoDoppler XP 300 Premium - 2010). All patients gave their informed consent for the study.

Two groups were formed: patients with stenotic ICA and patients presenting stenosis at the femoral artery bifurcation. The inclusion criteria for the first group were: asymptomatic ICA stenosis greater than 70%, history of TIA, history of minor stroke with self-sufficiency and 50-95% ICA stenosis. The patients in the second group meet the following inclusion criteria: arteriopathy stage III and IV with atherosclerotic lesions at the femoral bifurcation, regardless of the chosen surgical procedure.

The exclusion criteria were: autoimmune diseases, hypothyroidism, osteoporosis, hepatic insufficiency (GOT higher than 2.5 UI/ l), chronic kidney disease (creatinine above 2.0 mg / dl), ischemic heart disease class III, IV NYHA, atrial fibrillation and malignancies.

The comparison between these two groups started from the premise of the existence of a similar pattern for ICA deep femoral artery (DFA) and external carotid artery (ECA) - superficial femoral artery (SFA). Thus, the bifurcation of the CCA into the ICA and ECA anatomically resembles the bifurcation of common femoral artery (CFA) into DFA and SFA at each bifurcation there is an artery that will face increased resistance (ECA and SFA) and an artery that faces low resistance in the periphery (the ICA and DFA). Because of this, plaques at the two bifurcations are supposed to have a similar structure. Although clinically the manifestations of obstruction/stenosis of the ICA are much more severe than in obstruction/stenosis of DFA, the two models can be studied together in terms of atheromatous plaque progression.

US scans were performed on admission in all patients in both groups. B-mode settings were adjusted and then saved to ensure uniformity throughout the study (figure I.10). The stenosis grade was measured both in transversal and longitudinal section (figures I.11 and I.12).

Figure I.10. ICA and CCA B - mode US

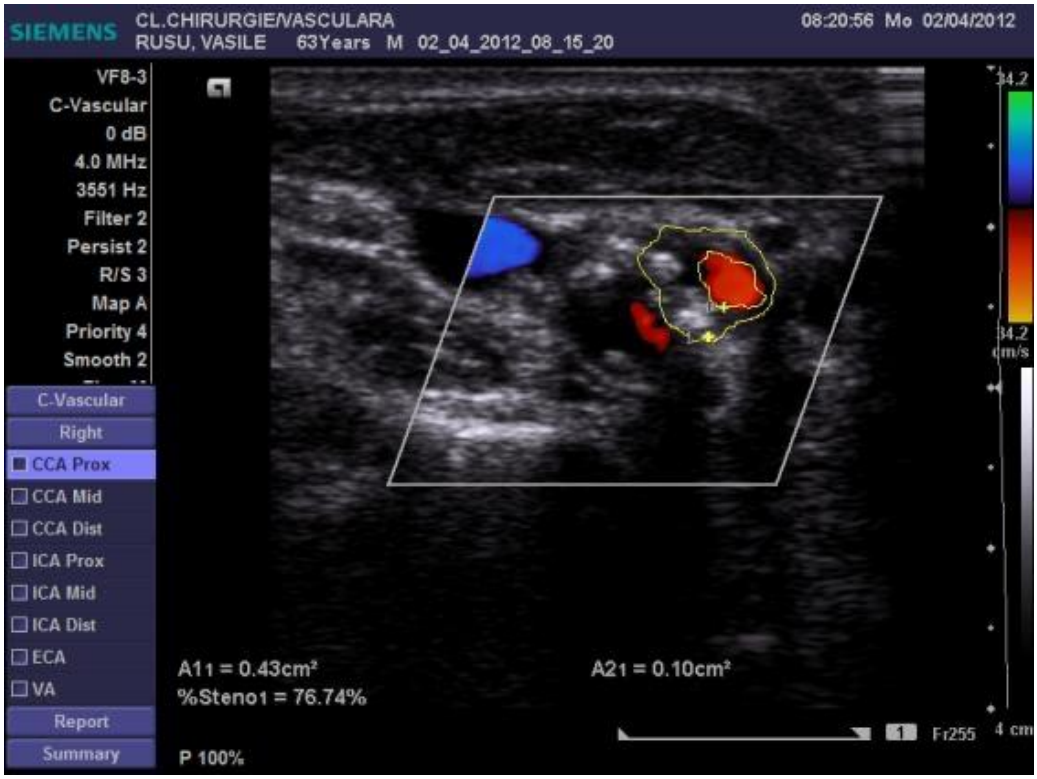

Figure I.11. Stenosis measurement on transversal section

Figure I.12. Stenosis measurement on longitudinal section

Two reference points were used for normalization of B-mode images, blood (black), and adventitia (white). Patients were examined supine with the neck-rotated 45 degrees to the opposite side. A peripheral vascular transducer was used. The image was “frozen”, stored and transferred to a computer in order to calculate the Gray Scale Median (GSM).

All images were normalized according to the method proposed by El-Atrozy et al. eliminating sonographic gain-induced variability of echogenicity in which the entire image is changed by a process of linear scaling to two reference points (blood and adventitia) with computer software (Adobe Photoshop 7.0). The GSM of the blood was set to 0, and the GSM of adventitia was set to 255. To determine the GSM for each stenotic plaque we acquired the histogram (82, 97, 141-143) (figures I.13 and I.14).

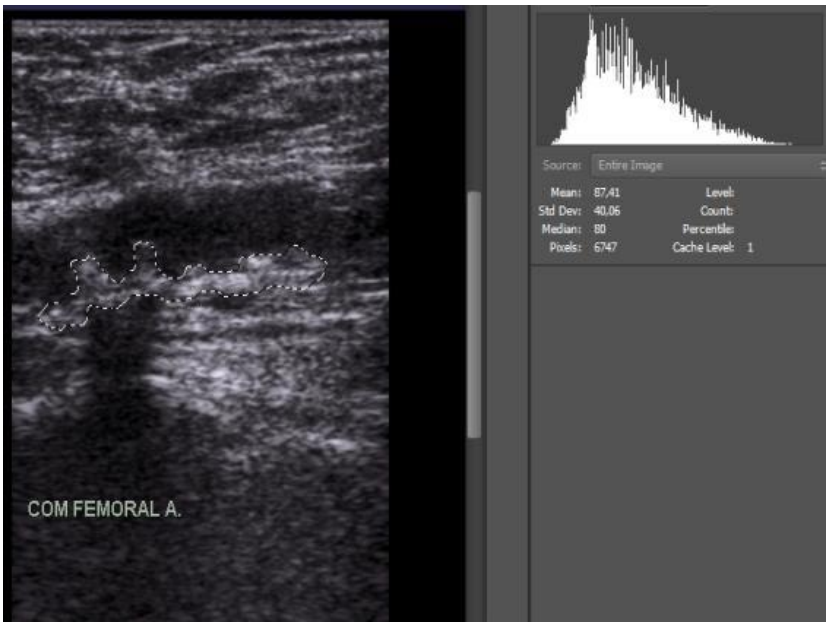

Figure I.13. Selected atheroma plaque and prenormalized histogram

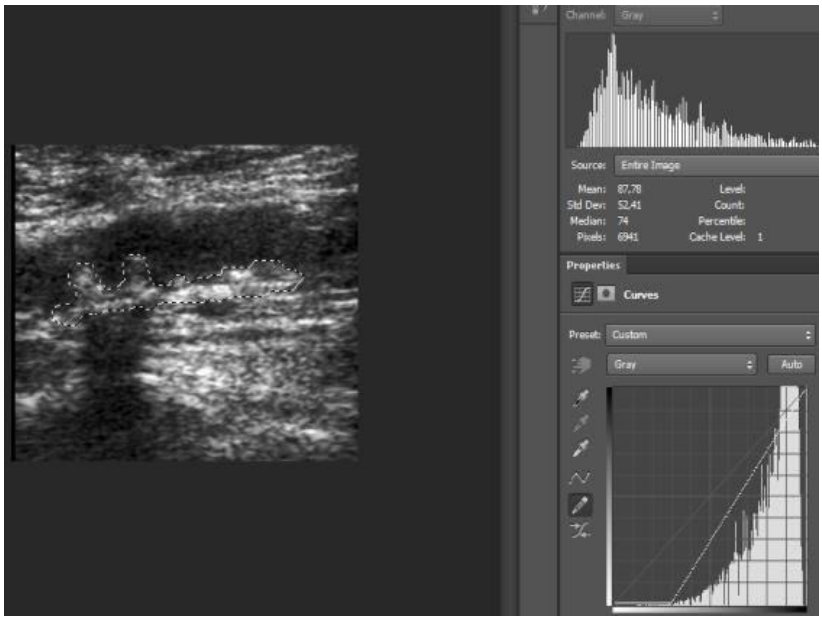

Figure I.14. Selected atheroma plaque and normalized histogram

The results were used to compare the groups with one another and to draw conclusions from each group. All patients underwent surgical interventions (endarterectomy and angioplasty in the patients with carotid artery stenosis or femoral artery stenosis and endarterectomy associated with bypasses in the patients with femoral artery stenosis) US was performed postoperatively and as follow-up at 1, 3, 6, 9 and 12 months (figures I.15 and I.16).

Figure I.15. Follow-up US - carotid angioplasty

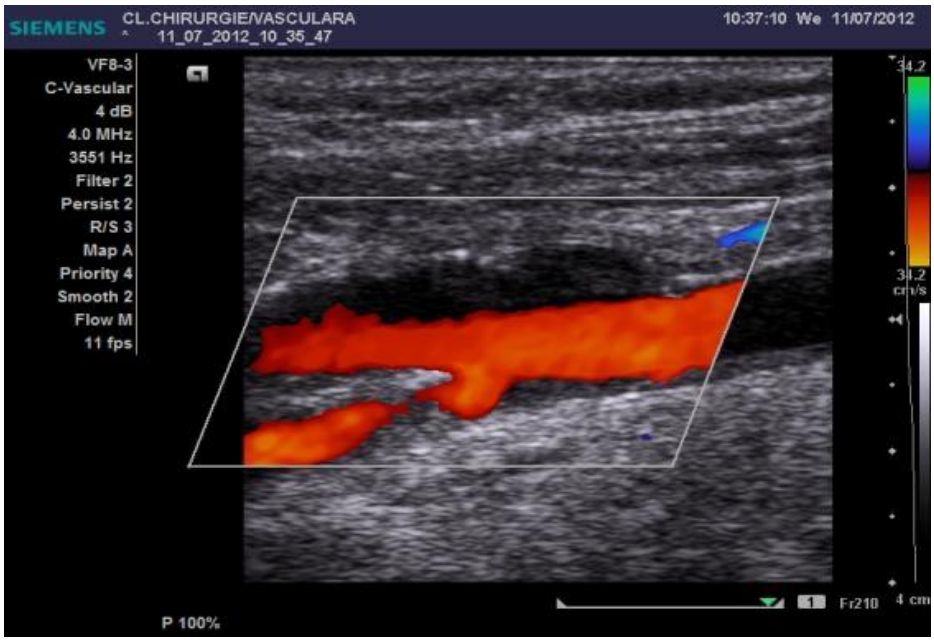

Figure I.16. Follow-up: carotid angioplasty Doppler US

I.1.5.3. Results

From January 1, 2012 to December 31, 2012 we included in the study 70 consecutive patients meeting all criteria, 35 patients in each group. Twelve patients with carotid lesions showed ICA stenosis greater than 90% stenosis.

Patients with femoral lesions had CFA stenosis greater than 50% associating in 13 cases DFA stenosis greater than 70%. No statistically significant differences in demographic characteristics, vascular risk factors or therapy were identified. Post-Hoc analysis (paired analysis) comparing the femoral or carotid plaque area before and after the normalization revealed the absence of statistical difference. The difference between prenormalization and normalization GSM values in each group were statistically significant (tables I.6 and I.7).

Table I.6. Post-Hoc GSM analysis (paired analysis)

Newman-Keuls test	P value	Statistics
prenormalized ICA vs. normalized ICA	0.014924	ss
prenormalized ICA vs. prenormalized DFA	0.142735	ns
normalized ICA vs. normalized DFA	0.036642	ss
prenormalized DFA vs. normalized DFA	0.001911	ss

Table legend: ICA- internal carotid artery; DFA- deep femoral artery; ss- statistically significant; ns- non-significant.

Table I.7. Post-Hoc aria analysis (paired analysis)

Newman-Keuls aria test	P value	Statistics
prenormalized ICA vs. normalized ICA	0.690022	ns
prenormalized ICA vs. prenormalized DFA	0.000028	ss
normalized ICA vs. normalized DFA	0.000036	ss
prenormalized DFA vs. normalized DFA	0.580894	ns

Table legend: ICA- internal carotid artery; DFA- deep femoral artery; ss- statistically significant; ns- non-significant.

The average carotid plaque area was twice as big as the average femoral plaque area (table I.8).

Table I.8. Statistical area values (mm) pre-normalized vs. normalized

		Avr	Average		SD	SE	Min	Max	Md
			-95%	+95%					
ICA	pre- N	2625.3	2136.1	3114.6	1424.3	240.7	615.9	5520.0	2322.2
	N	2729.9	2235.4	3224.4	1439.5	243.3	671.5	5800.5	2747.7
DFA	pre- N	1390.9	1196.4	1585.4	566.2	95.7	610.4	2487.9	1188.5
	N	1535.6	1321.7	1749.6	622.9	105.3	456.7	2906.7	1422.9
All		2070.4	1862.3	2278.6	1245.7	105.3	456.7	5800.5	1875.8

Table legend: ICA- internal carotid artery; DFA- deep femoral artery; pre-N- pre-normalized; N- normalized; Avr- average; SD- standard deviation; SE- standard error; Min- minimum; Max- maximum; Md- median.

Femoral plaque GSM values were higher in relation with hyperechogenity, highlighting the intensely calcified structure. Unstable plaques were more heterogenic, with higher transparency and lower GSM than stable plaques.

Carotid plaques average GSM was lower than the femoral one, meaning the carotid plaques are less stable. Minimum-maxim differences reveal a high grade of heterogenity in both groups (table I.9). Patients showed no carotid or femoral restenosis during the 1, 3, 6 and 12 months of US follow-up. Patients remained under surveillance.

Table I.9. Statistical GSM values [mm] pre-normalized versus normalized

		Average			**SD**	**SE**	**Min**	**Max**	**Md**
		Avg	-95%	+95%					
I C A	pre- N	41.17	34.17	48.17	20.37	3.44	13	86	40
	N	55.06	46.26	63.85	25.60	4.33	20	112	49
D F A	pre- N	48.49	42.91	54.06	16.23	2.74	23	78	44
	N	65.49	58.53	72.44	20.24	3.42	35	142	69
All		52.55	48.79	56.31	22.51	1.90	13	142	48

Table legend: ICA- internal carotid artery; DFA- deep femoral artery; pre-N- pre-normalized; N- normalized; Avr- average; SD- standard deviation; SE- standard error; Min- minimum; Max- maximum; Md- median.

I.1.5.4. Discussion and conclusions

Our study showed higher GSM values than those reported in the literature (105, 108). This is a consequence of the patients' tendency to present to the vascular surgeon in advanced disease stages.

The correlation of a lower GSM with plaque instability needs to be proved. During the US follow-up we aim at detecting the occurrence of restenosis.

Bifurcation plaques occurring in peripheral atherosclerotic disease are calcified and determine chronic ischemic symptoms (intermittent claudications, rest pain), while carotid bifurcation plaques are unstable and determine cerebral symptoms either by TIA or ischemic stroke.

US remain the gold standard noninvasive technique both for screening and diagnosis and set the therapeutic coordinates.

The GSM analysis is a new and versatile tool used to establish plaque characteristics and to assess the risk for acute events.

Chapter 2: Role of ultrasound examination for congenital heart abnormalities

I.2.1. State of art

The majority of congenital heart defects may be identified during pregnancy at the second trimester examination. Due to the fact that most of them occur in low-risk pregnancies and rely on the maternal obstetric provider to identify fetal cardiac abnormalities on obstetric screening anatomic ultrasonography, prenatal detection rates continue to be very varied.

Referrals for fetal echocardiography examination should be made for fetuses with abnormal findings on obstetric screening anatomic ultrasonography and/or risk factors for heart illness. Specialized sonographers should do fetal echocardiogram, and doctors who are familiar with the changing fetal cardiac anatomy and physiology during gestation should interpret the results.

Fetuses with congenital heart defects or other types of primary or secondary cardiac illness may be identified using a standardized and systematic method during a fetal echocardiography test, which can be performed starting in the late first trimester. Because fetal echocardiography allows for study of dynamic fetal heart physiology and evaluation of prospective fetal/neonatal therapy, the science of fetal cardiology has gone beyond the accurate prenatal diagnosis of simple and complicated congenital heart defects.

Fetal echocardiography still has the most effect in identifying serious CHD before birth, allowing for rapid cardiac treatment after delivery to lower newborn morbidity and death. Fetal cardiologists can prognose effects on the developing fetus, predict risk of postnatal hemodynamic instability, direct delivery planning through multidisciplinary collaboration, and foresee how the disease will affect the neonate after delivery by evaluating the severity of abnormal cardiac physiology in various forms of heart defects before birth.

The second chapter describes multiple imaging approaches for evaluating patent foramen ovale, as well as the role of 3-vessel-tracheal sections in screening for congenital cardiac anomalies.

Personal contributions:

1. Floria M, Năfureanu ED, Iov DE, Dranga M, **Popa RF**, Baroi LG, Sascău RA, Stătescu C, Tănase DM. Multimodality imaging approach of patent foramen ovale: Practical considerations for transient ischemic attack/stroke. J Clin Ultrasound. 2022 Oct;50(8):1166-1176. doi: 10.1002/jcu.23325. PMID: 36218207.
2. Gireadă R, Socolov D, Mihălceanu E, Matasariu R, Ursache A, Akad M, Bujor I, Scripcariu I, **Popa RF**, Socolov R. The Additional Role of the 3-Vessels and Trachea View in Screening for Congenital Heart Disease. Medicina (Kaunas). 2022 Feb 10;58(2):262. doi: 10.3390/medicina58020262. PMID: 35208585; PMCID: PMC8875090.

I.2.2. Multimodality imaging approach of patent foramen ovale: practical considerations for transient ischemic attack/stroke

I.2.2.1. Introduction

According to TOAST criteria, 1 patent foramen ovale (PFO) is a low-risk potential source of cardioembolic stroke, together with other interatrial septum anomalies such as atrial septum aneurysm (ASA) and atrial septum defect (ASD) (144). A PFO is present in up to

25% of the adult population and results from the incomplete fusion of the septum primum and secundum after birth (145). It causes paradoxical embolisms via a right-to-left shunting and it has an increased risk of stroke recurrence when associated with ASA, due to the nidus properties of the saccular like structure of the aneurysm (146, 147).

Likewise, the presence of Eustachian valve facilitates blood flow direction from the inferior vena cava toward the PFO, increasing the risk for stroke (145, 146). A tricuspid regurgitation flow directed to atrial septum may also result in a right-to-left shunt, favoring the passage of thrombi from the right to the left atrium. Besides stroke, the presence of PFO is associated with other clinical syndromes, the most known being migraine headaches and platypnea-orthodeoxia (145, 148).

There is no gold standard technique for assessing PFO and diagnosis is established based on multimodality imaging, with echocardiography being the most frequently used. The use of agitated saline as contrast when performing transthoracic (TTE) and transesophageal echocardiography (TTE) increases the sensitivity and sensibility of these methods by establishing right to left shunting (145, 149, 150).

According to TOAST criteria, 1 patent foramen ovale (PFO) is a low risk potential source of cardioembolic stroke, together with other interatrial septum anomalies such as atrial septum aneurysm (ASA) and atrial septum defect (ASD) (146). A PFO is present in up to 25% of the adult population and results from the incomplete fusion of the septum primum and secundum after birth (145). It causes paradoxical embolisms via a right-to-left shunting and it has an increased risk of stroke recurrence when associated with ASA, due to the nidus properties of the saccular like structure of the aneurysm (146, 147).

Likewise, the presence of Eustachian valve facilitates blood flow direction from the inferior vena cava toward the PFO, increasing the risk for stroke (145, 146). A tricuspid regurgitation flow directed to atrial septum may also result in a right-to-left shunt, favoring the passage of thrombi from the right to the left atrium. Besides stroke, the presence of PFO is associated with other clinical syndromes, the most known being migraine headaches and platypnea-orthodeoxia (145, 148).

There is no gold standard technique for assessing PFO and diagnosis is established based on multimodality imaging, with echocardiography. This paper aims to represent a practical guide for PFO multimodality imaging assessment in the setting of transient ischemic attack/stroke.

I.2.2.2. The embryology of patent foramen ovale

In order to achieve a better understanding of the difference between PFO and ASD, a few notions of the embryology of PFO should be understood. During fetal evolution, septation is the process that defines the development of the single chamber cardiac tubule into the known form of the four-chamber heart (Figure II.1). This process takes place between the fourth and seventh week of gestation, and is initiated by the development of septum primum from the roof of the primitive atrium (151-153).

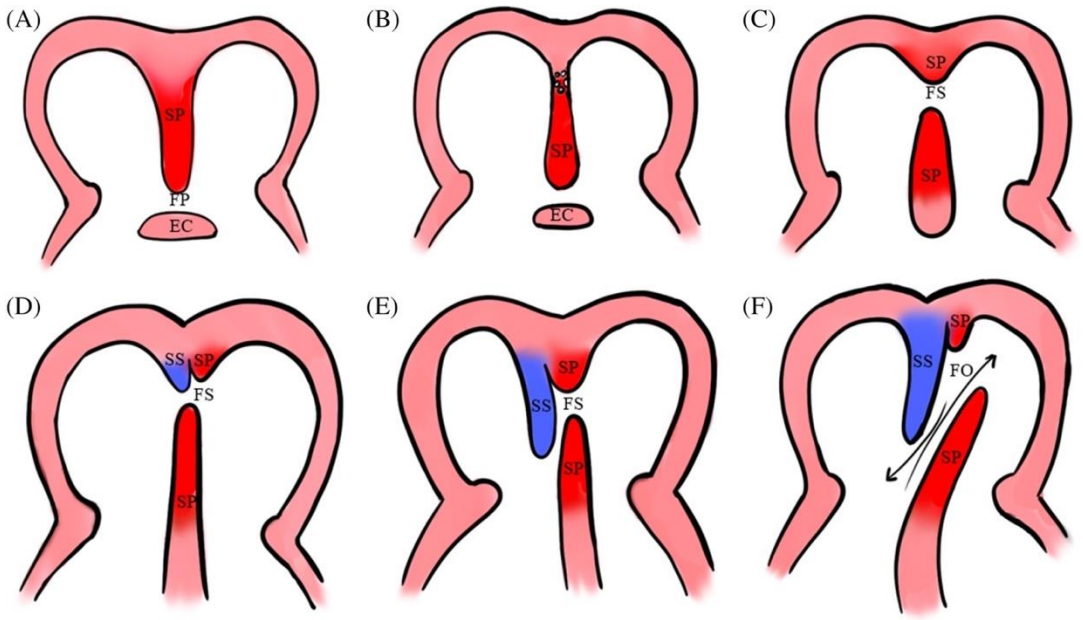

Figure II.1. Atrial septation. (A) septum primum growth toward endocardial cushions with the foramen primum between them; (B) fenestrated septum primum in the upper part; (C) fusion of septum primum with the endocardial cushions, closure of foramen primum and ful development of the foramen secundum; (D) start of development of the septum secundum on the right of septum primum; (E) growth of septum secundum toward septum secundum; (F) lack of fusion between septum primum and septum secundum, with foramen ovale between them. EC, endocardial cushions; FO, foramen ovale; FP, foramen primum; FS, foramen secundum; SP, septum primum; SS, septum secundum. Adapted after Jensen et al. (154)

Septum primum grows into a caudal manner toward the endocardial cushions. In the embryonic and fetal heart, a communication between the right and left part is necessary in order to allow blood coming from the placenta elude the pulmonary circulation of the fetus and enter into the systemic circulation (151, 154, 155). This is the reason why initially a free space remains between the inferior edge of the septum primum and the endocardial cushions, known as foramen primum.

Foramen primum closes by the end of the sixth week due to the full growth and fusion of septum primum with the endocardial cushions at the atrioventricular level, but this process happens simultaneously with the formation of a new opening, known as foramen secundum, in the superior part of the septum primum by its localized fragmentation (151-153).

Throughout the seventh week, the septum secundum appears at the right of the septum primum from an invagination of the atrial roof toward the atrioventricular junction. 8 Septum secundum obliterates the foramen secundum, but due to the lack of fusion with the endocardial cushions at its inferior edge, an opening remains.

This further forms an oblique orifice with the foramen secundum, which is known as the foramen ovale (152). The inferior part of the septum primum now acts as a flap valve for the foramen ovale, allowing the blood to flow only from the right toward the left cavities (152). At birth and soon after, due to respiration which causes inflation of the lungs, allows the pulmonary circulation to become functional and the left side pressure to increase, the foramen ovale closes by the permanent contact of the septum primum and septum secundum. This transforms foramen ovale into the fossa ovalis (153, 155).

I.2.2.3. Multimodality imaging of patent foramen ovale diagnosis

A PFO is not an ASD per se because it occurs as a consequence of the imperfect fusion of the septum primum and secundum and not due to loss of atrial septal tissue (145). Normally, given the higher pressures on the left side, the shunting through PFO is left to right; however, in situations with increased pressures in the right atrium or when other associated conditions are present (Table II.1), the foramen ovale opens in a transient or permanent manner, associating a right to left shunt (145). Due to its particular position within the interatrial septum and given the fact that expert consensuses on the subject did not establish a gold standard imaging technique, the diagnosis and evaluation of consequences of PFO are made using a rather patient, skilled and availability-based approach in which multiple tools can be used.

Table II.1. Conditions associated with PFO and right to left

Pulmonary hypertension (chronic or acute)
Sleep apnea syndrome
Right atrium dilation and remodeling
Valsalva maneuver
Interatrial septum aneurysm
Chiari network
Eustachian valve

The three pillars of PFO imaging assessment of are the various types of echography using contrast agents: contrast transcranial Doppler (c-TCD), contrast transthoracic echocardiography (c-TTE) and contrast transesophageal echocardiography (c-TEE), each with its own advantages, drawbacks and various specificity and sensibility percentages reported in studies (145, 149).

I.2.2.4. Transthoracic echocardiography

Transthoracic echocardiography is the first method which may rise clinical suspicion and could diagnose and evaluate the consequences of PFO; it also has the added benefit of being the most widely available imaging tool (149, 156). Diagnosis in TTE can be made based on imaging of the left to right or right to left shunting by using color Doppler or agitated saline contrast. The first view that allows to evaluate the integrity of the interatrial septum and PFO is the short parasternal axis, but without the possibility of correct assessment due to the parallel orientation of the ultrasound beam to the interatrial septum. In this regard, the preferred windows and views are those in which the ultrasound beam falls perpendicularly to the interatrial septum, such as the subcostal four-chamber view (Figure II.2A) and short axis view 3 (Figure II.2B).

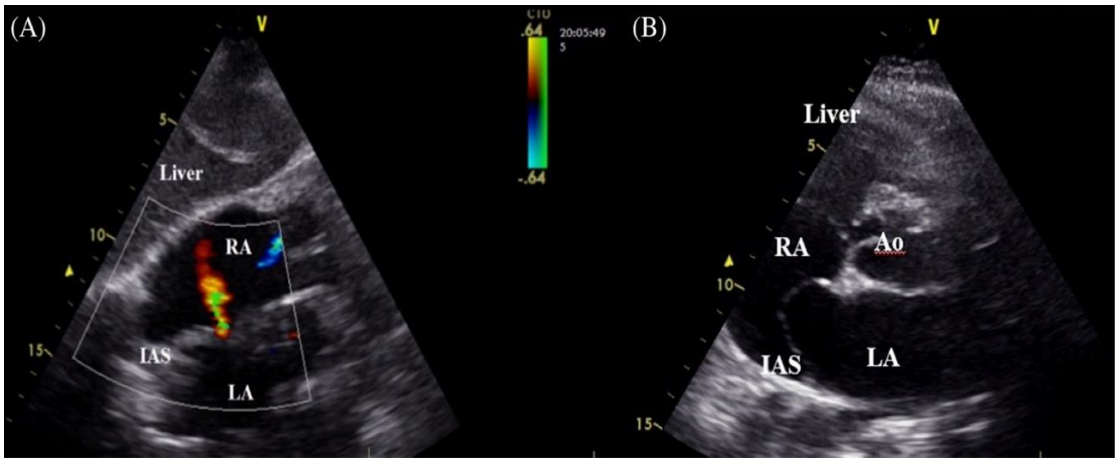

Figure II.2. Transthoracic echocardiography: (A) subcostal four chamber view, showing left to right shunt in color Doppler through a patent foramen ovale; (B) parasternal short axis view showing atrial septum aneurysm. Ao, aorta; IAS, interatrial septum; LA, left atrium; RA, right atrium

Bidimensional imaging in either window allows for an evaluation of the causes, consequences or anatomic variations associated with PFO. Apical four-chamber view should be used in order to measure an ASA (Figure II.3), evaluate the presence of Chiari network or thrombi, estimate atrial enlargement by measuring atrial volumes and assess the tricuspid gradient and the shunt by using an agitated saline contrast. The presence of some anatomic variations (Chiari network, ASA, presence of Eustachian valve and a lipomatous interatrial septum) classifies PFO as complex and should be carefully searched, especially when a patient with PFO is addressed for closure, as it can interfere with the procedure (157).

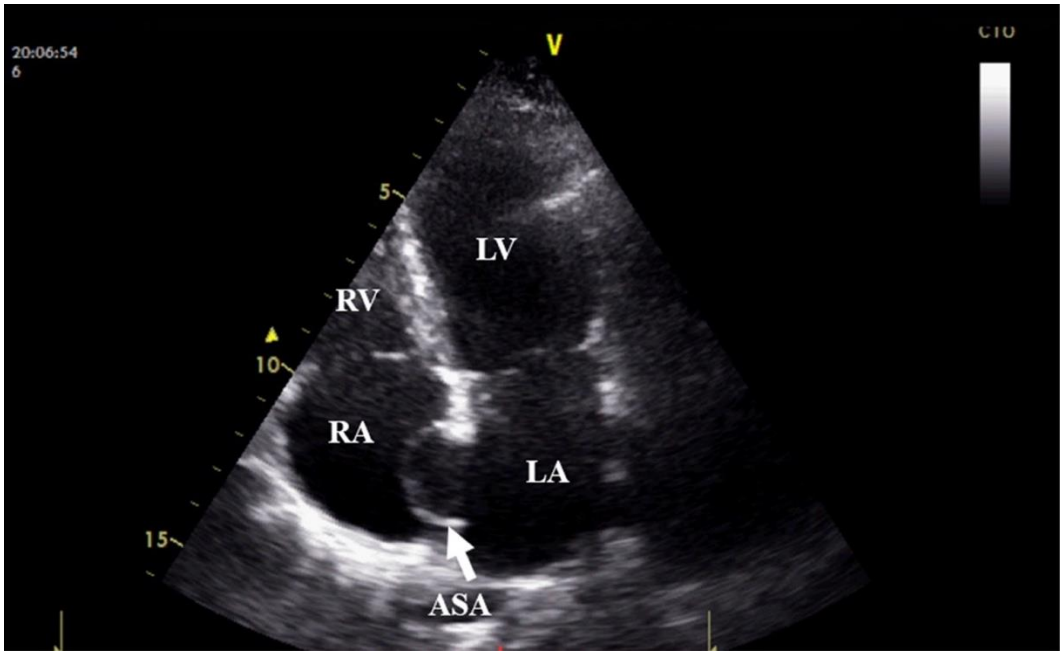

Figure II.3. Transthoracic echocardiography in apical four chamber view showing atrial septal aneurysm with left to right displacement. ASA, atrial septum aneurysm; LA, left atrium; LV, left ventricle; RA, right atrium; RV, right ventricle

When it comes to hemodynamic consequences of PFO with left to right shunting, one must be aware that due to its dimensions, it does not cause significant overload of the right cavities and other septal defects must be searched. In this situation, pulmonary to systemic flow ratio (Qp/Qs) and right ventricular dimensions and function assessments are mandatory.

Usually, a PFO does not modify the dimensions of the right atrium and ventricle by induced hemodynamic changes.

It is possible that in apical four chamber or subcostal view, the flow in color Doppler sometimes overlaps with that of the superior vena cava. Therefore, in this situation, the color Doppler sample should be greatly reduced to avoid overlapping.

I.2.2.5. Transesophageal echocardiography

Although currently there is a lack of a gold standard technique for PFO diagnosis, some authors and practitioners consider TEE the optimal tool as it offers more detailed information regarding the integrity of the interatrial septum and nearby structures. It allows differentiation between PFO and other types of atrial septal defects, especially in situations in which TTE does not provide sufficient information. The current guidelines for assessment of ASD and PFO from the American Society of Echocardiography and the European position paper on the management of patients with PFO stipulate that TEE should be used in patients who have a poor acoustic window when evaluated through TTE and in selecting and guiding transcatheter occlusion (145, 149).

A specific protocol must be followed when evaluating a PFO in TEE. 16 Five views are ideal for evaluation of the interatrial septum (Figure II.4): four midesophageal views (four chamber—Figure II.4B, long axis—Figure II.4D, aortic valve short axis—Figure II.4C, and bicaval—Figure II.4E) and one obtained from the upper esophagus (short axis—Figure II.4A) (145, 158, 159). Because of the foramen ovale's particular tunnel-like form within the interatrial septum, measurements of its total length and maximal size at the left and right atrial ends should be made whenever possible. Due to the fact that TEE is used in selecting patients which are candidates for PFO closure, an evaluation of PFO's distance to venae cavae must be performed (145, 158).

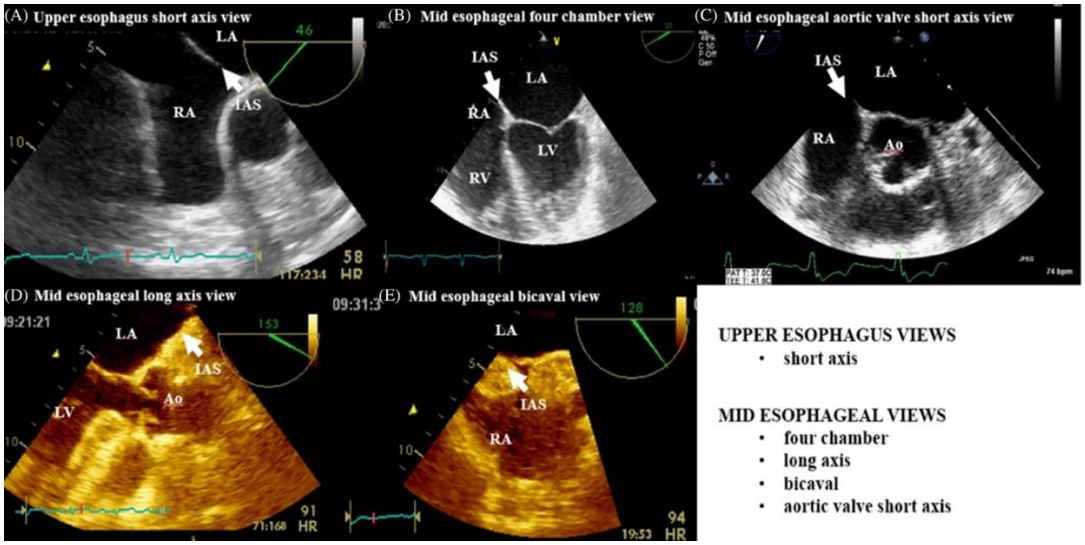

Figure II.4. The views for interatrial septum evaluation in transesophageal echocardiography: (A) Upper esophagus short axis view; (B) Mid esophageal four chamber view; (C) Mid esophageal aortic valve short axis view; (D) Mid esophageal long axis view (lipomatous hypertrophy of the interatrial septum); (E) Mid esophageal bicaval view (lipomatous hypertrophy of the interatrial septum). Ao, aorta; IAS, interatrial septum; LA, left atrium; LV, left ventricle; RA, right atrium; RV, right ventricle

Left to right shunting (or right to left shunting under Valsalva maneuver or specific conditions) through a PFO is evaluated in the same manner as with TEE, using color Doppler (Figure II.5A and II.5B) and agitated saline contrast (145).

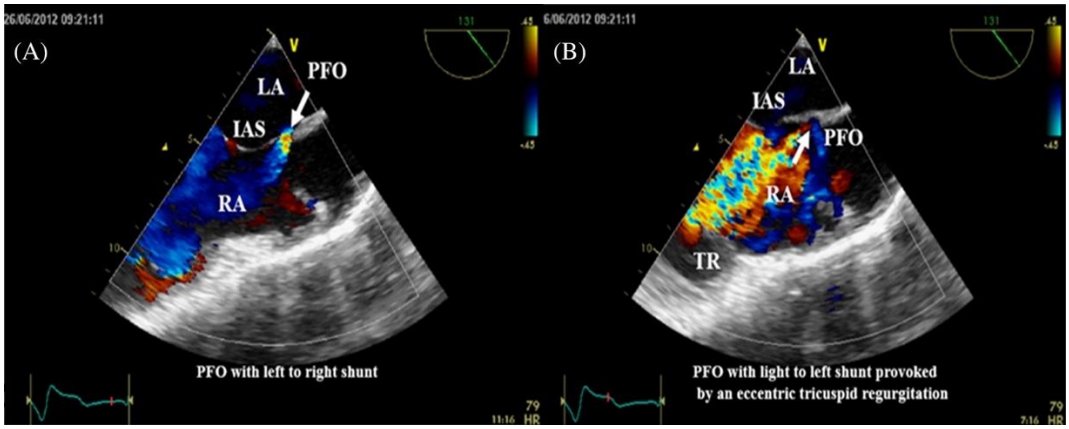

Figure II.5. Transesophageal echocardiography mid esophageal long axis view with color Doppler showing a patent foramen ovale with left to right shunting (A) and right to left shunting (B) facilitated by a regurgitant tricuspid flow (favorized by a ventricular pacemaker lead) directed toward the IAS. IAS, interatrial septum; LA, left atrium; PFO, patent foramen ovale; RA, right atrium; TR, tricuspid regurgitation

Regarding the ASA, this anatomic anomaly is defined as the movement of the interatrial septum of at least 10 mm into the left or right atrium from the plane or a combined left and right movement of 15 mm (Figure II.6) (145).

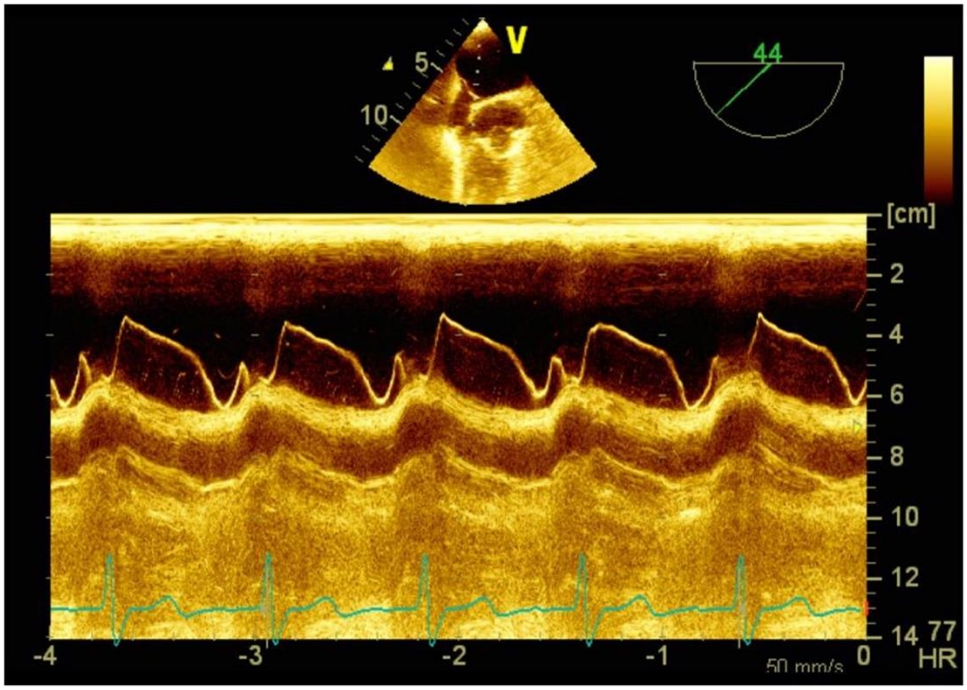

Figure II.6. Transesophageal echocardiography: excursion of the interatrial septum in M mode

The excursion of the interatrial septum in ASA could be assessed either in TTE or in TEE. ASA is present in about 4% 18 of cases of PFO and is associated with a high risk of paradoxical embolism due to the fact that the aneurysmal portion is a zone of capture for thrombi (146). Likewise, the presence of the Eustachian valve is associated with a higher risk of paradoxical embolism. This structure is a remnant of the inferior vena cava's valve present

in the embryo and fetus, whose role is to direct blood flow from the inferior vena cava toward the foramen ovale. A prominent Eustachian valve can cause a PFO because it comes into contact with the septum primum and blocks the fusion to the septum secundum.

Transesophageal echocardiography performed in experienced centers is a safe and easy procedure. However, overall complication rate during diagnostic and intraoperative TEE is 0.18%–2.8%. The absolute contraindications for TEE are perforated viscus, stricture, tumor, perforation, laceration or diverticulum of the esophagus and active upper gastrointestinal bleeding, while conditions such as a history of radiation to the neck and mediastinum, a history of gastrointestinal surgery, recent upper gastrointestinal bleed, Barrett's esophagus, a history of dysphagia, restriction of neck mobility (severe cervical arthritis, atlantoaxial joint disease), symptomatic hiatal hernia, esophageal varices, coagulopathy, thrombocytopenia, active esophagitis or active peptic ulcer disease constitute relative contraindications (160).

I.2.2.6. Agitated saline contrast echocardiography

Use of agitated saline while performing TTE (Figure II.7A) or TEE (Figure II.7B) is an inexpensive, ready to use method of assessing the right to left shunting in PFO. Agitated saline can also be used in assessing the right to left shunting when combined with transcranial Doppler (c-TCD).

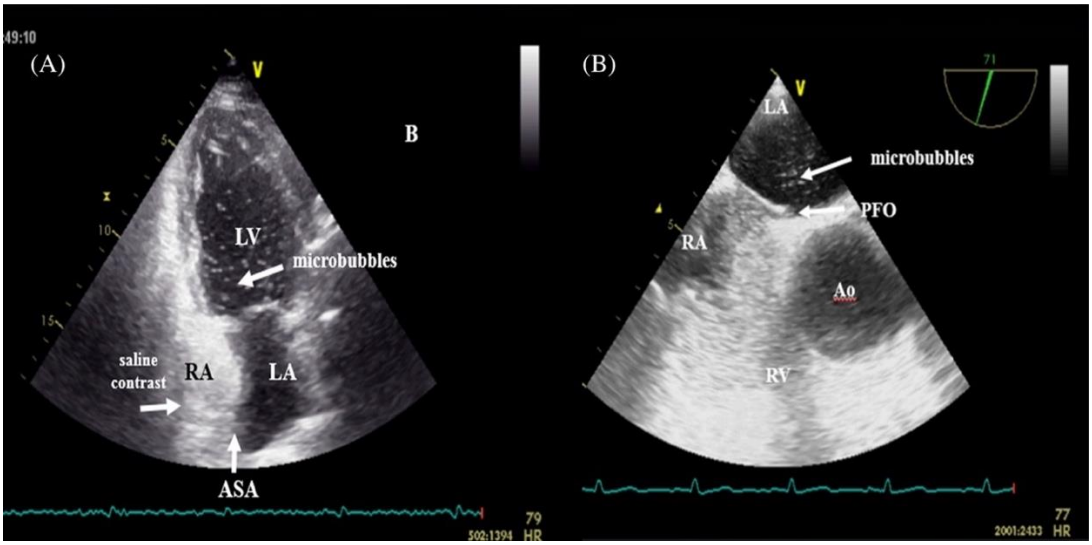

Figure II.7. Contrast echocardiography with microbubbles shows the presence of patent foramen ovale. (A) transthoracic echocardiography in apical four chamber view, showing right to left shunting through a patent foramen ovale during Valsava maneuver. (B) transesophageal echocardiography in mid esophageal short axis aorta view. Ao, aorta; ASA, atrial septum aneurysm; LA, left atrium; LV, left ventricle; PFO, patent foramen ovale; RA, right atrium; RV, right ventricle

Older studies comparing contrast transthoracic echocardiography using agitated saline to the other two contrast enhanced techniques concluded that c-TTE is the least useful diagnostic tool (161); however, more recent studies gave c-TTE the credibility of being a specific and sensitive mean for PFO diagnosis. This is probably mostly due to the fact that it is the first method used in the diagnostic algorithm for causes of stroke and its wide availability. Another reason could reside in the fact that performing a Valsalva maneuver during transesophageal echocardiography is more difficult (162, 163).

The technique (Table II.2, Figure II.8) which uses 80% saline, 10% air, and 10% patient's blood as the solution to be injected is preferred because studies have shown better

contrast intensity due to higher concentrations of microbubbles with added blood (164, 165). After injection of the solution in an arm vein, it is expected to see microbubbles in the right atrium. When performing this test, the inclusion of a well-trained nurse in the team is mandatory, in order to allow the imagist to correctly assess the presence of the PFO and the shunt.

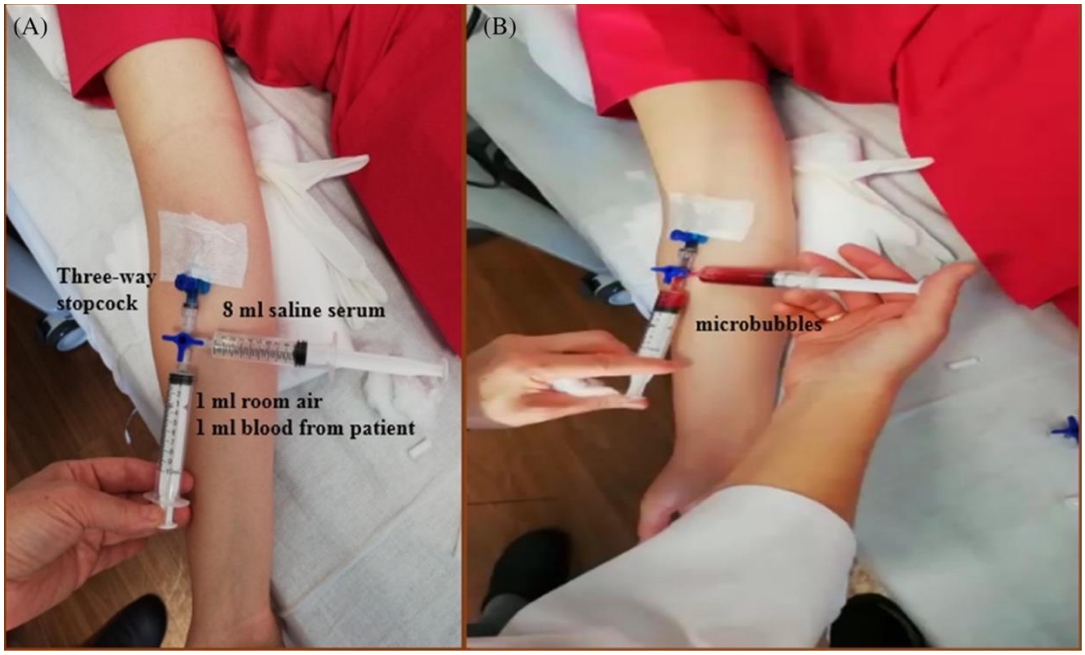

Figure II.8A and B. Agitated saline contrast technique (please see Table II.2 for details)

Table II.2. Materials needed and the technique of making microbubbles in six steps

Materials needed	Microbubbles protocol with technique details
• 2 syringes of 10 ml • intravenous catheter • 3-way stopcock • 8 ml saline • 1 ml of patient's blood	1. Place an intravenous catheter into an antecubital vein • attach a 3-way stopcock to it • please take sure that stopcock is very well screwed (to avoid syringes detaching during test) 2. Agitated saline preparation • mix it in a 10 ml syringe with 8 ml saline and 1 ml air • take 1 ml of patient's blood 3. Place the two syringes (the empty and the filled one) in the free orifices of the stopcock • close de orifice that connects the stopcock to the catheter 4. Start making microbubbles • move very fast the plungers back and forth for 10 s so the mixture will pass from a syringe to another • microbubbles must be visible in the syringes 5. Push the mixture into the vein

	• in order to do that, close de orifice connecting to the empty syringe and open the ones connecting the intravenous catheter to the filled syringe • microbubbles must be injected in bolus (very rapidly) 6. Repeat twice agitated saline test • for better recognition of a positive test and for reproducibility

When a right to left shunt is present, microbubbles will be seen entering the left atrium through the interatrial septum when performing a Valsalva maneuver (Figure II.9). As a rule of thumb, in order to establish a diagnosis of right to left shunting caused by a PFO, microbubbles should appear in the left atrium within three cardiac cycles. If microbubbles appear in the left atrium after more than three cardiac cycles, then the shunt is located intrapulmonary, with microbubbles entering the left atrium via the pulmonary veins (166). This is why when performing this test using transthoracic echocardiography, a subcostal four chamber view should be used in order to observe the passage of microbubbles from the right to left atrium via the interatrial septum.

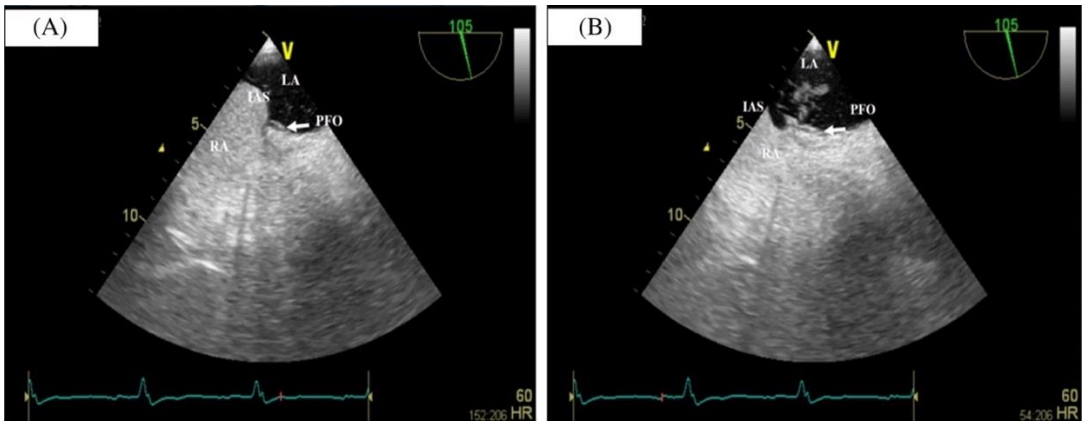

Figure II.9. Agitated saline contrast when performing c-TEE. (A) before Valsalva (no microbubbles seen in the LA). (B) after Valsalva (microbubbles seen in LA). IAS, interatrial septum; LA, left atrium; PFO, patent foramen ovale; RA, right atrium

When the subcostal window does not offer a clear image, an apical four chamber view must be used (Figure II.10) (167).

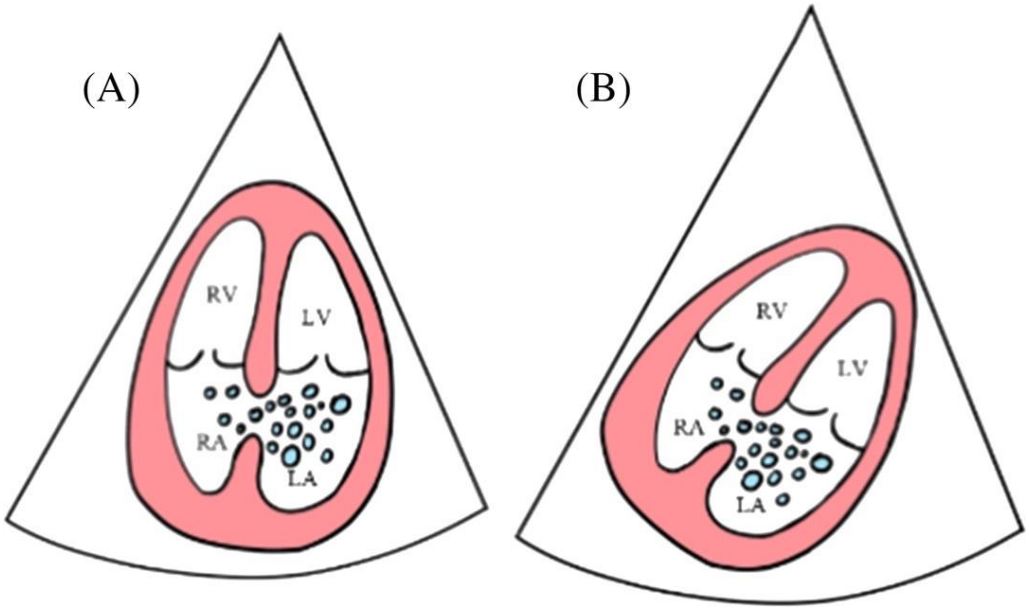

Figure II.10. Agitated saline TTE with microbubbles passing from right to left atrium in (A) apical four chamber view, (B) subcostal four chamber view. LA, left atrium; LV, left ventricle; RA, right atrium; RV, right ventricle. Adapted after Montrief et al. (168)

If this test is performed by TEE, the best views for the assessment of the right to left shunting are mid-esophageal bicaval and aortic short axis view (Figure II.11)

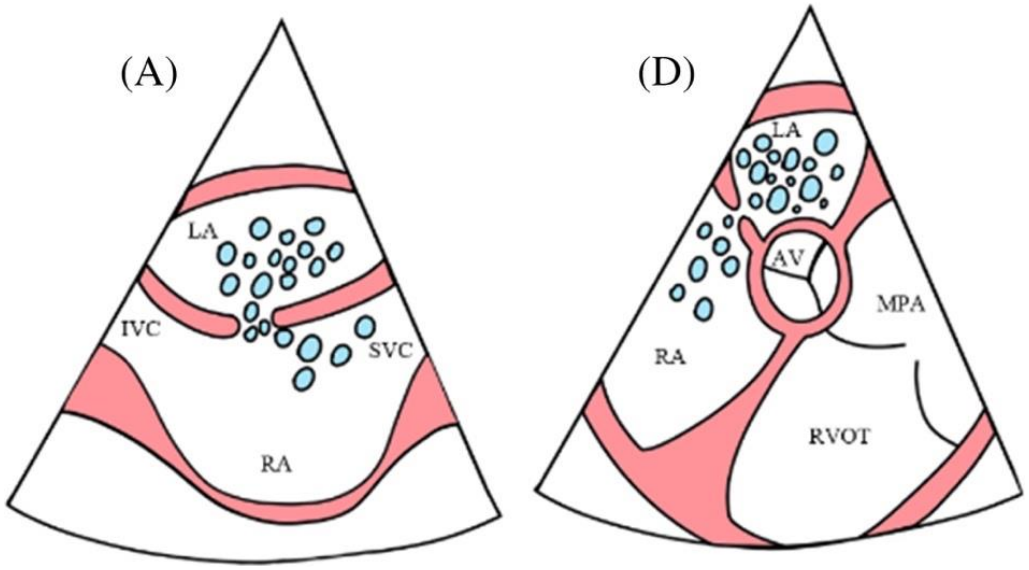

Figure II.11. Agitated saline TEE with microbubbles passing from right to left atrium in (A) midesophageal bicaval view and (B) midesophageal short axis aortic valve level view. AV, aortic valve; IVC, inferior vena cava; LA, left atrium; LV, left ventricle; MPA, main pulmonary artery; RA, right atrium; RV, right ventricle; RVOT, right ventricle outflow tract; SVC, superior vena cava. Adapted after Montrief et al. (168)

Agitated saline contrast echocardiography can allow a semiquantitative assessment of the right to left shunting based on the number of microbubbles seen in the left atrium. There is no standard classification of grades of right to left shunting, but most practitioners classify right to left shunting in three to five grades (table II.3) (169-171).

Table II.3. Severity grades of right to left shunt when assessed with agitated saline contrast

Author	Grade	Severity
Gonzalez-Alujas et al. (162)	3 grades	Mild: < 10 microbubbles Moderate: 10–20 microbubbles Severe: > 20 microbubbles
Vitarelli et al. (169)	4 grades	0: no microbubbles seen 1: < 10 bubble 2: ≥ 10 microbubbles 3: 25% opacification of left atrium
Rana et al. (170)	4 grades	1: < 5 microbubbles 2: 5–25 microbubbles 3: > 25 microbubbles 4: chamber opacification
Lee et al. (171)	5 grades	0: no microbubbles 1: 1–5 microbubbles 2: 6–20 microbubbles 3:21–50 microbubbles 4: > 50 microbubbles

An agitated saline contrast echocardiography does not lack false positive or false negative results. Various situations (Table II.4) can erroneously establish a diagnosis of PFO or, in contrast, may lead to missing it (171).

Table II.4. Situations that can result in a false negative or false positive agitated saline contrast echocardiography

False positive	False negative
Intrapulmonary shunts	Inadequate Valsalva maneuver
Unidentified ASDs	IVC flow creating a" wash out" effect
Sinus venosus septal defects	LV diastolic dysfunction
Poor acoustic image	Poor acoustic image

Sometimes inferior vena cava flow is directed toward the interatrial septum (Figure II.12), in some cases favored by the presence of Eustachian valve, thus leading to the opening of the foramen ovale. When the procedure is performed by injecting agitated saline into an arm vein, this may cause a subsequent "wash-out" effect of the contrast coming from the superior vena cava.

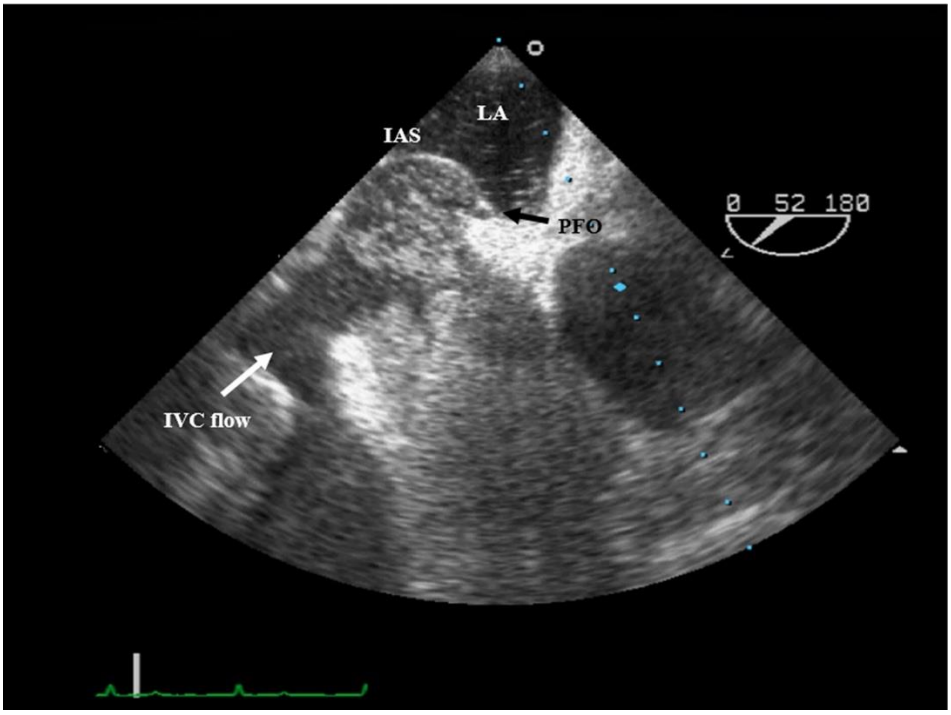

Figure II.12. Transesophageal echocardiography in midesophageal short axis view showing flow from IVC creating a "washout" effect of the saline contrast. IAS, interatrial septum; IVC, inferior vena cava; LA, left atrium; PFO, patent foramen ovale

I.2.2.7. Other imaging modalities

Several other techniques can be used in order to assess PFO, its associated anatomic variations and the resulting shunting, but some of them are less frequently used due to lower availability, high cost or lack of experience in performing and using them.

Contrast enhanced transcranial Doppler (c-TCD) uses the same principle as contrast echocardiography. It is performed by neurologists or radiologists following an established protocol that uses agitated saline as contrast and evaluates the appearance of microbubbles in the middle cerebral artery (172).

Thus, it establishes the presence of right to left shunting and rises a clinical suspicion of PFO in patients with paradoxical embolism. Results of studies comparing c-TCD to c-TTE and c-TEE are very non-homogeneous in terms of sensitivity and specificity, with older studies noting higher values in assessing right to left shunting. In spite of these findings, the major drawback of this method is its inability to establish the intra- or extracardiac nature of the shunt.2

Intracardiac echocardiography (ICE) and 3D echocardiography (3D-E) are two newer techniques used in guiding PFO closure because of their ability to assess the anatomy of the PFO and surrounding structures in great detail (173, 174).

Cardiac computed tomography (CCT) is less frequently used because of its inferiority to echocardiography. It can be performed with or without electrocardiography gating. It provides accurate anatomic descriptions of the interatrial septum and can raise suspicion of a PFO, but cannot clearly diagnose it. One major disadvantage is the fact that even in cases in which contrast agents are used, Valsalva maneuvers cannot be performed during image acquisition (175).

Cardiac magnetic resonance (CMR) has the advantage of a better estimation of right and left ventricular function by calculating volumes, but it is inferior to TEE when it comes to assessing shunting through a PFO, therefore its clinical use is limited (176).

Each imaging method has its advantages and disadvantages (Table II.5) and, in order to use the most suitable technique, a clinical rationale must be followed.

Table II.5. Advantages and disadvantages of imaging studies for the evaluation of PFO

Imaging modality	Advantages	Disadvantages
TTE/c-TTE	Accessible Repeatable Non-invasive Low costs	Poor image quality in some cases Need for an accredited cardiologist/imagist
TEE/c-TEE	Better image quality Semi-invasive Low costs	Semi-invasive (a small risk of esophageal injury) Need for a specialized cardiologist/imagist
c-TCD	Accessible Repeatable Non-invasive Low costs	Cannot establish the origin of shunt: intracardiac versus extracardiac
ICE	Limited personnel (can be performed by the interventionist) Limits exposure to radiation	Invasive: risk of arrhythmia and vascular injury Expensive when performed with single use catheter Needs a specialized practitioner
CCT	Assessment of other associated cardiac/ vascular disorders	Impossibility to perform Valsalva maneuver due to image acquisition protocol Radiation and contrast agent exposure Expensive Less accessible
CMR	Assessment of other associated cardiac/ vascular disorders	Inferior to echocardiography in shunt assessment Expensive Less accessible

Therefore, to summarize the multimodality imaging techniques for PFO diagnosis and management we propose the following flowchart (Figure II.13). As c-TCD is performed by neurologists and, moreover, it cannot indicate the origin of shunt (intracardiac or extracardiac) we therefore propose this flowchart from the cardiologist point of view.

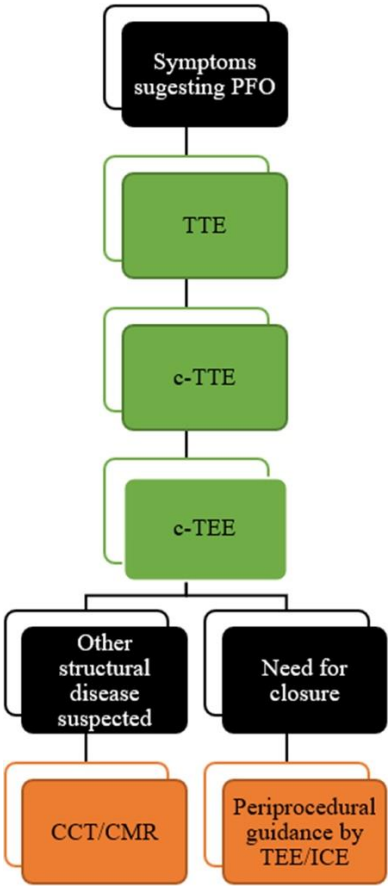

Figure II.13. Multimodality imaging techniques flowchart for PFO diagnosis and management

I.2.2.8. Indications for patent foramen ovale closure and periprocedural guidance

At the present moment, PFO closure is not standardized and the assembling of a multidisciplinary team is encouraged in order to make a therapeutic decision. 34 What is clearly stated in current guidelines (177) is the contraindication of performing closure as a primary prophylaxis method for stroke in patients with PFO.

Based on current literature data, PFO closure for the secondary prevention of stroke is made by a multidisciplinary team based on a multiple variable-based approach, including type of PFO (simple, complex) and age (usually between 18 and 60 years old), in patients with cryptogenic stroke, transient ischemic attack or other type of systemic embolism in whom the PFO is the certain the cause (177). In this regard, the RoPE score (risk of paradoxical embolism) has been proposed for estimating the probability that PFO is the causal agent of the stroke and guiding further therapy (178).

In patients who are candidates for PFO closure, a double-disc device could be implanted percutaneously, under TEE and/or fluoroscopic guidance. It is recommended that TEE be used to guide the closure because of better assessment of correct position and residual shunts by color Doppler and contrast. In addition to that, it has the added benefit of minimizing the radiation that is normally used when guidance is obtained based on fluoroscopy only (179).

It is essential that the device position is verified, focusing on a few key aspects: (1) the discs should be parallel to each other on eachside of the interatrial septum; (2) the rims and edges of the device should be securely fixed; (3) the occluder should not come in contact with other structures (such as the aorta, for example). For better image acquisition and guidance, 3D-TEE can be used (Figure II.14).

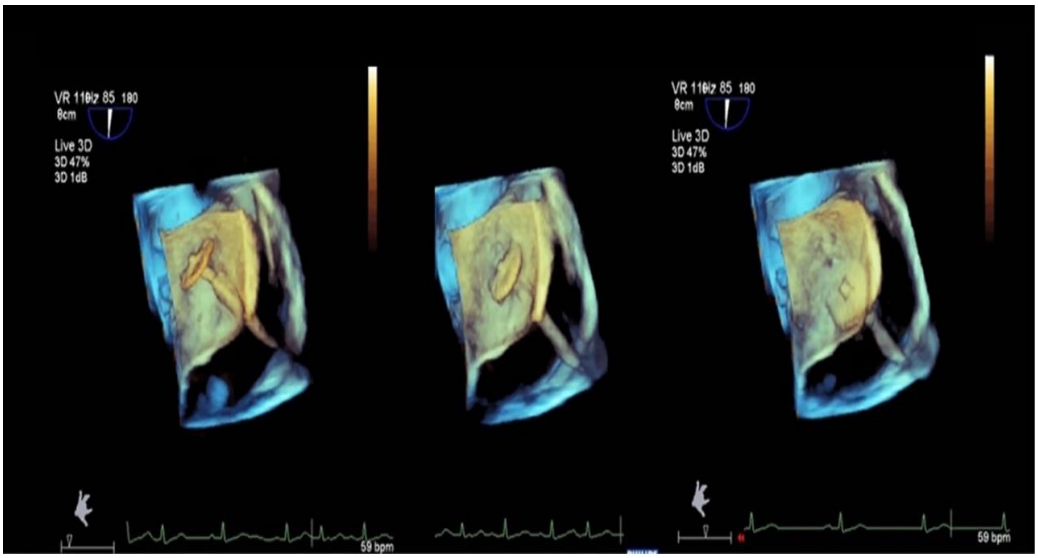

Figure II.14. 3D Transesophageal echocardiography images from PFO device closure guidance during positioning step

In spite of the fact that it is more invasive, as the probe is inserted via the right femoral vein into the right atrium under fluoroscopic guidance, intracardiac echocardiography is an excellent tool due to the proximity of the probe to the IAS and lower radiation exposure. In addition to that, it has the added advantage of requiring less personnel, because it can be performed by the same person who performs the closure and does not require an anesthesiologist due to lack of sedation (180).

Moreover, only two views are necessary for PFO closure (long and short atrial septal axis) (179). ICE with agitated saline contrast can also be used in order to evaluate the presence of right to left shunting, either for first assessment or in evaluating a residual shunt. However, ICE probes are expensive and therefore less accessible (174).

Another possibility for PFO closure is using a suture-mediated device. During this procedure, two sutures are done—the first on septum secundum and the subsequent one on septum primum—which are then tightened together by a small plastic knot (181). After closure, follow-up is carried out by TTE in apical and subcostal four chamber views (181).

I.2.2.9. Specific considerations for clinical practice

Based on the aforementioned facts, in clinical practice a few checkpoints should be followed in order to improve diagnosis and management of PFO closure.

• In order to correctly assess anatomic structures and shunts, evaluation of PFO should be centered on contrast enhanced echocardiography, either transthoracic or transesophageal, completed in selected cases by other multimodality imaging techniques.

• Based on the principle of the “heart team,” the decision for PFO closure should be made by a multidisciplinary cardio-neurology team; in order to accurately select cases that should be undergo this procedure, other specialists may be consulted depending on case complexity.

• Follow-up should be made by TTE.

• After closure, life-long antiplatelet therapy is mandatory in patients with a history of cryptogenic stroke or TIA, except for cases where anticoagulation must be used.

I.2.3. The additional role of the 3-vessels and trachea view in screening for congenital heart disease

I.2.3.1. Introduction

Congenital heart disease (CHD) affects 0.8% of the population, while the incidence of severe CHD goes up to 0.2% (182). Prenatal detection of CHD is crucial for planning delivery in cases that need immediate surgical treatment, and it helps parents decide the course of the pregnancy, especially when genetic testing is involved (183, 184).

Routine anatomy scans must follow the local/international guidelines, but there are great disparities between sonographers, from the allotted scan time to the anatomy checklist. The International Society of Ultrasound in Obstetrics and Gynecology (ISUOG) and the American Institute of Ultrasound in Medicine (AIUM) favor the sweep technique from the upper abdomen to the upper mediastinum, adding Color Doppler if possible (185, 186). However, the mandatory routine scan includes only situs, the 4-chamber view (4C), alongside the left and right ventricular outflow tracts (LVOT and RVOT) (185, 186). Although outflow tract inclusion increased prenatal CHD detection rate, this remains suboptimal and varies considerably according to the number of cardiac views (187).

The 3-vessels and trachea view (3VT) was introduced by Yagel as a complementary cardiac view to easily assess the aortic arch anomalies (188). The 3VT is the most cephalad cardiac transverse view, demonstrating the convergence of the aortic arch with the ductus arteriosus (DA), which communicates with the pulmonary artery at its bifurcation, near the origin of the left pulmonary artery (188). In the same plane, the trachea and the superior right vena cava can be seen at the right side of the transverse aorta (188).

Several anatomic landmarks can be assessed using 3VT: vessel number, alignment, arrangement, and size; trachea sidedness; and thymus size. A subjective caliber comparison between the transverse aorta and the pulmonary artery (especially toward their convergence) is sufficient to raise suspicion of an outflow tract anomaly, like aortic coarctation or pulmonary stenosis. By adding Color Doppler, we can evaluate the flow through the transverse aortic arch and the pulmonary artery/DA and, moving slightly more cephalad, we can demonstrate the normal course of the right subclavian artery and of the left brachiocephalic vein (LVBC) (188).

Although the 3VT view is deemed ‘desirable if technically feasible’ by both the ISUOG and AIUM screening guidelines (185, 186), especially due to its utility in detecting outflow tract anomalies (189-191), it is mandatory only in diagnostic echocardiography (192, 193). Hopefully, recommendations will change with future guideline revisions. The ISUOG guidelines were the screening reference in Romania, but national guidelines were adopted in 2019 for the 1st trimester (levocardia, situs solitus +/− 4C, and 3VT Color Doppler) and 2nd trimester (situs solitus, levocardia, 4C, LVOT, RVOT +/− 3 vessels, 3VT, and Color Doppler), and in 2020 for the 3rd trimester (4C, 3VT +/− Color Doppler) (194, 195).

This study aims to evaluate the additional role of 3VT in detecting CHD in an unselected Romanian population, with or without the use of Color Doppler, with an emphasis on CHD that could require immediate care after birth.

I.2.3.2. Materials and methods

This is a retrospective study conducted on unselected consecutive pregnant patients presenting at 11–37 weeks of gestation for a routine fetal anomaly scan in a private setting between 2019–2021. A total of 1608 fetuses were scanned (Figure II.15). We included only pregnancies with a known outcome that were scanned in their 2nd and/or 3rd trimester and

pregnancies that were scanned only in the 1st trimester due to early termination for fetal anomaly.

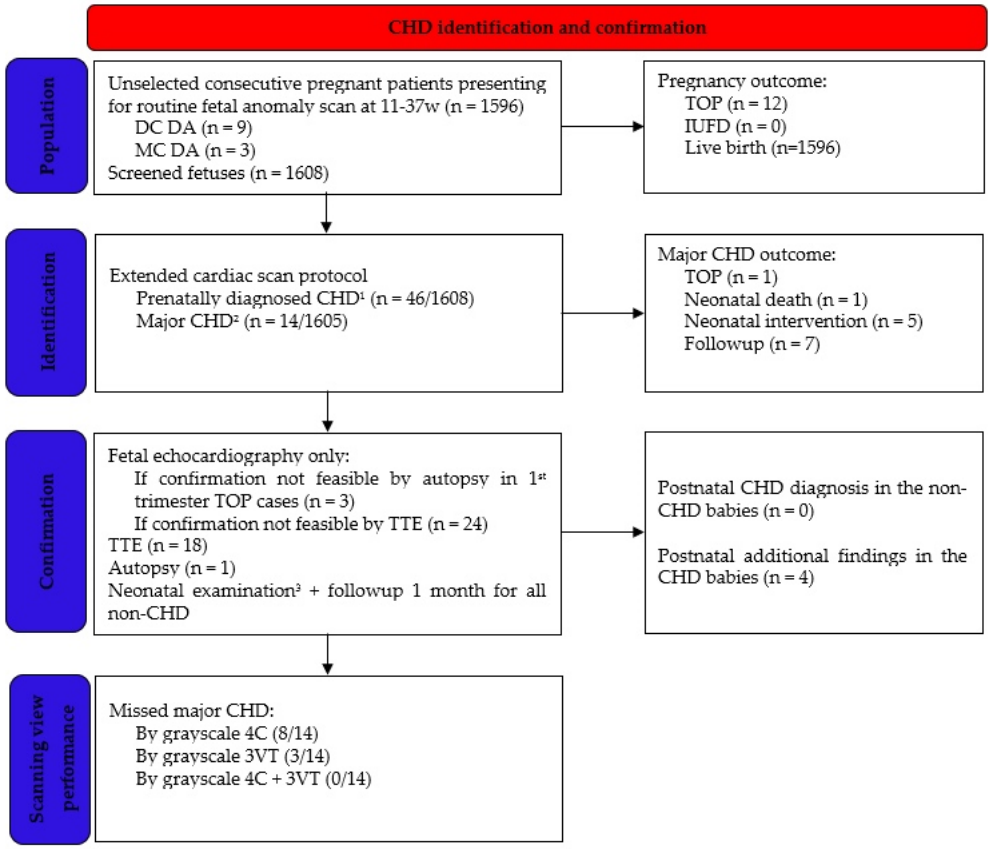

Figure II.15. Flowchart clarifying the selection of study population. [1]- Excluded CHD: cardiac rhythm disorders, persistent right umbilical vein, and umbilical vein varix. [2]- Hygroma-associated CHD with early TOP was excluded from major CHD definition (n = 3). [3]- General physical exam, heart auscultation, and preductal and postductal pulse oximetry. CHD, congenital heart disease; DC DA, dichorionic diamniotic twins; MC DA, monochorionic diamniotic twins; TOP, termination of pregnancy; IUFD, intrauterine fetal demise; TTE, transthoracic echocardiography; 4C, four chamber view; and 3VT, 3-vessels and trachea view

We collected data about demographics, ultrasound findings, prenatal genetic testing, and pregnancy outcome, by searching through the databases of the private clinics offering routine anomaly scans and of the hospitals where these patients gave birth, or by contacting patients via telephone or e-mail. We selected all cardiac/vascular anomalies detected by our scanning protocol, except for cardiac rhythm disorders, persistent right umbilical vein, and umbilical vein varix.

The scans were performed transabdominally and transvaginally by three specifically trained sonographers, using a Voluson E8, S10 or E10 ultrasound machine (GE Healthcare, Milwaukee, WI, USA), RAB6-D/RAB6-RS/RAB7-C abdominal convex probe, 2–8 MHz, or a vaginal IC9-RS 3.6–10 MHz probe. The preferred gestational age for scanning was 11–13 +6 weeks, 20–24 weeks, and 30–34 weeks.

In the 1st trimester, cardiac examination included situs, Color Doppler of the 4C and 3VT; the mandatory list also included the head (cranial vault, midline, cerebral ventricles, posterior fossa, facial profile with nasal bone, orbits with lenses, retronasal triangle, and mandibular gap), lungs, abdomen (diaphragm, stomach, kidneys, bladder, and abdominal wall), spine, limbs, and cord vessel number.

In the 2nd and 3rd trimesters, an extended cardiac protocol was followed using grayscale and Color Doppler, sweeping from abdominal situs to 4C (including Color Doppler examination of the atrioventricular septum in a horizontal orientation), left and right outflow tract, great vessels crossing, and 3VT (grayscale and Color Doppler, including a horizontal approach to further evaluate the supraaortic region for the course of the right subclavian artery and LVBC); aortic arch view, and bicaval view including identification of ductus venosus (DV). The routine anatomic survey for the 2nd and 3rd trimester also included the following elements: head (cranial vault, midline, cerebral ventricles, posterior fossa, corpus callosum, facial profile with nasal bone, orbits with lenses, lips, and nostrils), lungs, abdomen (diaphragm, stomach, gallbladder, intestine, kidneys, bladder, and abdominal wall), external genital organs, spine with cord insertion, limbs, and cord vessel number (the limbs and the abdominal wall were not mandatory in the 3rd trimester).

The allotted time for each patient was 45 min (75–90 min for twins), including history taking. The entire fetal anomaly scan lasted on average 35 min, while the cardiac examination itself took on average 10 min. Whenever protocol completion was not feasible due to inappropriate technical conditions, the patient was later rescanned. Upon fetal anomaly detection, a diagnostic ultrasound was performed by a fetal medicine specialist. Referral to a fetal cardiologist was made for all critical or ductal-dependent CHD, most likely requiring cardiac intervention shortly after birth, except for patients that opted for termination of pregnancy (TOP) after a 1st trimester diagnosis (in these cases, there was hygroma with multiple associated malformations).

The allotted time for each patient was 45 min (75–90 min for twins), including history taking. The entire fetal anomaly scan lasted on average 35 min, while the cardiac examination itself took on average 10 min. Whenever protocol completion was not feasible due to inappropriate technical conditions, the patient was later rescanned. Upon fetal anomaly detection, a diagnostic ultrasound was performed by a fetal medicine specialist. Referral to a fetal cardiologist was made for all critical or ductal-dependent CHD, most likely requiring cardiac intervention shortly after birth, except for patients that opted for termination of pregnancy (TOP) after a 1st trimester diagnosis (in these cases, there was hygroma with multiple associated malformations).

The 1st trimester TOP CHD cases were confirmed only by transvaginal ultrasound performed by a fetal medicine specialist. All 2nd trimester TOP CHD were confirmed by autopsy. All live-born babies (1596) were examined by the neonatologist in the first 3 days of life (general physical exam, heart auscultation, and preductal and postductal pulse oximetry). All children were followed up postnatally for 1 month.

All live-born babies with a prenatal CHD diagnosis underwent a transthoracic echocardiography, except for anomalies that could not be confirmed by this type of investigation, such as aberrant right subclavian artery (ARSA), persistent left superior vena cava (PLSVC), intrathymic LBCV, and DV agenesis. In addition, postnatal confirmation of atrial septal aneurysm (ASA) was not always possible due to its natural history toward physiological foramen ovale closure.

The complex/associated cardiac anomalies were classified according to the most severe or hemodynamically leading defect. CHD was considered major according to the possibility of requiring specialized care in the neonatal period. Under this spectrum, we decided to include all CHD with potential postnatal progression, such as mild pulmonary stenosis and PS; postnatal possible complications, such as extensive thrombosis from a DA aneurysm (DAA); and uncertain postnatal evolution, such as aortic coarctation. 1st trimester hygroma-associated CHD (3 cases) was excluded from the definition of major CHD, since parents usually opt for early TOP.

We evaluated the performance of the 4C and 3VT view ± Color Doppler in detecting all CHD and major CHD, respectively.

We performed a descriptive statistical analysis using Excel (Microsoft Office 2019 Professional Plus, Microsoft Corporation, Redmond, WA, USA). Continuous variables were expressed as mean ± standard deviation. Scalar variables were expressed as median and range. Categorical variables were counted and expressed as percentages.

The study was approved by the Institutional Review Board of each clinic and hospital involved (75122/2021, 25/2021, 2176/2021, 15075/2021, 15611/2021, and 10771/2021).

I.2.3.3. Results

The study population included 1596 pregnancies, with a total of 1608 fetuses (nine twin dichorionic diamniotic pregnancies and three twin monochorionic diamniotic pregnancies). There were 12 TOP for fetal anomaly: six were terminated before 15 weeks (three for hygroma with multiple structural defects, including CHD), and six were terminated at 16–22 weeks (one for isolated severe aortic stenosis). Table II.6 describes the demographics and pregnancy outcome of the 46 fetuses with prenatally diagnosed CHD (2.86% of the screened population).

Table II.6. Characteristics of the study group

Parameter	**Value**
Total patients, n	46
Maternal age, years (mean and standard deviation)	30 ± 4.85
Gravida (n%)	1 (1–4)
Nulliparity (n%)	67.3%
Male fetuses (n%)	60.4%
Syndromic/genetic (n%)	6.5% (3/46)
TOP (n%)	8.7% (4/46)
Livebirth (n%)	91.3% (42/46)
Neonatal death (n%)	2.1% (1/46)
Gestational age, weeks (mean and standard deviation)	39 ± 1.2
Birthweight, grams (mean and standard deviation)	3320 ± 497 (2250–4300)
Cesarean section (n%)	71.7%

Table II.7 lists all CHD with their ultrasound findings and associated anomalies. Only 14/1605 (0.87%) were considered major CHD: 9/14 were detected due to 3VT—aortic coarctation/hypoplastic aortic arch/interrupted aortic arch (IAoA), mild PS, tetralogy of Fallot, DAA, and D-transposition; and 5/14 were detected with grayscale 4C—severe aortic stenosis, hypoplastic left heart syndrome (HLHS), pulmonary atresia with intact ventricular septum (PA/IVS), cardiac rhabdomyoma, and hypertrophic cardiomyopathy. There was no postnatal diagnostics of genetic anomaly in CHD live births.

Some CHD-associated defects were diagnosed only postnatally: aortic valve malformation, mild supravalvular PS + facial dysmorphism, perimembranous ventricular septal defect (VSD), and hypospadias. There was no cardiac anomaly diagnosed in the first month of life in the nonCHD population.

Table II.7. Defects in 46 fetuses antenatally diagnosed with cardiac heart disease

Anomaly	Total	Associated, Prenatally [1]	Associated, Postnatally [1]	Main Suspicious View	Abnormal 3VT	1st	2nd	3rd	Detected at First Presentation
ASD type II	2	Late FGR	1 hypospadias	4C	-	0	1	1	2/2
ASA	9	1 hypoplastic aortic arch in 3rd T	1 aortic valve malformation + double ASD type II	4C	−/+	0	4	5	7/9
VSD, muscular	2	-	-	4C color	-	0	0	2	0/2
VSD, perimembranous	2	2 × T18 (hygroma + multiple defects)	-	other	-	2	0	0	2/2
AVSD, complete	1	hygroma + multiple defects (no genetics)	-	4C	-	1	0	0	1/1
Hypertrophic cardiomyopathy	1	gestational diabetes	-	4C	-	0	0	1	1/1
Left cardiac axis deviation 2	1	echogenic CSP	mild supravalvular PS + facial dysmorphism	4C	+	0	1	0	1/1
Severe aortic stenosis	1	-	-	4C	+	0	1	0	0/1
Aortic coarctation	3	1 × (hypoplastic NB and late FGR)	-	3VT	+	0	2	1	2/3
IAoA	1	perimembranous VSD	-	3VT	+	0	1	0	1/1
HLHS	1	mitral atresia + aortic atresia	-	4C	+	0	1	0	1/1
Valvular PS, mild	1	-	-	3VT	+	0	1	0	1/1
PA/IVS	1	-	-	4C	+	0	0	1	1/1
Fallot	1	-	-	3VT	+	0	1	0	1

Table legend: [1]- Structural and genetic defects. [2]- Cardiac axis normalized by the late 2nd trimester. [3]- The D-transposition had a reportedly normal 2nd trimester scan. ASD, atrial septal defect; FGR, fetal growth restriction; ASA, atrial septal aneurysm; VSD, ventricular septal defect; T18, trisomy 18; AVSD, atrioventricular septal defect; CSP, cavum septum pellucidum; PS, pulmonary stenosis; NB, nasal bone; IAoA, interrupted aortic arch; HLHS, hypoplastic left heart syndrome; PA/IVS, pulmonary atresia with intact ventricular septum; RAA, right aortic arch; ARSA, aberrant right subclavian artery; PLSVC, persistent left superior vena cava; LBCV, left brachiocephalic vein; DA, ductus arteriosus; DV, ductus venosus; 4C, 4-chamber; 3VT, 3-vessels and trachea

By analyzing the performance of the 4C and 3VT with and without Color Doppler, (Table II.8), we can see that by using only grayscale 4C we detected 47.8% of CHD, and by adding grayscale 3VT we achieved a 71.7% detection rate. Adding Color Doppler to our examination increased the detection of small septal defects (provided the septum was evaluated horizontally) and of anatomic variants, such as ARSA and intrathymic LBCV.

Table II.8. Prenatal ultrasound performance by scanning view

View	Detected CHD, All n = 46	Missed CHD, Major n = 14
Grayscale 4C only	47.8% (22/46)	57.1% (8/14)
Grayscale 3VT only	36.9% (17/46)	21.4% (3/14)
Color 3VT only	58.6% (27/46)	14.2% (2/14)
Grayscale 4C + 3VT	71.7% (33/46)	0% (0/14)

Hereafter, we present several cases of CHD with a normal 4C view but detected due to grayscale and/or color 3VT. The D-transposition was detected in the 3rd trimester, after reportedly normally crossing great vessels at the 2nd trimester anomaly scan (Figure II.16).

(**a**) (**b**)

Figure II.16. (a) D-transposition with normal 4C view; (b) Only two vessels (the aorta and the right superior vena cava) are seen on grayscale 3VT. Ao, aorta; RSVC, right superior vena cava; Tr, trachea (images from personal collection)

There was one case of interrupted aortic arch type B, with an associated malalignment VSD. Due to this association, the 4C seemed normal. On the 3-vessels view, the aorta was only slightly smaller than the pulmonary artery, but the ‘V’ was impossible to demonstrate on 3VT (Figure II.17).

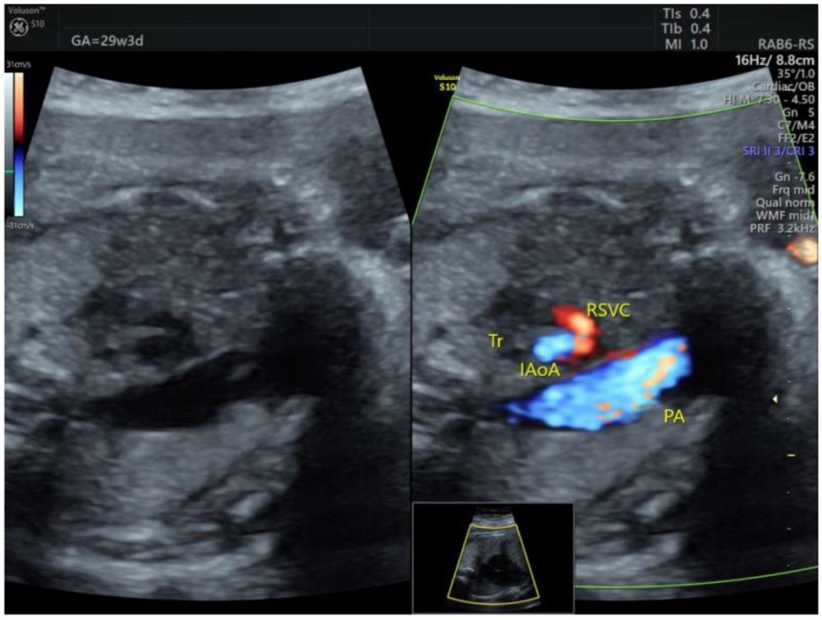

Figure II.17. Abnormal 3VT in a case of interrupted aortic arch type B with associated malalignment VSD. RSVC, right superior vena cava; Tr, trachea; IAoA, interrupted aortic arch; PA, pulmonary artery (images from personal collection)

In our tetralogy of Fallot case, there was also pulmonary atresia, so the 3VT was profoundly modified, with just a large aorta appearing instead of the 'V' (Figure II.18).

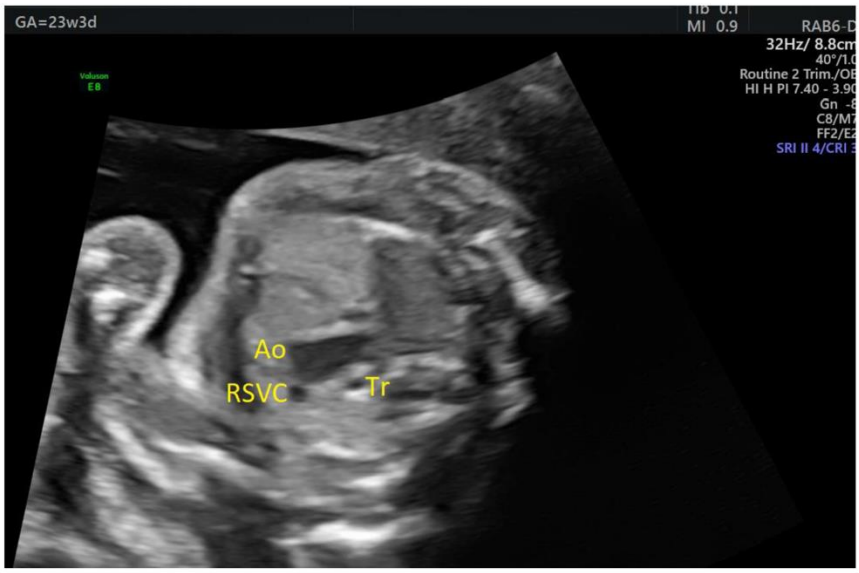

Figure II.18. Abnormal 3VT in a case of tetralogy of Fallot: there is a large aorta, and the pulmonary artery cannot be identified. Ao, aorta; RSVC, right superior vena cava; Tr, trachea (images from personal collection)

All cases of aortic coarctation were suspected due to a smaller transverse aortic arch on grayscale 3VT and confirmed by evaluating the aortic arch in a sagittal view. In one case, color 3VT seemed normal, but the transverse aorta was difficult to follow up to the DA (Figure II.19). Sagittal examination of the aortic arch demonstrated a contraductal shelf.

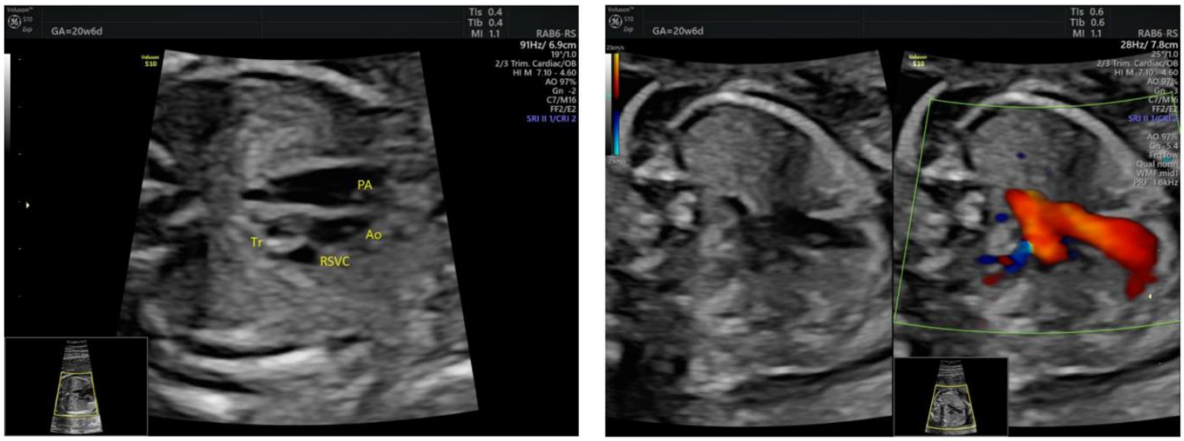

(**a**) (**b**)

Figure II.19. (a) Grayscale 3VT: the transverse aorta narrows gradually and is difficult to follow up to the ductus arteriosus; (b) Color 3VT: the aortopulmonary convergence appears normal, with great vessels seemingly having the same caliber. PA, pulmonary artery; Ao, aorta; RSCV, right superior vena cava; Tr, trachea (images from personal collection)

In one case of ASA detected in the 2nd trimester, aortic arch hypoplasia was suspected after evaluating the 3VT view in the 3rd trimester (Figure II.20). There was anterograde flow through the transverse aortic arch, but Color Doppler examination of the 4C view showed that the aneurysm became partially obstructive of the left ventricular inflow (Figure II.21). After birth, only a double atrial septal defect type II and a malformed nonstenotic aortic valve were found, so the cause of the smaller aortic arch was not certain.

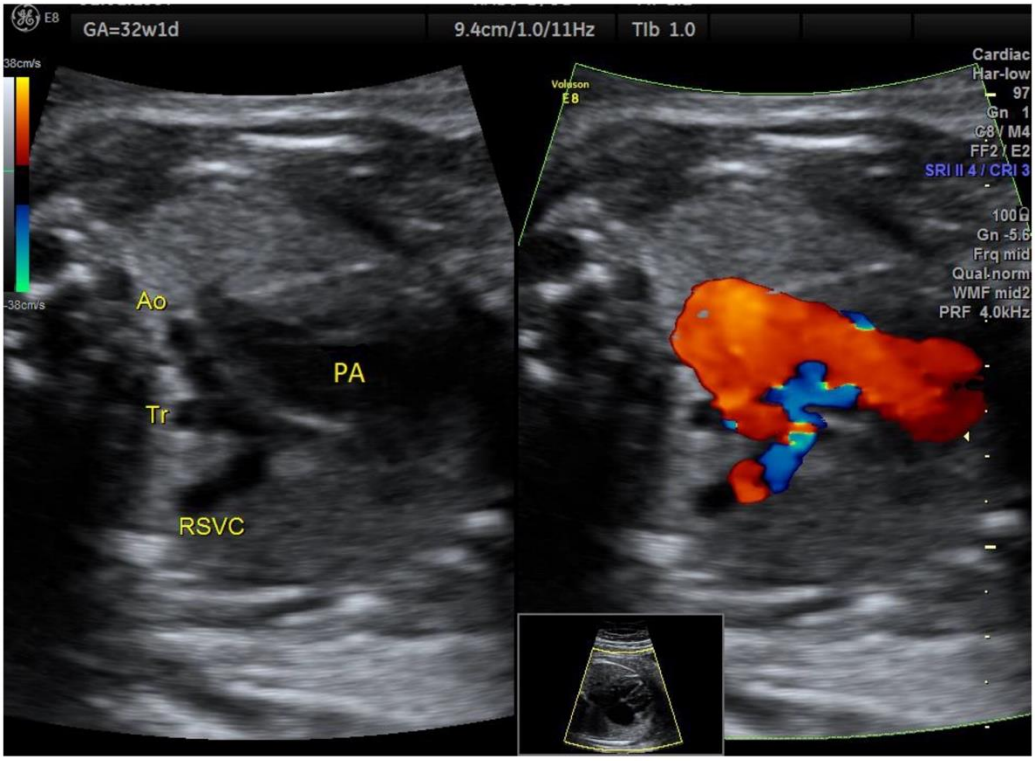

Figure II.20. Atrial septal aneurysm at 32w1d: the transverse aortic arch is smaller than the pulmonary artery on 3VT, but with anterograde flow. Ao, aorta, Tr, trachea; RSVC, right superior vena cava; PA, pulmonary artery (images from personal collection)

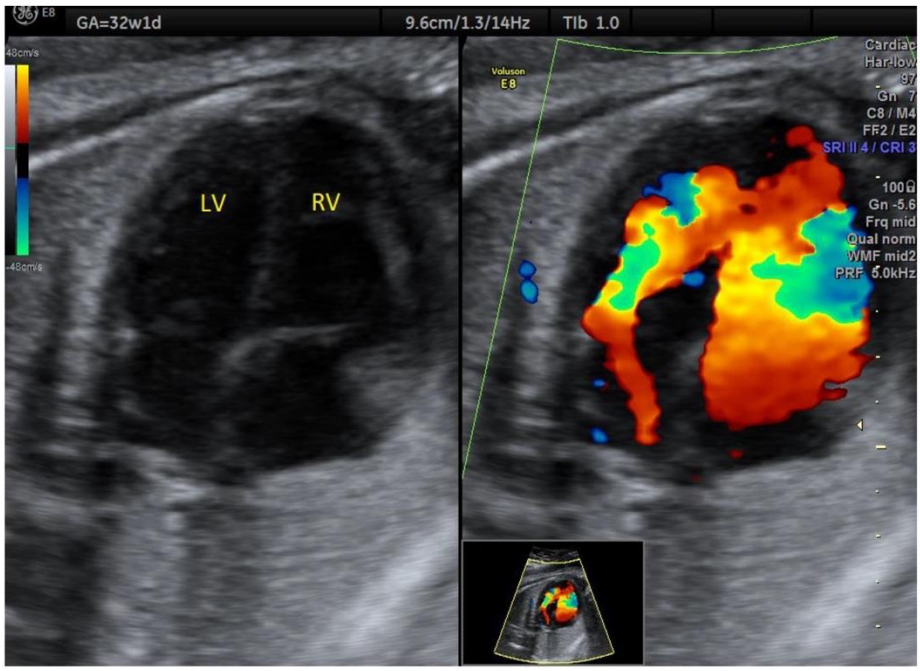

Figure II.21. Atrial septal aneurysm at 32w1d: diminished left ventricular inflow. LV, left ventricle; RV, right ventricle (images from personal collection)

We detected one case of mild PS in the 2nd trimester, based on the aortopulmonary discrepancy on grayscale 3VT (Figure II.22), which remained stable over time and had a good postnatal evolution.

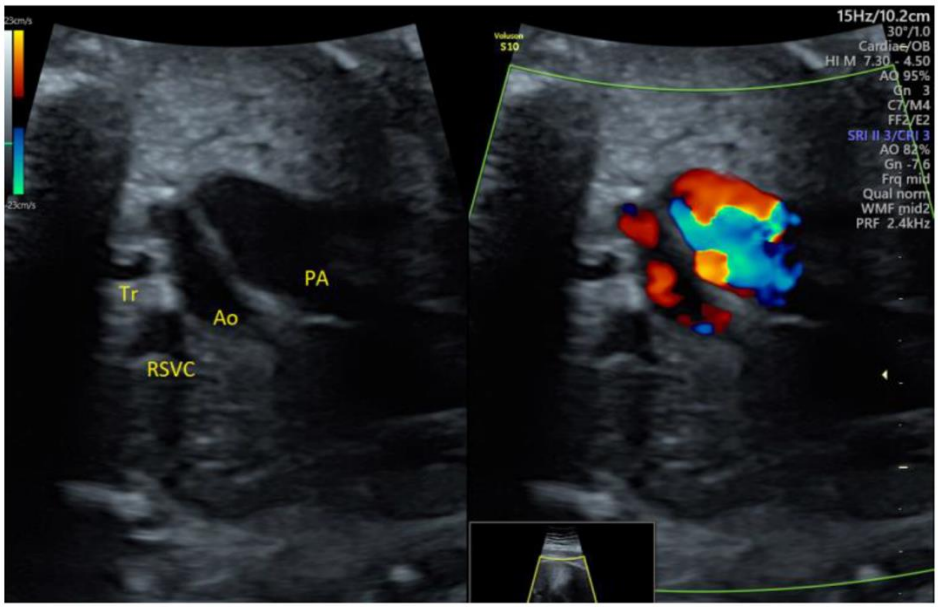

Figure II.22. Mild pulmonary stenosis stable in the 3rd trimester: enlarged pulmonary artery with turbulent flow. PA, pulmonary artery; Ao, aorta; RSVC, right superior vena cava; Tr, trachea (images from personal collection)

The DAA case diagnosed in the 3rd trimester (Figure II.23) had already presented a tortuous DA at 20w. There were no thrombotic complications before or after birth.

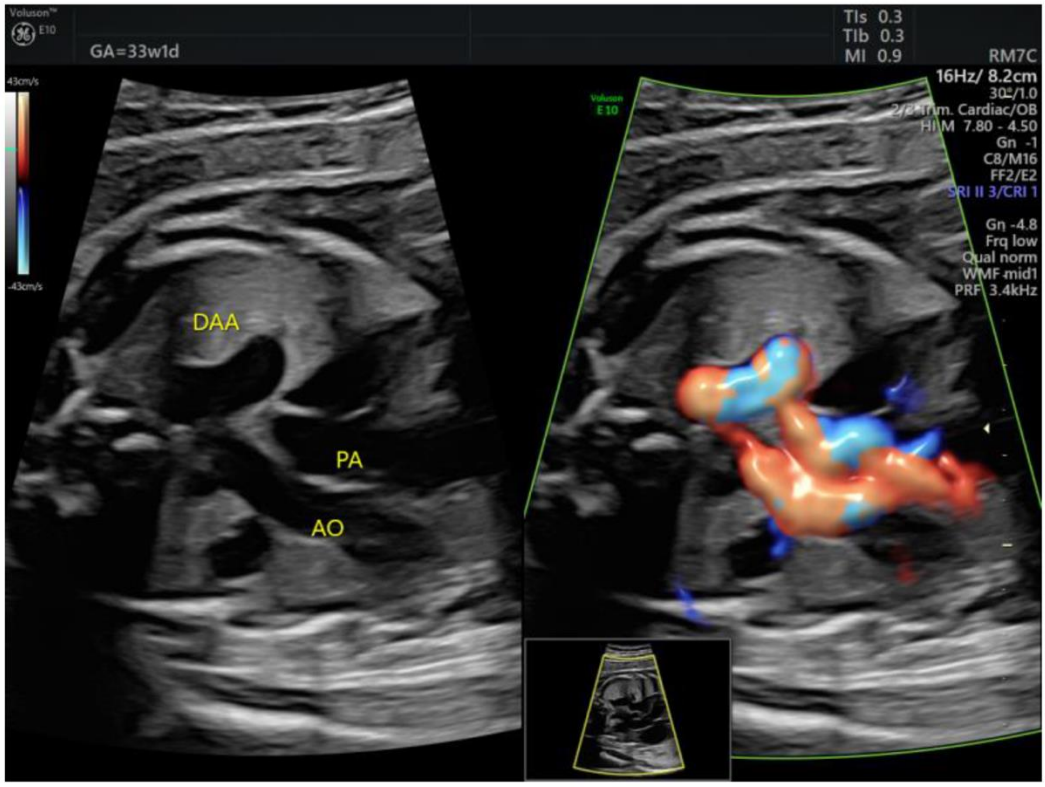

Figure II.23. The ductus arteriosus forms a tortuous loop, which is evident on grayscale 3VT. DAA, ductus arteriosus aneurysm; PA, pulmonary artery; Ao, aorta (images from personal collection)

The right aortic arch with left ductus arteriosus was detected at the 1st trimester scan (Figure II.24), and Color Doppler proved essential for early identification of this anomaly.

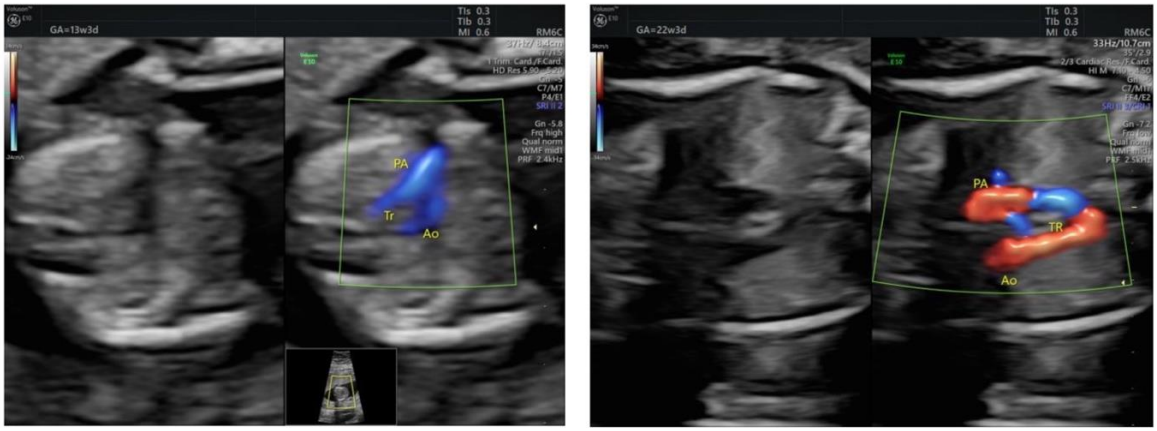

(**a**) (**b**)

Figure II.24. Right aortic arch with left ductus arteriosus showing its typical U shape on color 3VT (a) First trimester; (b) Second trimester. PA, pulmonary artery; Ao, aorta; Tr, trachea (images from personal collection)

ARSA can be identified by 3VT Color Doppler evaluation (Figure II.25). In our cohort, none of the prenatally isolated ARSA cases associated genetic anomalies, nor did they associate postnatal findings.

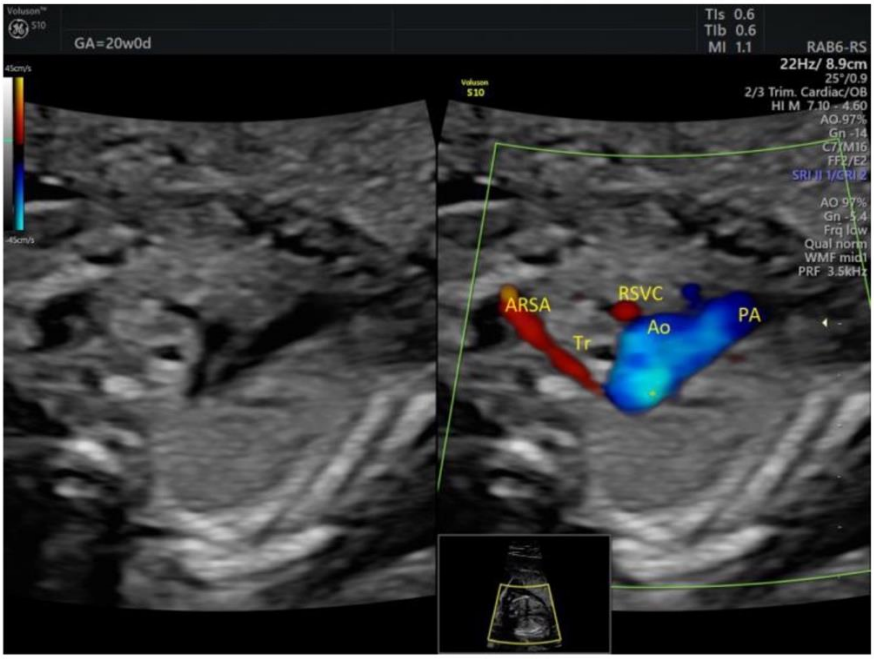

Figure II.25. Aberrant right subclavian artery coursing behind the trachea at 20w0d. ARSA, aberrant right subclavian artery; Tr, trachea; RSVC, right superior vena cava; Ao, aorta; PA, pulmonary artery (images from personal collection)

Color Doppler is also helpful in detecting PLSVC, although this can also be seen bordering the left atrium on a 4C view and on grayscale 3VT, it is easier detected upon failure to demonstrate a normal LBCV (Figure II.26). None of the PLSVC cases from our cohort associated aortic coarctation or genetic anomalies.

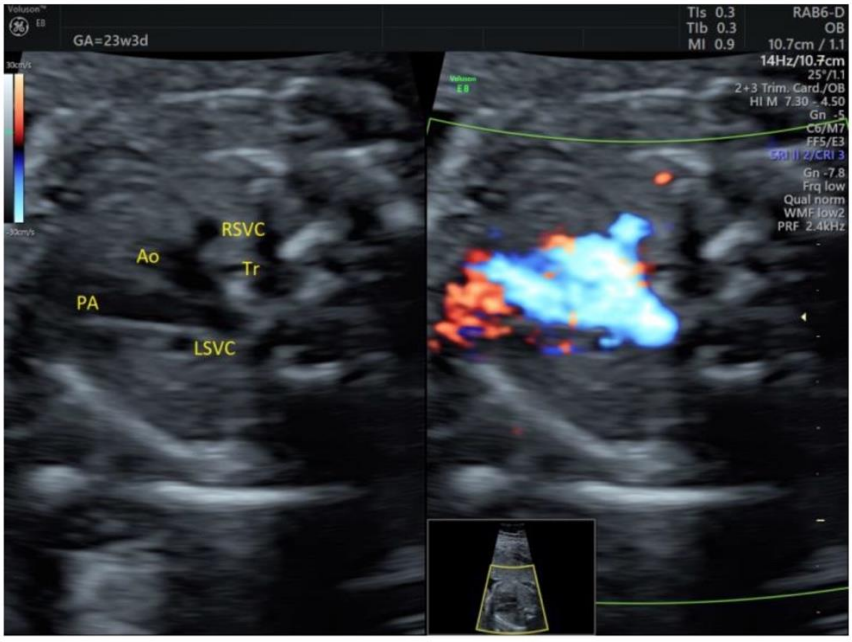

Figure II.26. Persistent left superior vena cava is identified as a fourth vessel on the 3VT view, seen on the left side of the pulmonary artery. RSVC, right superior vena cava; Tr, trachea; LSVC, left superior vena cava; Ao, aorta; PA pulmonary artery (images from personal collection)

I.2.3.4. Discussions

The overall CHD incidence was higher when compared to other studies: 2.86% versus 0.8%, mostly because minor anomalies were included, such as PLSVC, ARSA, and ASA. Our study also found a higher major CHD incidence: 0.87% versus 0.2% (182). That is partly because our definition of major CHD included some presumably nonsevere lesions, but potentially worsening after birth, such as mild PS (196, 197).

Since its introduction by Yagel, the 3VT view has been extensively studied [9,10,18,19,20] and included in the routine anatomy scan by experienced sonographers, proving its utility time and time again (198-200). Thus, a meta-analysis by Liu et al. proved that detection increases from 58% when using 4C + LVOT + RVOT to 73.5% by adding 3VT (187). Our study reports a comparable 3VT performance for detecting CHD (grayscale 4C + 3VT 71.7%).

3VT offers valuable clues leading to the diagnosis of both major and minor CHD. This study highlights the importance of 3VT in screening even without using Color Doppler. Just by adding grayscale 3VT examination to the 4C view, our study found that the detection rate increased 23.9%, with no major CHD being missed. It is noteworthy that the extra CHD detected by 3VT were outflow tract anomalies, whose outcome was significantly improved by prenatal diagnosis (D-transposition, coarctation of the aorta, and Fallot).

A simplified protocol scan using only grayscale 4C and 3VT could be employed during every scan, even when the referral reason is not an anatomic survey. This is especially useful for patients who never underwent an anatomy scan due to poor prenatal care access; for example, 78% of Romanian women underutilize free prenatal care (201). There is also a 'second opinion' benefit, for evolving CHD, such as valvular stenosis, or for missed CHD due to incorrect/incomplete initial scans, such as the D-transposition diagnosed in the 3rd trimester after a reportedly normal 2nd trimester scan.

Thus, combining 4C + 3VT proved to be a powerful tool in a low resource setting, whether that resource is available scan time, appropriate sonography training, or technical challenges.

Not only major CHD detection is of interest regarding perinatal mortality and morbidity, but also the detection of seemingly minor CHD, because of its potential evolution toward more serious CHD.

In fetal life, ASA is considered a normal evolution of an atrial septal defect toward spontaneous closure, so on postnatal echocardiograms it can present as normal, as a patent foramen ovale, or as an atrial septal defect (202).

Although generally considered a benign finding, on occasion ASA has been reported to become obstructive of the left ventricular inflow, with a consequent evolution toward mild left ventricle and aortic arch hypoplasia (203), so close follow up is advisable. This also happened in one of four ASA detected by our study in the 2nd trimester; fortunately, postnatal hemodynamic changes led to a nonobstructive ASA.

A tortuous DA is usually a minor ultrasound finding and considered a normal variant, but it is worth following up due to its potential evolution toward restrictive DA or DAA (204). In our series, there was no restrictive DA, but a tortuous DA detected in the 2nd trimester developed into a DAA in the 3rd trimester.

DAA can be associated with connective tissue disease (205) and can become complicated by prenatal thrombosis (206) or postnatal extension of the DA thrombus (whose formation is a physiologic event in order for the DA to close) to the adjacent pulmonary artery (207) or to the descending aorta (208). Thus, an antenatal diagnosis of DAA ensures a proper follow up, with planned delivery in a specialized center where surgical treatment is available.

Studying 4C and 3VT in grayscale is easy to learn and not time consuming. Because these are transverse views, one must just sweep cephalad from the upper abdomen, which is already routinely used to estimate fetal weight. In our opinion, under acceptable technical conditions, adding grayscale 4C and 3VT to a biometry scan would increase the examination time by maximum 1 min.

There are some pitfalls in using 3VT in routine anatomy scans in a low-risk population. 3VT also detects normal variants, mostly being asymptomatic; however, they still increase parental anxiety, especially in ARSA or PLSVC cases when genetic anomalies are brought into question (209, 210). Genetic testing is questionable if the ultrasound marker is isolated; our study did not demonstrate 'hidden' anomalies for isolated ARSA/PLSVC.

Although reported as easy to obtain and to interpret, sometimes a 'perfect V' cannot be easily obtained; that is, the aortopulmonary convergence is difficult to demonstrate, as if the transverse aorta and the DA were not in the same plane, and this can mislead the inexperienced sonographer to false-positive findings. However, if their caliber is rather equal all the way up to the descending aorta, even if not obvious in the same plane, there is no abnormality; the reason is either an incidence artifact or a tortuous DA, which is more obvious and frequent in the 3rd trimester (211).

Moreover, 3VT increases the cost of CHD screening as reflected by increased screening time if technical conditions are difficult and increased referrals to maternal–fetal units. Increased referral is also stressful for the parents and puts an extra burden on services that provide diagnostic ultrasound; however, all significant CHD detection is worthwhile, whether it is syndromic or requiring specialized postnatal care.

Lastly, 3VT cannot completely replace LVOT and RVOT examination, since it does not directly evaluate the aortic and pulmonary valves, valvular stenosis being among the most common CHD (182). As proven by the postnatal findings of this study, one mild PS and a malformed aortic valve were missed prenatally.

The strength of this study is the use of an extended scan protocol on an unselected population, thus detecting more cardiac and extracardiac anomalies than standard screening. Since most studies of extended cardiac examination performance are conducted on selected populations (either at risk for CHD or with suspicious screening results) (187), this study reflects more accurately the CHD frequency in an unselected fetal population. Also, some of these anomalies would be detected earlier according to our protocol. To our knowledge, this is the first study to report the routine use of 3VT in an unselected Romanian population.

There are several limitations to this study. There is an inclusion bias since private care is generally accessed by lower risk patients. Another study limitation is that children from the study population were followed up to 1 month, and there was no systematic postnatal echocardiographic examination, so there could be undetected CHD in our population.

In our study, the scans were performed by experienced sonographers, who are very familiar with 3VT and go beyond the minimal guideline recommendations and routinely use the ISUOG recommended 5-planes sweep, with an allotted screening time longer than in public settings (45 min versus usually 30 min).

Due to their experience in using 3VT (but also extra cardiac views), it is possible that that detection rates would be lower for inexperienced sonographers. Moreover, routine pulsed-wave Doppler was not used across the cardiac valves, so aortic/pulmonary stenosis may have been missed.

I.2.3.5. Conclusions

Fetal echocardiography can accurately diagnose most CHD, but it is not reasonable to expect experts to perform all screening scans. Ultimately, CHD detection relies on referral from screening sonographers, who apply simple and time-efficient protocols. For outflow tract anomalies, sonographer training is of utmost importance. A chain is as strong as its weakest link, so proper education of first-line sonographers is pivotal in improving prenatal CHD detection.

3VT proves ideal for CHD screening because it is fast to obtain, easy to learn, and sufficient to raise suspicion of outflow tract abnormality with subsequent referral to a specialist. In our opinion, grayscale 4C + 3VT is the perfect combination to screen for CHD: as shown by this study, no major anomaly would be missed by using this technique, even without the use of Color Doppler.

Chapter 3: Thrombosis and pregnancy

I.3.1. State of art

Thrombosis, or the formation of blood clots within the circulatory system, is a serious complication that can occur during pregnancy. Venous thromboembolism (VTE) is the most common type of thrombosis seen during pregnancy, and it encompasses both deep vein thrombosis (DVT) and pulmonary embolism (PE). The incidence of VTE in pregnant women is estimated to be approximately 1 in 1,000 (212).

Several risk factors contribute to the development of VTE during pregnancy, including a previous history of VTE, obesity, older maternal age, Cesarean delivery, and certain medical conditions such as thrombophilia (an inherited or acquired tendency to form blood clots) (213). The use of assisted reproductive technologies and multiple gestations also increase the risk of VTE during pregnancy.

Anticoagulation therapy is the mainstay of treatment and prevention of VTE during pregnancy. Low molecular weight heparin (LMWH) is the preferred anticoagulant as it has been shown to be effective and safe in pregnant women (214). Other anticoagulant medications such as unfractionated heparin (UFH) and warfarin are generally avoided due to their potential adverse effects on the developing fetus.

There has been significant research in recent years to improve the diagnosis, management, and prevention of VTE during pregnancy. The American College of Obstetricians and Gynecologists (ACOG) and the Royal College of Obstetricians and Gynecologists (RCOG) have both published guidelines for the management of VTE during pregnancy (215, 216). These guidelines emphasize the importance of risk assessment, appropriate prophylaxis, and prompt treatment of VTE in pregnant women.

In addition to medical management, lifestyle modifications such as regular exercise and healthy eating habits can also reduce the risk of VTE during pregnancy (217). Patient education and awareness of the signs and symptoms of VTE are also essential for early detection and prompt treatment.

Overall, while VTE remains a significant complication of pregnancy, advances in research and medical management have improved outcomes for pregnant women at risk for thrombosis. Ongoing efforts to refine risk assessment, prophylaxis, and treatment will continue to improve outcomes for pregnant women with VTE. This chapter will outline the influence of thrombotic disorders over the obstetrical and reproductive outcomes, as well as the DVT management during pregnancy.

Personal contributions:

1. Filip C, Socolov DG, Albu E, Filip C, Serban R, **Popa RF**. Serological Parameters and Vascular Investigation for a Better Assessment in DVT during Pregnancy-A Systematic Review. Medicina (Kaunas). 2021 Feb 10;57(2):160. doi: 10.3390/medicina57020160. PMID: 33578903; PMCID: PMC7916726.
2. Adam A-M, **Popa R-F**, Vaduva C, Georgescu CV, Adam G, Melinte-Popescu A-S, Popa C, Socolov D, Nechita A, Vasilache I-A, Mihalceanu E, Harabor A, Melinte-Popescu M, Harabor V, Neagu A, Socolov R. Pregnancy Outcomes, Immunophenotyping and Immunohistochemical Findings in a Cohort of Pregnant Patients with COVID-19—A Prospective Study. Diagnostics. 2023; 13(7):1345. https://doi.org/10.3390/diagnostics13071345
3. Maftei R, Doroftei B, **Popa R**, Harabor V, Adam AM, Popa C, Harabor A, Adam G, Nechita A, Vasilache IA, Mihalceanu E, Bivoleanu A, Lunguleac G, Cretu AM,

Armeanu T, Diaconu R, Cianga P. The Influence of Maternal KIR Haplotype on the Reproductive Outcomes after Single Embryo Transfer in IVF Cycles in Patients with Recurrent Pregnancy Loss and Implantation Failure-A Single Center Experience. J Clin Med. 2023 Feb 28;12(5):1905. doi: 10.3390/jcm12051905. PMID: 36902692; PMCID: PMC10004330.

I.3.2. Serological parameters and vascular investigation for a better assessment in DVT during pregnancy—a systematic review

I.3.2.1. Introduction

Deep vein thrombosis is an important medical problem, especially for women of childbearing potential. Deep vein thrombosis means the formation of a blood clot in the deep veins, especially in the lower limbs and only occasionally in the upper limbs.

The symptoms of the disease are swelling of the affected limb accompanied by pain, and redness and heat in the affected area, but almost half of the cases have no symptoms (218). Severe complications of the disease are pulmonary embolism and post-thrombotic syndrome. The occurrence of DVT can be idiopathic or as a result of risk factors such as contraceptives, obesity, surgical maneuvers, trauma, and so forth.

Venous thrombosis can be occlusive (acute) and non-occlusive (less symptomatic/asymptomatic) or chronic if it is symptomatic and persists for more than 10 days (219). Regarding the affected area, DVT is classified as proximal (ilio-femoral) when it is located above the knee and distal (in the leg) when it is located below the knee. In most cases DVT develops in the leg or thigh of the popliteal or ilio-femoral vein and evolves in the direction of venous flow to the heart and can reach the inferior vena cava (220).

An important aspect of DVT is a different pathophysiology compared to arterial thrombosis. Arterial thrombosis occurs as a result of a vascular wall injury in an environment with a normal oxygen content. The arterial clot contains a significant percentage of platelets. In contrast, DVT may occur in the absence of vascular damage in a low-oxygen environment. The venous clot contains mainly erythrocytes and fibrin but also white blood cells and platelets. The presence of white blood cells, which play an important role in the adhesion of cells to the surface of the endothelium, indicates an inflammatory phenomenon in the formation of clot (221). Hypoxemia, increased by venous stasis, activates certain cellular mechanisms that induce the association of monocytes with endothelial proteins, thus promoting clot formation (222).

In pregnancy, the deep vein thrombosis is characterized by the Virchow triad: venous stasis, hypercoagulability, and endothelial damage. Deep vein thrombosis is not a frequent complication but is a very serious medical problem. While in underdeveloped countries mortality at birth is caused by hemorrhage, in developed countries mortality is caused by the thromboembolic complications (223).

During pregnancy, DVT can be caused by prolonged rest/immobilization or obesity. Other responsible factors are preeclampsia, varicose veins, multiple pregnancies, and hereditary or acquired thrombophilia.

The frequency of DVT is similar over the three trimesters of pregnancy but increased in the first six weeks postpartum (223). Deep vein thrombosis associated with pulmonary thromboembolism is known as venous thromboembolism. In pregnancy the risk of venous thromboembolism is 5 times higher (224), and for the case of associated hereditary, thrombophilia is up to 30 times higher (218, 225).

Nowadays the first pregnancy currently occurs in older ages. In many cases, the age for the first pregnancy has moved to 35–45 years, so the number of pregnancies obtained through fertilization has constantly increased. We can say that these aspects characterize a so-called "contemporary pregnancy". Therefore, the contemporary pregnancy characterized by old age and/or assisted reproduction presents the following thrombotic risks: hyperstimulation that generates high levels of estradiol, which promotes hemoconcentration and immobilization, which favors hypercoagulability, which promotes DVT.

Regarding the location of the injured area and the moment of occurrence of DVT, literature indicates some particularities of DVT as follows (220):

- in more than 88% of cases, it affects the left lower limb as a result of the compression on the left common iliac vein accentuated by the growth of the uterus (224);
- it occurs most commonly in the third pregnancy trimester on the ilio-femoral vein;
- localization above the groin is much more common compared with other non-pregnant DVT patients;
- it frequently occurs, postpartum, in the first six weeks after birth.

I.3.2.2. Materials and methods

The literature search was done on Pub Med, ScienceDirect, Google Scholar, DOAJ, UpToDate in the last 20 years. Literature selection was made based on keywords: venous thromboembolism, pulmonary embolism, anticoagulants, thrombophilia.

The inclusion criteria covered the following aspects: reviews on basic pathophysiology, clinical evaluation in DVT, serological parameters currently used in the evaluation of DVT, serological parameters useful in the assessment of DVT envisaged for implementation, anticoagulant therapy.

The exclusion criteria were: normal non-DVT pregnancy, thrombosis and venous stroke, upper extremity thrombosis, surgical therapy of DVT during pregnancy, DVT pregnancy associated with non-thrombophilia pathology.

I.3.2.3. Epidemiology

Normal pregnancy and the postpartum period represent a condition characterized by a thrombotic predisposition. The hypercoagulable physiological state of pregnancy and postpartum seems to prevent blood loss during pregnancy and excessive bleeding at birth. For this reason, pregnant women develop DVT five times more frequently than non-pregnant women (218).

For patients with no thrombotic event in history, the overall incidence of DVT in pregnancy is up to 2/1000 (226). During normal pregnancy, the frequency of thrombosis is similar in all three trimesters. The frequency of thrombotic event is much higher in pregnancy with associated risk factor, such as: inherited or acquired thrombophilia, history of thrombosis, antiphospholipid syndrome, lupus (218).

Other independent risk factors are age 35 and older, zero parity, multiple pregnancies, obesity and immobility, which increase the risk by 1.5–2 times (222). Assisted reproduction is considered a risk factor, as it increases up to 10 times compared to natural pregnancy (218, 224). Finally, the postpartum period (six weeks) has an increased risk of DVT with an incidence up to 10 times higher compared to natural pregnancy (218).

I.3.2.4. Laboratory assessment of DVT

It is well known that normal pregnancy is associated with a hypercoagulation state generated by the modification of the serum concentration of specific parameters. Thus, coagulation factor II, VII, X, prothrombin, fibrinogen, and its degradation products (D-dimer) are increased. On the contrary, the fibrinolytic activity of the specific proteins involved in the process, such as protein C and protein S, is decreased.

This hypercoagulation state promotes thrombosis, but in normal pregnancy there are isolated acute events. If in the pregnant state additional factors that promote coagulation are added, the risk of a severe thrombotic event suddenly increases. Risk factors that promote DVT include: history of thrombotic event, thrombophilia (antithrombin deficiencies, antiphospholipid antibodies, Leiden factor V, methylenetetrahydrofolate reductase (MTHFR), etc.), use of contraceptives, and prolonged immobilization.

Particular situations such as older age and assisted reproduction can also be risk factors for a DVT occurring event. The literature specifies that, in the previously presented situations, the risk of DVT increases 1.5–2 times (224, 225).

For patients with no thrombotic event in history, the overall incidence of DVT in pregnancy and the puerperium is up to 2/1000 (226), thus supplementary tests for thrombophilia are not consider mandatary. On the contrary, laboratory investigation of thrombophilia is compulsory for the following pregnant patient categories: family history of DVT events in first-degree relatives (227, 228), patients with previous different thrombotic event, suspicion of antiphospholipid syndrome. During pregnancy, for all pregnant women with thrombophilia and for those in older age or in assisted reproduction pregnancies, the detection of DVT risk as early as possible prevents acute events such as miscarriage and allows the identification of patients who have contraindications to antithrombotic therapy.

Therefore, for a reliable assessment of a possible deep vein thrombosis event, two aspects must be followed: firstly, the evaluation of the coagulation/fibrinolysis parameters, and secondly, the determination of the extent of the contribution of the particular risk factors such as thrombophilia.

To estimate the level of risk of DVT during pregnancy, laboratory tests should follow a few steps to maximize the accuracy of the diagnosis.

A first step refers to the medical history of the patient that can highlight any medical event that may be associated with a disturbance of the coagulation–fibrinolysis balance. The medical history of the patients must be as complete as possible and must contain information about a possible antithrombotic therapy.

The second step regards the routine coagulation tests that include: fibrinogen, prothrombin time, thrombin time, activated partial thromboplastin time, fibrinogen and D-dimers. The purpose of this first group of analyses is to determine whether the patient has one or more of the risk factors that can trigger a DVT event (226). In the case of a positive test, the third step is the determination of the individual thrombophilia risk factors previously identified. The method/methods used for the individual risk factor determination must be selected according to the specificity and sensitivity of the method. The acquired data will be correlated to assess the extent of the DVT risk. A reliable assessment will facilitate the decision to choose the appropriate therapy to be followed.

For the evaluation of the coagulation/fibrinolysis balance in DVT, the following are currently determined: prothrombin time (PT), activated partial thromboplastin time (APTT), fibrinogen and D-dimers.

Currently for the diagnosis of DVT, the determination of D-dimers is considered the most reliable diagnosis tool in non-pregnant patients (229). D-dimers are produced after fibrinogen degradation under plasmin activity. They are generated when coagulation cascade

is activated. Regarding the determination of D-dimers during pregnancy, numerous studies (230, 231) indicate different reference values of D-dimers depending on the trimester of the pregnancy. Thus, plasma concentration of D-dimers increases progressively during pregnancy (232) with poor predictive value in excluding the diagnosis of deep vein thrombosis. Although there is some consensus in this regard, some authors believe that the risk of thromboembolism can be ruled out with certainty if D-dimer values are negative and compression duplex ultrasonography is normal and thus, the test presents high efficacy for the negative prediction of DVT rather than the positive one (191, 233).

During labor, D-dimers usually increase significantly, after which they decrease rapidly at three days postpartum and slowly return to normal values four weeks later. From this moment on, the test regains its usefulness. However, recent studies show that the onset of postpartum hemorrhage is preceded by hyperfibrinolysis. If D-dimers do not return to normal or their concentration increases, then postpartum hemorrhage should be considered (234).

If, after routine determination of the coagulation–fibrinolysis balance, one or more individual risk factors are identified, the laboratory investigation of the individual thrombophilia will begin.

In cases of inherited or acquired thrombophilia, the classification of the risk of DVT as small, moderate, or severe is of clinical importance (235-237) because it allows the individualization of therapy. As not all thrombophilia investigations are affordable or routine tests, the selection of the pregnant patients to be tested should be considered. A first strategy is that once a risk factor is identified, all known risk factors should be investigated.

Laboratory investigations of thrombophilia include the following individual risk factors: activated protein C resistance and V Leiden factor, prothrombin G20210A mutation, antithrombin deficiency, proteins C and S deficiencies, antiphospholipid antibodies, increased factor VIII level, as shown in Figure III.1, and hyperhomocysteinemia. In order to exclude false-positive results, specific confirmations are requested, as follows: mandatory repeating testing for antiphospholipid antibodies, increased factor VIII level, hyperhomocysteinemia or measurement of specific antigen for antithrombin deficiency, proteins C and S deficiencies.

For the inherited thrombophilia caused by deficiencies of activated protein C resistance and factor V Leiden or prothrombin G20210A mutation, literature shows that the associated risk of developing DVT is considered low for heterozygosity and highest for homozygosity (239). Thus, the most appropriate method of investigation is supposed to be DNA analysis. Because the DNA test is not routine, the first diagnosis is established based on the functional test for the activated protein C resistance and factor V Leiden. If a positive result occurs, then the DNA analysis is performed.

The inherited thrombophilia may occur in the deficiency of three individual risk factors: antithrombin, protein C, and protein S. From the clinical point of view, these parameters are considered as being very reliable markers for a moderate risk of DVT (239). The protein deficiencies come from two different causes: a low synthesis that generates insufficient quantities of the protein or a low quality of the synthesized protein that generates poor activity. As a consequence, two ways of investigation are available to determine these deficiencies: a functional test that assesses the activity and the immunoassay test that assesses the quantity of these proteins. As a general rule, both tests are performed in order to avoid a false-positive test. The deficiencies of all these tree proteins are rare, but among them antithrombin and protein C are considered a preponderant hereditary thrombophilia risk factor.

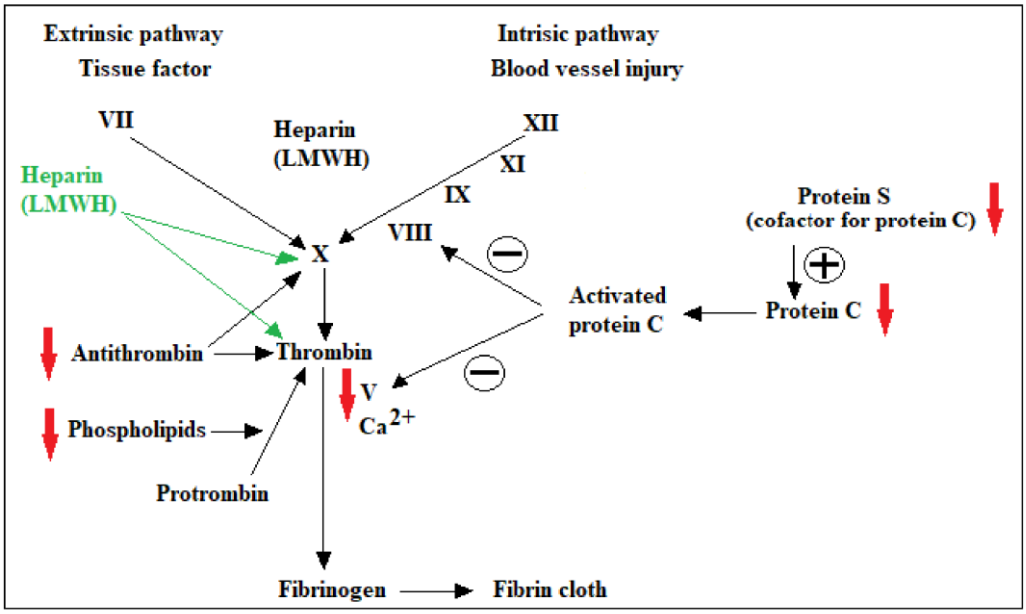

Figure III.1. Specific proteins of the coagulation cascade that can become risk factors in acquired or inherited deficiencies, thus promoting hypercoagulation. Targeted factors for antithrombotic therapy. Adapted after Turpie et al. (238)

Another thrombophilia risk factor is the presence of antiphospholipid antibodies that trigger the antiphospholipid syndrome. Antiphospholipid syndrome is considered one of the important thrombophilia risk factors. It is involved in both arterial and venous thromboembolism and in miscarriage as well. In patients with a history of recurrent pregnancy loss, old age, and assisted reproduction, the earlier assessment of antiphospholipid antibodies is recommended in order to establish and to start the appropriate therapy. To avoid false-positive results, the laboratory determination should be performed twice at a distance of about 12 weeks.

Hyperhomocysteinemia (HHC) is another thrombophilia risk factor. HHC is characterized by increased concentration of homocysteine (HC) in plasma, and is associated with both venous and arterial thrombosis (240-243). It is generally accepted that HHC disrupts normal endothelial functions, which are the relaxation of blood vessels and the state of anticoagulation of the blood, thus disturbing coagulation–fibrinolysis balance (244, 245). Hyperhomocysteinemia is caused by an inherited or acquired deficiency of the enzymes involved in its metabolism (methylenetetrahydrofolate reductase or cystathionine beta synthetase) or a deficiency of vitamins belonging to the group of B vitamins.

Based only on serological routine factors and on additional individual risk factor, Dargaud et al. (246) proposed a Lyon DVT score in order to assess as accurately as possible the risk of the DVT event. Lyon DVT score indicates the severity and the initiation of the therapy as follows: <3 there is no antenatal prophylaxis; 3–5 LMWH starting on the third trimester; ≥6 LMWH starting during the first trimester (VTE, venous thromboembolism; DVT, deep venous thrombosis; LMWH, low-molecular-weight heparin) (246).

I.3.2.5. Clinical vascular evaluation of DVT

During pregnancy, a large number of women experience vascular events that are generally moderate such as superficial varicose veins, or more important ones such as compression of the abdominal vessels as a result of the evolution of pregnancy. Acute events that may also occur, although less frequent, are of major importance and life threatening.

Acute thrombotic events mainly include venous thromboembolism and post-thrombotic syndrome. The DVT investigation from the vascular point of view includes the same steps that can not only improve the diagnosis but also detect earlier a hidden pathology.

From the vascular point of view, DVT detection can be accomplished by the following steps:

- the examination of the lower limbs should be performed on both the whole limb and on segments, for patients with suspicion/risk of DVT (according to current literature recommendations (247).

- examination by ultrasonography as the first line of investigation in DVT due to lack of risks. It is less sensitive than venography but it is an affordable and available tool. Even so, it has low accuracy in pelvic vein thrombosis. Although ultrasonography is the main DVT method of determination, magnetic resonance imaging (MRI) is recommended when ultrasound is inconclusive and the clinical symptoms persist. A high-quality study (248) shows that the prevalence of venography over ultrasonography in DVT identification in asymptomatic patients is about 22%. Even so, the study concluded that particularly for the proximal veins, ultrasound is accurate in diagnosing DVT in asymptomatic patients having a 95% confidence. For the distal vein, the ultrasound accuracy in DVT detection is inconclusive due to anatomical particularities.

- examination of venography only where other investigations are inconclusive. Venography is generally accepted as the gold standard in detecting DVT. Its limitation comes from the invasive method of investigation, and thus non-invasive diagnostic tests like ultrasound replace venography in routine screening for DVT, particularly in pregnant patients. In conclusion, the ultrasound investigation is the gold standard in particular cases of pregnancy.

Comprehensive information on the tools used by clinicians to detect and assess the extent of a thrombotic event, including DVT, in patients of all categories, including coronavirus disease-2019 patients, can be found in the literature (249-252).

In conclusion, a general summary for the clinical DVT investigation in pregnancy is presented in Figure III.2.

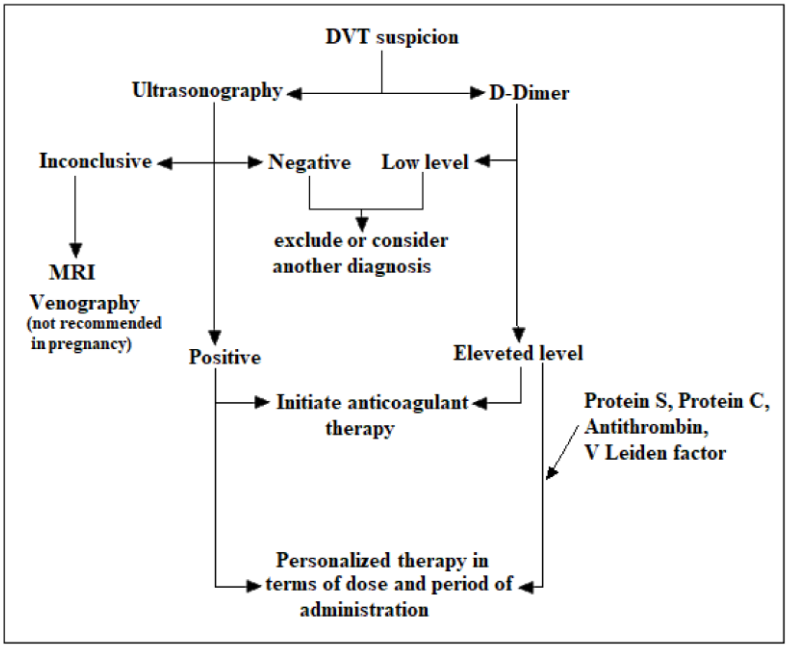

Figure III.2. Clinical and serological investigation of deep vein thrombosis (DVT) in pregnancy. Adapted after Khan et al. (253)

I.3.2.6. Diagnosis and therapeutic steps

The diagnosis of DVT is generally made on clinical grounds. The most common symptom of DVT is swelling and discomfort in the lower extremities in the absence of trauma as shown in Table III.1. DVT can be present in normal and complicated pregnancies as well as in the postpartum period.

Table III.1. Symptomatology of DVT

Symptoms and Signs of Deep Venous Thrombosis
Leg swelling
Leg pain or discomfort and walking difficulty
Increased temperature and edema
Tenderness
Lower abdominal pain (sometimes associated)

The clinical diagnosis is accompanied by laboratory tests that, in this case, aim to highlight particular situations such as thrombophilia.

D-dimer represents the choice analysis of screening in thrombophilia and has a high negative predictive value. However, D-dimer levels increase during normal or complicated pregnancy as well as in the postpartum period, which makes this parameter less reliable. For this reason, the investigation of fibrinolytic-specific parameters, presented in Table III.2, appears to be mandatary particularly in thrombophilia.

Table III.2. Blood/serum investigation in DVT diagnosis

Blood and Serum Modification in Deep Venous Thrombosis Tests/Measurements
Elevated white cell count
Prothrombin time (PT) and a partial thromboplastin time (PTT)
Homocysteine levels (to detect inherited or acquired deficiencies)
Factor V Leiden and prothrombin (factor II) 20210 mutation (to detect inherited risk factors)
Protein C and protein S (to detect inherited risk factors or deficiency in blood clotting factors)
Lupus anticoagulant testing (to diagnose antiphospholipid syndrome)

I.3.2.7. Therapeutic steps during pregnancy

Anticoagulation with heparin is the therapy of choice in DVT. However, the choice of treatment must take into account certain particular factors/steps:

Before initiating treatment, laboratory tests must establish the thrombophilia state. Although a positive result does not significantly influence the therapy, the type of thrombophilia may influence the doses and duration of anticoagulants.

DVT treatment must prevent not only the thromboembolism but also prevent PTS? The renal condition is decisive in choosing the type of anticoagulant. Thrombolytic therapy with plasminogen activators (tPA, urokinase, and streptokinase) is relatively contraindicated in pregnancy because of the theoretical risk of massive abruption.

International experts from the National Institute of Health Care and Excellence (NICE) established the general guidelines for antithrombotic therapy including pregnant patients (254, 255). The guidelines contain indication for deep vein thrombosis as well as pulmonary embolism (PE).

I.3.2.8. General guidelines in DVT and PE

In case of suspicion of DVT or PE, the optimal moment for the early initiation of anticoagulant treatment will be decided, so that it can continue even after the diagnosis is confirmed. In March 2020, direct-acting anticoagulants and some low-molecular-weight heparins (LMWH) were considered off-label for indication in the treatment of suspected cases of DVT or PE (256).

Before initiating the anticoagulant therapy, biological tests must be performed (complete blood count, renal and hepatic function, prothrombin time, activated partial thromboplastin time) and anticoagulation must be initiated until results are received and doses adjusted accordingly within the next 24 h (257).

In confirmed cases of DVT or PE, anticoagulant therapy is performed for three months. Comorbidities (obesity, hemodynamic instability, neoplasms, renal failure, antiphospholipid syndrome) are taken into account when initiating anticoagulant treatment (257).

Either apixaban or rivaroxaban should be indicated in patients with proximal DVT or confirmed PE (258). If they are not available, LMWH will be administered for at least five days followed by dabigatran or edoxaban or LMWH simultaneously with a vitamin K antagonist (VKA) for at least five days or until the international normalized ratio (INR) is at least 2.0 in two consecutive readings, followed by VKA monotherapy. Unfractionated heparin (UFH) is usually not associated with a VKA for the proximal DVT or confirmed PE therapy, except in cases of renal impairment or an increased risk of bleeding.

In patients with proximal DVT or PE both confirmed and with renal impairment (creatinine clearance estimated between 15 mL/min and 50 mL/min), one of the following will be chosen (258): (a) apixaban, rivaroxaban, LMWH for at least five days, followed by edoxaban or (b) dabigatran if the estimated creatinine clearance is 30 mL/min or greater, (c) LMWH or UFH, co-administered with a VKA for at least five days or until the INR is at least 2.0 in two consecutive determinations, followed by a VKA monotherapy.

In patients with proximal DVT or PE both confirmed with pre-existing renal impairment (estimated creatinine clearance less than 15 mL/min), choose one of the following (258): (a) LMWH, UFH, LMWH or (b) UFH simultaneously with VKA for at least five days or until the INR is at least 2.0 in two consecutive determinations, followed by a VKA alone. Long-term anticoagulation for secondary prevention will be decided after assessing the benefits and risks that may occur from continuing, stopping, or changing the anticoagulant.

Catheter thrombolytic therapy will be considered in patients with DVT with symptoms lasting less than 14 days, good functional status (ECOG 0-1), life expectancy of more than one year, and low risk of bleeding (259). Pharmacological systemic thrombolytic therapy is recommended in patients with hemodynamic instability PE. In patients with proximal DVT or in whom anticoagulation is contraindicated or in whom an episode of PE occurred during anticoagulant treatment, a filter in the inferior vena cava is indicated.

As for therapy in pregnancy, the guideline indicates the use of heparin (small molecule) as it can reduce the risk of obstetric adverse events. In the particular case of thrombophilia (inherited or acquired), the use of low doses of low-molecular-weight aspirin may or may not be associated with heparin during the pregnancy (260).

When a single thrombotic risk factor is present, prophylaxis with LMWH heparin is recommended both before and after childbirth (239). When two thrombotic risk factors are present, LMWH heparin prophylaxis is recommended starting from the 28th week of pregnancy and continuing after birth. As a general rule, LMWH heparin prophylaxis for the postnatal period recommends a general period of six weeks of administration.

I.3.2.9. Conclusions

Pregnancy, thrombophilia, deep vein thrombosis, and thromboembolism are causally linked.

The diagnosis of DVT is made on clinical symptoms and D-dimers, after which a general scheme of anticoagulant treatment is applied. Thus, the presence of a hidden thrombophilia risk may be missed.

Therefore, the chosen therapy may be excessive or not fully efficient. Although there are recommendations for the detection, evaluation, and treatment of thrombophilia during pregnancy, the ultimate goal is to select the appropriate investigations to make the best possible therapeutic decision.

Our study focused on the importance of selecting investigational tools and highlighted relevant serological factors that, when included in routine analyses of pregnancy tests, allow treatment to be personalized.

I.3.3. Pregnancy outcomes, immunophenotyping and immunohistochemical findings in a cohort of pregnant patients with COVID-19- a prospective study

I.3.3.1. Introduction

Severe acute respiratory syndrome coronavirus 2 (SARS-CoV-2) is the causative agent of coronavirus disease 2019 (COVID-19) (261). Since the World Health Organization (WHO) declared the SARS-CoV-2 a pandemic on March 11, 2020, new questions have emerged as to whether this virus can affect pregnancy outcomes (262). Many studies have estimated that between 3 and 20% of pregnant women presenting for labor and delivery were infected with this virus (263, 264). However, because universal screening was not widely used, it is challenging to offer an exact estimate for the prevalence of this viral infection in the population of pregnant patients.

Until now, several studies have outlined an association of SARS-CoV-2 infection and poor pregnancy outcomes (265). For example, it was demonstrated that miscarriage, intrauterine death, fetal growth restriction and high maternal-fetal morbidity rates were more prevalent in patients infected with this type of virus (266-270). Wei et al., performed a meta-analysis on 42 studies involving 438 548 pregnant patients, which evaluated the association between SARS-CoV-2 infection during pregnancy and adverse pregnancy outcomes. The authors demonstrated that the risk of developing preeclampsia (OR 1.33, 95% CI 1.03 to 1.73), preterm birth (OR 1.82, 95% CI 1.38 to 2.39) and stillbirth (OR 2.11, 95% CI 1.14 to 3.90) were higher in infected patients, and that severe forms of viral infection were associated with higher odds of developing preeclampsia, preterm birth, gestational diabetes or to deliver a newborn with low birth weight (271).

The risk of maternal complications appears to be increased in severe forms of COVID-19. A retrospective cohort study by Ko et al., on 489 471 delivery hospitalizations evaluated the maternal complications for 6550 pregnant patients with COVID-19 (272). The authors demonstrated that this viral infection was associated with increased risk for acute respiratory distress syndrome, death, sepsis, mechanical ventilation, shock, intensive care unit admission, acute renal failure, thromboembolic disease, and adverse cardiac events. The risk factors for severe COVID-19 disease are poorly explored in the literature, but recent data suggests that maternal diabetes, obesity, asthma, lower respiratory symptoms, and the extent of pulmonary disease on imaging studies constitute important independent risk factors for this maternal intensive care admission (269, 273-276).

On the other hand, it was shown that the prevalence of adverse pregnancy outcomes was reduced in vaccinated patients. For example, a recent meta-analysis by Prasad et al., indicated that messenger ribonucleic acid (mRNA) vaccination was a safe and effective method for reducing the rate of stillbirth by 15% in pregnant patients with confirmed SARS-CoV-2 infection (pooled odds ratio-OR: 0.85; 95% confidence interval- CI: 0.73-0.99, 66,067 vaccinated vs. 424,624 unvaccinated, I^2 = 93.9%) (277). The safety of mRNA vaccines has been outlined by many observational studies that compared perinatal outcomes between vaccinated and unvaccinated pregnant patients, and did not demonstrate harmful effects on pregnancy or the newborn (278-280).

There are ongoing efforts to investigate placentas from COVID-19 patients in order to better comprehend and predict the consequences of SARS-CoV-2 on pregnant women and newborns. The placenta acts as a barrier, preventing the fetus from being exposed to maternal illnesses (281). On the other hand, the receptor angiotensin-converting enzyme 2 (ACE2) used by SARS-CoV-2 for infecting pulmonary cells was also found in placental tissue (282-284), supporting the idea of vertical transmission for this type of infection (285, 286). Recent investigations of placental pathologies indicated the presence of feto-maternal vascular malperfusion, and placental inflammation with excessive infiltration of CD3+ CD8+ lymphocytes, CD68+ macrophages and CD20+ lymphocytes (287-289).

Given the scarcity of data on placental changes in the context of SARS-CoV-2 infection, the goal of this study was to assess the immunohistochemical changes of the umbilical cord, amniotic membranes and placental fragments, the immunophenotyping alterations, as well as pregnancy outcomes, in a cohort of patients with this type of viral infection.

I.3.3.2. Materials and methods

We conducted an observational prospective study of pregnant patients with COVID-19 admitted to the Obstetrics and Gynecology Hospital 'Buna Vestire', Galati, between October 2020 and November 2021. The SARS-CoV-2 infection was confirmed after the evaluation of nasopharyngeal swabs using the polymerase chain reaction (PCR) assay. The main circulating variants of SARS-CoV-2 were Alpha, for October 2020- September 2021 time frame, and Delta, for October- November 2021 time frame (290, 291).

Ethical approval for this study was obtained from the Institutional Ethics Committees of University of Medicine and Pharmacy 'Grigore T. Popa' (No.27/04.01.2021), and 'Buna Vestire' Obstetrics and Gynecology Hospital (No. 6793/08.09.2020). Informed consent was obtained from all participants included in the study. All methods were carried out in accordance with relevant guidelines and regulations.

Exclusion criteria comprised patients who had multiple pregnancies, ectopic pregnancies, first and second trimester abortions, fetal intrauterine demise, fetuses with chromosomal or structural abnormalities, incomplete medical records, or who were unable to offer informed consent due to various reasons (age less than 18 years old, intellectual deficits, psychiatric disorders, etc.).

52 patients were segregated into two groups depending on the presence of SARS-CoV-2 infection: with confirmed infection (n= 26) or without infection (n=26). The following variables were recorded: demographic data, the patient's medical history, clinical manifestations, laboratory parameters at admission, pregnancy outcomes, imaging findings, the treatment received, their clinical evolution, and the neonatal outcomes (gestational age, birthweight, Apgar score at 5 min).

For investigating the immunophenotyping changes, we further segregated the group of patients with COVID-19 into two subgroups depending on the disease severity: mild disease

(subgroup 1, n= 14 patients), and moderate-severe disease (subgroup 2, n= 12 patients). The criteria for inclusion in the mild disease subgroup were derived from the National Guidelines (292), and were represented by: patients with confirmed SARS-CoV-2 infection, with any signs or symptoms of respiratory tract infection such as fever, cough, rhinorrhea, sore throat, malaise, headache, or myalgia, but without breathing difficulties, dyspnea or thoracic imaging findings suggestive of pneumonia.

On the other hand, patients with mild or severe forms of COVID-19 were considered in case of confirmed SARS-CoV-2 infection, fever and signs of non-severe pneumonia, without needing supplementary oxygen or who manifested important dyspnea (respiratory frequency≥ 30/min), newly onset hypoxemia (oxygen saturation≤ 94%), a ratio of arterial oxygen partial pressure (mmHg) to fractional inspired oxygen (PaO_2/FiO_2)≤ 300 mmHg, rapid evolution of pulmonary imaging in the last 24-48 hours (> 50%), a progressive reduction in the lymphocytes number or a rapid increase in serum lactate levels.

A blood sample (5 mL) was drawn from pregnant patients diagnosed with COVID-19 in tubes containing ethylenediaminetetraacetic acid (EDTA). The frequency and number of CD4+ T cells, CD8+ T cells, CD19+B cells, CD16+ or CD56+, and NK cells, were measured by flow cytometry method using human monoclonal antibodies (BD Biosciences), according to the manufacturer's instructions. Flow cytometric acquisition was performed on a Partec PAS flow cytometer system (Partec GmBH), and the results were analyzed using Flowjo software (Treestar).

After delivery, two fragments of umbilical cord, amniotic membranes, and placenta underwent fixation in 10% buffered formalin and histopathological examination in the Pathology Department. Sections underwent routine processing, embedding, sectioning at 4 μm and staining with Hematoxylin & Eosin (H&E). For each Formalin-Fixed Paraffin-Embedded (FFPE) tissue sample, five additional 4 μm sections were made for immunohistochemical (IHC) assays, which were performed on the DAKO Autostainer LINK 48.

IHC antigen retrieval was performed using Target retrieval solution high pH (prediluted, pH 9.0) for 20 minutes at 97ºC. Specimens were incubated at room temperature as it follows: for 5 minutes with Peroxidase blocking reagent, then with primary antibodies for 20 minutes, followed by Horseradish peroxidase for 20 minutes, then with DAB chromogen for 10 minutes and they were then counterstained with hematoxylin. The primary antibodies (CD19, CD3, CD4, CD8 and CD56) were monoclonal, prediluted (ready to use (RTU)), were produced by Agilent and their characteristics are mentioned in table III.3.

Table III.3. Commercial antibodies for immunohistochemistry

Product number	Name	Species	Clone
IR65661-2	CD19	Mouse mAb	LE-CD19
IR50361-2	CD3	Mouse mAb	F7.2.38
IR64961-2	CD4	Mouse mAb	4B12
IR62361-2	CD8	Mouse mAb	C8/144B
IR62861-2	CD56	Mouse mAb	123C3

In the first stage of the statistical analysis, each variable was evaluated with chi-squared and Fisher’s exact tests for categorical variables, which were presented as frequencies with corresponding percentages, and t-tests for continuous variables, which were presented as means and standard deviations (SD).

A conditional logistic regression (CLR) model was applied for the evaluation of associations between adverse pregnancy outcomes and the presence of SARS-CoV-2 infection and the adjusted odd ratios (aOR) with 95% Confidence Intervals (CI) were

calculated for each variable of interest. A *p* value less than 0.05 was considered statistically significant. The statistical analyses were performed using STATA SE (version 17, 2022, StataCorp LLC, College Station, TX, USA).

In the second stage of the analysis, we described the immunohistochemical changes of the umbilical cord, amniotic membranes and placental fragments for pregnant patients infected with SARS-CoV-2.

I.3.3.3. Results

This prospective study evaluated 52 pregnant patients, segregated into two groups: with COVID-19 (group 1, n= 26 patients), and without COVID-19 (group 2, n= 26 patients). The clinical characteristics of the evaluated groups and the results from the univariate analysis are presented in Table III.4. We found a statistically significant difference between the two groups regarding personal history of pulmonary disease (*p*= 0.038) and smoking habit (*p*= 0.037). Even though we could not find a significant difference between groups regarding their body mass index (BMI), we noted a median value of 30 kg/m^2 for this index, meaning that most pregnant patients had increased body weight.

Table III.4. Univariate analysis of the clinical characteristics for the patients included in our study

Patient's data		**Group 1 (with COVID-19, n=26 patients)**	**Group 2 (without COVID-19, n=26 patients)**	***p* value**
Demographics	Maternal age, years (mean and standard deviation)	29.73± 5.86	29.69± 6.74	0.98
	Medium (n/%)	Rural= 13 (50%) Urban=13 (50%)	Rural= 11 (42,3%) Urban= 15 (57,7%)	0.39
	BMI, kg/m^2, (mean and standard deviation)	30.05± 5.99	29.93± 6.11	0.47

Clinical parameters	Smoking (n/%)	Yes= 5 (19,2%)	Yes= 2 (7,7%)	0.037
	Pulmonary disease (n/%)	Yes= 4 (15,4%)	Yes= 0 (0%)	0.038
	Personal history of thrombosis (n/%)	Yes= 2 (7,7%)	Yes= 0 (0%)	0.14
	Diabetes (n/%)	Yes= 1 (3,8%)	Yes= 0 (0%)	0.31
	Thrombophilia (n/%)	Yes= 4 (15,4%)	Yes= 2 (7,7%)	0.38
	Lower limb varicose veins (n/%)	Yes= 2 (7,7%)	Yes= 1 (3,8%)	0.55

Table legend: BMI- body mass index;

For patients infected with COVID-19 the most prevalent symptoms were anosmia and cough (n= 7, 26,9%), ageusia (n= 6, 23,1%), fever (n= 5, 19,2%), followed by dyspnea (n= 4, 15,4%), myalgia and joint pain (n= 3, 11,5%), and diarrhea (n=1, 3,8%). In two cases (7,7%), the imaging examinations revealed aspects of interstitial pneumonia. The univariate analysis of the main laboratory parameters revealed a significantly higher frequency of inflammatory syndrome (elevated C-reactive protein, procalcitonin and ferritin) in the group of patients diagnosed with COVID-19 compared with controls ($p< 0.05$) (Table III.5).

Table III.5. Univariate analysis of the paraclinical parameters at admission for patients included in our study

Laboratory parameters	**Group 1 (with COVID-19, n=26 patients)**	**Group 2 (without COVID-19, n=26 patients)**	***p* value**
Leucocytes/mm^3 (mean, standard deviation)	9730± 3173.48	8900± 1839.83	0.57
Neutrophils, %, (mean, standard deviation)	76.48± 6.99	72.36± 6.80	0.11
Lymphocytes, %, (mean, standard deviation)	11.96± 6.46	13.2± 4.96	0.34
Monocytes, %, (mean, standard deviation)	5.70± 1.59	6.62± 0.98	0.22
Eosinophils, %, (mean, standard deviation)	0.93± 0.66	1.06± 0.60	0.35
Basophils, %, (mean, standard deviation)	0.98± 0.33	1.18 ± 0.37	0.12
Thrombocytes/mm^3 (mean, standard deviation)	264,692.3± 124,452	208,200 ± 79,948.1	0.17
C- reactive protein, mg/dL (mean, standard deviation)	13.2± 7.35	1.47± 0.29	< 0.001
Procalcitonin, ng/mL (mean, standard deviation)	5.7± 6.85	0.14± 0.06	< 0.001
Glutamic-oxaloacetic transaminase (TGO), U/L (mean, standard deviation)	55.5± 6.82	39.4± 2.95	0.38
Glutamic pyruvic transaminase (TGP), U/L (mean, standard deviation)	63.73± 1.53	18.91± 17.44	0.43
Ferritin, ng/ml (mean, standard deviation)	620.05± 248.89	1344.58± 444.92	< 0.001

Table legend: TGO- Glutamic-oxaloacetic transaminase, TGP- Glutamic pyruvic transaminase.

Our results failed to indicate a statistically significant difference between the two groups regarding the pregnancy outcomes: gestational age at birth (p= 0.42), birth weight (p= 0.39), mode of delivery (p= 0.56), preterm labour before 37 weeks of gestation (p= 0.22), and neonatal intensive care unit admission (p= 0.31), respectively (Table III.6). Only Apgar score 5 minutes was significantly lower for the first group (p=0.005), and patients with COVID-19 had a higher chance of delivering a newborn with lower Apgar score (OR: 4.11; 95%CI: 1.211-13.974). All newborns were tested for SARS-CoV-2 infection, but none of them became positive during admission.

All patients with moderate-severe forms of COVID-19 received treatment with an antiviral (Remdesivir), thromboprophylaxis with low molecular weight heparin (LMWH), and

antibiotic therapy. One maternal death was recorded due to interstitial pneumonia with acute respiratory distress syndrome, and multiorgan system failure. None of the pregnant patients were vaccinated against COVID-19.

Table III.6. Pregnancy outcomes for the two groups of patients included in the study

Pregnancy outcomes	**Group 1 (with COVID-19, n=26 patients)**	**Group 2 (without COVID-19, n=26 patients)**	**OR and 95%CI**	***p* value**
Gestational age, weeks (mean, standard deviation)	38.19± 1.91	38.53± 1.10	0.99 (0.998-1.001)	0.42
Birth weight, g (mean, standard deviation)	3151.92± 564.70	3189.23± 406.08	0.70 (0.46- 1.06)	0.39
Apgar score 5 minutes (mean, standard deviation)	8.38± 0.63	8.88± 0.58	4.11 (1.211-13.974)	0.005
Mode of delivery (n/%)	Cesarean= 15 (57.7%) Vaginal= 11 (42.3%)	Cesarean= 17 (65.4%) Vaginal= 9 (34.6%)	1.12 (0.320-3.924)	0.56
Intrauterine growth restriction (n/%)	Yes= 4 (15,4%)	Yes= 2 (7,7%)	0.32 (0.03-3.12)	0.38
Preterm labour (n/%)	Yes= 5 (19,2%)	Yes= 2 (7,7%)	0.98 (0.96- 1.00)	0.22
Neonatal intensive care unit admission (n/%)	Yes= 1 (3,8%)	Yes= 0 (0%)	1.01 (0.98- 1.05)	0.31

Table legend: OR- Odds ratio; CI- confidence interval.

The pregnant patients with COVID-19 were segregated into two subgroups depending of the form of disease: mild disease (subgroup 1, n= 14 patients), and moderate-severe disease (subgroup 2, n= 12 patients). We compared the lymphocyte populations as determined by immunophenotyping between subgroups using univariate analysis that is presented in table III.7. Our results indicated that patients with moderate- severe forms of COVID-19 had a significantly reduced population of lymphocytes, CD4+ T cells, CD8+ T cells (only numeric), and CD4+/CD8+ index compared with patients who presented with mild forms of COVID-19 ($p< 0.05$). Additionally, the populations of B lymphocytes and natural killer (NK) cells were significantly diminished in the first subgroup ($p< 0.05$).

Table III.7. Univariate analysis of lymphocyte populations among the evaluated subgroups

Parameters evaluated	**Moderate-severe form (subgroup 1, n= 12 patients)**	**Mild form (subgroup 2, n= 14 patients)**	***p* value**
Lymphocyte number/mm^3 (mean, standard deviation)	746.0± 429.75	1927.85± 717.30	< 0.001
Lymphocyte percentage	68.41± 6.76	79.21± 5.60	0.002
CD4+ T cells number/mm^3 (mean, standard deviation)	531.08± 350.42	1538.78± 588.09	< 0.001
CD4+ T cells percentage	32.25 ± 11.17	47.92± 8.85	0.003

CD8+ T cells number/mm^3 (mean, standard deviation)	275± 248.85	950.71± 393.79	< 0.001
CD8+ T cells percentage	30.16± 3.45	29.07± 7.16	0.31
CD4+/CD8+ index	1.12± 0.55	1.77± 0.63	0.005
B lymphocytes number/mm^3 (mean, standard deviation)	101.08± 66.37	227.5± 141.77	0.004
B lymphocytes percentage	13.58± 3.67	11.14± 4.89	0.08
Natural killer cells number/mm^3 (mean, standard deviation)	83.75± 28.96	134.85± 42.67	0.001
Natural killer cells percentage	12± 1.85	8.35± 4.74	0.02

The immunohistochemistry analysis of sections from umbilical cord, amniotic membranes and placental fragments from pregnant patients with COVID-19 failed to demonstrate positivity for the following markers: CD19, CD3, CD4, CD8 and CD56. These antibodies were used in order to find the inflammatory cells in the analyzed tissues, as follows: CD19 for B cells, CD3 for T cells, CD4 for T helper cells, CD8 for cytotoxic T cells and CD56 for Natural Killer (NK) cells.

Acquired images from H&E-stained slides, as well as immunohistochemical markings were presented in figures III.3-5.

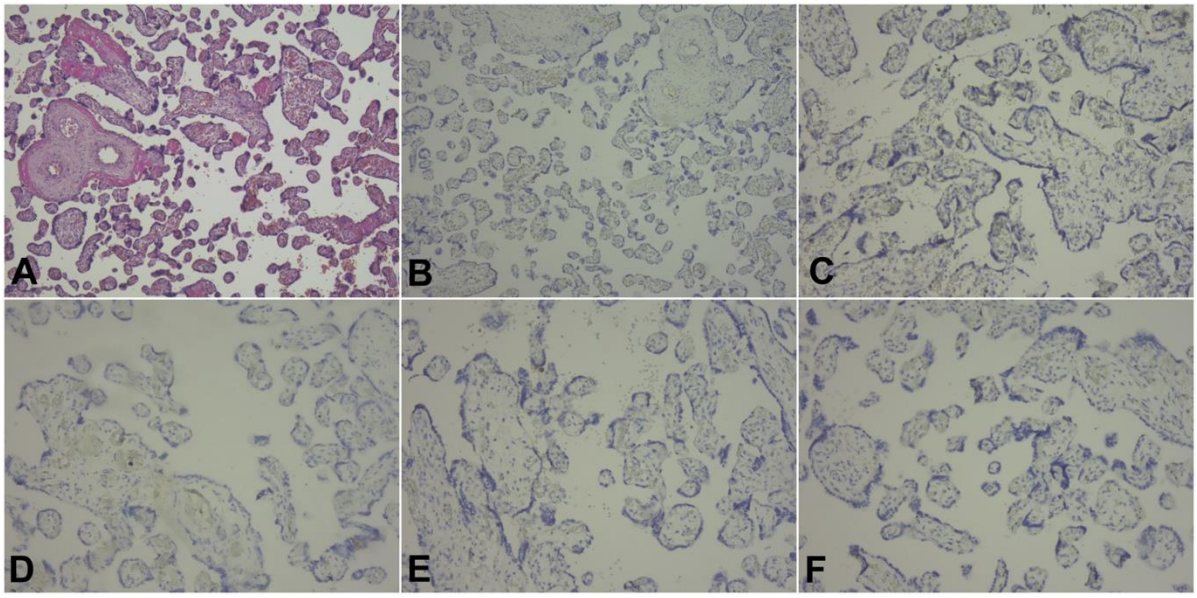

Figure III.3. Selected microscopic aspects from placental sections. A. Presence of intramural fibrin deposition and lack of inflammatory cells, H&E stain, x100 magnification. B-F. Negativity for the immune markings: B. CD4, x100 magnification, C. CD8, x200 magnification, D. CD19, x200 magnification, E. CD3, x200 magnification, F. CD56, x200 magnification

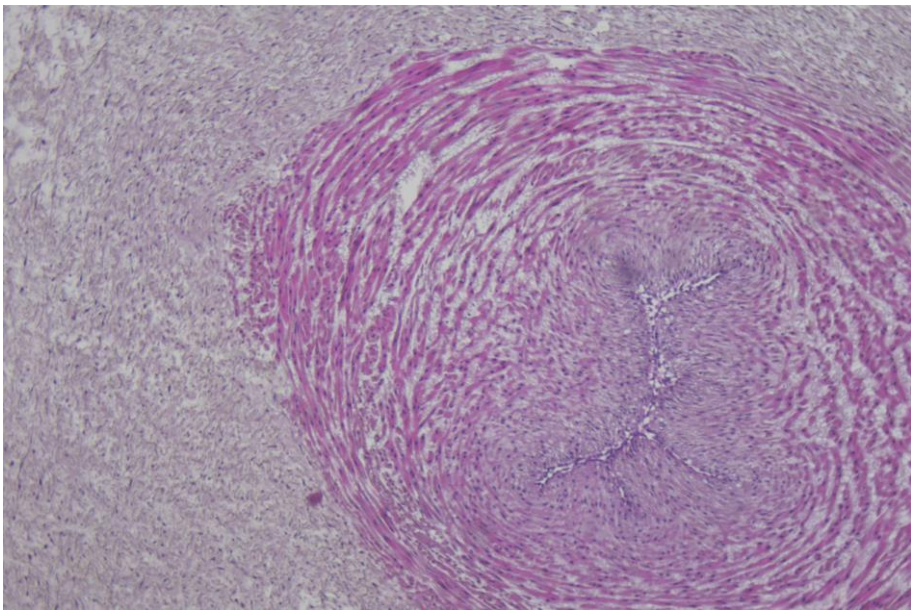

Figure III.4. Histological aspect of umbilical cord section, lacking inflammatory reactions, H&E stain, x100 magnification

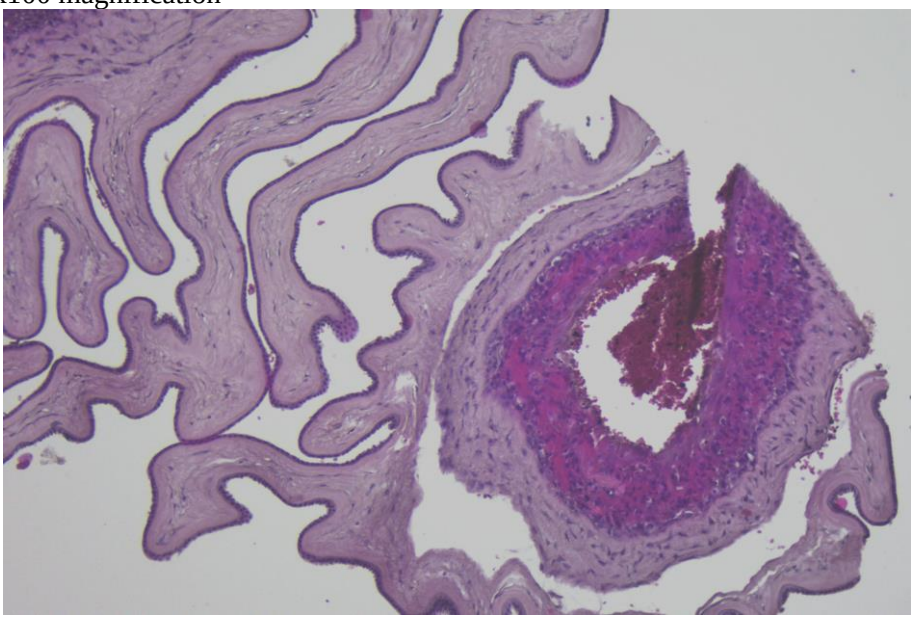

Figure III.5. Amniotic membrane section, without inflammatory cells, H&E stain, x100 magnification

I.3.3.4. Discussions and conclusions

In this prospective study, we assessed the immunohistochemical changes of the umbilical cord, amniotic membranes and placental fragments, the immunophenotyping alterations, and pregnancy outcomes in a cohort of patients with this Sars-CoV-2 infection. Personal history of pulmonary disease and smoking habit were more prevalent for pregnant patients with this viral infection. Regarding the patient's symptomatology, anosmia, cough, ageusia, and fever were the most frequently encountered manifestations at admission.

Previous research revealed similar results in terms of risk factors for COVID-19 development and its clinical picture. For example, in a Mendelian randomization study by Yeung et al., on a large cohort of adult patients, the authors demonstrated that smoking increased the risk of developing COVID-19 (OR: 1.19, 95% CI: 1.11-1.27), as well as the disease severity (293). Moreover, a recent study by Radzikowska et al., that evaluated

different SARS-CoV-2 receptors in primary human cells and tissues, demonstrated that airway epithelium in asthma and chronic obstructive pulmonary disease (COPD) had a gene signature that potentially can facilitate viral entry and internalization into cells (294).

Anosmia and ageusia are frequently encountered symptoms in COVID-19 patients (295), and a recent systematic review and meta-analysis confirmed our findings regarding the clinical manifestations of pregnant patients, by citing cough, fever, fatigue, and anosmia/ageusia as the most commonly reported symptoms in the literature (296).

The univariate analysis of the main laboratory parameters revealed a significantly higher frequency of inflammatory syndrome (elevated C-reactive protein, procalcitonin and ferritin) in the group of patients diagnosed with COVID-19. As expected, the inflammatory syndrome associated with COVID-19 was also outlined in various studies on pregnant patients (297-299). Moreover, it was demonstrated that elevated serum levels of procalcitonin and ferritin were associated with severe forms of disease (300, 301).

On the other hand, our results failed to indicate a statistically significant difference between the two groups regarding the adverse pregnancy outcomes such as preterm labour and neonatal intensive care unit admission. A multicentric cohort study by Oncel et al., revealed high rates of cesarean section (71.2%), prematurity (26.4%), and low-birthweight infant rates (12.8%) for a cohort of patients with COVID-19 (302). Another retrospective multicentric study indicated higher rated of NICU admission among offspring of symptomatic women (303). We hypothesize that the small cohort of patients represents the main reason for our findings in contrast with the published data.

The subgroup analysis of pregnant patients using immunophenotyping indicated that patients with moderate- severe forms of COVID-19 had a significantly reduced population of lymphocytes, CD4+ T cells, CD8+ T cells (only numeric), and CD4+/CD8+ index Additionally, the populations of B lymphocytes and natural killer (NK) cells were significantly diminished in the first subgroup. Several studies demonstrated that lymphopenia and decreased NK cells were associated with progression to severe forms of COVID-19 in pregnancy (304-308). Moreover, it was demonstrated that the absolute lymphocyte count (ALC) (AUC = 0.80), and neutrophil to lymphocyte ratio (NLR) (AUC= 0.86) were highly sensitive for progression to severe illness (306).

The lymphocytopenia could be due to viral attachment, immunological damage caused by proinflammatory cytokines, or extravasation of circulating lymphocytes into lung tissues (304). In a prospective study by Wang et al., that evaluated the levels of peripheral lymphocyte subsets in 60 hospitalized COVID-19 patients, the authors demonstrated a decrease in total lymphocytes, CD4+ T, CD8+ T, B, and NK cells, especially in severe forms. Additionally, the authors showed a significant association between inflammatory status of patients and decreased levels of CD8+ T cells and CD4+/CD8+ ratio (309).

Finally, our immunohistochemistry analysis of umbilical cord, amniotic membranes and placental fragments retrieved in the third trimester of pregnancy failed to demonstrate positivity for CD19, CD3, CD4, CD8 and CD56 markers. In a recent study by Levitan et al., the authors evaluated 64 placentas using immunohistochemical staining for SARS-CoV-2 nucleocapsid protein, and found that none of the specimens were positive for this marker (310). Another study that analyzed the immunohistochemical staining of placental specimens for various leukocytes revealed an increased CD68+ macrophages infiltration (311).

Resta et al. investigated the association between the symptoms' severity and different placental histological characteristics using immunohistochemical investigations for CD4 + and CD8 + T lymphocytes, and CD68 + macrophage (286). Their authors did not observe significant differences patients with mild of severe forms of COVID-19 and controls for CD4. CD8 expression was significantly higher in placentas from patients with severe forms

compared with controls, while the CD68 expression were significantly different between the evaluated groups.

Finally, Juttukonda et al., characterized the decidual immune response depending on the timing of infection during gestation, and demonstrated that for an infection acquired in the third trimester of pregnancy, decidual tissues presented significantly more macrophages (CD14+), NK cells (CD56+), and T cells (CD3+) (312). For the infection acquired in the second trimester of pregnancy, only T cells (CD3+) were significantly more expressed in the evaluated placentas.

This study has the advantage of presenting the immunophenotyping and immunohistochemical findings from pregnant patients with acquired COVID-19 infection in the third trimester of pregnancy. However, the results outlined in this paper must be evaluated considering the following limitations: small cohort of patients, and reduced timeframe for the prospective assessment.

Further studies, on larger cohort of patients, could determine the extent of immunological decidual response in patients with various forms of COVID-19, and for different timing of infection during gestation.

I.3.4. The influence of maternal KIR haplotype on the reproductive outcomes after single embryo transfer in IVF cycles in patients with recurrent pregnancy loss and implantation failure- a single center experience

I.3.4.1. Introduction

The definition of recurrent pregnancy loss (RPL) varies in the literature, but one of the most used definitions describes this disorder as the spontaneous loss of two or more pregnancies (313). The prevalence of pregnancy loss is difficult to estimate since it depends on how early women discover their pregnancy, the study population, and the use of multiple criteria to diagnose this disorder. Recent reports indicate an average prevalence of recurrent pregnancy loss between 1% and 4% of all women who achieve pregnancy (314, 315).

On the other hand, recurrent implantation failure (RIF) refers to cases in which women have had three failed in vitro fertilization (IVF) attempts with good quality embryos (316). The definition of RIF is also heterogeneously reported in the literature, so an accurate epidemiological profile of this disorder cannot be properly specified. However, one recent retrospective cohort study by Pirtea et al., on 4,429 women with anatomically normal uterus, who underwent up to three consecutives frozen euploid single embryo transfers estimated an RIF prevalence of less than 5% (317).

Both RPL and RIF appear to have in common a deficient maternal adaptation to the semi-allogeneic fetus (318-321). An important element in the pathophysiology of these illnesses is represented by the natural killer (NK) cells, and their interaction with various ligands (322). Because of their ability to release cytokines and destroy target cells without prior sensitization, NK cells play a fundamental role in the innate immune response. Due to their cytotoxic nature, NK cells must be able to distinguish normal self-tissue in order to prevent self-destruction (323). Interactions between members of the killer immunoglobulin-like receptor (KIR) family expressed by NK cells and trophoblast human leukocyte antigen-C (HLA-C) molecules are of special relevance in terms of allorecognition since both maternal KIR and fetal HLA-C genes are highly variable (324).

In any pregnancy, the maternal KIR genotype could be AA (no activating KIRs), AB, or BB (activating KIRs) (325). HLA-C ligands for KIRs are classified into two types: HLA-C1 and HLA-C2. The inhibitory receptors KIR2DL2 (B haplotype) and KIR2DL3 (A

haplotype) are ligands for the C1 group allotypes, while the activating KIR2DS1 receptors are ligands for the C2 group allotypes (B haplotype). C2 is a more potent ligand than C1 (326).

In recent years, several studies have outlined the association of various KIR polymorphisms with infertility, and pregnancy related disorders, but there is still great heterogeneity over the reporting of specific KIR haplotypes and their influence on the reproductive outcomes (327-329). The aim of this study was to evaluate the influence of maternal KIR haplotype on the reproductive outcomes after single embryo transfer in IVF cycles in patients with recurrent pregnancy loss and implantation failure in a cohort of patients from Romania.

I.3.4.2. Materials and methods

In this study patients with RIF and RPL who presented for consultations at Origyn Fertility Center from Iasi, Romania, were prospectively enrolled between January 2020 and December 2022. Ethical approval for this study was obtained from the Institutional Ethics Committee of University of Medicine and Pharmacy 'Grigore T. Popa' (No. 143/18.03.2019). Informed consent was obtained from all participants included in the study. All methods were carried out in accordance with relevant guidelines and regulations.

The inclusion criteria taken into consideration were: pregnant patients with RPL or RIF, age ≥ 18, with/without previous IVF procedure. We considered RPL as the spontaneous loss of two or more pregnancies (313), and RIF as three failed in vitro fertilization (IVF) attempts with good quality embryos (316). Exclusion criteria comprised patients who had ectopic pregnancies, fetal intrauterine demise, fetuses with chromosomal or structural abnormalities, incomplete medical records, or who were unable to offer informed consent.

All of the women and their partners were subjected to a comprehensive fertility screening. This included a complete clinical history, physical examination, viral serology (hepatitis B, hepatitis C, and human immunodeficiency virus), hormonal analysis (thyroid-stimulating hormone- TSH, free thyroxin- fT4, anti-thyroid peroxidase antibodies ATPO, anti-mullerian hormone- AMH, and 25-hydroxy vitamin D- 25(OH)D), male sperm analysis, and pelvic ultrasound.

The following tests were performed: parental karyotype, thrombophilic disorders screening, immunological screening for anticardiolipin and anti-b-2-glycoprotein, and lupus anticoagulant.

A blood sample (5 mL) was drawn from each participant in tubes containing ethylenediaminetetraacetic acid (EDTA). DNA was extracted, and KIR typing was performed using polymerase chain reaction with sequence-specific primers (PCR/SSP) for the following KIRs: 2DL1, 2DL2, 2DL3, 2DL4, 2DL5, 2DS1, 2DS2, 2DS3, 2DS4, 2DS4N, 2DS5, 3DL1, 3DL2, 3DL3, 3DS1, 2DP1 and 3DP1. If any of the genes, 2DL2, 2DL5, 3DS1, 2DS1, 2DS2, 2DS3, and 2DS5, were present, the genotype was accepted as B. When none of these were present, the genotype was accepted as AA.

The HLA-C genotypes were also investigated using PCR analysis. The HLA-C genes of all partners or egg donors were analyzed and classified as C1 HLA-C or C2 HLA-C. All HLA-C alleles found in populations are classified as C1 or C2, depending on which amino acid (asparagine or lysine) is present at position 80 of the HLA-C molecule. KIRs bind to the HLA-C molecules in this site, to the KIR binding C1 or C2 epitope. The genetic testing for both KIR and HLA-C was performed at 'Queen Mary's' Genetic Center from Bucharest, Romania.

We chose to use a theoretical score proposed by Alecsandru et al. (324), and defined as the number of C2 alleles from both gamete providers, multiplied by the number of embryos

transferred, minus the number of C2 alleles held by the mother for evaluation of excessive maternal HLA-C2 presence.

We included in this study 108 patients out of 123 patients initially evaluated, and we divided them into three subgroups: subgroup 1 (AA genotype, n= 31), subgroup 2 (BB genotype, n= 72), and subgroup 3 (AB genotype, n= 5). The following reproductive outcomes were assessed: the pregnancy rate, the miscarriage rates, and the live birth rates. These reproductive outcomes were further segregated depending on the mode of achieving a pregnancy (IVF or spontaneous).

In the first stage of the statistical analysis, each variable was evaluated with chi-squared and Fisher's exact tests for categorical variables, which were presented as frequencies with corresponding percentages, and *t*-tests for continuous variables, which were presented as means and standard deviations (SD).

ANOVA analysis with the Bonferroni post-hoc test was used to determine whether or not there is a statistically significant difference between the subgroups regarding their paraclinical characteristics. The statistical analyses were performed using STATA SE (version 17, 2021, StataCorp LLC, College Station, TX, USA).

A conditional logistic regression (CLR) model was applied for the evaluation of associations between reproductive outcomes and KIR haplotypes and the adjusted odd ratios (aOR) with 95% Confidence Intervals (CI) were calculated for each variable of interest. A *p* value less than 0.05 was considered statistically significant.

I.3.4.3. Results

A total of 108 patients were evaluated in our prospective study. Their clinical characteristics are presented in table III.8, segregated into the following groups: RPL (group 1, 30 patients), and RIF (group 2, 78 patients). The personal history of systemic lupus erythematosus (SLE)/antiphospholipid syndrome (APS) (p= 0.005), thrombophilia (p= 0.002), and thrombosis (p= 0.008) were significantly more prevalent in the group of patients with recurrent pregnancy loss.

Table III.8. Clinical characteristics of the patients included in the main groups

Patient's characteristics	**Group 1 (RPL, n= 30)**	**Group 2 (RIF, n= 78)**	***P* value**
Age, years (mean ± SD)	33.56± 3.95	33.92± 4.23	0.69
Medium (n/ %)	Urban= 16 (53.3%) Rural= 14 (46.7%)	Urban= 35 (44.9%) Rural= 43 (55.1%%)	0.43
Obesity (n/ %)	Yes= 8 (26.7 %)	Yes= 19 (24.4%)	0.80
Hypertension (n/ %)	Yes= 3 (9%)	Yes= 7 (10%)	0.86
Renal disease (n/ %)	Yes= 0 (0%)	Yes= 2 (2.6%)	0.37
Diabetes (n/ %)	Yes= 1 (3.3%)	Yes= 2 (2.6%)	0.82
SLE/APS (n/ %)	Yes= 7 (23.3%)	Yes= 4 (5.1 %)	0.005

Thrombophilia (n/ %)	Yes= 6 (20%)	Yes= 2 (2.6%)	0.002
Thrombosis (n/ %)	Yes= 5 (16.7%)	Yes= 2 (2.6%)	0.008
Endometriosis (n/ %)	Yes= 7 (23.3%)	Yes= 22 (28.2%)	0.60
Autoimmune thyroiditis (n/ %)	Yes= 6 (20%)	Yes= 8 (10.3%)	0.17
Rheumatoid arthritis (n/ %)	Yes= 0 (0%)	Yes= 1 (1.3%)	0.55
Autoimmune thrombocytopenic purpura (n/ %)	Yes= 0 (0%)	Yes= 1 (1.3%)	0.55

Table legend: RPL- recurrent pregnancy loss; RIF: recurrent implantation failure; SD- standard deviation; APS- antiphospholipid syndrome; SLE- systemic lupus erythematosus;

The paraclinical characteristics of the main groups are presented in table III.9. Our results indicated that the serum levels of ATPO were significantly higher in the RPL group compared to RIF group (140.32± 378.48 versus 50.89± 156.99 UI/mL, *p*= 0.005). Moreover, the vitamin D serum levels were significantly lower in the RPL group compared to RIF group (32.76± 21.98 versus 39.91± 20.13 ng/mL, *p*= 0.006). Although the prevalence of AA haplotypes was higher in the RPL group, and the prevalence of AB haplotype was higher in the RIF group, the difference was not statistically significant.

Table III.9. Paraclinical characteristics of the patients included in the main groups

Patient's characteristics	**Group 1 (RPL, n= 30)**	**Group 2 (RIF, n= 78)**	***P* value**
AA haplotype (n/ %)	Yes= 10 (33.3 %)	Yes= 21 (26.9 %)	0.51
AB haplotype (n/ %)	Yes= 0 (0%)	Yes= 4 (5.71%)	0.20
BB haplotype (n/ %)	Yes= 20 (66.7%)	Yes= 53 (66.7%)	0.99
Maternal HLA- C1/C2 (n/ %)	Yes= 14 (46.7%)	Yes= 33 (42.3%)	0.68
Maternal HLA- C2/C2 (n/ %)	Yes= 7 (23.3%)	Yes= 14 (17.9%)	0.52
Maternal HLA- C1/C1 (n/ %)	Yes= 31 (39.7%)	Yes= 14 (17.9%)	0.20
Partner's HLA- C1/C2 (n/ %)	Yes= 18 (60%)	Yes= 43 (55.1%)	0.64
Partner's HLA- C2/C2 (n/ %)	Yes= 2 (6.7%)	Yes= 13 (16.7%)	0.17
Partner's HLA- C1/C1 (n/ %)	Yes= 10 (33.3%)	Yes= 22 (28.2%)	0.60

Score (mean ± SD)	0.73± 0.58	0.85± 0.67	0.37
TSH, μUI/mL, (mean ± SD)	2.10± 1.07	1.88± 0.98	0.33
fT4, pmol/L, (mean ± SD)	11.48± 4.18	12.88± 3.77	0.14
ATPO, UI/mL, (mean ± SD)	140.32± 378.48	50.89± 156.99	0.005
Vitamin D, ng/mL, (mean ± SD)	32.76± 21.98	39.91± 20.13	0.006
AMH, ng/mL, (mean ± SD)	2.98± 2.18	2.89± 1.99	0.41

Table legend: RPL- recurrent pregnancy loss; RIF: recurrent implantation failure; SD- standard deviation; TSH- thyroid stimulating hormone; fT4- free thyroxine; ATPO- anti-thyroid peroxidase antibodies; AMH- anti-müllerian hormone.

We further comparatively analyzed the paraclinical characteristics of the following subgroups: subgroup 1 (AA genotype, n= 22), subgroup 2 (BB genotype, n= 94), and subgroup 3 (AB genotype, n= 88) (Table III.10). The ANOVA analysis with the Bonferroni post-hoc test indicated that there is no statistically significant difference in terms of variance between the exanimated subgroups regarding their clinical parameters.

Table III.10. Comparison of paraclinical characteristics for the patients included in the analyzed subgroups

		Sum of Squares	**Mean Square**	**F score**	***P* value**
Score	Between Groups	0.427	0.213	0.496	0.611
TSH	Between Groups	1.371	0.685	0.667	0.516
fT4	Between Groups	4.656	2.328	0.149	0.861
ATPO	Between Groups	22904.490	11452.245	0.201	0.818
AMH	Between Groups	3.024	1.512	0.360	0.698
Vitamin D	Between Groups	250.316	125.158	0.473	0.625

Table legend: TSH- thyroid stimulating hormone; fT4- free thyroxine; ATPO- anti-thyroid peroxidase antibodies; AMH- anti-müllerian hormone.

A comparison of reproductive outcomes was presented in table III.11. Our results indicated that miscarriage rate was significantly lower (6.9%, p= 0.018), and the live birth rate (87.5%) was significantly higher for BB haplotype compared to other haplotypes. On the other hand, no statistically significant difference could be determined between haplotypes regarding the pregnancy rate.

Table III.11. Comparison of reproductive outcomes between patients with various haplotypes

Reproductive outcome	**AA**	**AB**	**BB**	**P value**
PR	25 (80.6%)	4 (80%)	68 (94.4%)	0.08
MR	7 (22.6%)	1 (20%)	5 (6.9%)	0.018
LBR	18 (58.1%)	3 (60%)	63 (87.5%)	0.003

Table legend: PR- pregnancy rate; MR: miscarriage rate; LBR- live birth rate.

The reproductive outcomes were further comparatively analyzed based on the KIR genotype (Table III.12). Patients with an AA haplotype had significantly more chances of miscarriage if they underwent an IVF procedure (aOR: 4.15, 95%CI: 1.39- 6.50, p= 0.032) compared with those who spontaneously achieved a pregnancy. The chances of obtaining a pregnancy were also significantly higher for those patients with an AA haplotype who underwent an IVF procedure (aOR: 2.57, 95% CI: 0.85- 6.75, p= 0.023), but at the same time live birth odds did not significantly differ between the evaluated haplotypes.

Table III.12. Comparison of reproductive depending on the mode of achieving a pregnancy for the patients included in the analyzed subgroups

Kir haplotype	**MR *(Odds ratio, 95%CI lower limit- upper limit)*** LBR		
	S	IVF	*P* value
AA	2.36 (0.84- 8.38)	4.15 (1.39- 6.50)	0.032
AB	0.70 (0.46- 1.06)	1.01 (0.98- 1.05)	0.314
BB	0.43 (0.16- 1.14)	0.98 (0.96- 1.00)	0.051
Kir haplotype	**PR *(Odds ratio, 95%CI lower limit- upper limit)***		
	S	IVF	*P* value
AA	1.04 (0.97-1.11)	2.57 (0.85- 6.75)	0.023
AB	1.01 (0.98- 1.05)	1.03 (0.97- 1.08	0.251
BB	0.98 (0.96- 1.00)	1.15 (0.74- 1.78)	0.518
Kir haplotype	**LBR (Odds ratio, 95%CI lower limit- upper limit)**		
	S	IVF	*P* value

AA	0.51	0.18	1.44	0.84	0.64	1.09	0.174
AB	0.75	0.12	4.59	0.94	0.30	2.92	0.759
BB	1.12	0.94	1.34	1.62	0.27	6.70	0.189

Table legend: PR- pregnancy rate; MR: miscarriage rate; LBR- live birth rate; S- spontaneous pregnancy; IVF- pregnancy obtained by in vitro fertilization.

I.3.4.4. Discussion

In this prospective study, we have assessed the influence of maternal KIR haplotypes on reproductive outcomes after single embryo transfer in IVF cycles in patients with recurrent pregnancy loss and implantation failure. Our results indicated that miscarriage rate was significantly lower (6.9%, p= 0.018), and the live birth rate (87.5%) was significantly higher for BB haplotype compared to other haplotypes. On the other hand, when we stratified the reproductive outcomes using the modality of achieving a pregnancy, patients with an AA haplotype had significantly more chances of miscarriage if they underwent an IVF procedure (aOR: 4.15, 95%CI: 1.39- 6.50, p= 0.032) compared with those who spontaneously achieved a pregnancy. Moreover, it appeared that the same haplotype increased the chances of obtaining a pregnancy for patients who underwent an IVF procedure (aOR: 2.57, 95% CI: 0.85- 6.75, p= 0.023).

These findings are complementary to those published in previous literature. For example, in a retrospective study by Alecsandru et al.(330), on a cohort of 291 women, with recurrent miscarriage (RM) or RIF, who underwent 1304 assisted reproductive cycles, the authors evaluated the influence of maternal KIR haplotype on the pregnancy, miscarriage rates and live birth rates after single (SET) or double embryo transfer (DET) when categorized by the origin of the oocytes. The authors identified higher rates of early miscarriage per cycle after DET with the patient's own oocytes in mothers with the KIR AA haplotype (22.8%) followed by those with the KIR AB haplotype (16.7%) compared with mothers with the KIR BB haplotype (11.1%) were observed (p= 0.03). However, they could not confirm the same findings on the SET cohort of patients.

Another study by Alecsandru et al. (324), with a prospective design, evaluated the reproductive outcomes in 204 patients who underwent IVF according to maternal KIR genes expressed by uterine natural killer cells and paternal or oocyte donor HLA-C genes. The authors identified a higher miscarriage rate after DETs in KIR AA mothers (47.8% egg donation and 37.5% in IVF) compared with KIR AB (10.5% egg donation and 12.5% IVF) or KIR BB (6.7% egg donation and 0% IVF). Moreover, they observed a significantly decreased LBR after DETs with oocyte donation in KIR AA patients (4.3%) compared with KIR AB (26.3%) or BB (46.7%), and further decrease in the LBR as the fetal HLA-C2 load increased in KIR AA women.

In this study we did not have access to miscarriage tissue not have the possibility to test the newborns for HLA-C genotyping. Our results showed that there was not statistically significant difference regarding the parental HLA-C genotypes between groups of patients with RIF and RPL. For this reason, the theoretical score proposed by Alecsandru et al.(324), that we chose to use for analysis, did not significantly differ among our groups.

On the other hand, a recent case-control study on 140 patients, investigated the association between KIR gene polymorphisms and unexplained recurrent pregnancy loss. The authors demonstrated that the KIR 2DL1, 2DL2, 2DL3, 2DL4, 2DS1, 2DS2, 2DS4, and 2DS5 polymorphisms, as well as Bx haplotypes were associated with URPL (323). In our study the

BB haplotype had equal prevalence in the RPL and RIF groups (66.7%), and no statistically significant difference between these groups could be determined regarding this aspect.

The recent literature outlined the immunological background for both RPL and RIF (319, 320, 331-334), and in this study we also evaluated if the personal history of autoimmune disorders varies in these cohorts of patients. The clinical data indicated that the personal history of SLE/ APS, thrombophilia, and thrombosis were significantly more prevalent in the group of patients with recurrent pregnancy loss.

A systematic review and meta-analysis indicated that pregnant women with hereditary thrombophilia have an increased risk of RPL, especially in the presence of G1691A mutation of the factor V Leiden (FVL) gene, the G20210A mutation of the prothrombin gene (PGM), and deficiency of protein S (PS) (335). On the other hand, autoimmune disorders such as rheumatoid polyarthritis, autoimmune thyroiditis, and autoimmune thrombocytopenic purpura were not significantly associated with RPL or RIF.

An interesting finding resulted from the analysis of paraclinical characteristics of the evaluated patients. Our findings outlined that the serum levels of ATPO were significantly higher in the RPL group compared to RIF group, and that the vitamin D serum levels were significantly lower in the RPL group compared to RIF group.

In a case-control study by Yan et al., the authors compared the serum levels of vitamin D and the vitamin D receptors (VDR) expression in the chorionic villi and decidua, obtained during surgical evacuation of uterus of 40 women with RPL (336). Their results indicated a reduced serum level of vitamin D, as well as reduced VDR expression in the chorionic villi and decidua of patients with RPL. Moreover, a recent literature review suggested vitamin D supplementation might be beneficial for patients with RPL, although stronger evidence is needed before including this substance in the therapeutic scheme (337).

One of the limitations of our study is represented by the small sample size, which can constitute a selection bias. Also, the heterogeneity of the clinical and paraclinical findings constitutes a limitation in the relationship with the above-mentioned caveats. A greater cohort of patients recruited from multiple centers would allow for a more comprehensive picture of the issue.

I.3.4.5. Conclusions

Adverse reproductive outcomes are becoming more prevalent nowadays, especially in the context of an ascending trend of assisted reproductive techniques. It is important to clearly determine the association between clinical and paraclinical risk factors and adverse reproductive outcomes, as this would allow and improved patient's management.

This is the first prospective study that evaluated the influence of maternal KIR haplotypes on reproductive outcomes after single embryo transfer in IVF cycles in patients with recurrent pregnancy loss and implantation failure from Romania.

Our results indicated that patients with an AA haplotype had significantly more chances of miscarriage if they underwent an IVF procedure, and it appeared that the same haplotype increased the chances of obtaining a pregnancy for patients who underwent an IVF procedure.

In this study we found out that the serum levels of vitamin D were significantly lower in the RPL group compared to RIF, suggesting that vitamin D supplementation might be beneficial for this category of patients, although further research is needed.

Chapter 4: COVID-19, thrombosis and vasculopathy- is there a link?

I.4.1. State of art

COVID-19, the disease caused by the SARS-CoV-2 virus, has been associated with an increased risk of thrombosis and vascular complications. Thrombosis has been reported in patients with severe COVID-19, particularly those requiring hospitalization in intensive care units (ICUs) (338). Additionally, vascular complications such as arterial and venous thromboembolism, stroke, and myocardial infarction have been observed in some COVID-19 patients.

There are several mechanisms that may contribute to the increased risk of thrombosis and vascular complications in COVID-19 (339). One of the main mechanisms is thought to be the activation of the coagulation system and inflammation due to the virus-induced cytokine storm. The cytokine storm causes an imbalance in the coagulation system, leading to a hypercoagulable state and the formation of blood clots. The virus may also directly infect endothelial cells, leading to endothelial dysfunction, inflammation, and damage to blood vessels.

Several studies have reported an association between COVID-19 and thrombosis. A meta-analysis of 17 studies involving over 4,000 patients with COVID-19 found that the incidence of venous thromboembolism was 14.1%, and the incidence of arterial thrombotic events was 3.6% (340). The risk of thrombosis was found to be higher in patients with severe COVID-19 and those requiring ICU admission (341).

The use of anticoagulation therapy has been proposed as a potential treatment option for COVID-19 patients with thrombosis and those at high risk of thrombosis. However, the optimal duration and dosing of anticoagulation therapy in COVID-19 patients is still unclear and requires further research (342).

In addition to thrombosis, COVID-19 has also been associated with vasculopathy, or damage to blood vessels (343). The virus may directly infect endothelial cells, leading to endothelial dysfunction and inflammation. This may contribute to the development of vascular complications such as stroke, myocardial infarction, and pulmonary embolism.

In summary, there appears to be a link between COVID-19, thrombosis, and vasculopathy. The mechanisms underlying this association are still being studied, and further research is needed to fully understand the relationship between COVID-19 and vascular complications. Clinicians should remain vigilant for the development of thrombosis and vascular complications in COVID-19 patients and consider anticoagulation therapy in high-risk patients.

Personal contributions:

1. Luca MC, Loghin II, Mihai IF, **Popa R,** Vâţă A, Manciuc C. Liver Damage Associated with SARS-CoV-2 Infection-Myth or Reality? J Pers Med. 2023 Feb 17;13(2):349. doi: 10.3390/jpm13020349. PMID: 36836583; PMCID: PMC9965594.
2. Loghin II, Mihai IF, Roşu MF, Diaconu IE, Vâţă A, **Popa R**, Luca MC. Characteristics and Trends of COVID-19 Infection in a Tertiary Hospital in Romania: A Retrospective Study. J Pers Med. 2022 Nov 18;12(11):1928. doi: 10.3390/jpm12111928. PMID: 36422104; PMCID: PMC9698915.

I.4.2. Characteristics and trends of COVID-19 infection in a tertiary hospital in Romania: a retrospective study

I.4.2.1. Introduction

The end of 2019 brought to the fore a new coronavirus that infects humans, called SARS-CoV-2, that emerged in Wuhan and rapidly spread to other regions of China and around the world (344). COVID-19, the name of the disease caused by this pathogen, is described as a complex spectrum of signs and symptoms, such as cough, shortness of breath, sore throat, in association with fever, also adding anosmia, ageusia, and gastrointestinal symptoms such as nausea, vomiting, and diarrhea, by various severity degrees (345).

On 11 March 2020, the World Health Organization (WHO) characterized COVID-19 as a pandemic disease and public health threat of international interest (346), in the context of the excessive increase in the number of COVID-19 confirmed cases with a wide geographical distribution (347).

Regarding the appearance of COVID-19 in Romania, the first case was confirmed on 26 February 2020 in county Gorj, of a person who was in close contact with a citizen from Italy, the most endemic area at that time (290). Since then, until the time when this article was written (3 September 2022) in Romania, there have been 3,224,382 cases of COVID-19 and 66,751 deaths with a total number of 609,584,678 cases worldwide and 6,501,648 deaths globally.

Regarding pathogenesis, the SARS-CoV-2 enters the human body being transmitted by a respiratory way and infects human cells. Later, the infection stage is reached by binding to the cell surface protein angiotensin-converting enzyme 2 (ACE2) through the Receptor Binding Domain (RBD) of its spike (S) protein. Finally, it infiltrates and circulates in the cells of the immune system. In addition, the cellular transmembrane serine protease 2 (TMPRSS2) is required for the priming of the virus S protein (265, 294). At the epithelial cells, a complex mechanism can occur through the invasion of SARS-CoV-2 with ACE-2 receptors such as renal distal tubules, the hepatocytes, pancreas cell, and the mucosa of the intestine (348). At the same time, noble organs can be affected, such as the brain, heart, and spleen, but also the lymphatic system (lymph nodes and other lymphoid tissues) (349).

Since the beginning the COVID-19 pandemic, numerous mutations of the SARS-CoV-2 have been identified, but it turns out that only a few managed to modify the immune features of the virus. The most significant variants influencing the function of the virus originated in the United Kingdom, South Africa, Brazil, and India (350). They were named using the letters of the Greek alphabet, namely Alpha (B. 1. 1. 7), Beta (B. 1. 351), Gamma (P. 1), Delta (B. 1. 617. 2), and Omicron (B. 1. 1. 529).

The Alpha strain (B1.1.7 or British variant) was discovered In September 2020 and represents one of the first distinct variants. The second variant of the coronavirus, the Beta variant (B.1.351), was detected in South Africa on 20 May 2020. The Beta variant was also the first to generate discussion about the effectiveness of vaccines against virus mutations. The Gamma strain, the third variant of the coronavirus, was detected in Brazil in November 2020. The fourth variant of the coronavirus was detected in India in October 2020. Called Delta, it is the most virulent strain, which has generated a new wave pandemic despite the fact that in most of the developed countries the vaccination process had begun. The last strain, Omicron (B. 1.1. 529), was described in November 2021 in South Africa (351).

All these strains represent mutations of the SARS-CoV-2 from the beginning of the pandemic until now. Some of these, due to their increased transmissibility, high mortality, or hospitalization rates, have been called variants of concern (352)

The Delta variant is one of the variants of concern strain of the SARS-CoV-2. Globally it is considered the determining agent of the most severe wave of diseases. At the same time, the Delta variant caused the highest number of deaths of COVID-19, among all other strains (353).

More than two and half years after the pandemic, we have learned that the clinical picture can range from asymptomatic forms or forms with mild or moderate symptoms to severe or critical cases (354). The clinical features include a wide variety of manifestations, from respiratory symptoms, digestive symptoms, or skin rashes, to neurological damage (355). Studies have shown that some groups of patients were treated at home or they were outpatients and others who developed a moderate to severe illness requiring mechanical ventilation were hospitalized in intensive care departments.

A high mortality was recorded in cases which associated multiorgan dysfunction syndrome (356). SARS-CoV-2 has affected infants, adolescents, and adults, people without comorbidities or with various underlying diseases (357). The need to discover a vaccine which can induce SARS-CoV-2 specific neutralizing antibodies was the perfect and imperative solution in the absence of a specific treatment targeting life cycle of SARS-CoV-2 (358).

During the pandemic, great efforts were made to establish a national protocol for follow-up, diagnosis, and treatment of patients with SARS-CoV-2 infection. The research teams, doctors, and health and governmental institutions updated and made decisions based on the increased number of cases in each wave, as well as the identification of the predominant circulating strain, all this to ensure the good health of population in each territory, to keep the situation under control, to inform citizens, in order to remove some panic situations. Moreover, specific vaccines were launched, which were administered in a controlled manner. At the same time, SARS-CoV-2 testing was instituted in large communities with medical activity, in school communities, or among tourists.

In the context of a paradoxical, enigmatic, and relentless COVID-19, the objective of the current study was to evaluate the characteristics and the evolution of patients with SARS-CoV-2 infection, hospitalized in “St. Parascheva” Clinical Hospital of Infectious Diseases (Iasi, Romania).

I.4.2.2. Materials and methods

We conducted a retrospective study using the medical database recorded between July and November 2021 in order to assess the characteristics and evolution of SARS-CoV-2 infection in patients belonging to the northeastern region of Romania.

In our study the inclusion criteria represented all in-patients confirmed with COVID-19 by reverse transcriptase-polymerase chain reaction (RT-PCR), hospitalized in the “St. Parascheva” Clinical Hospital of Infectious Diseases, Iasi in the previously mentioned period. The exclusion criteria in our study were patients that had a negative result in RT-PCR for SARS-CoV-2 infection.

The analysis included demographic data, medical history, clinical, laboratory and imagistic findings, the treatment administered, and patient’s evolution. The positive diagnostic was established after RT-PCR tests performed in our hospital molecular biology laboratory or in approved accredited laboratories from Iasi, Romania.

Study limitations: this is a retrospective study based on medical records, laboratory, and imagistic findings; furthermore, the identification of circulating variants was not possible in all cases, due to limitations related to the availability of RT-q PCR kits for detection of SARS-CoV-2 in the molecular biology laboratory of the “St. Parascheva” Clinical Hospital of Infectious Diseases, Iasi.

I.4.2.3. Results

During July to November 2021, a total of 1732 SARS-CoV-2 infected patients with complete dataset were admitted at “St. Parascheva” Clinical Hospital of Infectious Diseases in Iasi.

The demographic characteristics of the patients (table IV.1) show that the mean age was 67 ± 3.4 years, most of the patients affected being aged 65–74 years old (474 cases; 27.36%). Predominantly, the patients in our study were over the age of 50, having associated multiple comorbidities with deficient immunity, this age group being likely to develop moderate-severe forms of COVID-19. The lower percentage of patients (16.95%) in our study was represented by group age of young adults (18–44 years old) and pediatric ones (under 18 years), which we correlated with a better immune status, in the absence of an underlying disease. Feminine gender was most affected, compared with the masculine gender (987 cases; 56.99% vs. 745 cases; 43.01%). Most cases were from urban areas (982 patients; 56.70%) compared to rural areas (750 patients; 43.30%).

Table IV.1. Demographic characteristics of patients

Characteristics	**Number**	**%**
Total Patients	1732	100
Age (years)	Mean	67 ± 3.4 years
	0–14 years	52
	15–24 years	29
	25–34 years	57
	35–44 years	157
	45–54 years	247
	55–64 years	323
	65–74 years	474
	>75 years	393
Gender	Female	987
	Male	745
Residence	Urban	982
	Rural	750

Of the 1732 hospitalized patients, 1242 (71.71%) patients had at least one underlying disease, such as cardiovascular pathology: hypertension (527 cases; 30.42%), atrial fibrillation (62 cases; 3.57%), heart failure (105 cases; 6.06%), chronic peripheral venous insufficiency (56 cases; 3.32%); metabolic pathology: diabetes (285 cases; 16.45%), mostly type 2, obesity (343 cases; 19.80%), chronic kidney disease (78 cases; 4.50%); but also oncological pathology (87 cases; 5.02%) (figure IV.1).

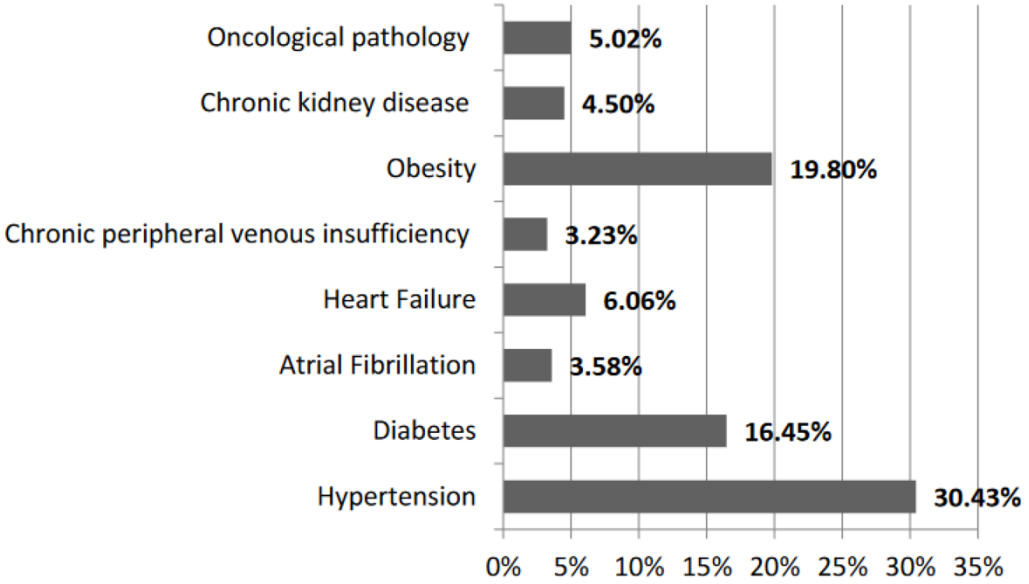

Figure IV.1**.** Associated pathologies in our patients

The first clinical symptoms at the majority of patients with SARS-CoV-2 infection were: physical asthenia (99.88%) in varying degrees, fever (1230 cases; 71.01%), cough (982 cases; 56.69%), chest pain (870 cases; 50.23%), sore throat (930 cases; 53.69%), but also myalgia (675 cases; 38.98%), arthralgia (564 cases; 32.56%), anosmia (431 cases; 24.88%), ageusia (232 cases; 13.39%), abdominal pain (482 cases; 27.82%), diarrhea (387 cases; 22.34%), and loss of appetite (1110 cases; 64.08%), (see figure IV.2) with an average duration from onset to hospitalization of 7 ± 3 days. Regarding the clinical stage of the disease, in our study, the moderate form predominated (814 cases; 47%). There were also 669 severe forms (38.63%) and 249 mild forms (14.38%).

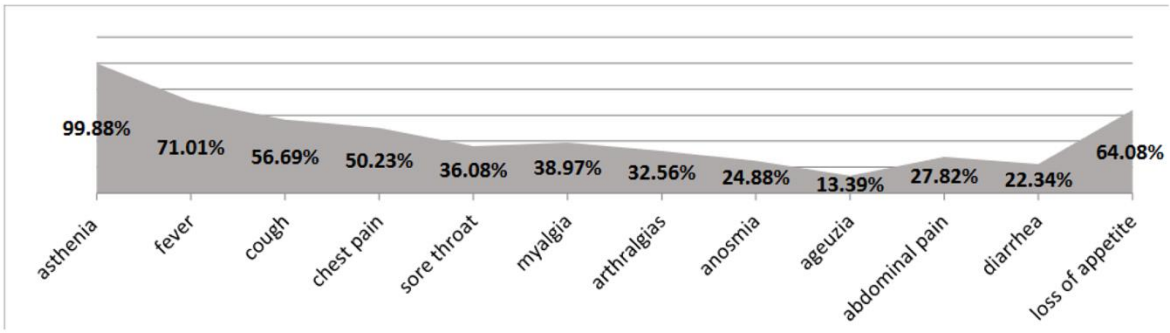

Figure IV.2**.** Symptoms at patients from our study

Each patient in the study was examined paraclinically (hematological, biochemical, serological) and by imaging (computer tomography or chest radiography). The most frequent anomalies that we could observe in this study were the decreased number of white blood cells and lymphopenia, elevated liver-function values and inflammatory markers (CRP and LDH levels) and thrombocytopenia.

During the period of our study, in Romania, the dominant spreading variant was Delta. Therefore, the sequencing was performed especially in severe cases, the Delta variant (B. 1. 617. 2) being identified by RT-PCR in 282 patients.

The necessary imaging investigations included, for each patient, lung radiography or chest computer tomography. The most pulmonary imaging changes were found in 1042

(60.16%) cases, such as viral pneumonia 850 (49.07%) cases, interstitial pneumonia 138 (7.97%) cases, bronchopneumonia 38 (2.20%) cases, and 18 (1.03%) cases of lobar pneumonia.

Biological therapy with tocilizumab and anakinra, antivirals such as remdesivir and favipiravir, and new monoclonal antibody therapies were used as treatment for these patients. Most of them received antivirals (56.76%), biological therapy (20.09%), monoclonal antibody therapy (0.58%), and in 8.66% of cases were used both antivirals and biologic therapy (figure IV.3).

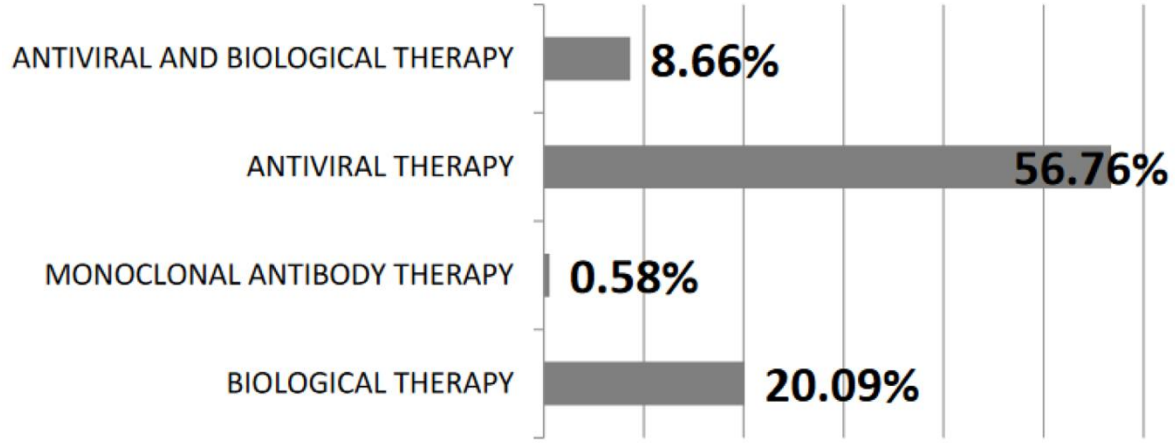

Figure IV.3. Therapies used in SARS-CoV-2 infection

In all cases, pathogenic and symptomatic treatment was associated. Most received anticoagulant treatment according to current guidelines and intravenous rebalancing infusions. In the case of patients with comorbidities, chronic treatment was also administered during hospitalization, and patients with acute respiratory failure needed oxygen therapy.

The median length of hospitalization was 9.5 days; 1359 (78.46%) patients were discharged cured, 48 (2.77%) were transferred to other services by decompensating the associated pathologies, 302 (17.43%) patients needed extensive support in the intensive care unit, and there were 325 (18.76%) deaths (figure IV.4).

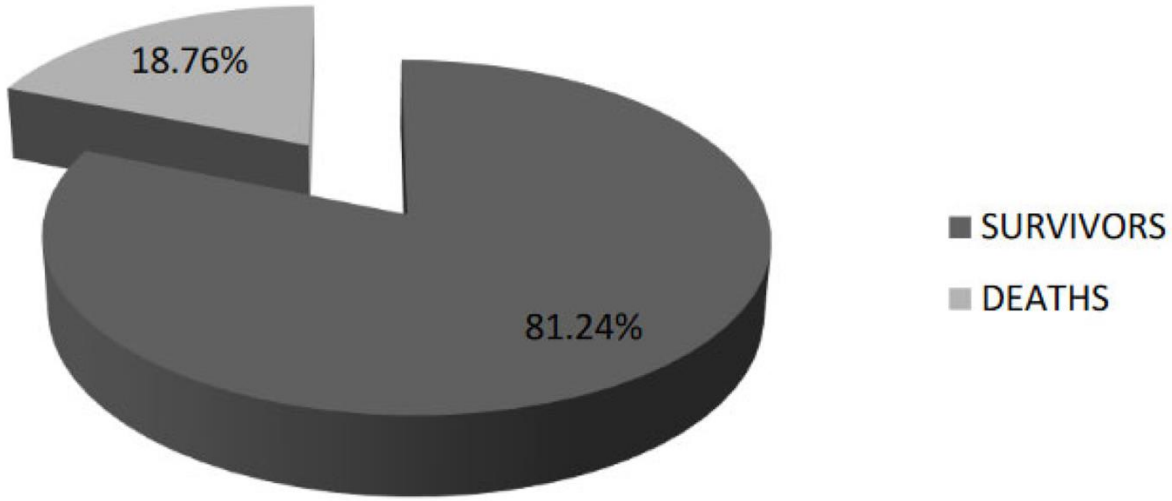

Figure IV.4. Evolution of the cases with SARS-CoV-2 infection in our study (deaths and survivors)

The most frequent deaths were recorded in the 65–74 age group (30.15%) and over 75 years old (45.84%), predominantly among male patients (55.69%) from urban area (63.38%), (table IV.2). The underlying diseases often registered in the death's cases were hypertension (41.84%), obesity (16.30%), and diabetes mellitus (14.46%). The applied treatment in severe cases, according to the national protocol, involved administration of dexamethasone, remdesivir, anakinra, tocilizumab, monotherapy, or other associated treatments. In addition, these patients received anticoagulants and additional high-flow nasal oxygen. In cases of acute respiratory distress syndrome, noninvasive ventilation and endotracheal intubation were used.

Table IV.2. Characteristics of death cases in our study

Characteristics	**Number**	**%**
Deaths		
	325	100
Age (years)		
0–14 years	0	-
15–24 years	0	-
25–34 years	0	-
35–44 years	3	0.92%
45–54 years	21	6.64%
55–64 years	54	16.61%
65–74 years	98	30.15%
>75 years	149	45.84%
Gender		
Female	144	44.30%
Male	181	55.70%
Residence		
Urban	206	63.38%
Rural	119	36.62%

I.4.2.4. Discussions

In early December 2019, 41 cases of respiratory infection were evaluated and confirmed positive by RT-PCR for COVID-19, then named "2019-nCoV" (359). In those moments, probably no one had any idea of the impact that the new virus would produce.

Since the beginning of the pandemic, around the world, multiple cases of SARS-CoV-2 infection have been reported with various strains that have emerged and put pressure on public health system by rapidly spreading and potentially evading immune protection through vaccination (360). Genetic mutations were acquired faster than expected because previous coronaviruses usually mutate at lower rates compared with other RNA viruses, such as influenza and HIV (361).

Three months after the appearance of the first cases in Wuhan, Romania reported on 26 February 2020 the first case of SARS-CoV-2 infection in the national territory, a 20-year-old male patient from Gorj county. This person came in close contact with a citizen from Italy who had been newly diagnosed with coronavirus and recently visited Romania (362). From then until the hospitalization of the first case with SARS-CoV-2 infection in the "St Parascheva" Clinical Hospital of Infectious Diseases, in Iasi, was a matter of a few days. Thus, on 4 March 2020, a 71-year-old man, who had returned from Lombardy complaining of respiratory symptoms, was confirmed to have COVID-19 and became the first patient

hospitalized in our clinic (290). Starting that time and until now, more than 10,000 COVID-19 patients have required hospitalization in our hospital.

The period to which the present study refers coincides with the 4th wave of SARS-CoV-2 infection in Romania, in which the dominant spread variant was Delta (B. 1. 617. 2), with most severe forms of COVID-19 and a high death rate recorded.

In the current study, we analyzed the clinical characteristics, treatment, and evolution of patients with SARS-CoV-2 infection admitted at "St. Parascheva" Clinical Hospital of Infectious Diseases in Iasi, for a period of 5 months (between July and November 2021), including in the study all patients with a diagnosis of COVID-19 confirmed by RT-PCR. In that period, the share of moderate cases of SARS-CoV-2 infection constituted almost half (47%) of the total number of studied cases. According to a large study from China, more than 80% of confirmed cases of coronavirus are not severe forms. However, even such a long persistence of symptoms could make the epidemic more difficult to control (363).

Statistics show that the elderly were the most susceptible category to COVID. Regarding the gender distribution, globally, there is no clear trend regarding the predisposition to infection with COVID-19. However, in the vast majority of countries, a clear pattern of mortality emerged; men appear more likely than women to die from COVID-19 once infected. In the present study, the majority of those affected were over 60 years old. The female gender and people from urban areas predominated. The number of deaths recorded during the study period was 325, 165 (50.77%) being male patients.

The predominance of the urban environment may be because of large population, public transit, and crowded travel conditions. Several studies showed that the current socio-geographical context of some countries can lead to an increased number of COVID-19 cases, and this was also observed in our region. Tourism was the main cause involved in SARS-CoV-2 infection spreading, therefore travelers developed a higher risk of infection (364).

COVID-19 can affect anyone, young or adult, with or without associated pathologies. However, advanced age and the presence of associated diseases may represent major factors in developing of severe stages and for increasing death rates (365, 366). According to our study, severe infection was observed in older patients with COVID-19 and in 1242 (71.71%) cases was found at least one associated disease.

Respiratory impairment, represented by cough and febrile episodes, was encountered in most cases, while other patients presented different symptoms, such as diarrhea, anosmia, and ageusia, but in a smaller percentage. If we refer to the changes in laboratory values, the most frequent anomalies that we could observe in this study were the leukopenia and lymphopenia, as well as the increase in CRP and LDH levels, data consistent with most studies (295, 367).

Since the start of the COVID-19 pandemic, scientists have conducted numerous studies to identify suitable therapeutic agents to treat COVID-19. Various drugs approved by the World Health Organization (WHO) and the Food and Drug Administration (FDA) were used during the pandemic. Antibiotics, antivirals, anti-inflammatories, anticoagulants, and some common medications along with combination therapies are part of the treatment or supportive care of COVID-19 patients (368). Biological therapy (20.09%) with tocilizumab and anakinra, antivirals (56.76%) such as remdesivir and favipiravir, and new monoclonal antibody therapies (0.58%) were used as treatment for the patients from our study.

I.4.2.5. Conclusions

The novelty brought in the present study is to highlight the profile of patients and the characteristics of severe forms of COVID-19, in the northeastern region of Romania, during the 4th pandemic wave.

The epidemiological characteristics of SARS-CoV-2 infection recorded in our study were mostly the same with characteristics of COVID-19 from all over the world. We found that in our hospital, most of the cases presented a moderate form of SARS-CoV-2 infections (47%) and it was an increased number of patients with severe forms (38.80%). Mortality was increased in these patients with 18.76% deaths. Furthermore, as all around the word, treatments according to protocols were used with antivirals, monoclonal antibodies, and biological therapy.

The hospital serves the entire northeastern area of Romania, providing care and treatment for admitted patients with severe forms of COVID-19, who required monitoring and treatment in Intensive Care Unit also. During the pandemic, a new extended area dedicated to patients with SARS-CoV-2 infection was opened, thus supplementing the necessary beds, especially those with the possibility of providing additional oxygen support through concentrators and mechanical ventilators. It was a real exercise of strength that through a good collaboration and interdisciplinary involvement, we passed through the very difficult pandemic COVID-19 waves.

The identification of the most frequently affected age groups, the characteristics of the patients with SARS-CoV-2 infection, the risk of mortality among patients with associated pathologies, the predominant variant, and the need for hospitalization in intensive care departments of severe cases can raise an alarm signal regarding the protection of the categories of persons at risk. Implementation of information and awareness programs such as the need for vaccination are required. In the event of a new pandemic, the population, physicians, and researchers, therefore, will know what to expect, the latter being able to develop new therapies and new standards of care in order to respond better to patients' needs.

I.4.3. Liver damage associated with SARS-CoV-2 infection—myth or reality?

I.4.3.1. Introduction

Severe acute respiratory syndrome coronavirus 2 (SARS-CoV-2) is the third strain of the Coronaviridae family responsible for causing a pandemic. Coronavirus disease 2019 (COVID-19), the respiratory disease responsible for the ongoing COVID-19 pandemic is caused by the SARS-CoV-2 virus. Its appearance in December 2019 in Wuhan, China and its rapid spread in over 216 countries led to an unprecedented global crisis with repercussions on the medical and economic system, but also on the quality of life of individuals (369). The similarity in the clinical manifestations of SARS-CoV-2 infection with other diseases, the unpredictability of the clinical and paraclinical evolution, the uncertainties regarding side effects and the treatment of the infection, and the impact of the self-isolation/isolation/quarantine regime were real challenges (370).

The experience of the current pandemic has shown us that SARS-CoV-2 can affect various organs and systems such as the cardiovascular, respiratory, neurological, digestive, metabolic systems, and more. Older adults and patients with a significant personal history of medical pathology (i.e., metabolic syndrome, cardiovascular disease, neurological disease, oncological, or liver disease) may be at an increased risk for the severe COVID-19 form (366). Oxygen saturation (SpO2) < 94% in room temperature air at sea level, the ratio of arterial oxygen partial pressure (PaO2 in mmHg) to fractional inspired oxygen (PaO2/FiO2) < 300 mm Hg, a respiratory rate > 30 breaths/min, or lung infiltrates > 50% defines a severe SARS-CoV-2 illness. These patients present with an evolution towards rapid clinical deterioration.

Liver disease is among the main extrapulmonary manifestations. Liver damage associated with SARS-CoV-2 infection is defined as any liver damage occurring during the

disease course and treatment of COVID-19 in patients with or without pre-existing liver disease. According to the statistical data up to now, in one out of five patients diagnosed with SARS-CoV-2 infection, we also find liver damage (371). In such cases, blood test results highlight elevated liver enzymes such as alanine aminotransferase (ALT) and aspartate aminotransferase (AST). Also, alkaline phosphatase (ALP) and gamma-glutamyl transferase (GGT) are enzymes that suggest liver damage. Some studies have shown that people with pre-existing liver disease (chronic liver disease, cirrhosis, or related complications) who have been diagnosed with COVID-19 have a higher risk of death than people without pre-existing liver disease (346, 372).

Mechanically, SARS-CoV-2 infection involves the binding of the viral spike protein to angiotensin-converting enzyme 2 (ACE2) as an entry receptor on the cell surface. This binding facilitates the penetration of the virus into the cell, viral replication, and intercellular transmission (373). Due to the ubiquitous distribution of ACE2, SARS-CoV-2 causes systemic disease, with possible involvement of the heart, kidneys, liver, or other organs, causing changes in circulating lymphocytes and the immune system. Liver ACE2 receptors are expressed mainly in cholangiocytes (59.7% of cells), minimally expressed in hepatocytes (2.6% of cells), and absent in Kupffer cells. Thus, it is confirmed that SARS-CoV-2 infection affects liver function by direct cytotoxicity due to the continuous replication of the virus in the previously mentioned cell populations (374, 375).

The inflammatory immune response may be responsible for hepatic impairment in COVID-19. This is demonstrated by the presence of elevated values of inflammatory markers (e.g., C-reactive protein (CRP), interleukin-6 (IL-6), interleukin-2 (IL-2), lactate dehydrogenase (LDH), ferritin, D-dimers) suggesting a direct link between the presence of cytokine storm syndrome and the severity of the disease (376).

In addition, there are other factors that contribute to impaired liver function, including medication used to treat SARS-CoV-2 infection (e.g., umifenovir, remdesivir, tocilizumab, lopinavir/ritonavir) or the treatment of associated bacterial infections (antibiotics, antipyretics, steroids), pre-existing liver disease, congestion liver, or ischemic hypoxic lesions.

Our goal was to highlight the effects of SARS-CoV-2 infection on the liver. For this purpose, we conducted a study on a group of patients diagnosed with SARS-CoV-2 infection. Finally, we used data and developing theories from the literature and corroborated them with the data obtained by our research.

I.4.3.2. Materials and methods

We conducted a retrospective clinical study focusing on hospital-based medical records of patients from “Sf. Parascheva” Clinic Hospital of Infectious Diseases from Iasi, having the objective of evaluating patients diagnosed with SARS-CoV-2 infection and associated liver injuries. Patients included were hospitalized between the 1 October 2021 and 31 December 2021.

All hospitalized patients over 18 years of age who tested positive for SARS-CoV-2 infection and had transaminase levels more than three times the normal value in the absence of pre-existing liver damage were included in the study. Diagnosis of SARS-CoV-2 infection was based on real-time reverse transcriptase-polymerase chain reactions (RT-PCR) performed on either nasopharyngeal swabs (NPS) or oropharyngeal swabs (OPS). Patients who tested positive for infection but had no evidence of liver damage with normal or quasi-abnormal transaminases or had a known pre-existing liver disease were excluded from this study.

We collected from each patient’s medical database: demographic data (age, sex), medical history, clinical features, blood tests, in-hospital treatment and outpatient outcomes (severe COVID-19, intensive care unit (ICU), mechanical ventilation, and death). Liver test

abnormalities were defined according to reference laboratory standards: AST (aspartate aminotransferase) > 37 U/L, ALT (alanine aminotransferase) > 40 U/L, ALP (serum alkaline phosphatase) outside the range of 98–279 U/L, TBIL (total-value bilirubin) > 1 mg/dL, and gamma-glutamyl transferase (GGT) > 49 U/L. All blood tests were performed by the hospital's central laboratory. RT-PCR tests were performed either by the hospital's molecular biology laboratory or by other accredited laboratories, on either nasopharyngeal swabs (NPS) or oropharyngeal swabs (OPS).

Only patients whose transaminase values were increased more than three times were included in the study because we wanted to do a statistically significant analysis of liver damage due to SARS-CoV-2 infection. The chosen period, namely October to December 2021, was representative due to the predominance of the Delta strain in Romania. This was the period with the most admissions in the entire pandemic, the most serious cases, and an increase in the number of deaths.

Correlations between demographic parameters, clinical data, and outcomes were performed using Pearson test in XLSTAT version 2019 software. Kendall's Tau correlation coefficients were calculated (377). Statistical analysis was performed using Statistical Software for Excel (XLSTAT) version 2019.

I.4.3.3. Results

During the abovementioned period in the "St. Parascheva" Clinical Hospital of Infectious Diseases from Iasi, 1552 patients confirmed to have SARS-CoV-2 infection by reverse transcriptase real-time quantitative polymerase chain reaction (RT-PCR SARS-CoV-2 RNA) were hospitalized. All patients were tested for SARS-CoV-2 infection before or on the day of hospitalization. From the total number of hospitalized cases in the mentioned period, 500 cases with liver damage were observed. After excluding pre-existing liver pathology (chronic hepatitis, liver cirrhosis, portal hypertension syndrome, ascites, jaundice, liver failure, and biliary colic), 207 patients demonstrated transaminase levels more than three times the normal value in the absence of pre-existing liver damage. Our study includes an analysis of the 207 cases mentioned above.

The age of the patients varied between 18 and 94 years, with an average age of 61 years. The most affected patients were those in the age group of 60–79 years (102 patients, 49.27%) (Figure IV.5).

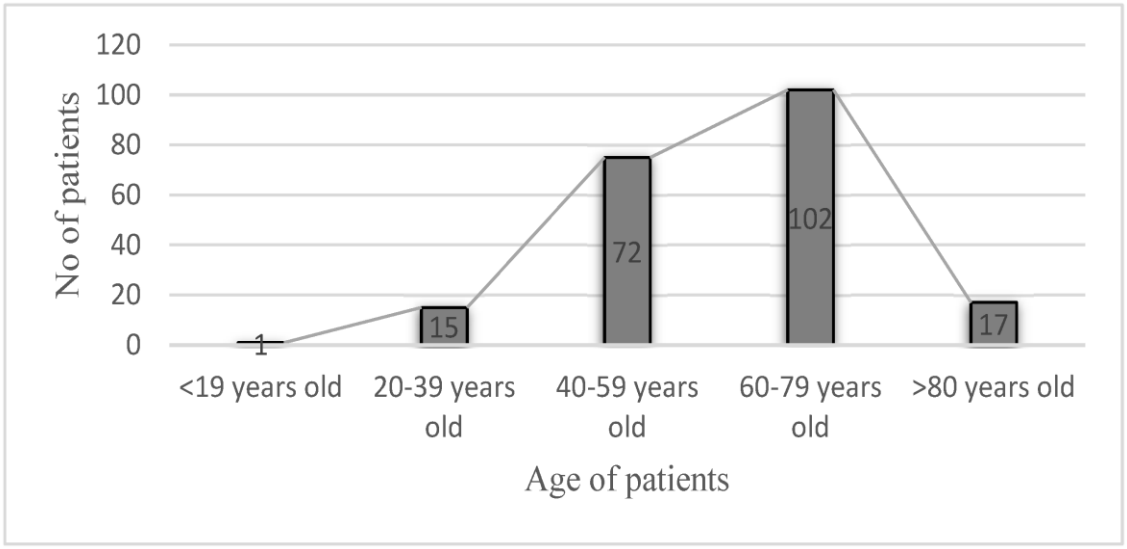

Figure IV.5. Number of patients according to age group

The total group of patients included in the study (207 in total) was divided into two groups. We called them group A and group B. Group A (48 patients, 23.19%) was represented by the category of patients with whom an increase in transaminase values was observed since the beginning of hospitalization; we considered an increase of more than three times of the normal value statistically significant. Group A also included patients where, after hospitalization and the initiation of treatment, the values decreased to the normal value or demonstrated values close to normal.

Group B (159 patients, 76.81% of the total) included patients who had normal values of transaminases or values close to normal at the time of hospitalization and those who had more than three times increase in the values normal for AST and ALT during the hospitalization and the initiation of the treatment.

The gender distribution and residence of patients showed a slightly higher share of male patients (52.65% vs. 47.34% female patients, 109 males vs. 98 female, $p < 0.05$) and those living in urban areas (56.52% vs. 43.48% in rural areas, $p < 0.05$) (Table IV.3).

Table IV.3. Demographic characteristics of the patients enrolled in our study

	Number of Patients Enrolled	%	**p value**
Gender			< 0.05
Male	109	52.65	
Female	98	47.34	
Residence			< 0.05
Urban	117	56.52	
Rural	90	43.38	

The detailed anamnesis of the patients highlighted the fact that the average time from symptom onset to hospital admission was 7.7 days. Eighteen patients (8.17%) had a complete COVID-19 vaccination scheme at hospitalization, 6 patients (2.90%) had an incomplete vaccination scheme, and the remaining 183 patients (88.40%) did not have specific anti-SARS-CoV-2 prophylaxis. A total of 39.47% (61/207) patients had no comorbidities. More than half of them had pre-existing pathologies. Excluding liver damage, patients in the study had cardiovascular disease (56 patients, 27.37%), kidney disease (47 patients, 22.70%), diabetes (27 patients, 13.04%), and neurological impairment (17 patients, 8.21%).

According to the definitions developed by the World Health Organization, the classification of COVID-19 in terms of clinical form is mild, moderate, or severe depending on the degree of respiratory function. Regarding the patients in the study group, most developed a severe form of SARS-CoV-2 infection (108 patients, 52.17%). Four (1.93%) patients developed a mild form and 95 (48.89%) developed a moderate form.

Hepatic impairment was highlighted primarily by increased transaminases (AST, ALT). All cases with elevated transaminases were determined to be secondary to SARS-CoV-2 infection. In 48 cases (23.19%), transaminase abnormalities were highlighted since the beginning of hospitalization and then subsequently normalized (group A) (Figure IV.6). In 159 cases (76.81%) an increase in liver enzymes was observed after 6 days of hospitalization, with a decrease towards the normal level (group B) (Figure IV.7).

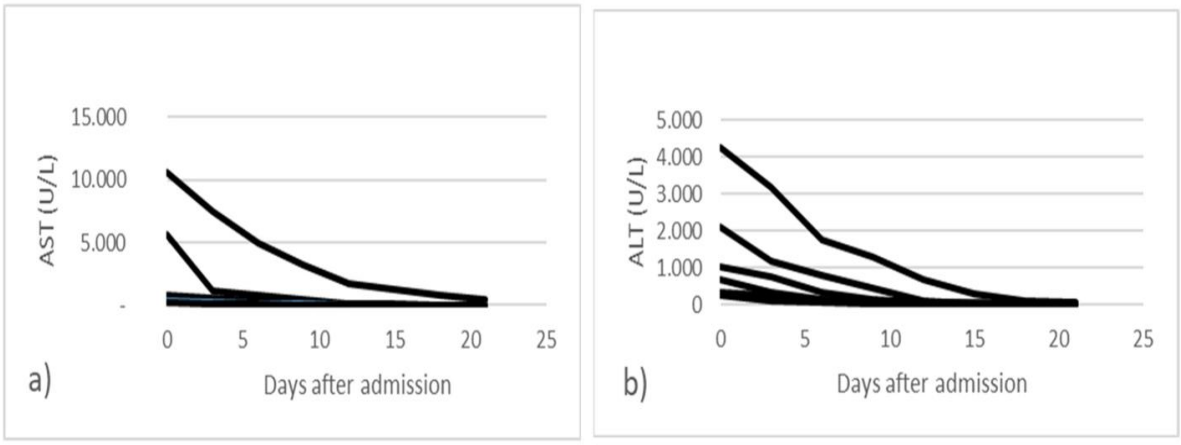

Figure IV.6**.** Dynamic changes in transaminase levels in all patients from group A; (**a**) aspartate aminotransferase and (**b**) alanine transaminase

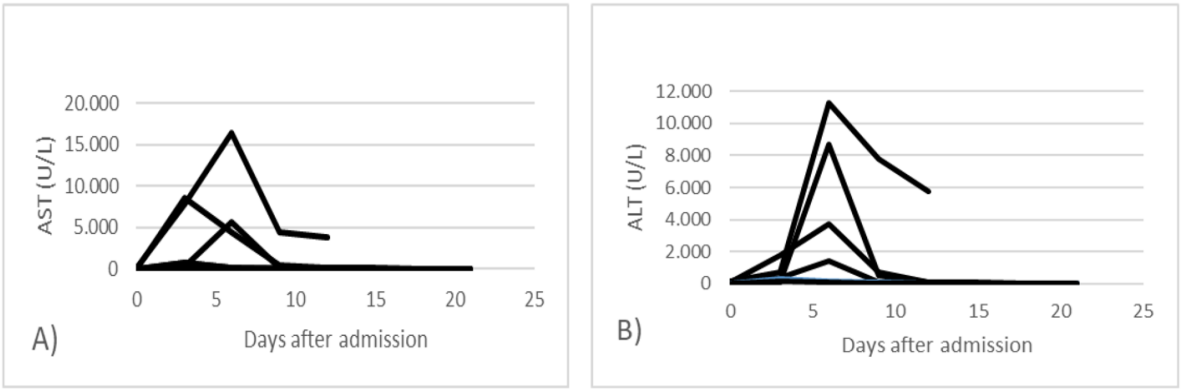

Figure IV.7. Dynamic changes in transaminase levels in all patients from group B; (**A**) aspartate aminotransferase and (B) alanine transaminase

In the graphs above, the changes in laboratory values regarding liver enzymes AST and ALT are exemplified in the case of all patients. In group A there were 5 cases with AST and ALT values over 250 U/L and in group B, in 15 cases an increase of over 250 U/L was observed during hospitalization. In the other cases, a transient increase of up to 250 U/L of transaminases was observed.

Correlated with transaminase values, we also evaluated the level of total bilirubin, with a predilection for indirect bilirubin, gamma-glutamate dehydrogenase, and alkaline phosphatase. We evaluated platelet numbers, total proteins, and prothrombin values in all patients in the study. An analysis of laboratory data showed patients with hepatic impairment had elevated indirect bilirubin (19 cases, 9.17%) and increases in gamma glutamate dehydrogenase (GGT) (72 cases, 34.78%), thrombocytopenia (46 cases, 22.21%), and hypoalbuminemia (18 cases, 8.70%).

In hospital the treatment used for SARS-CoV-2 infection was in accordance with the legislation in force at that time. The following medications were administered to patients: antibiotics such as Ceftriaxone (137 cases, 66.18%), Imipenem/cilastin (62 cases, 29.95%), and Linezolid (50 cases, 24.15%); antivirals such as Favipiravir (109 cases, 52.65%) and Remdesivir (46 cases, 22.22%); anti-inflammatory and immunomodulatory medications such as Anakinra (82 cases, 39.61%) and Tocilizumab (16 cases, 7.72%) (Figure IV.8); and vitamins according to symptoms. Hepatoprotectives and amino acids have been used for liver damage due to their detoxifying effect on the liver.

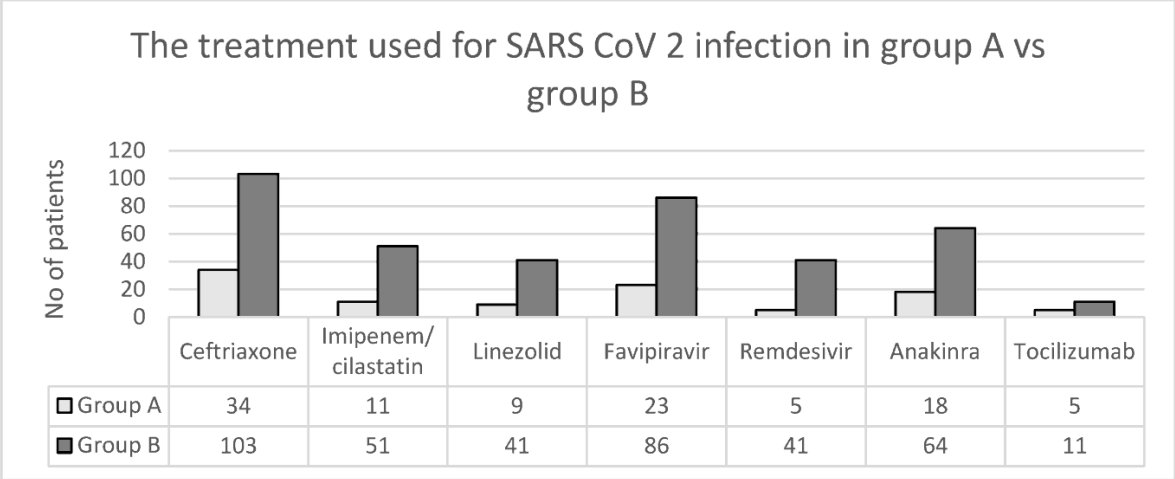

Figure IV.8. The treatment used for SARS-CoV-2 infection in group A versus group B

Prior to hospitalization all patients reported self-administration of various treatments, with most of them being symptomatic. A percentage of 18.84% (39/207) patients combined antibiotic/antiviral treatments at home (Figure IV.9).

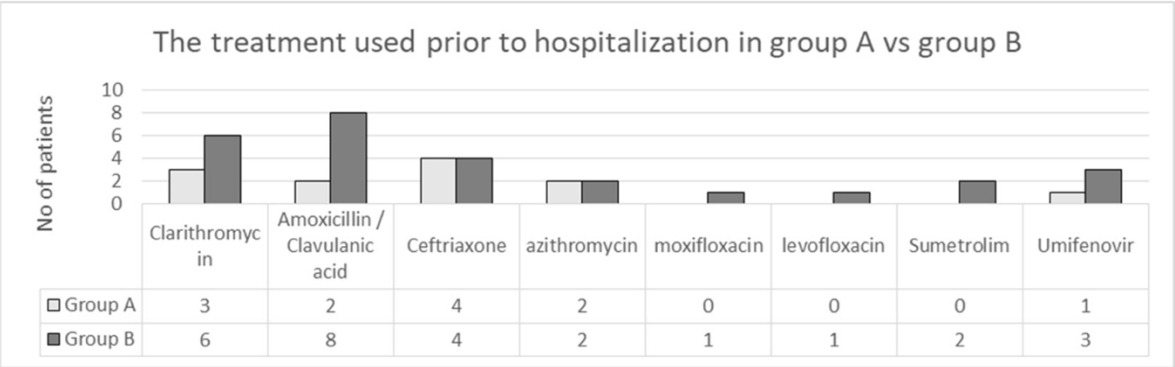

Figure IV.9. The treatment used prior to hospitalization in group A versus group B

The average time from hospital admission to discharge/interhospital transfer/death was 12.4 days. The evolution was favorable in more than half of the cases. Out of the total number of patients, 76 (36.71%) required hospitalization in the intensive care unit. In 19 cases (9.17%) patients were transferred to specialized clinics depending on the associated comorbidities and in 50 cases (24.15%) death occurred (32 cases due to multiple organ dysfunction and 18 cases due to severe respiratory failure).

In group A, 8 deaths were reported, two of which were associated with severe liver failure since admission (case 1 of a 65-year-old male patient with a severe form of COVID-19 who had AST 10 618 U/L and ALT 4260 U/L and case 2 of an 85-year-old woman with a severe form of COVID-19 who had an AST of 5700 U/L and an ALT of 2115 U/L). In both cases, the evolution was slow and worsening, with the need to monitor and continue treatment in the intensive care unit for more than 20 days.

Group B recorded a statistically higher percentage of deaths (84%). There were 4 cases in which the patients had associated liver failure. Only in one case did the death occur due to worsening liver function—the case of the 37-year-old patient with a severe form of COVID-19 who had an ALT of 11,255 U/L and an AST of 16,455 U/L.

I.4.3.4. Discussions

The new coronavirus began to be talked about at the end of 2019 after five cases of a respiratory disease of unknown origin were identified, with patients showing symptoms similar to viral pneumonia (378). From then until now (6 February 2023), after almost 3 years of the COVID-19 pandemic, more than 675 million cases of SARS-CoV-2 infection have been identified globally, with more than 6 million deaths. A new reason for concern for the entire medical system was the appearance of new variant strains that presented several mutations of the virus. They were named Alpha (British strain—B. 1. 1. 7), Beta (South Africa—B. 1. 351), Gamma (Brazilian strain—P. 1), Delta (Indian strain—B. 1. 617. 2), and Omicron (South Africa—B. 1. 1. 529) (379). Variant B1617.2 (Delta), or the Indian strain, is considered the most adapted of the four viral variants of concern, with a high degree of infectivity twice that of the original strain and about 60% greater than the Alpha variant, known as the British strain. Detected variants of coronavirus have caused fears at the global level so a great emphasis has been placed on vaccination campaigns (380).

Although a pathology of the respiratory system which was unknown to the whole world at the beginning of 2020, the SARS-CoV-2 infection proved to be multisystemic, affecting several organs and systems. From respiratory, digestive, and skin system damage to liver, metabolic, and cardiovascular damage, the clinical picture of SARS-CoV-2 infection proved to be diverse.

Liver disease has been reported since the beginning of the discovery of the novel coronavirus, frequently being described as a common manifestation, although its clinical significance was not fully understood, especially for patients with underlying chronic liver disease (CLD) (381). Both in the case of patients with pre-existing liver damage as well as in the case of patients with de novo liver damage, liver damage in hospitalized patients is mainly manifested by changes in biochemical markers in the liver (382).

Liver damage presenting with increased liver enzymes and lactate dehydrogenase was first reported in a study of 99 patients in early 2020 (383). Of the total, 43 (43.43%) had varying degrees of liver damage and impaired liver function with ALT or AST above the normal range. In one case, the value of transaminases indicated severe acute impairment of liver function, with serum ALT and AST levels increased up to 7590 and 1445 U/L, respectively, in a patient with the severe form of COVID-19 (372). A review article reported abnormal levels of ALT and AST during COVID-19 ranging from 14% to 53% (384).

Another study of nearly 1100 patients in China observed that elevated serum AST levels were found in approximately 18% of patients with moderate or mild COVID-19 disease and in approximately 56% of patients with the severe COVID-19 form. Moreover, in that study, elevated serum ALT levels were observed in nearly 20% of patients with mild or moderate COVID-19 disease and in approximately 28% of patients with severe COVID-19 disease (385). In cases of COVID-19 resulting in death, the incidence of liver injury might reach as high as 58.06 and 78% (386).

Liver test abnormalities were defined as the elevation of the following liver enzymes in serum: ALT > 40 U/L, AST > 37 U/L, GGT > 49 U/L, ALP outside the range of 98–279 U/L, and TBIL > 1 mg/dL (372). In our study, it was highlighted that 500 patients had liver damage, with 293 cases having pre-existing liver damage. Most of the cases did not have a significant deterioration of liver function and, for this reason, they were excluded from the study. We focused on the 207 cases, showing that liver involvement during COVID-19 infection with ALT or AST three times above the normal value may affect less than a quarter of patients admitted to the clinic (207 cases out of a total of 1552, 13.34%). In group A there were 5 cases with AST and ALT values over 250 U/L and in group B, in 15 cases an increase

of over 250 U/L was observed during hospitalization. In the other cases, a transient increase of up to 250 U/L in transaminase values was observed.

According to the statistical data published so far, the increase in ALT was observed between day 4 and day 17 of hospitalization, at an average of 7.3 ± 3.0 days in severe forms compared to 10.7 ± 4.1 days in mild forms ($p = 0.048$) (387). The batch studied by us was divided into two groups based on the moment of occurrence of de novo liver damage. Thus, we called them group A and group B. Group A (48 patients, 23.19%) was represented by the category of patients with whom increased values of liver enzymes were present from the first day of hospitalization; we considered an increase of more than three times the normal value statistically significant. Group A also included patients with whom, after hospitalization and the initiation of treatment, the values decreased to the normal value or demonstrated values close to normal.

Group B (159 patients, 76.81% of the total) included patients who had normal values of transaminases or values close to normal at the time of hospitalization and those who had more than three times increase in the values normal for AST and ALT during the hospitalization and the initiation of the treatment. In these cases, the increase in transaminase values was highlighted in the first week of hospitalization, after the 6th day.

Although serum transaminases may have been elevated before COVID-19, results from clinical reports and autopsy studies suggest that liver dysfunction may be an expression of a more severe course of the disease and that an increase in transaminases alone is likely to be indirect expression of systemic inflammation.

In another study of 417 patients with COVID-19, abnormal liver tests (i.e., AST, ALT, total bilirubin, GGT) were present in 76.3% and 21.5% developed liver damage during hospitalization, especially within the first two weeks after admission.

Studies have shown that patients with abnormal liver tests have a higher risk of progressing to severe disease and liver impairment is closely linked to mortality in patients with COVID-19. In our study, the severe form of COVID-19 was found in 108 cases (52.17%), accounting for more than half of all cases. Also, correlating the value of transaminases with the severity of COVID-19, we observed that in severe forms of the disease, the transaminases had a value 10 times higher than the normal one, in the case of ALT in 27 patients (9.9%) and in the case of AST in 15 patients (5.4%). The highest value was recorded in a 37-year-old patient with a severe form of COVID-19 (ALT 11,255 U/L, AST 16,455 U/L) from group B who presented at the hospital on the third day after the onset of symptoms. On the day of admission, the values of the laboratory analysis showed the following values: ALT 159 U/L, AST 109 U/L, GGT 334 U/L, ALP 437 U/L, and BT 2.68 mg/dL. The evolution in the case of this patient was unfavorable. Being a severe form of COVID-19, it required continuous oxygen therapy, supervision, and treatment in the intensive care unit, exhibiting a rapid deterioration of organs and systems. It was the first case in the study in which liver failure was one of the causes of death.

Regarding the evolution of the cases, improvement was noticed in more than half of the cases, with an average time from hospital admission to discharge/interhospital transfer/death of 12.4 days. Out of the total number of patients, 76 (36.71%) required hospitalization in the intensive care unit. In 19 cases (9.17%) patients were transferred to specialized clinics depending on the associated comorbidities and in 50 cases (24.15%) death occurred (32 cases due to multiple organ dysfunction and 18 cases due to severe respiratory failure).

In group A, 8 deaths were reported, two of which were associated with severe liver failure present since admission (case 1 of a 65-year-old male patient with the severe form of COVID-19 who had AST 10,618 U/L and ALT 4260 U/L and case 2 of an 85-year-old woman with the severe form of COVID-19 who had AST 5700 U/L and ALT 2115 U/L). In

both cases, the evolution was slow and worsening, with the need for monitoring and continuing treatment in the intensive care unit for more than 20 days.

Group B recorded a statistically higher number of deaths. There were 4 cases in which the patients had associated liver failure and only in one case did the death occur due to worsening liver function, that being the case of the 37-year-old patient with the severe form of COVID-19 who had ALT 11,255 U/L and AST 16,455 U/L.

The prevalence of abnormal liver tests may also be due to the medications used during hospitalization. In a study conducted at the Third People's Hospital of Shenzhen from China (387), among a total of 170 patients, 84% used lopinavir/ritonavir during hospitalization, which was reported to cause liver damage and affect liver tests. In our study, the medications administered to the patients were: antiviral treatment: Favipiravir (109 cases—52.65%) and Remdesivir (46 cases—22.22%); anti-inflammatory and immunomodulatory medication: Anakinra (82 cases—39.61%) and Tocilizumab (16 cases—7.72%); along with vitamins, hepatoprotectives, and amino acids according to symptoms, the latter of which is used for liver damage due to its detoxifying effect on the liver.

In addition to the increase in transaminase values, we were able to observe in our study increases in indirect bilirubin and gamma-glutamate dehydrogenase, with unchanged levels of alkaline phosphatase. Among patients with pre-existing liver pathology, it was also possible to observe a decrease in platelet values and a decrease in total proteins, especially albumin.

Hepatic impairment in mild cases of COVID-19 is often transient and may return to normal without special treatment. However, when severe liver damage occurs, liver protection treatment should be given to patients (388).

Therefore, if we refer to the causes of liver damage in our study, we refer to pre-existing liver damage, the direct expression of viral infection in the liver, and the toxic liver action of the medication used in treatment. Also, if we refer to the hepatic effects of SARS-CoV-2 infection on the patients in the study, there were increases in liver enzymes, increased total bilirubin, increases in glutamate dehydrogenase, decreased platelets, decreased bilirubin, and unchanged alkaline phosphatase.

I.4.3.5. Conclusions

Liver damage in the case of patients diagnosed with SARS-CoV-2 infection is one of the main manifestations of the infection, especially in hospitalized patients, and its presence has been associated with an increased risk of complications, including death. The cause of liver damage is most likely viral infection of bile duct cells or functional impairment caused by the use of antiviral drugs.

The present study revealed that high AST and ALT at hospital admission was associated with severe forms of COVID-19 and a high mortality risk in COVID-19 patients. Therefore, abnormal liver test results can be a significant prognostic indicator of outcomes in COVID-19 patients.

In COVID-19 elevated liver enzymes are usually mild and generally recover with hepatoprotective treatment or regimens and rest. However, the increased values of transaminases in the context of severe forms of COVID-19 or as a consequence of antiviral therapies with effects on the liver should not be neglected. It is therefore necessary to distinguish in clinical practice if the onset of abnormal liver function occurs at diagnosis or during treatment.

The mechanism of liver damage in patients with SARS-CoV-2 infection is multifactorial and requires additional research to improve the therapeutic approach in this category of patients.

Even if the pandemic is officially over, cases of infection are still being diagnosed all over the world so future research should continue. Deciphering virus–host interactions will certainly give us more clues about the detailed molecular mechanisms of liver failure following SARS-CoV-2 infection.

SECTION II

Directions for future professional development and scientific research

I will persist in prioritizing the quality of the didactic process, which is contingent upon both the didactic material's content and the pedagogical approach employed. The primary objective is to achieve success in knowledge transfer while ensuring an effective evaluation of students' knowledge and skill acquisition. In order to optimize the acquisition of knowledge during practical workshops in vascular surgery, it is suggested that a student-centered approach be employed, which emphasizes active and participatory learning. The proposal is to implement the concepts acquired in the "Train-the-Trainers" course by forming work teams to promote individual work and foster a collaborative and team-oriented mindset. The objective is to enhance the ability to analyze and self-assess the work of others.

My objective is to participate in the creation of a practice guide focused on medical vascular surgery, specifically tailored for students who are learning at General Medicine Faculty.

With regards to the training of residents, I propose the incorporation of scientific analysis sessions aimed at discussing studies and articles published in the national and international scientific community.

As part of my didactic activity, I intend to coordinate a minimum of three undergraduate theses annually for students in their final years at the University of Medicine and Pharmacy "Gr. T. Popa" Iași, encompassing both the Romanian and foreign language-speaking sections.

• Facilitate and direct student involvement in oral presentations during student communication sessions, symposiums, and congresses.

• Coordinate student workshops aimed at enhancing knowledge and practical skills.

• Conduct thematic seminars and clinical case sessions with residents.

Regarding my scientific and clinical future directions of research, I will continue to follow my main points of interests: vascular surgery, cardiac surgery, and thrombotic complications of pregnancy.

The narrowing of the carotid artery is a widely recognized predisposing element for the occurrence of ischemic stroke. The prioritization of identifying optimal primary and secondary stroke prevention strategies for both asymptomatic and symptomatic patients with carotid stenosis is of utmost importance. The present guidelines pertaining to the management of symptomatic and asymptomatic atherosclerosis are founded on randomized trials that compare medical therapy with surgical interventions. These trials utilize the degree of stenosis and symptom status as the basis for comparison, without taking into account plaque morphology and composition.

Since the initial publication of the NASCET report (389), which established a correlation between high-grade stenosis and patient outcomes, significant advancements have been made in both surgical techniques and medical interventions. The incidence of morbidity and mortality associated with revascularization procedures, particularly carotid endarterectomy, has demonstrated a decline, resulting in a decrease in severe complications and mortality rates (390).

Furthermore, multiple clinical trials have presented findings that support the efficacy of conservative medical interventions for carotid disease. These interventions include high-dose statin therapy and anti-inflammatory therapy targeting the interleukin-1β innate immunity pathway, both of which have demonstrated protective effects. Recent meta-analyses have presented evidence indicating the possibility of reversing atherosclerosis, also known as

"plaque regression," through high-dose lipid-lowering therapy. Additionally, high-dose statins have the potential to convert vulnerable plaque from a high lipid content to a more stable calcified plaque (391).

The imaging of the morphology of carotid plaque has the potential to provide a more precise representation of the pathobiology of the plaque, thereby enabling the assessment of plaque risk. This has the potential to result in a more economical choice of costly endovascular or surgical treatment alternatives (392). I am aiming to incorporate new imaging markers identified using MRI, CT and ultrasound that are associated with future cerebrovascular events. My team and I will write a grant proposal for the study of imaging biomarkers such as carotid wall volume, CT density and the plaque/muscle ratio for the prediction of plaque instability.

Compared to their nonpregnant counterparts, all pregnant patients have a greater chance of developing VTE, although certain gravidae have an increased risk compared to others (393). Although it is now advised that all obstetric patients should have their risk of VTE evaluated, there is no agreement on the best ways to do so. The necessity for high-quality research on the appropriate risk-stratification of obstetric patients is highlighted by the fact that there are several contradicting suggestions and guidelines.

The need for an accurate risk-scoring method stems from the fact that both over- and under-prophylaxis may have negative effects. Over-prophylaxis is expensive, requires patients to get frequent injections, and exposes them to uncommon side effects including hemorrhage or thrombocytopenia brought on by heparin. The incidence of VTE may rise with inadequate prevention. Therefore, the development of a precise VTE risk-stratification system for pregnancy necessitates the immediate completion of large prospective trials.

Me and my team are interested in developing different risk-scoring algorithms based on artificial intelligence and machine learning techniques, that will allow better stratification of patients at risk of VTE, and an individualized management. These algorithms would incorporate a large number of clinical and paraclinical data, collected both retrospectively and prospectively, and their performance would be assessed in terms of positive predictive value, negative predictive value, accuracy, value of area under the curve, and recall.

Another future direction of research would be based on our current work at the clinic that involves vascular repermeabilization techniques for various disorders such as diabetic arteriopathy or large vessels stenosis. The objective of creating human tissue material for vascular repair, replacement, or reconstruction is to provide a convenient, readily available substitute for autologous conduits. This substitute should possess comparable immunogenicity and long-term functionality, while also eliminating the need for wound care and operating time associated with harvesting patients' own vessels.

The demand for replacement vascular conduits among patients is consistently increasing (394). The demand for replacement vessels is crucial in the context of peripheral artery disease (PAD) and vascular injuries, which encompass both civilian and military traumatic injuries (395). Patients suffering from end-stage renal disease who are undergoing hemodialysis require frequent access to their circulatory system, which is facilitated by either a central catheter or a surgically created superficial arteriovenous loop access. The upper limb is the most common location for the arteriovenous conduit, which can be achieved through the use of the patient's vessels (known as arteriovenous fistula) or through the implantation of a synthetic graft, such as expanded polytetrafluoroethylene. The increasing prevalence of such disorders outlines the need for novel materials (396).

Currently, there are four primary sources from which vascular grafts are derived: synthetic polymers, xenogeneic tissues, allogeneic or autologous tissues, and engineered tissues. Although all of these vascular replacements have demonstrated some level of functionality, they’re in vivo outcomes vary significantly. The most common modes of failure

observed are infection, inflammation, occlusion, and degradation (397). One of the primary obstacles in the implementation of vascular grafts is their integration with the host and capacity to undergo tissue remodeling. We aim to establish a multicentric partnership with specialists from the European Union and Israel in order to study the clinical efficacy of various endoluminal grafts such as those for aortic aneurysm. Our desire is to implement, together with the use of these endografts, new procedures and materials that are already part of the panoply of procedures for inserting such type of devices. The testing of some materials and the use of new techniques for inserting these grafts can be topics for our team of research that can be included in international grants.

SECTION III

REFERENCES

1. Wolf D, Ley K. Immunity and inflammation in atherosclerosis. Circulation research. 2019;124(2):315-27.
2. Cravioto ST. Inflammation in atherosclerosis. Archivos de Cardiología de México. 2003;73(s1):141-5.
3. Timmis A, Townsend N, Gale CP, Torbica A, Lettino M, Petersen SE, et al. European Society of Cardiology: cardiovascular disease statistics 2019. European heart journal. 2020;41(1):12-85.
4. Virani SS, Alonso A, Benjamin EJ, Bittencourt MS, Callaway CW, Carson AP, et al. Heart disease and stroke statistics—2020 update: a report from the American Heart Association. Circulation. 2020;141(9):e139-e596.
5. Libby P, Ridker PM, Hansson GK. Progress and challenges in translating the biology of atherosclerosis. Nature. 2011;473(7347):317-25.
6. Stone GW, Maehara A, Lansky AJ, De Bruyne B, Cristea E, Mintz GS, et al. A prospective natural-history study of coronary atherosclerosis. New England Journal of Medicine. 2011;364(3):226-35.
7. Yusuf S, Hawken S, Ôunpuu S, Dans T, Avezum A, Lanas F, et al. Effect of potentially modifiable risk factors associated with myocardial infarction in 52 countries (the INTERHEART study): case-control study. The lancet. 2004;364(9438):937-52.
8. Bentzon JF, Otsuka F, Virmani R, Falk E. Mechanisms of plaque formation and rupture. Circulation research. 2014;114(12):1852-66.
9. Stefanadis C, Antoniou CK, Tsiachris D, Pietri P. Coronary atherosclerotic vulnerable plaque: current perspectives. Journal of the American Heart Association. 2017;6(3):e005543.
10. Roy P, Orecchioni M, Ley K. How the immune system shapes atherosclerosis: roles of innate and adaptive immunity. Nature Reviews Immunology. 2022;22(4):251-65.
11. Balakumar P, Alqahtani A, Khan NA, Alqahtani T, A T, Jagadeesh G. The physiologic and physiopathologic roles of perivascular adipose tissue and its interactions with blood vessels and the renin-angiotensin system. Pharmacological Research. 2021;173.
12. Queiroz M, Sena CM. Perivascular adipose tissue in age-related vascular disease. Ageing Research Reviews. 2020;59.
13. Weigle DS, Cummings DE, Newby PD, Breen PA, Frayo RS, Matthys CC, et al. Roles of leptin and ghrelin in the loss of body weight caused by a low fat, high carbohydrate diet. Journal of Clinical Endocrinology and Metabolism. 2003;88(4):1577-86.
14. Davies JS, Kotokorpi P, Eccles SR, Barnes SK, Tokarczuk PF, Allen SK, et al. Ghrelin induces abdominal obesity via GHS-R-dependent lipid retention. Molecular Endocrinology. 2009;23(6):914-24.
15. Papotti M, Ghè C, Cassoni P, Catapano F, Deghenghi R, Ghigo E, et al. Growth hormone secretagogue binding sites in peripheral human tissues. Journal of Clinical Endocrinology and Metabolism. 2000;85(10):3803-7.
16. Tesauro M, Schinzari F, Rovella V, Di Daniele N, Lauro D, Mores N, et al. Ghrelin restores the endothelin 1/nitric oxide balance in patients with obesity-related metabolic syndrome. Hypertension. 2009;54(5):995-1000.
17. Mengozzi A, Masi S, Virdis A. Obesity-Related Endothelial Dysfunction: moving from classical to emerging mechanisms. Endocrine and Metabolic Science. 2020;1(3-4).

18. Tesauro M, Schinzari F, Iantorno M, Rizza S, Melina D, Lauro D, et al. Ghrelin improves endothelial function in patients with metabolic syndrome. Circulation. 2005;112(19):2986-92.
19. Cardillo C, Kilcoyne CM, Cannon Iii RO, Panza JA. Interactions between nitric oxide and endothelin in the regulation of vascular tone of human resistance vessels in vivo. Hypertension. 2000;35(6):1237-41.
20. Antonopoulos AS, Papanikolaou P, Tousoulis D. The role of perivascular adipose tissue in microvascular function and coronary atherosclerosis. Microcirculation: From Bench to Bedside2019. p. 77-94.
21. Acosta JR, Tavira B, Douagi I, Kulyté A, Arner P, Rydén M, et al. Human-Specific Function of IL-10 in Adipose Tissue Linked to Insulin Resistance. Journal of Clinical Endocrinology and Metabolism. 2019;104(10):4552-62.
22. Contreras GA, Yang Y, Flood ED, Garver H, Bhattacharya S, Fink GD, et al. Blood pressure changes PVAT function and transcriptome: use of the mid-thoracic aorta coarcted rat. American Journal of Physiology - Heart and Circulatory Physiology. 2020;319(6):H1313-H24.
23. Rajsheker S, Manka D, Blomkalns AL, Chatterjee TK, Stoll LL, Weintraub NL. Crosstalk between perivascular adipose tissue and blood vessels. Current Opinion in Pharmacology. 2010;10(2):191-6.
24. Malka KT, Clum P, Tero B, Huang C, Vary C, Liaw L. Perivascular Adipose Tissue Surrounding Healthy and Diseased Human Aorta Represent Two Distinct Populations of Adipocytes. J Vasc Surg. 2021;74:e325-e6.
25. Verhagen SN, Vink A, van der Graaf Y, Visseren FLJ. Coronary perivascular adipose tissue characteristics are related to atherosclerotic plaque size and composition. A post-mortem study. Atherosclerosis. 2012;225(1):99-104.
26. Verhagen SN, Buijsrogge MP, Vink A, Van Herwerden LA, Van Der Graaf Y, Visseren FLJ. Secretion of adipocytokines by perivascular adipose tissue near stenotic and non-stenotic coronary artery segments in patients undergoing CABG. Atherosclerosis. 2014;233(1):242-7.
27. Shan B, Shao M, Zhang Q, Hepler C, Paschoal VA, Barnes SD, et al. Perivascular mesenchymal cells control adipose-tissue macrophage accrual in obesity. Nature Metabolism. 2020;2(11):1332-49.
28. Choi K, Roh SG, Hong YH, Shrestha YB, Hishikawa D, Chen C, et al. The role of ghrelin and growth hormone secretagogues receptor on rat adipogenesis. Endocrinology. 2003;144(3):754-9.
29. Lelis DDF, Freitas DFD, Machado AS, Crespo TS, Santos SHS. Angiotensin-(1-7), Adipokines and Inflammation. Metabolism: Clinical and Experimental. 2019;95:36-45.
30. Yasuda T, Masaki T, Kakuma T, Yoshimatsu H. Centrally administered ghrelin suppresses sympathetic nerve activity in brown adipose tissue of rats. Neuroscience Letters. 2003;349(2):75-8.
31. Ukkola O. Ghrelin and atherosclerosis. Current Opinion in Lipidology. 2015;26(4):288-91.
32. Achike FI, To NHP, Wang H, Kwan CY. Obesity, metabolic syndrome, adipocytes and vascular function: A holistic viewpoint. Clinical and Experimental Pharmacology and Physiology. 2011;38(1):1-10.
33. Avallone R, Demers A, Rodrigue-Way A, Bujold K, Harb D, Anghel S, et al. A growth hormone-releasing peptide that binds scavenger receptor CD36 and ghrelin receptor up-regulates sterol transporters and cholesterol efflux in macrophages through a peroxisome proliferator-activated receptor γ-dependent pathway. Molecular Endocrinology. 2006;20(12):3165-78.

34. Ai W, Wu M, Chen L, Jiang B, Mu M, Liu L, et al. Ghrelin ameliorates atherosclerosis by inhibiting endoplasmic reticulum stress. Fundamental and Clinical Pharmacology. 2017;31(2):147-54.
35. Yang Y, Zhou Q, Gao A, Chen L, Li L. Endoplasmic reticulum stress and focused drug discovery in cardiovascular disease. Clinica Chimica Acta. 2020;504:125-37.
36. Ringel C, Dittrich J, Gaudl A, Schellong P, Beuchel CF, Baber R, et al. Association of plasma trimethylamine N-oxide levels with atherosclerotic cardiovascular disease and factors of the metabolic syndrome. Atherosclerosis. 2021;335:62-7.
37. Lin X, Ouyang S, Zhi C, Li P, Tan X, Ma W, et al. Focus on ferroptosis, pyroptosis, apoptosis and autophagy of vascular endothelial cells to the strategic targets for the treatment of atherosclerosis. Archives of Biochemistry and Biophysics. 2022;715.
38. Carbone F, Mach F, Montecucco F. The role of adipocytokines in atherogenesis and atheroprogression. Current Drug Targets. 2015;16(4):320.
39. Virdis A, Lerman LO, Regoli F, Ghiadoni L, Lerman A, Taddei S. Human ghrelin: A gastric hormone with cardiovascular properties. Current Pharmaceutical Design. 2016;22(1):52-8.
40. Zhang M, Wang S, Pan Z, Ou T, Ma J, Liu H, et al. AMPK/NF-κB signaling pathway regulated by ghrelin participates in the regulation of HUVEC and THP1 Inflammation. Molecular and Cellular Biochemistry. 2018;437(1-2):45-53.
41. Zhang M, Qu X, Yuan F, Yang Y, Xu L, Dai J, et al. Ghrelin receptor deficiency aggravates atherosclerotic plaque instability. Frontiers in Bioscience - Landmark. 2015;20(4):604-13.
42. Lilleness BM, Frishman WH. Ghrelin and the cardiovascular system. Cardiology in Review. 2016;24(6):288-97.
43. Conconi MT, Nico B, Guidolin D, Baiguera S, Spinazzi R, Rebuffat P, et al. Ghrelin inhibits FGF-2-mediated angiogenesis in vitro and in vivo. Peptides. 2004;25(12):2179-85.
44. Mirzaei Bavil F, Karimi-Sales E, Alihemmati A, Alipour MR. Effect of ghrelin on hypoxia-related cardiac angiogenesis: involvement of miR-210 signalling pathway. Archives of Physiology and Biochemistry. 2022;128(1):270-5.
45. Cui H, López M, Rahmouni K. The cellular and molecular bases of leptin and ghrelin resistance in obesity. Nature Reviews Endocrinology. 2017;13(6):338-51.
46. Dixit VD, Schaffer EM, Pyle RS, Collins GD, Sakthivel SK, Palaniappan R, et al. Ghrelin inhibits leptin- and activation-induced proinflammatory cytokine expression by human monocytes and T cells. Journal of Clinical Investigation. 2004;114(1):57-66.
47. Perpétuo L, Voisin PM, Amado F, Hirtz C, Vitorino R. Ghrelin and adipokines: An overview of their physiological role, antimicrobial activity and impact on cardiovascular conditions. Vitamins and Hormones2021. p. 477-509.
48. Bedendi I, Alloatti G, Marcantoni A, Malan D, Catapano F, Ghé C, et al. Cardiac effects of ghrelin and its endogenous derivatives des-octanoyl ghrelin and des-Gln14-ghrelin. European Journal of Pharmacology. 2003;476(1-2):87-95.
49. Yu Y, Fernandez ID, Meng Y, Zhao W, Groth SW. Gut hormones, adipokines, and pro- and anti-inflammatory cytokines/markers in loss of control eating: A scoping review. Appetite. 2021;166.
50. Rodríguez A. Novel molecular aspects of ghrelin and leptin in the control of adipobiology and the cardiovascular system. Obesity Facts. 2014;7(2):82-95.
51. Shu ZW, Yu M, Chen XJ, Tan XR. Ghrelin could be a candidate for the prevention of in-stent restenosis. Cardiovascular Drugs and Therapy. 2013;27(4):309-14.

52. Virdis A, Taddei S. Endothelial Dysfunction in Resistance Arteries of Hypertensive Humans: Old and New Conspirators. Journal of Cardiovascular Pharmacology. 2016;67(6):451-7.
53. Schrottmaier WC, Mussbacher M, Salzmann M, Assinger A. Platelet-leukocyte interplay during vascular disease. Atherosclerosis. 2020;307:109-20.
54. Wang L, Tang C. Targeting platelet in atherosclerosis plaque formation: Current knowledge and future perspectives. International Journal of Molecular Sciences. 2020;21(24):1-23.
55. Ed Rainger G, Chimen M, Harrison MJ, Yates CM, Harrison P, Watson SP, et al. The role of platelets in the recruitment of leukocytes during vascular disease. Platelets. 2015;26(6):507-20.
56. Elbatarny HS, Netherton SJ, Ovens JD, Ferguson AV, Maurice DH. Adiponectin, ghrelin, and leptin differentially influence human platelet and human vascular endothelial cell functions: Implication in obesity-associated cardiovascular diseases. European Journal of Pharmacology. 2007;558(1-3):7-13.
57. Arici OF, Çetin N. Protective role of ghrelin against carbon tetrachloride (CCl4)-induced coagulation disturbances in rats. Regulatory Peptides. 2011;166(1-3):139-42.
58. Nishimura S, Manabe I, Nagasaki M, Seo K, Yamashita H, Hosoya Y, et al. In vivo imaging in mice reveals local cell dynamics and inflammation in obese adipose tissue. Journal of Clinical Investigation. 2008;118(2):710-21.
59. Costa RM, Filgueira FP, Tostes RC, Carvalho MHC, Akamine EH, Lobato NS. H2O2 generated from mitochondrial electron transport chain in thoracic perivascular adipose tissue is crucial for modulation of vascular smooth muscle contraction. Vascular Pharmacology. 2016;84:28-37.
60. Azul L, Leandro A, Boroumand P, Klip A, Seiça R, Sena CM. Increased inflammation, oxidative stress and a reduction in antioxidant defense enzymes in perivascular adipose tissue contribute to vascular dysfunction in type 2 diabetes. Free Radical Biology and Medicine. 2020;146:264-74.
61. Landecho MF, Tuero C, Valentí V, Bilbao I, de la Higuera M, Frühbeck G. Relevance of leptin and other adipokines in obesity-associated cardiovascular risk. Nutrients. 2019;11(11).
62. Rossi F, Castelli A, Bianco MJ, Bertone C, Brama M, Santiemma V. Ghrelin inhibits contraction and proliferation of human aortic smooth muscle cells by cAMP/PKA pathway activation. Atherosclerosis. 2009;203(1):97-104.
63. Okumura H, Nagaya N, Enomoto M, Nakagawa E, Oya H, Kangawa K. Vasodilatory effect of ghrelin, an endogenous peptide from the stomach. Journal of Cardiovascular Pharmacology. 2002;39(6):779-83.
64. Mao Y, Tokudome T, Kishimoto I. Ghrelin and Blood Pressure Regulation. Current Hypertension Reports. 2016;18(2):1-6.
65. Kawczynska-Drozdz A, Olszanecki R, Jawien J, Brzozowski T, Pawlik WW, Korbut R, et al. Ghrelin Inhibits Vascular Superoxide Production in Spontaneously Hypertensive Rats. American Journal of Hypertension. 2006;19(7):764-7.
66. Carraro G, Albertin G, Aragona F, Forneris M, Casale V, Spinazzi R, et al. Age-dependent decrease in the ghrelin gene expression in the human adrenal cortex: A real-time PCR study. International Journal of Molecular Medicine. 2006;17(2):319-21.
67. Cappellari GG, Semolic A, Cremasco G, Vinci P, Zanetti M, Barazzoni R. Unacylated ghrelin plasma levels are lower and predict 5-year low muscle mass in elderly obese subjects. Nutrition. 2021;87:111316.
68. Lindqvist A, Shcherbina L, Prasad RB, Miskelly MG, Abels M, Martínez-Lopéz JA, et al. Ghrelin suppresses insulin secretion in human islets and type 2 diabetes

patients have diminished islet ghrelin cell number and lower plasma ghrelin levels. Molecular and Cellular Endocrinology. 2020;511.

69. Adebayo O, Adeoye AM. Atherosclerosis: A Journey Around the Terminology. Gianturco L, editor. IntechOpen
2020.

70. Herrington W, Lacey B, Sherliker P, Armitage J, Lewington S. Epidemiology of Atherosclerosis and the Potential to Reduce the Global Burden of Atherothrombotic Disease. Circ Res. 2016;118(4):535-46.

71. Forouzanfar MH, Moran AE, Flaxman AD, Roth G, Mensah GA, Ezzati M, et al. Assessing the global burden of ischemic heart disease, part 2: analytic methods and estimates of the global epidemiology of ischemic heart disease in 2010. Glob Heart. 2012;7(4):331-42.

72. Otsuka F, Yasuda S, Noguchi T, Ishibashi-Ueda H. Pathology of coronary atherosclerosis and thrombosis. Cardiovasc Diagn Ther. 2016;6(4):396-408.

73. Stary HC, Chandler AB, Dinsmore RE, Fuster V, Glagov S, Insull W, Jr., et al. A definition of advanced types of atherosclerotic lesions and a histological classification of atherosclerosis. A report from the Committee on Vascular Lesions of the Council on Arteriosclerosis, American Heart Association. Circulation. 1995;92(5):1355-74.

74. Rader DJ, Daugherty A. Translating molecular discoveries into new therapies for atherosclerosis. Nature. 2008;451(7181):904-13.

75. Pedicino D, Giglio AF, Galiffa VA, Cialdella P, Trotta F, Graziani F, et al. Infections, immunity and atherosclerosis: pathogenic mechanisms and unsolved questions. Int J Cardiol. 2013;166(3):572-83.

76. Tabas I, García-Cardeña G, Owens GK. Recent insights into the cellular biology of atherosclerosis. J Cell Biol. 2015;209(1):13-22.

77. Brown RA, Shantsila E, Varma C, Lip GY. Current Understanding of Atherogenesis. Am J Med. 2017;130(3):268-82.

78. Wang T, Butany J. Pathogenesis of atherosclerosis. Diagnostic Histopathology. 2017;23(11):473-8.

79. Nakahara T, Dweck MR, Narula N, Pisapia D, Narula J, Strauss HW. Coronary Artery Calcification: From Mechanism to Molecular Imaging. JACC Cardiovasc Imaging. 2017;10(5):582-93.

80. Abedin M, Tintut Y, Demer LL. Vascular calcification: mechanisms and clinical ramifications. Arterioscler Thromb Vasc Biol. 2004;24(7):1161-70.

81. Collin-Osdoby P. Regulation of vascular calcification by osteoclast regulatory factors RANKL and osteoprotegerin. Circ Res. 2004;95(11):1046-57.

82. Kadoglou NP, Gerasimidis T, Moumtzouoglou A, Kapelouzou A, Sailer N, Fotiadis G, et al. Intensive lipid-lowering therapy ameliorates novel calcification markers and GSM score in patients with carotid stenosis. Eur J Vasc Endovasc Surg. 2008;35(6):661-8.

83. Kahles F, Findeisen HM, Bruemmer D. Osteopontin: A novel regulator at the cross roads of inflammation, obesity and diabetes. Mol Metab. 2014;3(4):384-93.

84. Denhardt DT, Noda M. Osteopontin expression and function: role in bone remodeling. J Cell Biochem Suppl. 1998;30-31:92-102.

85. Kwon HM, Hong BK, Kang TS, Kwon K, Kim HK, Jang Y, et al. Expression of osteopontin in calcified coronary atherosclerotic plaques. J Korean Med Sci. 2000;15(5):485-93.

86. Momiyama Y, Ohmori R, Fayad ZA, Kihara T, Tanaka N, Kato R, et al. Associations between plasma osteopontin levels and the severities of coronary and aortic atherosclerosis. Atherosclerosis. 2010;210(2):668-70.

87. Reid P, Holen I. Pathophysiological roles of osteoprotegerin (OPG). Eur J Cell Biol. 2009;88(1):1-17.

88. Scatena M, Liaw L, Giachelli CM. Osteopontin: a multifunctional molecule regulating chronic inflammation and vascular disease. Arterioscler Thromb Vasc Biol. 2007;27(11):2302-9.

89. Heymann MF, Herisson F, Davaine JM, Charrier C, Battaglia S, Passuti N, et al. Role of the OPG/RANK/RANKL triad in calcifications of the atheromatous plaques: comparison between carotid and femoral beds. Cytokine. 2012;58(2):300-6.

90. Rochette L, Meloux A, Rigal E, Zeller M, Cottin Y, Vergely C. The Role of Osteoprotegerin and Its Ligands in Vascular Function. Int J Mol Sci. 2019;20(3).

91. Van Campenhout A, Golledge J. Osteoprotegerin, vascular calcification and atherosclerosis. Atherosclerosis. 2009;204(2):321-9.

92. Oates CP, Naylor AR, Hartshorne T, Charles SM, Fail T, Humphries K, et al. Joint recommendations for reporting carotid ultrasound investigations in the United Kingdom. Eur J Vasc Endovasc Surg. 2009;37(3):251-61.

93. Naylor AR, Ricco JB, de Borst GJ, Debus S, de Haro J, Halliday A, et al. Editor's Choice - Management of Atherosclerotic Carotid and Vertebral Artery Disease: 2017 Clinical Practice Guidelines of the European Society for Vascular Surgery (ESVS). Eur J Vasc Endovasc Surg. 2018;55(1):3-81.

94. Barnett HJM, Taylor DW, Haynes RB, Sackett DL, Peerless SJ, Ferguson GG, et al. Beneficial effect of carotid endarterectomy in symptomatic patients with high-grade carotid stenosis. N Engl J Med. 1991;325(7):445-53.

95. MRC European Carotid Surgery Trial: interim results for symptomatic patients with severe (70-99%) or with mild (0-29%) carotid stenosis. European Carotid Surgery Trialists' Collaborative Group. Lancet. 1991;337(8752):1235-43.

96. el-Barghouty N, Nicolaides A, Bahal V, Geroulakos G, Androulakis A. The identification of the high risk carotid plaque. Eur J Vasc Endovasc Surg. 1996;11(4):470-8.

97. Elatrozy T, Nicolaides A, Tegos T, Zarka AZ, Griffin M, Sabetai M. The effect of B-mode ultrasonic image standardisation on the echodensity of symptomatic and asymptomatic carotid bifurcation plaques. Int Angiol. 1998;17(3):179-86.

98. Popa RF, Strobescu C, Baroi G, Raza A, Fotea V. Complex utrasound study of the atherosclerotic plaque. Rev Med Chir Soc Med Nat Iasi. 2013;117(2):424-30.

99. Strobescu-Ciobanu C PR, Giuşcă SE, Rusu A, Lupaşcu CD. Correlations between grayscale and histopathological proprieties of carotid atherosclerotic plaque. . Rev Med Chir Soc Med Nat Iasi. 2020;124(1):79–85.

100. Gray-Weale AC, Graham JC, Burnett JR, Byrne K, Lusby RJ. Carotid artery atheroma: comparison of preoperative B-mode ultrasound appearance with carotid endarterectomy specimen pathology. J Cardiovasc Surg (Torino). 1988;29(6):676-81.

101. Lovett JK, Redgrave JN, Rothwell PM. A critical appraisal of the performance, reporting, and interpretation of studies comparing carotid plaque imaging with histology. Stroke. 2005;36(5):1091-7.

102. Makris GC, Nicolaides AN, Geroulakos G. Histological analysis of the carotid plaque post-endarterectomy: a waste of time or a wasted piece of information? Eur J Vasc Endovasc Surg. 2011;42(1):13-4.

103. Rothwell PM, Eliasziw M, Gutnikov SA, Fox AJ, Taylor DW, Mayberg MR, et al. Analysis of pooled data from the randomised controlled trials of endarterectomy for symptomatic carotid stenosis. Lancet. 2003;361(9352):107-16.

104. Rothwell PM, Eliasziw M, Gutnikov SA, Warlow CP, Barnett HJ. Endarterectomy for symptomatic carotid stenosis in relation to clinical subgroups and timing of surgery. Lancet. 2004;363(9413):915-24.

105. Tegos TJ, Sohail M, Sabetai MM, Robless P, Akbar N, Pare G, et al. Echomorphologic and histopathologic characteristics of unstable carotid plaques. AJNR Am J Neuroradiol. 2000;21(10):1937-44.

106. Ratliff DA, Gallagher PJ, Hames TK, Humphries KN, Webster JH, Chant AD. Characterisation of carotid artery disease: comparison of duplex scanning with histology. Ultrasound Med Biol. 1985;11(6):835-40.

107. Carotid artery plaque composition--relationship to clinical presentation and ultrasound B-mode imaging. European Carotid Plaque Study Group. Eur J Vasc Endovasc Surg. 1995;10(1):23-30.

108. Reiter M, Horvat R, Puchner S, Rinner W, Polterauer P, Lammer J, et al. Plaque imaging of the internal carotid artery - correlation of B-flow imaging with histopathology. AJNR Am J Neuroradiol. 2007;28(1):122-6.

109. de Bray JM, Baud JM, Delanoy P, Camuzat JP, Dehans V, Descamp-Le Chevoir J, et al. Reproducibility in ultrasonic characterization of carotid plaques. Cerebrovasc Dis. 1998;8(5):273-7.

110. Arnold JA, Modaresi KB, Thomas N, Taylor PR, Padayachee TS. Carotid plaque characterization by duplex scanning: observer error may undermine current clinical trials. Stroke. 1999;30(1):61-5.

111. Denzel C, Balzer K, Müller KM, Fellner F, Fellner C, Lang W. Relative value of normalized sonographic in vitro analysis of arteriosclerotic plaques of internal carotid artery. Stroke. 2003;34(8):1901-6.

112. Meiliana A DN, Wijaya A. . Mesenchymal stem cell secretome: cell-free therapeutic strategy in regenerative medicine. . Indones Biomed J. 2019;11(2):113–124.

113. Golledge J, McCann M, Mangan S, Lam A, Karan M. Osteoprotegerin and osteopontin are expressed at high concentrations within symptomatic carotid atherosclerosis. Stroke. 2004;35(7):1636-41.

114. Kadoglou NP, Gerasimidis T, Golemati S, Kapelouzou A, Karayannacos PE, Liapis CD. The relationship between serum levels of vascular calcification inhibitors and carotid plaque vulnerability. J Vasc Surg. 2008;47(1):55-62.

115. Butler WT. The nature and significance of osteopontin. Connect Tissue Res. 1989;23(2-3):123-36.

116. Icer MA, Gezmen-Karadag M. The multiple functions and mechanisms of osteopontin. Clin Biochem. 2018;59:17-24.

117. Lok ZSY, Lyle AN. Osteopontin in Vascular Disease. Arterioscler Thromb Vasc Biol. 2019;39(4):613-22.

118. Myers DL, Harmon KJ, Lindner V, Liaw L. Alterations of arterial physiology in osteopontin-null mice. Arterioscler Thromb Vasc Biol. 2003;23(6):1021-8.

119. Chiba S, Okamoto H, Kon S, Kimura C, Murakami M, Inobe M, et al. Development of atherosclerosis in osteopontin transgenic mice. Heart Vessels. 2002;16(3):111-7.

120. Wolak T, Sion-Vardi N, Novack V, Greenberg G, Szendro G, Tarnovscki T, et al. N-terminal rather than full-length osteopontin or its C-terminal fragment is associated with carotid-plaque inflammation in hypertensive patients. Am J Hypertens. 2013;26(3):326-33.

121. Herisson F, Heymann MF, Chétiveaux M, Charrier C, Battaglia S, Pilet P, et al. Carotid and femoral atherosclerotic plaques show different morphology. Atherosclerosis. 2011;216(2):348-54.

122. Kim J, Song TJ, Yang SH, Lee OH, Nam HS, Kim YD, et al. Plasma osteoprotegerin levels increase with the severity of cerebral artery atherosclerosis. Clin Biochem. 2013;46(12):1036-40.

123. Blázquez-Medela AM, García-Ortiz L, Gómez-Marcos MA, Recio-Rodriguez JI, Sánchez-Rodríguez A, López-Novoa JM, et al. Osteoprotegerin is associated with cardiovascular risk in hypertension and/or diabetes. Eur J Clin Invest. 2012;42(5):548-56.

124. Halak S, Östling G, Edsfeldt A, Kennbäck C, Dencker M, Gonçalves I, et al. Spotty Carotid Plaques Are Associated with Inflammation and the Occurrence of Cerebrovascular Symptoms. Cerebrovasc Dis Extra. 2018;8(1):16-25.

125. Davaine JM, Quillard T, Brion R, Lapérine O, Guyomarch B, Merlini T, et al. Osteoprotegerin, pericytes and bone-like vascular calcification are associated with carotid plaque stability. PLoS One. 2014;9(9):e107642.

126. Truelsen T, Piechowski-Jóźwiak B, Bonita R, Mathers C, Bogousslavsky J, Boysen G. Stroke incidence and prevalence in Europe: a review of available data. Eur J Neurol. 2006;13(6):581-98.

127. Nichols M, Townsend N, Scarborough P, Rayner M. Cardiovascular disease in Europe: epidemiological update. Eur Heart J. 2013;34(39):3028-34.

128. Leon-Constantin MM ea. The impact of subclinical atherosclerosis to the patients with stroke and diabetes. . Rev Med Chir Soc Med Nat Iasi 2019;123(3): 419-425.

129. Grant EG, Benson CB, Moneta GL, Alexandrov AV, Baker JD, Bluth EI, et al. Carotid artery stenosis: gray-scale and Doppler US diagnosis--Society of Radiologists in Ultrasound Consensus Conference. Radiology. 2003;229(2):340-6.

130. Langsfeld M, Gray-Weale AC, Lusby RJ. The role of plaque morphology and diameter reduction in the development of new symptoms in asymptomatic carotid arteries. J Vasc Surg. 1989;9(4):548-57.

131. Geroulakos G, Ramaswami G, Nicolaides A, James K, Labropoulos N, Belcaro G, et al. Characterization of symptomatic and asymptomatic carotid plaques using high-resolution real-time ultrasonography. Br J Surg. 1993;80(10):1274-7.

132. Geroulakos G, Domjan J, Nicolaides A, Stevens J, Labropoulos N, Ramaswami G, et al. Ultrasonic carotid artery plaque structure and the risk of cerebral infarction on computed tomography. J Vasc Surg. 1994;20(2):263-6.

133. Sztajzel R. Ultrasonographic assessment of the morphological characteristics of the carotid plaque. Swiss Med Wkly. 2005;135(43-44):635-43.

134. Bassiouny HS, Sakaguchi Y, Mikucki SA, McKinsey JF, Piano G, Gewertz BL, et al. Juxtalumenal location of plaque necrosis and neoformation in symptomatic carotid stenosis. J Vasc Surg. 1997;26(4):585-94.

135. Tsuruda JS, Saloner D, Anderson C. Noninvasive evaluation of cerebral ischemia. Trends for the 1990s. Circulation. 1991;83(2 Suppl):I176-89.

136. Zwiebel WJ. Duplex sonography of the cerebral arteries: efficacy, limitations, and indications. AJR Am J Roentgenol. 1992;158(1):29-36.

137. Hunink MG, Polak JF, Barlan MM, O'Leary DH. Detection and quantification of carotid artery stenosis: efficacy of various Doppler velocity parameters. AJR Am J Roentgenol. 1993;160(3):619-25.

138. Carroll BA. Carotid sonography. Radiology. 1991;178(2):303-13.

139. Moneta GL, Edwards JM, Chitwood RW, Taylor LM, Jr., Lee RW, Cummings CA, et al. Correlation of North American Symptomatic Carotid Endarterectomy Trial (NASCET) angiographic definition of 70% to 99% internal carotid artery stenosis with duplex scanning. J Vasc Surg. 1993;17(1):152-7; discussion 7-9.

140. Wilterdink JL, Feldmann E, Easton JD, Ward R. Performance of carotid ultrasound in evaluating candidates for carotid endarterectomy is optimized by an approach based on clinical outcome rather than accuracy. Stroke. 1996;27(6):1094-8.

141. Wijeyaratne SM, Jarvis S, Stead LA, Kibria SG, Evans JA, Gough MJ. A new method for characterizing carotid plaque: multiple cross-sectional view echomorphology. J Vasc Surg. 2003;37(4):778-84.
142. Casella IB, Fukushima RB, Marques AB, Cury MV, Presti C. Comparison between a new computer program and the reference software for gray-scale median analysis of atherosclerotic carotid plaques. J Clin Ultrasound. 2015;43(3):194-8.
143. Russell DA, Wijeyaratne SM, Gough MJ. Relationship of carotid plaque echomorphology to presenting symptom. Eur J Vasc Endovasc Surg. 2010;39(2):134-8.
144. Camen S, Haeusler KG, Schnabel RB. Cardiac imaging after ischemic stroke: Echocardiography, CT, or MRI? Herz. 2019;44(4):296-303.
145. Silvestry FE, Cohen MS, Armsby LB, Burkule NJ, Fleishman CE, Hijazi ZM, et al. Guidelines for the Echocardiographic Assessment of Atrial Septal Defect and Patent Foramen Ovale: From the American Society of Echocardiography and Society for Cardiac Angiography and Interventions. Journal of the American Society of Echocardiography. 2015;28(8):910-58.
146. Alkhouli M, Sievert H, Holmes DR. Patent foramen ovale closure for secondary stroke prevention. European Heart Journal. 2019;40(28):2339-49.
147. Meschia JF, Bushnell C, Boden-Albala B, Braun LT, Bravata DM, Chaturvedi S, et al. Guidelines for the primary prevention of stroke: A statement for healthcare professionals from the American heart association/American stroke association. Stroke. 2014;45(12):3754-832.
148. Floria M, Gabriel L, Schroeder E, Chenu P, Ambăruş V, Marchandise B. Stroke and an unexplained dyspnea in an elderly patient: Platypnea-orthodeoxia syndrome. Geriatrics and Gerontology International. 2012;12(2):356-8.
149. Pristipino C, Sievert H, D'Ascenzo F, Louis Mas J, Meier B, Scacciatella P, et al. European position paper on the management of patients with patent foramen ovale. General approach and left circulation thromboembolism. European Heart Journal. 2019;40(38):3182-95.
150. D'Andrea A, Dweck MR, Holte E, Fontes-Carvalho R, Cameli M, Aboumarie HS, et al. EACVI survey on the management of patients with patent foramen ovale and cryptogenic stroke. European Heart Journal Cardiovascular Imaging. 2021;22(2):135-41.
151. Lamers WH, Moorman AFM. Cardiac septation: A late contribution of the embryonic primary myocardium to heart morphogenesis. Circulation Research. 2002;91(2):93-103.
152. Naqvi N, McCarthy KP, Ho SY. Anatomy of the atrial septum and interatrial communications. Journal of Thoracic Disease. 2018;10:S2837-S47.
153. Anderson RH, Brown NA, Webb S. Development and structure of the atrial septum. Heart. 2002;88(1):104-10.
154. Jensen B, Spicer DE, Sheppard MN, Anderson RH. Development of the atrial septum in relation to postnatal anatomy and interatrial communications. Heart. 2017;103(6):456-62.
155. Yee K, Lui F. Anatomy, Thorax, Heart Foramen Ovale. 2021.
156. Falanga G, Carerj S, Oreto G, Khandheria BK, Zito C. How to understand patent foramen ovale clinical significance: Part i. Journal of Cardiovascular Echography. 2014;24(4):114-21.
157. Grecu M, Floria M, Tinică G. Complication due to entrapment in the Chiari apparatus. Europace : European pacing, arrhythmias, and cardiac electrophysiology : journal of the working groups on cardiac pacing, arrhythmias, and cardiac cellular electrophysiology of the European Society of Cardiology. 2014;16(4):577.

158. Hahn RT, Abraham T, Adams MS, Bruce CJ, Glas KE, Lang RM, et al. Guidelines for performing a comprehensive transesophageal echocardiographic examination: Recommendations from the american society of echocardiography and the society of cardiovascular anesthesiologists. Journal of the American Society of Echocardiography. 2013;26(9):921-64.

159. Puchalski MD, Lui GK, Miller-Hance WC, Brook MM, Young LT, Bhat A, et al. Guidelines for Performing a Comprehensive Transesophageal Echocardiographic: Examination in Children and All Patients with Congenital Heart Disease: Recommendations from the American Society of Echocardiography. Journal of the American Society of Echocardiography. 2019;32(2):173-215.

160. Hahn RT, Saric M, Faletra FF, Garg R, Gillam LD, Horton K, et al. Recommended Standards for the Performance of Transesophageal Echocardiographic Screening for Structural Heart Intervention: From the American Society of Echocardiography. Journal of the American Society of Echocardiography. 2022;35(1):1-76.

161. Mojadidi MK, Roberts SC, Winoker JS, Romero J, Goodman-Meza D, Gevorgyan R, et al. Accuracy of transcranial Doppler for the diagnosis of intracardiac right-to-left shunt: A bivariate meta-analysis of prospective studies. JACC: Cardiovascular Imaging. 2014;7(3):236-50.

162. González-Alujas T, Evangelista A, Santamarina E, Rubiera M, Gómez-Bosch Z, Rodríguez-Palomares JF, et al. Diagnosis and quantification of patent foramen ovale. Which is the reference technique? Simultaneous study with transcranial doppler, transthoracic and transesophageal echocardiography. Revista Espanola de Cardiologia. 2011;64(2):133-9.

163. Li Y, Ya-Nan Z, Li-Qun W. Which technique is better for detection of right-to- Left shunt in patients with patent foramen ovale: Comparing contrast transthoracic echocardiography with contrast transesophageal echocardiography. Echocardiography. 2014;31(9):1050-5.

164. Fan S, Nagai T, Luo H, Atar S, Naqvi T, Birnbaum Y, et al. Superiority of the combination of blood and agitated saline for routine contrast enhancement. Journal of the American Society of Echocardiography. 1999;12(2):94-8.

165. Jeon DS, Luo H, Iwami T, Miyamoto T, Brasch AV, Mirocha J, et al. The usefulness of a 10% air-10% blood-80% saline mixture for contrast echocardiography: Doppler measurement of pulmonary artery systolic pressure. Journal of the American College of Cardiology. 2002;39(1):124-9.

166. Porter TR, Abdelmoneim S, Belcik JT, McCulloch ML, Mulvagh SL, Olson JJ, et al. Guidelines for the cardiac sonographer in the performance of contrast echocardiography: A focused update from the American society of echocardiography. Journal of the American Society of Echocardiography. 2014;27(8):797-810.

167. Kawano T, Cui J, Koezuka Y, Toura I, Kaneko Y, Motoki K, et al. CD1d-restricted and TCR-mediated activation of valpha14 NKT cells by glycosylceramides. Science. 1997;278(5343):1626-9.

168. Montrief T, Alerhand S, Denault A, Scott J. Point-of-care echocardiography for the evaluation of right-to-left cardiopulmonary shunts: a narrative review. Canadian Journal of Anesthesia/Journal canadien d'anesthésie. 2020;67(12):1824-38.

169. Vitarelli A, Mangieri E, Capotosto L, Tanzilli G, D'Angeli I, Toni D, et al. Echocardiographic findings in simple and complex patent foramen ovale before and after transcatheter closure. European Heart Journal Cardiovascular Imaging. 2014;15(12):1377-85.

170. Rana BS, Thomas MR, Calvert PA, Monaghan MJ, Hildick-Smith D. Echocardiographic evaluation of patent foramen ovale prior to device closure. JACC: Cardiovascular Imaging. 2010;3(7):749-60.

171. Lee M, Oh JH. Echocardiographic diagnosis of right-to-left shunt using transoesophageal and transthoracic echocardiography. Open Heart. 2020;7(2).

172. Jauss M, Zanette E. Detection of right-to-left shunt with ultrasound contrast agent and transcranial Doppler sonography. Cerebrovascular Diseases. 2000;10(6):490-6.

173. Enriquez A, Saenz LC, Rosso R, Silvestry FE, Callans D, Marchlinski FE, et al. Use of intracardiac echocardiography in interventional cardiology working with the anatomy rather than fighting it. Circulation. 2018;137(21):2278-94.

174. Bartel T, Müller S, Biviano A, Hahn RT. Why is intracardiac echocardiography helpful? Benefits, costs, and how to learn. European Heart Journal. 2014;35(2):69-76.

175. Nicolay S, Salgado RA, Shivalkar B, Van Herck PL, Vrints C, Parizel PM. CT imaging features of atrioventricular shunts: what the radiologist must know. Insights into Imaging. 2016;7(1):119-29.

176. Nusser T, Höher M, Merkle N, Grebe OC, Spiess J, Kestler HA, et al. Cardiac Magnetic Resonance Imaging and Transesophageal Echocardiography in Patients With Transcatheter Closure of Patent Foramen Ovale. Journal of the American College of Cardiology. 2006;48(2):322-9.

177. Kleindorfer DO, Towfighi A, Chaturvedi S, Cockroft KM, Gutierrez J, Lombardi-Hill D, et al. 2021 Guideline for the prevention of stroke in patients with stroke and transient ischemic attack; A guideline from the American Heart Association/American Stroke Association. Stroke. 2021:E364-E467.

178. Kent DM, Saver JL, Ruthazer R, Furlan AJ, Reisman M, Carroll JD, et al. Risk of Paradoxical Embolism (RoPE)-Estimated Attributable Fraction Correlates with the Benefit of Patent Foramen Ovale Closure: An Analysis of 3 Trials. Stroke. 2020:3119-23.

179. Agricola E, Meucci F, Ancona F, Sanz AP, Zamorano JL. Echocardiographic guidance in transcatheter structural cardiac interventions. EuroIntervention. 2022;17(15):1205-26.

180. . How to Close a PFO With ICE Guidance Cardiac Interventions Today. 0000.

181. Vendrusculo V, de Souza VP, LA MF, MG MDO, Banzato TP, Monteiro PA, et al. Synthesis of novel perillyl-dihydropyrimidinone hybrids designed for antiproliferative activity. Medchemcomm. 2018;9(9):1553-64.

182. Liu Y, Chen S, Zühlke L, Black GC, Choy MK, Li N, et al. Global birth prevalence of congenital heart defects 1970-2017: Updated systematic review and meta-analysis of 260 studies. International Journal of Epidemiology. 2019;48(2):455-63.

183. Sanapo L, Pruetz JD, Słodki M, Goens MB, Moon-Grady AJ, Donofrio MT. Fetal echocardiography for planning perinatal and delivery room care of neonates with congenital heart disease. Echocardiography. 2017;34(12):1804-21.

184. Huang H, Cai M, Wang Y, Liang B, Lin N, Xu L. Snp array as a tool for prenatal diagnosis of congenital heart disease screened by echocardiography: Implications for precision assessment of fetal prognosis. Risk Management and Healthcare Policy. 2021;14:345-55.

185. The International Society of Ultrasound in O, Gynecology. ISUOG Practice Guidelines (updated): sonographic screening examination of the fetal heart. Ultrasound in obstetrics & gynecology : the official journal of the International Society of Ultrasound in Obstetrics and Gynecology. 2013;41(3):348-59.

186. AIUM–ACR–ACOG–SMFM–SRU Practice Parameter for the Performance of Standard Diagnostic Obstetric Ultrasound Examinations. Journal of Ultrasound in Medicine. 2018;37(11):E13-E24.

187. Liu H, Zhou J, Feng QL, Gu HT, Wan G, Zhang HM, et al. Fetal echocardiography for congenital heart disease diagnosis: A meta-analysis, power analysis and missing data analysis. European Journal of Preventive Cardiology. 2015;22(12):1531-47.
188. Yagel S, Arbel R, Anteby EY, Raveh D, Achiron R. The three vessels and trachea view (3VT) in fetal cardiac scanning. Ultrasound in Obstetrics and Gynecology. 2002;20(4):340-5.
189. Pasternok M, Nocun A, Knafel A, Grzesiak M, Orzechowski M, Konarska K, et al. YSign at the level of the 3-Vessel and trachea view: An effective fetal marker of aortic dextroposition anomalies in the first trimester. Journal of Ultrasound in Medicine. 2018;37(8):1869-78.
190. Palatnik A, Grobman WA, Cohen LS, Dungan JS, Gotteiner NL. Role of the 3-Vessel and trachea view in antenatal detection of tetralogy of fallot. Journal of Ultrasound in Medicine. 2016;35(8):1799-809.
191. Edwards H, Hamilton R. Single centre audit of early impact of inclusion of the three vessel and trachea view in obstetric screening. Ultrasound. 2018;26(2):93-100.
192. Lee W, Allan L, Carvalho JS, Chaoui R, Copel J, Devore G, et al. ISUOG consensus statement: What constitutes a fetal echocardiogram? Ultrasound in Obstetrics and Gynecology. 2008;32(2):239-42.
193. AIUM Practice Parameter for the Performance of Fetal Echocardiography. Journal of Ultrasound in Medicine. 2020;39(1):E5-E16.
194. . Ghid de Examinare Ecografică de Screening pentru Anomalii de Sarcină in Trimestru 1. 2019.
195. . Ghid de Examinare Ecografică de Screening pentru Anomalii de Sarcină in Trimestru 2. 2019.
196. Bronshtein M, Blumenfeld Z, Khoury A, Gover A. Diverse outcome following early prenatal diagnosis of pulmonary stenosis. Ultrasound in Obstetrics and Gynecology. 2017;49(2):213-8.
197. Guirado L, Crispi F, Masoller N, Bennasar M, Marimon E, Carretero J, et al. Biventricular impact of mild to moderate fetal pulmonary valve stenosis. Ultrasound in Obstetrics and Gynecology. 2018;51(3):349-56.
198. Fricke K, Liuba P, Weismann CG. Fetal Echocardiographic Dimension Indices: Important Predictors of Postnatal Coarctation. Pediatric Cardiology. 2021;42(3):517-25.
199. Familiari A, Morlando M, Khalil A, Sonesson SE, Scala C, Rizzo G, et al. Risk Factors for Coarctation of the Aorta on Prenatal Ultrasound: A Systematic Review and Meta-Analysis. Circulation. 2017;135(8):772-85.
200. Zheng MM, Tang HR, Zhang Y, Ru T, Li J, Xu BY, et al. Contribution of the fetal cardiac axis and v-sign angle in first-trimester screening for major cardiac defects. Journal of Ultrasound in Medicine. 2019;38(5):1179-87.
201. Stativa E, Rus AV, Suciu N, Pennings JS, Butterfield ME, Wenyika R, et al. Characteristics and prenatal care utilisation of Romanian pregnant women. European Journal of Contraception and Reproductive Health Care. 2014;19(3):220-6.
202. Pinette MG, Pan Y, Pinette SG, Blackstone J, Stubblefield PG. Fetal atrial septal aneurysm: Prenatal diagnosis by ultrasonography. Journal of Reproductive Medicine for the Obstetrician and Gynecologist. 1997;42(8):459-62.
203. Sun HY, Fripp RR, Printz BF. Unusual consequence of a fetal atrial septal aneurysm. Clin Case Rep. 2015;3(6):368-9.
204. Gewillig M, Brown SC, Roggen M, Eyskens B, Heying R, Givron P, et al. Dysfunction of the foetal arterial duct results in a wide spectrum of cardiovascular pathology. Acta Cardiologica. 2017;72(6):625-35.

205. Liang M, Wen H, Li S. Two fetuses in one family of arterial tortuosity syndrome: prenatal ultrasound diagnosis. BMC Pregnancy and Childbirth. 2021;21(1).
206. Aly SA, Contreras J, Honjo O, Villemain O. Antenatal occlusion of a ductal arteriosus aneurysm: A potential postnatal surgical emergency. Case report and literature review. Cardiology in the Young. 2020;30(11):1750-2.
207. Takajo D, Kobayashi D. Ductus arteriosus aneurysm with left pulmonary artery obstruction. Echocardiography. 2021;38(7):1128-30.
208. Doğan V, Aksoy ÖN, Sayıcı İU, Çitli R. Thrombosis of isolated ductus arteriosus aneurysm in a newborn. Echocardiography. 2021;38(4):716-7.
209. Ranzini AC, Hyman F, Jamaer E, Van Mieghem T. Aberrant right subclavian artery: Correlation between fetal and neonatal abnormalities and abnormal genetic screening or testing. Journal of Ultrasound in Medicine. 2017;36(4):785-90.
210. Minsart AF, Boucoiran I, Delrue MA, Audibert F, Abadir S, Lapierre C, et al. Left Superior Vena Cava in the Fetus: A Rarely Isolated Anomaly. Pediatric Cardiology. 2020;41(2):230-6.
211. Abuhamad A, Chaoui R. The Three-Vessel-Trachea View and Upper Mediastinum. A Practical Guide to Fetal Echocardiography: Normal and Abnormal Hearts. 2016:115-6.
212. Heit JA, Kobbervig CE, James AH, Petterson TM, Bailey KR, Melton LJ, 3rd. Trends in the incidence of venous thromboembolism during pregnancy or postpartum: a 30-year population-based study. Ann Intern Med. 2005;143(10):697-706.
213. Alsheef MA, Alabbad AM, Albassam RA, Alarfaj RM, Zaidi ARZ, Al-Arfaj O, et al. Pregnancy and Venous Thromboembolism: Risk Factors, Trends, Management, and Mortality. Biomed Res Int. 2020;2020:4071892.
214. Kalaitzopoulos DR, Panagopoulos A, Samant S, Ghalib N, Kadillari J, Daniilidis A, et al. Management of venous thromboembolism in pregnancy. Thromb Res. 2022;211:106-13.
215. ACOG Practice Bulletin No. 196: Thromboembolism in Pregnancy. Obstet Gynecol. 2018;132(1):e1-e17.
216. Touqmatchi D, Cotzias C, Girling J. Venous thromboprophylaxis in pregnancy: the implications of changing to the 2010 RCOG guidelines. J Obstet Gynaecol. 2012;32(8):743-6.
217. Bagaria SJ, Bagaria VB. Strategies for diagnosis and prevention of venous thromboembolism during pregnancy. J Pregnancy. 2011;2011:206858.
218. Devis P, Knuttinen MG. Deep venous thrombosis in pregnancy: Incidence, pathogenesis and endovascular management. Cardiovascular Diagnosis and Therapy. 2017;7:S300-S19.
219. Conklin P, Soares GM, Dubel GJ, Ahn SH, Murphy TP. Acute deep vein thrombosis (DVT): evolving treatment strategies and endovascular therapy. Medicine and health, Rhode Island. 2009;92(12):394-7.
220. Kesieme E, Kesieme C, Jebbin N, Irekpita E, Dongo A. Deep vein thrombosis: A clinical review. J Blood Med. 2011;2(2):59-69.
221. Chan WS, Spencer FA, Ginsberg JS. Anatomic distribution of deep vein thrombosis in pregnancy. CMAJ Canadian Medical Association Journal. 2010;182(7):657-60.
222. Martinelli I, Bucciarelli P, Mannucci PM. Thrombotic risk factors: Basic pathophysiology. Critical Care Medicine. 2010;38(SUPPL. 2):S3-S9.
223. Chen H, Wu L, Dou Q, Qin J, Li S, Cheng JZ, et al. Ultrasound Standard Plane Detection Using a Composite Neural Network Framework. IEEE Trans Cybern. 2017;47(6):1576-86.

224. de Jong PG, Coppens M, Middeldorp S. Duration of anticoagulant therapy for venous thromboembolism: Balancing benefits and harms on the long term. British Journal of Haematology. 2012;158(4):433-41.
225. Marik PE, Plante LA. Venous thromboembolic disease and pregnancy. New England Journal of Medicine. 2008;359(19):2025-33.
226. Margetic S. Diagnostic algorithm for thrombophilia screening. Clinical Chemistry and Laboratory Medicine. 2010;48(SUPPL. 1):S27-S39.
227. Lindhoff-Last E, Luxembourg B. Evidence-based indications for thrombophilia screening. Vasa - Journal of Vascular Diseases. 2008;37(1):19-30.
228. Lussana F, Dentali F, Abbate R, d'Aloja E, D'Angelo A, De Stefano V, et al. Screening for thrombophilia and antithrombotic prophylaxis in pregnancy: Guidelines of the Italian Society for Haemostasis and Thrombosis (SISET). Thrombosis Research. 2009;124(5):e19-e25.
229. Chan WS. Diagnosis of venous thromboembolism in pregnancy. Thrombosis Research. 2018;163:221-8.
230. Ercan S, Özkan S, Yücel N, Orçun A. Establishing reference intervals for D-dimer to trimesters. Journal of Maternal-Fetal and Neonatal Medicine. 2015;28(8):983-7.
231. Hedengran KK, Andersen MR, Stender S, Szecsi PB. Large D-Dimer Fluctuation in Normal Pregnancy: A Longitudinal Cohort Study of 4,117 Samples from 714 Healthy Danish Women. Obstetrics and Gynecology International. 2016;2016.
232. Kline JA, Richardson DM, Than MP, Penaloza A, Roy PM. Systematic review and meta-analysis of pregnant patients investigated for suspected pulmonary embolism in the emergency department. Academic Emergency Medicine. 2014;21(9):949-59.
233. Morse M. Establishing a normal range for D-dimer levels through pregnancy to aid in the diagnosis of pulmonary embolism and deep vein thrombosis [7]. Journal of Thrombosis and Haemostasis. 2004;2(7):1202-4.
234. Ducloy-Bouthors AS, Duhamel A, Kipnis E, Tournoys A, Prado-Dupont A, Elkalioubie A, et al. Postpartum haemorrhage related early increase in D-dimers is inhibited by tranexamic acid: Haemostasis parameters of a randomized controlled open labelled trial. British Journal of Anaesthesia. 2016;116(5):641-8.
235. Middeldorp S. Thrombophilia and pregnancy complications: Cause or association? Journal of Thrombosis and Haemostasis. 2007;5(SUPPL. 1):276-82.
236. Dalen JE. Should Patients with Venous Thromboembolism Be Screened for Thrombophilia? American Journal of Medicine. 2008;121(6):458-63.
237. Cohn DM, Vansenne F, Kaptein AA, De Borgie CAJM, Middeldorp S. The psychological impact of testing for thrombophilia: A systematic review. Journal of Thrombosis and Haemostasis. 2008;6(7):1099-104.
238. Turpie A, Esmon C. Venous and arterial thrombosis - Pathogenesis and the rationale for anticoagulation. Thrombosis and haemostasis. 2011;105:586-96.
239. Bates SM, Greer A, Middeldorp S, Veenstra DL, Prabulos AM, Vandvik PO. VTE, thrombophilia, antithrombotic therapy, and pregnancy - Antithrombotic therapy and prevention of thrombosis, 9th ed: American College of Chest Physicians evidence-based clinical practice guidelines. Chest. 2012;141(2 SUPPL.):e691S-e736S.
240. Den Heijer M, Köster T, Blom HJ, Bos GMJ, Briët E, Reitsma PH, et al. Hyperhomocysteinemia as a risk factor for deep-vein thrombosis. New England Journal of Medicine. 1996;334(12):759-62.
241. Debreceni L. Homocysteine--a risk factor for atherosclerosis. Orvosi hetilap. 2001;142(27):1439-44.
242. Milosević-Tosić M, Borota J. Hyperhomocysteinemia--a risk factor for development of occlusive vascular diseases. Medicinski pregled. 2002;55(9-10):385-91.

243. Falcon CR, Cattaneo M, Panzeri D, Martinelli I, Mannucci PM. High prevalence of hyperhomocyst(e)inemia in patients with juvenile venous thrombosis. Arteriosclerosis, Thrombosis, and Vascular Biology. 1994;14(7):1080-3.

244. Badulescu OV, Ciocoiu M, Filip N, Veringa V. The efficiency of substitutive treatment with Moroctocog alfa in managing hemostasis in patients with hemophilia A without inhibitors with total knee arthroplasties. Revista de Chimie. 2018;69(12):3702-4.

245. Badulescu OV, Filip N, Sirbu PD, Bararu-Bojan I, Vladeanu M, Bojan A, et al. Current practices in haemophilic patients undergoing orthopedic surgery a systematic review. Experimental and Therapeutic Medicine. 2020;20(6).

246. Dargaud Y, Rugeri L, Fleury C, Battie C, Gaucherand P, Huissoud C, et al. Personalized thromboprophylaxis using a risk score for the management of pregnancies with high risk of thrombosis: a prospective clinical study. Journal of Thrombosis and Haemostasis. 2017;15(5):897-906.

247. De Maeseneer MGR, Bochanen N, Van Rooijen G, Neglén P. Analysis of 1,338 Patients with Acute Lower Limb Deep Venous Thrombosis (DVT) Supports the Inadequacy of the Term "proximal DVT". European Journal of Vascular and Endovascular Surgery. 2016;51(3):415-20.

248. Kassaï B, Boissel JP, Cucherat M, Sonie S, Shah NR, Leizorovicz A. A systematic review of the accuracy of ultrasound in the diagnosis of deep venous thrombosis in asymptomatic patients. Thrombosis and Haemostasis. 2004;91(4):655-66.

249. Dua A, Thondapu V, Rosovsky R, Hunt D, Latz C, Waller HD, et al. Deep Vein Thrombosis Protocol Optimization to Minimize Healthcare Worker Exposure in Coronavirus Disease-2019. 0000.

250. Shabani Varaki E, Gargiulo GD, Penkala S, Breen PP. Peripheral vascular disease assessment in the lower limb: A review of current and emerging non-invasive diagnostic methods. BioMedical Engineering Online. 2018;17(1).

251. Laurence N, Cronan John J, Lilly Michael P, Merli Geno J, Srikar A, Hertzberg Barbara S. Ultrasound for lower extremity deep venous thrombosis. Circulation. 2018;137:1505-15.

252. Zitek JA, Baydoun J, Baird J. Tools for the Clinician: The essentials of bedside (ED or ICU) ultrasound for deep vein thrombosis. Curr Emerg Hosp Med Rep. 2013;1(2):65-70.

253. Khan F, Vaillancourt C, Bourjeily G. Diagnosis and management of deep vein thrombosis in pregnancy. BMJ. 2017;357:j2344.

254. Sucker C. Prophylaxis and Therapy of Venous Thrombotic Events (VTE) in Pregnancy and the Postpartum Period. Geburtshilfe und Frauenheilkunde. 2020;80(1):48-59.

255. Alsheef MA, Alabbad AM, Albassam RA, Alarfaj RM, Zaidi ARZ, Al-Arfaj O, et al. Pregnancy and Venous Thromboembolism: Risk Factors, Trends, Management, and Mortality. BioMed Research International. 2020;2020.

256. Lim W, Eikelboom JW, Ginsberg JS. Inherited thrombophilia and pregnancy associated venous thromboembolism. British Medical Journal. 2007;334(7607):1318-21.

257. Voicu DI, Munteanu O, Gherghiceanu F, Arsene LV, Bohiltea RE, Gradinaru DM, et al. Maternal inherited thrombophilia and pregnancy outcomes. Exp Ther Med. 2020;20(3):2411-4.

258. James AH, Rhee E, Thames B, Philipp CS. Characterization of antithrombin levels in pregnancy. Thrombosis research. 2014;134(3):648-51.

259. Fleck D, Albadawi H, Shamoun F, Knuttinen G, Naidu S, Oklu R. Catheter-directed thrombolysis of deep vein thrombosis: literature review and practice considerations. Cardiovasc Diagn Ther. 2017;7(Suppl 3):S228-s37.

260. Khare M, Nelson-Piercy C. Acquired thrombophilias and pregnancy. Best Practice and Research: Clinical Obstetrics and Gynaecology. 2003;17(3):491-507.

261. Muralidar S, Ambi SV, Sekaran S, Krishnan UM. The emergence of COVID-19 as a global pandemic: Understanding the epidemiology, immune response and potential therapeutic targets of SARS-CoV-2. Biochimie. 2020;179:85-100.

262. Cucinotta D, Vanelli M. WHO declares COVID-19 a pandemic. Acta bio medica: Atenei parmensis. 2020;91(1):157.

263. LaCourse SM, Kachikis A, Blain M, Simmons LE, Mays JA, Pattison AD, et al. Low prevalence of severe acute respiratory syndrome coronavirus 2 among pregnant and postpartum patients with universal screening in Seattle, Washington. Clinical Infectious Diseases. 2021;72(5):869-72.

264. Vintzileos WS, Muscat J, Hoffmann E, John NS, Vertichio R, Vintzileos AM, et al. Screening all pregnant women admitted to labor and delivery for the virus responsible for coronavirus disease 2019. American Journal of Obstetrics & Gynecology. 2020;223(2):284-6.

265. Săndulescu MS, Văduva CC, Siminel MA, Dijmărescu AL, Vrabie SC, Camen IV, et al. Impact of COVID-19 on fertility and assisted reproductive technology (ART): a systematic review. Rom J Morphol Embryol. 2022;63(3):503-10.

266. Wang CL, Liu YY, Wu CH, Wang CY, Wang CH, Long CY. Impact of COVID-19 on Pregnancy. Int J Med Sci. 2021;18(3):763-7.

267. Di Toro F, Gjoka M, Di Lorenzo G, De Santo D, De Seta F, Maso G, et al. Impact of COVID-19 on maternal and neonatal outcomes: a systematic review and meta-analysis. Clin Microbiol Infect. 2021;27(1):36-46.

268. Di Mascio D, Khalil A, Saccone G, Rizzo G, Buca D, Liberati M, et al. Outcome of coronavirus spectrum infections (SARS, MERS, COVID-19) during pregnancy: a systematic review and meta-analysis. Am J Obstet Gynecol MFM. 2020;2(2):100107.

269. Adam AM, Vasilache IA, Socolov D, Stuparu Cretu M, Georgescu CV, Vicoveanu P, et al. Risk Factors Associated with Severe Disease and Intensive Care Unit Admission of Pregnant Patients with COVID-19 Infection-A Retrospective Study. J Clin Med. 2022;11(20).

270. Mullins E, Hudak ML, Banerjee J, Getzlaff T, Townson J, Barnette K, et al. Pregnancy and neonatal outcomes of COVID-19: coreporting of common outcomes from PAN-COVID and AAP-SONPM registries. Ultrasound Obstet Gynecol. 2021;57(4):573-81.

271. Wei SQ, Bilodeau-Bertrand M, Liu S, Auger N. The impact of COVID-19 on pregnancy outcomes: a systematic review and meta-analysis. Cmaj. 2021;193(16):E540-e8.

272. Ko JY, DeSisto CL, Simeone RM, Ellington S, Galang RR, Oduyebo T, et al. Adverse Pregnancy Outcomes, Maternal Complications, and Severe Illness Among US Delivery Hospitalizations With and Without a Coronavirus Disease 2019 (COVID-19) Diagnosis. Clin Infect Dis. 2021;73(Suppl 1):S24-s31.

273. La Verde M, Riemma G, Torella M, Cianci S, Savoia F, Licciardi F, et al. Maternal death related to COVID-19: A systematic review and meta-analysis focused on maternal co-morbidities and clinical characteristics. Int J Gynaecol Obstet. 2021;154(2):212-9.

274. Karimi L, Makvandi S, Vahedian-Azimi A, Sathyapalan T, Sahebkar A. Effect of COVID-19 on Mortality of Pregnant and Postpartum Women: A Systematic Review and Meta-Analysis. J Pregnancy. 2021;2021:8870129.

275. Péju E, Belicard F, Silva S, Hraiech S, Painvin B, Kamel T, et al. Management and outcomes of pregnant women admitted to intensive care unit for severe pneumonia related to SARS-CoV-2 infection: the multicenter and international COVIDPREG study. Intensive Care Med. 2022;48(9):1185-96.

276. Kalafat E, Prasad S, Birol P, Tekin AB, Kunt A, Di Fabrizio C, et al. An internally validated prediction model for critical COVID-19 infection and intensive care unit admission in symptomatic pregnant women. Am J Obstet Gynecol. 2022;226(3):403.e1-.e13.

277. Prasad S, Kalafat E, Blakeway H, Townsend R, O'Brien P, Morris E, et al. Systematic review and meta-analysis of the effectiveness and perinatal outcomes of COVID-19 vaccination in pregnancy. Nat Commun. 2022;13(1):2414.

278. Kalafat E, Heath P, Prasad S, P OB, Khalil A. COVID-19 vaccination in pregnancy. Am J Obstet Gynecol. 2022;227(2):136-47.

279. Fell DB, Dhinsa T, Alton GD, Török E, Dimanlig-Cruz S, Regan AK, et al. Association of COVID-19 Vaccination in Pregnancy With Adverse Peripartum Outcomes. Jama. 2022;327(15):1478-87.

280. Shimabukuro TT, Kim SY, Myers TR, Moro PL, Oduyebo T, Panagiotakopoulos L, et al. Preliminary Findings of mRNA Covid-19 Vaccine Safety in Pregnant Persons. N Engl J Med. 2021;384(24):2273-82.

281. Wastnedge EA, Reynolds RM, Van Boeckel SR, Stock SJ, Denison FC, Maybin JA, et al. Pregnancy and COVID-19. Physiological reviews. 2021;101(1):303-18.

282. Pathangey G, Fadadu PP, Hospodar AR, Abbas AE. Angiotensin-converting enzyme 2 and COVID-19: patients, comorbidities, and therapies. Am J Physiol Lung Cell Mol Physiol. 2021;320(3):L301-l30.

283. Gengler C, Dubruc E, Favre G, Greub G, de Leval L, Baud D. SARS-CoV-2 ACE-receptor detection in the placenta throughout pregnancy. Clin Microbiol Infect. 2021;27(3):489-90.

284. Malinowski AK, Noureldin A, Othman M. COVID-19 susceptibility in pregnancy: Immune/inflammatory considerations, the role of placental ACE-2 and research considerations. Reprod Biol. 2020;20(4):568-72.

285. Azinheira Nobrega Cruz N, Stoll D, Casarini DE, Bertagnolli M. Role of ACE2 in pregnancy and potential implications for COVID-19 susceptibility. Clin Sci (Lond). 2021;135(15):1805-24.

286. Resta L, Vimercati A, Cazzato G, Fanelli M, Scarcella SV, Ingravallo G, et al. SARS-CoV-2, Placental Histopathology, Gravity of Infection and Immunopathology: Is There an Association? Viruses. 2022;14(6).

287. Ezechukwu HC, Shi J, Fowora MA, Diya CA, Elfaki F, Adegboye OA. Fetoplacental transmission and placental response to SARS-CoV-2: Evidence from the literature. Front Med (Lausanne). 2022;9:962937.

288. Tallarek A-C, Urbschat C, Fonseca Brito L, Stanelle-Bertram S, Krasemann S, Frascaroli G, et al. Inefficient placental virus replication and absence of neonatal cell-specific immunity upon sars-CoV-2 infection during pregnancy. Frontiers in immunology. 2021;12:698578.

289. Peiris S, Mesa H, Aysola A, Manivel J, Toledo J, Borges-Sa M, et al. Pathological findings in organs and tissues of patients with COVID-19: A systematic review. PloS one. 2021;16(4):e0250708.

290. Heath. RNIoP. Analiza epidemiologică a 385 de cazuri de COVID-19 confirmate cu noi varianteale SARS-CoV-2. 2021. . Available online: http://wwwcnscbtro/indexphp/analiza-cazuri-confirmate-covid19/2329-cazuri-covid-19-cu-noi-variante-analiza-epidemiologica-a-385-cazuri/file (accessed on 10 February 2023) 2021.

291. (ECDC). ECfDPaC. Variants of interest and concern in the EU/EE. . Available online: https://gisecdceuropaeu/portal/apps/opsdashboard/indexhtml#/25b6e879c076412aaa9ae7adb78d3241 (accessed on 10 February 2023) 2020.

292. Ministry RH. PROTOCOL din 1 iulie 2021 pentru suportul respirator non-invaziv al pacienților adulți diagnosticați cu COVID-19 în afara secțiilor ATI. MONITORUL OFICIAL nr 661 bis din 5 iulie 2021. 2021;Available at: https://legislatie.just.ro/Public/DetaliiDocument/244114 (Accesed on 20 December 2022).
293. Au Yeung SL, Li AM, He B, Kwok KO, Schooling CM. Association of smoking, lung function and COPD in COVID-19 risk: a two-step Mendelian randomization study. Addiction. 2022;117(7):2027-36.
294. Radzikowska U, Ding M, Tan G, Zhakparov D, Peng Y, Wawrzyniak P, et al. Distribution of ACE2, CD147, CD26, and other SARS-CoV-2 associated molecules in tissues and immune cells in health and in asthma, COPD, obesity, hypertension, and COVID-19 risk factors. Allergy. 2020;75(11):2829-45.
295. Tanasa IA, Manciuc C, Carauleanu A, Navolan DB, Bohiltea RE, Nemescu D. Anosmia and ageusia associated with coronavirus infection (COVID-19) - what is known? Exp Ther Med. 2020;20(3):2344-7.
296. Lassi ZS, Ana A, Das JK, Salam RA, Padhani ZA, Irfan O, et al. A systematic review and meta-analysis of data on pregnant women with confirmed COVID-19: Clinical presentation, and pregnancy and perinatal outcomes based on COVID-19 severity. J Glob Health. 2021;11:05018.
297. Zaigham M, Andersson O. Maternal and perinatal outcomes with COVID-19: A systematic review of 108 pregnancies. Acta Obstet Gynecol Scand. 2020;99(7):823-9.
298. Vakili S, Savardashtaki A, Jamalnia S, Tabrizi R, Nematollahi MH, Jafarinia M, et al. Laboratory Findings of COVID-19 Infection are Conflicting in Different Age Groups and Pregnant Women: A Literature Review. Arch Med Res. 2020;51(7):603-7.
299. Yamamoto R, Asano H, Umazume T, Takaoka M, Noshiro K, Saito Y, et al. C-reactive protein level predicts need for medical intervention in pregnant women with SARS-CoV2 infection: A retrospective study. J Obstet Gynaecol Res. 2022;48(4):938-45.
300. Fisher SA, Goldstein JA, Mithal LB, Isaia AL, Shanes ED, Otero S, et al. Laboratory analysis of symptomatic and asymptomatic pregnant patients with SARS-CoV-2 infection. Am J Obstet Gynecol MFM. 2021;3(6):100458.
301. Gandini O, Criniti A, Ballesio L, Giglio S, Galardo G, Gianni W, et al. Serum Ferritin is an independent risk factor for Acute Respiratory Distress Syndrome in COVID-19. J Infect. 2020;81(6):979-97.
302. Oncel MY, Akın IM, Kanburoglu MK, Tayman C, Coskun S, Narter F, et al. A multicenter study on epidemiological and clinical characteristics of 125 newborns born to women infected with COVID-19 by Turkish Neonatal Society. Eur J Pediatr. 2021;180(3):733-42.
303. Vila-Candel R, González-Chordá VM, Soriano-Vidal FJ, Castro-Sánchez E, Rodríguez-Blanco N, Gómez-Seguí A, et al. Obstetric-Neonatal Care during Birth and Postpartum in Symptomatic and Asymptomatic Women Infected with SARS-CoV-2: A Retrospective Multicenter Study. Int J Environ Res Public Health. 2022;19(9).
304. Gao YD, Ding M, Dong X, Zhang JJ, Kursat Azkur A, Azkur D, et al. Risk factors for severe and critically ill COVID-19 patients: A review. Allergy. 2021;76(2):428-55.
305. Al-Saadi E, Abdulnabi MA. Hematological changes associated with COVID-19 infection. J Clin Lab Anal. 2022;36(1):e24064.
306. Lasser DM, Chervenak J, Moore RM, Li T, Knight C, Teo HO, et al. Severity of COVID-19 Respiratory Complications during Pregnancy are Associated with Degree of Lymphopenia and Neutrophil to Lymphocyte Ratio on Presentation: A Multicenter Cohort Study. Am J Perinatol. 2021;38(12):1236-43.

307. Covali R, Socolov D, Socolov R, Pavaleanu I, Carauleanu A, Akad M, et al. Complete Blood Count Peculiarities in Pregnant SARS-CoV-2-Infected Patients at Term: A Cohort Study. Diagnostics (Basel). 2021;12(1).

308. Covali R, Socolov D, Pavaleanu I, Carauleanu A, Boiculese VL, Socolov R. SARS-CoV-2 Infection Susceptibility of Pregnant Patients at Term Regarding ABO and Rh Blood Groups: A Cohort Study. Medicina (Kaunas). 2021;57(5).

309. Wang F, Nie J, Wang H, Zhao Q, Xiong Y, Deng L, et al. Characteristics of Peripheral Lymphocyte Subset Alteration in COVID-19 Pneumonia. J Infect Dis. 2020;221(11):1762-9.

310. Levitan D, London V, McLaren RA, Jr, Mann JD, Cheng K, Silver M, et al. Histologic and Immunohistochemical Evaluation of 65 Placentas From Women With Polymerase Chain Reaction–Proven Severe Acute Respiratory Syndrome Coronavirus 2 (SARS-CoV-2) Infection. Archives of Pathology & Laboratory Medicine. 2021;145(6):648-56.

311. Zhao S, Xie T, Shen L, Liu H, Wang L, Ma X, et al. An Immunological Perspective: What Happened to Pregnant Women After Recovering From COVID-19? Front Immunol. 2021;12:631044.

312. Juttukonda LJ, Wachman EM, Boateng J, Jain M, Benarroch Y, Taglauer ES. Decidual immune response following COVID-19 during pregnancy varies by timing of maternal SARS-CoV-2 infection. J Reprod Immunol. 2022;151:103501.

313. Definitions of infertility and recurrent pregnancy loss: a committee opinion. Fertil Steril. 2020;113(3):533-5.

314. Magnus MC, Wilcox AJ, Morken NH, Weinberg CR, Håberg SE. Role of maternal age and pregnancy history in risk of miscarriage: prospective register based study. Bmj. 2019;364:l869.

315. Rasmark Roepke E, Matthiesen L, Rylance R, Christiansen OB. Is the incidence of recurrent pregnancy loss increasing? A retrospective register-based study in Sweden. Acta Obstet Gynecol Scand. 2017;96(11):1365-72.

316. Bashiri A, Halper KI, Orvieto R. Recurrent Implantation Failure-update overview on etiology, diagnosis, treatment and future directions. Reprod Biol Endocrinol. 2018;16(1):121.

317. Pirtea P, De Ziegler D, Tao X, Sun L, Zhan Y, Ayoubi JM, et al. Rate of true recurrent implantation failure is low: results of three successive frozen euploid single embryo transfers. Fertil Steril. 2021;115(1):45-53.

318. Franasiak JM, Alecsandru D, Forman EJ, Gemmell LC, Goldberg JM, Llarena N, et al. A review of the pathophysiology of recurrent implantation failure. Fertil Steril. 2021;116(6):1436-48.

319. Günther V, Otte SV, Freytag D, Maass N, Alkatout I. Recurrent implantation failure - an overview of current research. Gynecol Endocrinol. 2021;37(7):584-90.

320. Mekinian A, Cohen J, Alijotas-Reig J, Carbillon L, Nicaise-Roland P, Kayem G, et al. Unexplained Recurrent Miscarriage and Recurrent Implantation Failure: Is There a Place for Immunomodulation? Am J Reprod Immunol. 2016;76(1):8-28.

321. Sheikhansari G, Pourmoghadam Z, Danaii S, Mehdizadeh A, Yousefi M. Etiology and management of recurrent implantation failure: A focus on intra-uterine PBMC-therapy for RIF. J Reprod Immunol. 2020;139:103121.

322. Freitag N, Pour SJ, Fehm TN, Toth B, Markert UR, Weber M, et al. Are uterine natural killer and plasma cells in infertility patients associated with endometriosis, repeated implantation failure, or recurrent pregnancy loss? Arch Gynecol Obstet. 2020;302(6):1487-94.

323. Ay ME, Ay Ö, Çayan FE, Tekin S, Karakaş Ü, Derici Yildirim D, et al. Genetic Predisposition to Unexplained Recurrent Pregnancy Loss: Killer Cell Immunoglobulin-Like Receptor Gene Polymorphisms as Potential Biomarkers. Genet Test Mol Biomarkers. 2019;23(1):57-65.

324. Alecsandru D, Barrio A, Garrido N, Aparicio P, Pellicer A, Moffett A, et al. Parental human leukocyte antigen-C allotypes are predictive of live birth rate and risk of poor placentation in assisted reproductive treatment. Fertil Steril. 2020;114(4):809-17.

325. Uhrberg M, Valiante NM, Shum BP, Shilling HG, Lienert-Weidenbach K, Corliss B, et al. Human diversity in killer cell inhibitory receptor genes. Immunity. 1997;7(6):753-63.

326. Winter CC, Gumperz JE, Parham P, Long EO, Wagtmann N. Direct binding and functional transfer of NK cell inhibitory receptors reveal novel patterns of HLA-C allotype recognition. J Immunol. 1998;161(2):571-7.

327. Xu WH, Chen JJ, Sun Q, Wang LP, Jia YF, Xuan BB, et al. Chlamydia trachomatis, Ureaplasma urealyticum and Neisseria gonorrhoeae among Chinese women with urinary tract infections in Shanghai: A community-based cross-sectional study. J Obstet Gynaecol Res. 2018;44(3):495-502.

328. Varla-Leftherioti M, Keramitsoglou T, Parapanissiou E, Kurpisz M, Kontopoulou-Antonopoulou V, Tsekoura C, et al. HLA-DQA1*0505 sharing and killer immunoglobulin-like receptors in sub fertile couples: report from the 15th International Histocompatibility Workshop. Tissue Antigens. 2010;75(6):668-72.

329. Nowak I, Wilczyńska K, Wilczyński JR, Malinowski A, Radwan P, Radwan M, et al. KIR, LILRB and their Ligands' Genes as Potential Biomarkers in Recurrent Implantation Failure. Arch Immunol Ther Exp (Warsz). 2017;65(5):391-9.

330. Alecsandru D, Garrido N, Vicario JL, Barrio A, Aparicio P, Requena A, et al. Maternal KIR haplotype influences live birth rate after double embryo transfer in IVF cycles in patients with recurrent miscarriages and implantation failure. Hum Reprod. 2014;29(12):2637-43.

331. Deshmukh H, Way SS. Immunological Basis for Recurrent Fetal Loss and Pregnancy Complications. Annu Rev Pathol. 2019;14:185-210.

332. Von Woon E, Greer O, Shah N, Nikolaou D, Johnson M, Male V. Number and function of uterine natural killer cells in recurrent miscarriage and implantation failure: a systematic review and meta-analysis. Hum Reprod Update. 2022;28(4):548-82.

333. Dong AC, Morgan J, Kane M, Stagnaro-Green A, Stephenson MD. Subclinical hypothyroidism and thyroid autoimmunity in recurrent pregnancy loss: a systematic review and meta-analysis. Fertil Steril. 2020;113(3):587-600.e1.

334. Vicoveanu P, Vasilache IA, Scripcariu IS, Nemescu D, Carauleanu A, Vicoveanu D, et al. Use of a Feed-Forward Back Propagation Network for the Prediction of Small for Gestational Age Newborns in a Cohort of Pregnant Patients with Thrombophilia. Diagnostics (Basel). 2022;12(4).

335. Liu X, Chen Y, Ye C, Xing D, Wu R, Li F, et al. Hereditary thrombophilia and recurrent pregnancy loss: a systematic review and meta-analysis. Hum Reprod. 2021;36(5):1213-29.

336. Yan X, Wang L, Yan C, Zhang X, Hui L, Sheng Q, et al. Decreased expression of the vitamin D receptor in women with recurrent pregnancy loss. Arch Biochem Biophys. 2016;606:128-33.

337. Gonçalves DR, Braga A, Braga J, Marinho A. Recurrent pregnancy loss and vitamin D: A review of the literature. Am J Reprod Immunol. 2018;80(5):e13022.

338. Bikdeli B, Madhavan MV, Jimenez D, Chuich T, Dreyfus I, Driggin E, et al. COVID-19 and Thrombotic or Thromboembolic Disease: Implications for Prevention,

Antithrombotic Therapy, and Follow-Up: JACC State-of-the-Art Review. J Am Coll Cardiol. 2020;75(23):2950-73.

339. Ali MAM, Spinler SA. COVID-19 and thrombosis: From bench to bedside. Trends Cardiovasc Med. 2021;31(3):143-60.

340. Kollias A, Kyriakoulis KG, Lagou S, Kontopantelis E, Stergiou GS, Syrigos K. Venous thromboembolism in COVID-19: A systematic review and meta-analysis. Vasc Med. 2021;26(4):415-25.

341. Klok FA, Kruip M, van der Meer NJM, Arbous MS, Gommers D, Kant KM, et al. Incidence of thrombotic complications in critically ill ICU patients with COVID-19. Thromb Res. 2020;191:145-7.

342. Connors JM, Levy JH. COVID-19 and its implications for thrombosis and anticoagulation. Blood. 2020;135(23):2033-40.

343. Flaumenhaft R, Enjyoji K, Schmaier AA. Vasculopathy in COVID-19. Blood. 2022;140(3):222-35.

344. Liu YC, Kuo RL, Shih SR. COVID-19: The first documented coronavirus pandemic in history. Biomedical Journal. 2020;43(4):328-33.

345. Lovato A, de Filippis C, Marioni G. Upper airway symptoms in coronavirus disease 2019 (COVID-19). American Journal of Otolaryngology - Head and Neck Medicine and Surgery. 2020;41(3).

346. World Health O. Coronavirus disease 2019 (COVID-19) situation report—44. Coronavirus Disease 2019 (covid-19) Situation Report-29. 2020.

347. Wang L, Gao YH, Lou LL, Zhang GJ. The clinical dynamics of 18 cases of COVID-19 outside of Wuhan, China. European Respiratory Journal. 2020;55(4).

348. Gupta A, Madhavan MV, Sehgal K, Nair N, Mahajan S, Sehrawat TS, et al. Extrapulmonary manifestations of COVID-19. Nature Medicine. 2020;26(7):1017-32.

349. Fiorino S, Gallo C, Zippi M, Sabbatani S, Manfredi R, Moretti R, et al. Cytokine storm in aged people with CoV-2: possible role of vitamins as therapy or preventive strategy. Aging Clinical and Experimental Research. 2020;32(10):2115-31.

350. Jogalekar MP, Veerabathini A, Gangadaran P. SARS-CoV-2 variants: A double-edged sword? Experimental Biology and Medicine. 2021;246(15):1721-6.

351. Sanyaolu A, Okorie C, Marinkovic A, Haider N, Abbasi AF, Jaferi U, et al. The emerging SARS-CoV-2 variants of concern. Therapeutic Advances in Infectious Disease. 2021;8.

352. Samieefar N, Rashedi R, Akhlaghdoust M, Mashhadi M, Darzi P, Rezaei N. Delta Variant: The New Challenge of COVID-19 Pandemic, an Overview of Epidemiological, Clinical, and Immune Characteristics. Acta bio-medica : Atenei Parmensis. 2022;93(1):e2022179.

353. Alexandar S, Ravisankar M, Kumar RS, Jakkan K. A comprehensive review on Covid-19 Delta variant. Int J Pharmacol Clin Res. 2021;5(2):83-5.

354. Hu B, Guo H, Zhou P, Shi ZL. Characteristics of SARS-CoV-2 and COVID-19. Nature Reviews Microbiology. 2021;19(3):141-54.

355. Trougakos IP, Stamatelopoulos K, Terpos E, Tsitsilonis OE, Aivalioti E, Paraskevis D, et al. Insights to SARS-CoV-2 life cycle, pathophysiology, and rationalized treatments that target COVID-19 clinical complications. Journal of Biomedical Science. 2021;28(1).

356. Dascalu S. The Successes and Failures of the Initial COVID-19 Pandemic Response in Romania. Frontiers in Public Health. 2020;8.

357. Runwal P. Two Years Later, Coronavirus Evolution Still Surprises Experts Here's why National Geographic Science Coronavirus Coverage 11 March 2022. 0000.

358. Lipsitch M, Krammer F, Regev-Yochay G, Lustig Y, Balicer RD. SARS-CoV-2 breakthrough infections in vaccinated individuals: measurement, causes and impact. Nature Reviews Immunology. 2022;22(1):57-65.

359. Allam Z. The first 50 days of COVID-19: A detailed chronological timeline and extensive review of literature documenting the pandemic. Surveying the Covid-19 Pandemic and its Implications. 2020:1-7.

360. Surleac M, Casangiu C, Banica L, Milu P, Florea D, Sandulescu O, et al. Short Communication:Evidence of Novel SARS-CoV-2 Variants Circulation in Romania. AIDS Research and Human Retroviruses. 2021;37(4):329-32.

361. Farzanegan MR, Gholipour HF, Feizi M, Nunkoo R, Andargoli AE. International Tourism and Outbreak of Coronavirus (COVID-19): A Cross-Country Analysis. Journal of Travel Research. 2021;60(3):687-92.

362. Ficiu L. Details about the First Romanian Diagnosed with the New Coronavirus He Is 20 Years Old and Lives in Prigoria Commune—UPDATE Mediafax 27 February 2020. 0000.

363. Wang Y, Wang Y, Chen Y, Qin Q. Unique epidemiological and clinical features of the emerging 2019 novel coronavirus pneumonia (COVID-19) implicate special control measures. Journal of Medical Virology. 2020;92(6):568-76.

364. Volkmann C, Tokarski KO, Dincă VM, Bogdan A. The Impact of COVID-19 on Romanian Tourism. An Explorative Case Study on Prahova County, Romania. Amfiteatru Economic. 2021;23(56):163-.

365. Córdova LDS, Vega APM, Luján-Carpio E, Parodi JF, Moncada-Mapelli E, Armacanqui-Valencia I, et al. Clinical characteristics of older patients with COVID-19: A systematic review of case reports. Dementia e Neuropsychologia. 2021;15(1):1-15.

366. Manciuc C, Nemescu D, Vata A, Lacatusu GA. SARS-CoV-2 infection and diabetes mellitus: A North Eastern Romanian experience. Exp Ther Med. 2021;21.

367. Vâţă A, Anita A, Manciuc CD, Savuta G, Luca CM, Roșu FM, et al. Clinical significance of early IgA an-ti-SARS-CoV-2 antibody detection in patients from a Romanian referral COVID-19 hospital. Exp Ther Med. 2022;23:391.

368. Niknam Z, Jafari A, Golchin A, Danesh Pouya F, Nemati M, Rezaei-Tavirani M, et al. Potential therapeutic options for COVID-19: an update on current evidence. European Journal of Medical Research. 2022;27(1).

369. Lalchhandama K. The chronicles of coronaviruses: the bronchitis, the hepatitis and the common cold. Science Vision. 2020;20(1):43-53.

370. Lacatusu GA, Vasilescu C, Mihai IF, Filip-Ciubotaru F, Vata A, Manciuc C. COVID-19 and air conditioning-is there an environmental link? Environ Eng Manag J EEMJ. 2020;1:19.

371. Gracia-Ramos AE, Jaquez-Quintana JO, Contreras-Omaña R, Auron M. Liver dysfunction and SARS-CoV-2 infection. World Journal of Gastroenterology. 2021;27(26):3951-70.

372. Zhang C, Shi L, Wang FS. Liver injury in COVID-19: management and challenges. The Lancet Gastroenterology and Hepatology. 2020;5(5):428-30.

373. Devaux CA, Rolain JM, Raoult D. ACE2 receptor polymorphism: Susceptibility to SARS-CoV-2, hypertension, multi-organ failure, and COVID-19 disease outcome. Journal of Microbiology, Immunology and Infection. 2020;53(3):425-35.

374. Warner FJ, Rajapaksha H, Shackel N, Herath CB. ACE2: From protection of liver disease to propagation of COVID-19. Clinical Science. 2020;134(23):3137-58.

375. Cichoż-Lach H, Michalak A. Liver injury in the era of COVID-19. World Journal of Gastroenterology. 2021;27(5):377-90.

376. Fara A, Mitrev Z, Rosalia RA, Assas BM. Cytokine storm and COVID-19: a chronicle of pro-inflammatory cytokines: Cytokine storm: The elements of rage! Open Biology. 2020;10(9).
377. McLeod AI. Kendall rank correlation and mann-kendall trend test. R Package Kendall. 2005.
378. Huang C, Wang Y, Li X, Ren L, Zhao J, Hu Y, et al. Clinical features of patients infected with 2019 novel coronavirus in Wuhan, China. The Lancet. 2020;395(10223):497-506.
379. El-Shabasy RM, Nayel MA, Taher MM, Abdelmonem R, Shoueir KR, Kenawy ER. Three waves changes, new variant strains, and vaccination effect against COVID-19 pandemic. International Journal of Biological Macromolecules. 2022;204:161-8.
380. Duong D. Alpha, Beta, Delta, Gamma: What's important to know about SARS-CoV-2 variants of concern? CMAJ : Canadian Medical Association journal = journal de l'Association medicale canadienne. 2021;193(27):E1059-E60.
381. Garrido I, Liberal R, Macedo G. Review article: COVID-19 and liver disease—what we know on 1st May 2020. Alimentary Pharmacology and Therapeutics. 2020;52(2):267-75.
382. Huang YK, Li YJ, Li B, Wang P, Wang QH. Dysregulated liver function in SARS-CoV-2 infection: Current understanding and perspectives. World Journal of Gastroenterology. 2021;27(27):4358-70.
383. Chen N, Zhou M, Dong X, Qu J, Gong F, Han Y, et al. Epidemiological and clinical characteristics of 99 cases of 2019 novel coronavirus pneumonia in Wuhan, China: a descriptive study. The Lancet. 2020;395(10223):507-13.
384. Cai Q, Huang D, Yu H, Zhu Z, Xia Z, Su Y, et al. COVID-19: Abnormal liver function tests. Journal of Hepatology. 2020;73(3):566-74.
385. Guan W, Ni Z, Hu Y, Liang W, Ou C, He J, et al. Clinical characteristics of coronavirus disease 2019 in China. New England Journal of Medicine. 2020;382(18):1708-20.
386. Huang Y, Zhou H, Yang R, Xu Y, Feng X, Gong P. Clinical characteristics of 36 non-survivors with COVID-19 in Wuhan, China. medRxiv. 2020(10229).
387. Liu Q, Wang RS, Qu GQ. Gross Examination Report of a COVID-19 Death Autopsy. Journal of Forensic Medicine. 2020;36(1):21-3.
388. Loghin II, Mihai IF, Roşu MF, Diaconu IE, Vâţă A, Popa R, et al. Characteristics and Trends of COVID-19 Infection in a Tertiary Hospital in Romania: A Retrospective Study. Journal of Personalized Medicine. 2022;12(11).
389. Ferguson GG, Eliasziw M, Barr HW, Clagett GP, Barnes RW, Wallace MC, et al. The North American Symptomatic Carotid Endarterectomy Trial : surgical results in 1415 patients. Stroke. 1999;30(9):1751-8.
390. Kumamaru H, Jalbert JJ, Nguyen LL, Gerhard-Herman MD, Williams LA, Chen C-Y, et al. Surgeon case volume and 30-day mortality after carotid endarterectomy among contemporary medicare beneficiaries: before and after national coverage determination for carotid artery stenting. Stroke. 2015;46(5):1288-94.
391. Karlöf E, Seime T, Dias N, Lengquist M, Witasp A, Almqvist H, et al. Correlation of computed tomography with carotid plaque transcriptomes associates calcification with lesion-stabilization. Atherosclerosis. 2019;288:175-85.
392. Kapadia M, Mehri-Basha M, Madhavan R, Rajamani K, Chaturvedi S. High rate of inappropriate carotid endarterectomy in an urban medical center. Journal of stroke and cerebrovascular diseases. 2009;18(4):277-80.
393. Bothamley J. Thromboembolism in pregnancy. Emergencies Around Childbirth: Routledge; 2017. p. 65-86.

394. Tsao CW, Aday AW, Almarzooq ZI, Alonso A, Beaton AZ, Bittencourt MS, et al. Heart disease and stroke statistics—2022 update: a report from the American Heart Association. Circulation. 2022;145(8):e153-e639.

395. Fowkes FGR, Rudan D, Rudan I, Aboyans V, Denenberg JO, McDermott MM, et al. Comparison of global estimates of prevalence and risk factors for peripheral artery disease in 2000 and 2010: a systematic review and analysis. The lancet. 2013;382(9901):1329-40.

396. Saran R, Robinson B, Abbott KC, Bragg-Gresham J, Chen X, Gipson D, et al. US renal data system 2019 annual data report: epidemiology of kidney disease in the United States. American Journal of Kidney Diseases. 2020;75(1):A6-A7.

397. Ravi S, Chaikof EL. Biomaterials for vascular tissue engineering. Regenerative medicine. 2010;5(1):107-20.